

Artificial Gravity: The Role of Graviceptive Information during Cross-Coupled Rotation
in Context-Specific Adaptation

By

Nathaniel J Newby

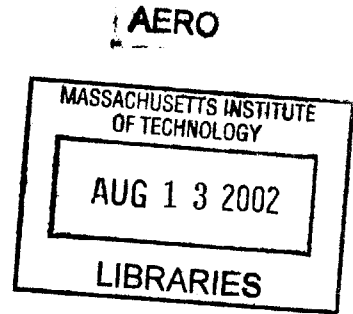
B.S. Biomedical Engineering
Milwaukee School of Engineering

SUBMITTED TO THE DEPARTMENT OF AERONAUTICS AND ASTRONAUTICS
IN PARTIAL FULFILLMENT OF THE REQUIREMENTS FOR THE DEGREE OF

MASTER OF SCIENCE IN AERONAUTICS AND ASTRONAUTICS AT THE
MASSACHUSETTS INSTITUTE OF TECHNOLOGY

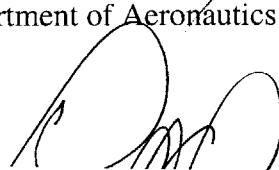
JUNE 2002

© 2002 Massachusetts Institute of Technology. All rights reserved.



Signature of Author:

Department of Aeronautics and Astronautics
May 24, 2002



Certified by:

Laurence R. Young, Sc.D.
Apollo Program Professor of Astronautics
Thesis Supervisor

Accepted by:

Wallace E. Vander Velde
Professor of Aeronautics and Astronautics
Chairman, Committee for Graduate Students

Artificial Gravity: The Role of Graviceptive Information during Cross-Coupled Rotation in Context-Specific Adaptation

by
Nathaniel J Newby

Submitted to the Department of Aeronautics and Astronautics
on May 24, 2002 in partial fulfillment of the
Requirements for the Degree of Master of Science in Aeronautics and Astronautics

Abstract

Extended periods of time spent in microgravity can lead to several debilitating physiological and performance effects on the human body. Short-radius centrifugation provides a means of countering some of these negative effects. However, out of plane head movements in a rotating environment can induce inappropriate reflex components, disorientation, and motion sickness. As a result, an adaptation protocol to the resultant action of the cross-coupled rotational stimuli on the semicircular canals must be developed if short-radius centrifugation is ever to be used in an effective manner. It is possible that the gravito-inertial environment itself specifies this context for adaptation. During space flight, the linear acceleration force is either absent or minimized, which will impact the manner in which the canals reinterpret stimulation arising from head movements in a rotating environment.

The goal of this study was to investigate the role of graviceptive information as a possible influencing factor for adaptation to short-radius centrifugation and is based upon Aim 5 of the NSBRI Neurovestibular Aspects of Artificial Gravity Proposal (Young, et al, 2000). Previous studies on MIT's centrifuge indicate that the duration of illusory motion sensations induced by yaw head movements in the rotating environment depend, in part, upon the head's position with respect to gravity (Aim 1, experiment 2 of the NSBRI Neurovestibular Aspects of Artificial Gravity Proposal by Young, et al, 2000). The conflicting sensation decayed faster during head movements toward ear down than for similar head movements toward nose up. A number of plausible explanations exist for this asymmetry including: different velocity profiles per each type of head turn, different absolute head turn angles, differing responses based on the relationship of the head with respect to the trunk of one's body, or that otolithic information is modulating the semicircular canal response. Seventeen subjects participated in this study designed to locate the root cause of this asymmetry. The results indicate that the latter explanation is responsible for the pronounced difference between nose up and ear down head movements made in the rotating environment in the presence of Earth's gravity.

Thesis Supervisor: Dr. Laurence Young, Apollo Program Professor of Astronautics
Department of Aeronautics and Astronautics

This work was supported by the National Space Biomedical Research Institute (NSBRI) through a cooperative agreement with NASA (NCC9-58). Grant number NSBRI-00-01-014.

Acknowledgements

This work was supported by the National Space Biomedical Research Institute (NSBRI) through a cooperative agreement with the National Aeronautics and Space Administration (NCC 9-58).

I am deeply indebted to my thesis supervisor, Dr. Laurence Young, for providing me with an opportunity to participate in this research as well as continued guidance in all aspects of this work.

I would like to thank the co-investigator of this study, Dr. Fred Mast, for all of his hard work, knowledge and expertise in psychophysics.

I would like to acknowledge the instructive assistance of Dr. Charles Oman and Dr. Dan Merfeld for helping me understand vestibular physiology from an engineering system's approach.

Thank you Dr. Heiko Hecht for your competent management of the Artificial Gravity team. You have provided invaluable assistance throughout not only this study, but my graduate career.

I could not have performed the statistical analysis of data without the beneficial aid of Dr. Alan Natapoff. I would also like to thank Liz Zotos for work done beyond the call of duty in helping me order parts, learn my way around the lab, and for supplying answers to a million other questions.

Special thank you to fellow graduate student Erika Brown for many enlightening conversations, help with all aspects of this study, moral support, and continued friendship.

I would like to acknowledge all those MVL graduates who helped me get started including: Kathy Sienko for taking the time to teach me data analysis techniques, Carol Chueng for showing me the ins and outs of the SRC and its control system, and Lisette Lyne for initiating me to experimentation with human subjects.

Thanks to all of the UROPs especially Nathan Shapiro, Dylan Chavez, Elliot Vasquez, and Jane Wu for their dedication and contributions to both this work and other artificial gravity research endeavors. I also wish to recognize all the people who participated as subjects in this study.

Finally, I'd like to thank my wife, Nicole, and daughter, Abigail, for adding so much to my life and making my dreams come true. And, above all, thanks to my Heavenly Father, without whom, none of this would be possible.

Table of Contents

Chapter 1 Introduction	8
1.2 Countermeasures	10
1.3 Artificial Gravity	10
1.4 Rationale	12
1.5 Motivation	13
1.6 Hypothesis	15
1.7 Thesis Outline	15
Chapter 2 Background	18
2.0 Chapter Introduction	18
2.1 Artificial Gravity: Physics and Implications	19
2.2 Vestibular Anatomy/Physiology	20
2.2.1 The Maculae – Detection of Head Orientation with Respect to Gravity	21
2.2.2 Directional Sensitivity of the Hair Cells	21
2.2.3 Semicircular Canals	23
2.3 Vestibular Ocular Reflex (VOR)	24
2.4 Nystagmus	25
2.5 Vestibular Physiology: An Engineering Approach	26
2.5.1 Torsion Pendulum Model of the Semicircular Canals	26
2.5.2 Modeling the Otolith Organs	30
2.5.3 Modeling the Vestibulo-Ocular Reflex	32
2.5.4 Modeling Velocity Storage	34
2.6 Stimulus Provided to the Vestibular System during SRC	36
2.7 Physical Responses to SRC Stimulus	38
2.8 GIF Conflict Resolution Theory	39
2.9 Modification of the Semicircular Response by the Utricular and Saccular Maculae	40
2.10 Context-Specific Adaptation	42
Chapter 3 Experimental Methods	44
3.1 Experimental Design	44
3.2 Subjects	47
3.3 Equipment	48
3.3.1 Short-Radius Centrifuge	49
3.3.2 Head Restraint	51
3.3.3 ISCAN Video Eye Imaging Hardware and Software	54
3.3.4 Subjective Visual Vertical	54
3.3.5 Subjective Measures	55
3.3.5.1 Motion Sickness Survey	55
3.3.5.2 Verbal Accounts of Magnitude Estimation	56
3.3.5.3 Verbal Accounts of Direction and Degrees	57
3.3.5.4 Estimated Duration of Sensations	57
3.4 Experimental Procedure	58
Chapter 4 Analysis Techniques	66
4.1 Eye Data	66

4.2 Normalized SPV.....	70
4.3 Head Movements.....	71
4.4 Missing Data Points.....	71
Chapter 5 Results.....	73
5.1 Head Movements.....	73
5.2 Subjective Magnitude Estimates.....	75
5.3 Duration of Illusory Sensations.....	78
5.4 Normalized Slow Phase Eye Velocity (NSPV).....	79
5.5 Subjective Visual Vertical (SVV).....	81
5.6 Subjective Descriptions of Self-motion.....	81
Chapter 6 Discussion.....	87
6.0 Main Findings.....	87
6.1 Semicircular Canals and Normalized Slow Phase Eye Velocity (NSPV).....	88
6.2 Neck Proprioceptors.....	89
6.3 Head Turn Properties.....	90
6.4 Perception of Angular Rotation.....	92
6.5 Graviceptive Information.....	93
6.5.1 Otolith Asymmetries.....	93
6.5.2 Otolith-Canal Interaction.....	96
6.5.3 CNS Processing of Otolith-Canal Interactions.....	97
6.5.3.1 Subjective Descriptions of Illusory Motion.....	98
6.5.3.2 Subject Grouping by Amount of GIF Conflict.....	98
6.5.3.3 Analysis of GIF Conflict Groups.....	100
6.5.3.4 Possible Concerns with GIF Conflict Theory.....	101
6.6 Pragmatic Aspects of this Study.....	102
6.5 Recommendations.....	103
Chapter 7 Conclusion.....	105
References.....	107
APPENDIX A: Consent Form.....	113
APPENDIX B: Medical Disqualifications.....	116
APPENDIX C: Experimental Protocols.....	117
APPENDIX D: Individual Subject Data.....	122
APPENDIX E: Raw Data.....	139
APPENDIX F: Matlab Source Code.....	201

List of Tables and Figures

Figure 1: Von Braun’s vision of artificial gravity. Source: October 18, 1952 issue of Collier’s.....	11
Figure 2: Illusory sensations decay faster for yaw head turns to ear down than for nose up head turns in the rotating environment. Hecht, et al (2001).....	14
Figure 3 – Anatomy of the Inner Ear.....	20
Figure 4: Detail of semicircular canal ampula and rotational dynamics.....	23
Figure 5: Illustration of slow and fast phase nystagmus.....	26
Figure 6: Simplified circular canal without cupula, illustrating the fundamental integrating function of canal hydrodynamics. V. Wilson and G. Jones (1979) p.44.....	27
Figure 7: Bode plot for the Torsion-Pendulum model of the semicircular canals.....	30
Figure 8: A: Mechanical linkage between the macula and overlying structures. B: Mechanical analogy. \ddot{x} , Linear acceleration of head relative to space; \ddot{y} , acceleration of otoconia relative to space; ξ , relative displacement of otoconia and macula; t_0 , position of end organ at commencement of acceleration; t , position after time t	31
V. Wilson and G. Jones (1979) p.71.....	31
Figure 9: Model of the VOR. Source: Paige, 1983.....	34
Figure 10: Raphan model of the velocity storage mechanism, where E_H is eye position in the head, E_S is eye position in space, H is head position in space, $Th(s)$ is semicircular canal dynamics, and W is the viewed image’s position. All terms are first derivatives indicating velocity rather than position. Velocity storage mechanism is represented in a feedback loop by a gain term K , and integration term $\int dt$	35
Figure 11: Experimental setup.....	36
Figure 12: Right-hand coordinate frame.....	36
Figure 13: Effect of orientation to gravity on decay of nystagmus. Benson and Bodin (1966).....	41
Figure 14: Short Radius Centrifuge and experimental equipment.....	49
Figure 15: MIT’s Short-radius Centrifuge.....	51
Figure 16: Head restraint device designed for this study.....	54
Figure 17: Protocol.....	63
Table 1: Subjects’ body positions for various experimental phases.....	65
Figure 18: Data collected from subject 13, phase 9, head turn number 12. From top to bottom: head position during yaw movement, eye position, SPV, and subject’s estimate of the duration of illusory motion sensations.....	69
Figure 19: Exponentially decaying curve fit for the SPV depicted in Figure X. Amplitude equal to -19.31 with a time constant of 4.49 seconds.....	70
Table 2: Missing dependent variable data points. Grayed boxes denote variables that were not statistically analyzed. Items in black indicate the number of points replaced using averaging schema.....	72
Figure 20: Average head turn velocity for supine versus right shoulder down body positions.....	74
Figure 21: Average turn velocity as a function of whether it occurred in the early or late set of turns for a particular body position.....	75

Figure 22: Subjective magnitude estimates of illusory motion for head turns toward nose up and toward right ear down. NU vs. RED differences were significant for both body positions..... 76

Figure 23: Magnitude estimates habituate as a function of head turn repetition. 77

Figure 24: Magnitude estimates habituate over repetitions, and adapt across phases. 77

Figure 25: Longer illusory sensations were experienced for NU than for RED head turns. No significant effect of body position was observed. 78

Figure 26: Duration of illusory sensations is significantly shorter in the later than in the earlier phase for a given body position. 79

Figure 27: NSPV for head turn direction was not significantly different in either body orientation..... 80

Figure 28: Histogram of time constant of decay of nystagmus. 80

Table 3: Results from SVV testing. 81

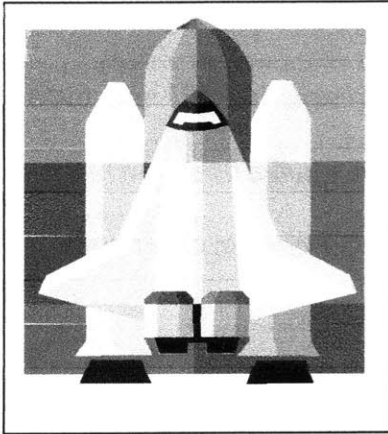
Figure 29: Group 1 average self-motion; magnitude and direction. 83

Figure 30: Group 2 average self-motion; magnitude and direction. 83

Figure 31: Group 3 average self-motion; magnitude and direction. 84

Table 4: Average subjective magnitude estimates for head turns toward NU and RED. . 85

Table 5: Average subjective duration estimates for head turns toward NU and RED..... 85



Chapter 1

Introduction

1.1 Physiological Effects of Long-duration Space Flight

Long-term human exposure to microgravity contributes to cardiovascular deconditioning, muscle atrophy, bone loss, and overall weakening of the body's immune system (National Research Council Space Studies Board, 1998; Churchill, 1997). Many of these side effects of space flight are manageable or can be considered negligible for short earth orbit missions, as medical expertise is readily available upon return to the earth.

However, as human exploration carries us further from home, these issues take on greater importance. For example, on a manned mission to Mars, the crew will not be able to rely on medical support upon arrival. In addition to the per-voyage threat of radiation exposure, the results of a six to eight month weightless journey may have catastrophic effects upon entry into the Martian gravitational environment (Young 1999).

Immediately after entry into weightlessness, a headwards shift of fluid occurs due to the lack of a hydrostatic gradient. Baroreceptors become stretched causing the body to react

to this fluid shift as an increase in fluid volume. The body removes this excess volume via sodium excretion, which increases urine flow, and through hypothalamic modification of one's thirst, so less water is drunk. The heart is no longer pumping against a gravity gradient, and over time cardiac muscle mass is lost. In other words, the cardiovascular system optimally adapts to the micro-g environment (Young, 1999). Problems arise when an astronaut adapted to the weightless environment transitions to a gravitational environment. The reduced sensitivity of the baroreflex response can lead to orthostatic intolerance and episodes of syncope (White, Nyberg, White, Grimes, Finney, 1965).

In much the same way that cardiac muscle mass is lost; muscles that oppose gravity also atrophy as a function of time spent in the weightless environment. Extended periods of spaceflight result in a loss of lean body mass and muscular strength, a greater fast-to-slow twitch muscle fiber ratio, and a flexor versus extensor muscle bias Caiozzo, V. J. Baker, M.J., Herrick, R.E., Tao, M., and K. M. Baldwin. (1994). A report by the National Space Biomedical Research Institute (NSBRI) showed that contractile properties of leg extensors were decreased by 40% by the 4th – 7th day of flight (Shenkman and Kozlovskaya, 2000). As with the cardiovascular system, serious problems arise during the transition from micro-gravity to a gravitational environment. Given the extent of overall muscle degradation, we can expect serious performance decrements and possibly even injury occurring upon re-entry.

Bone loss may be the most formidable obstacle to long duration space-flight. Current research indicates that dynamic loading and strains are a prerequisite for strong, healthy

bones. Both dynamic and static loads are negligible in the micro-g environment, which may lead to substantial amounts of bone loss (Churchill, 1997). Cosmonaut data indicate that overall bone mineral density decreases occur on the order of one to two percent per month spent in weightlessness with no apparent plateau. Even more pronounced losses have been observed in the bones of the back, spine, and legs. Furthermore, recovery of these losses is extremely limited. Astronauts traveling to Mars risk serious injury and even fracture as they set foot upon the surface.

In addition to bone, muscle, and cardiovascular degradation, other physiological systems suffer from extended duration space-flight. Coordination of movement and locomotion is affected after long-duration space-flight. Circadian rhythms are disrupted due to varying day-night cycles. Immune response is weakened. Radiation hazards increase as a function of time spent in space. The neurovestibular system is also impacted and may lead to disorientation illusions and nausea.

1.2 Countermeasures

Several countermeasures have been proposed and developed which attempt to address each of these individual debilitating physiological effects. Taken as a whole, the majority of these countermeasures neglect the root problem itself, namely the lack of a gravito-inertial environment. Creation of an artificial gravity environment via centrifugation, however, provides a solution that directly attacks the core difficulty underlying long-duration spaceflight.

1.3 Artificial Gravity

Artificial gravity is a concept that can be traced back to the mid 1800s and the dawn of serious thought about human space travel. The Russian scientist, E. K. Tsiolkovsky, discussed the convenience and efficacy of artificial gravity as early as 1911 (Tsiolkovsky, 1911). Perhaps the most popular version of an artificial gravity device is the one sketched by Wernher Von Braun in 1953. His vision, depicted in the film *2001: A Space Odyssey* consisted of a large, rotating torus where the crew happily transitioned between rotating and non-rotating portions of the spacecraft.



Figure 1: Von Braun's vision of artificial gravity. Source: October 18, 1952 issue of Collier's.

Such large-radius rotating structures are an unlikely possibility in the near term, because of the engineering complexity and cost associated with such designs. A short-radius centrifuge capable of being carried on board a craft or station is a feasible, low cost alternative solution. Given its elegance and simplicity of design, it is somewhat surprising that there have been no human studies conducted during spaceflight with such a device. The fact that no deconditioning was observed in rats spun continuously at 1-g for several days is promising (Gurovsky, Gazenko, Adamovich, Ilyin, Genin, Korolkov, Shipov, Kotovskaya, Kondratyeva, Serova, Kondratyev, Yu, 1980). However, several questions remain unanswered about short-radius centrifugation, such as whether or not we require continuous gravity or can we get by with a daily gravity “bath”? Is 1-g the optimum level, 1/2-g, 2-g? If artificial gravity is used intermittently should it just be administered during sleep or should appropriate exercise protocols be developed and implemented as well?

1.4 Rationale

As the radial arm of the rotating structure is decreased the angular velocity must be increased in order to maintain the same level of centrifugal acceleration. For example, a 2m-radius centrifuge, such as MIT’s, requires an angular velocity of 23 revolutions per minute to be maintained to achieve a 1G force at the feet of a subject. A person making out of plane head movements in such a rotating environment results in inappropriate eye reflex components, illusory sensations, disorientation, and motion sickness. One solution to this problem is to restrict an astronaut’s ability to make head movements while on a centrifuge. Other than being uncomfortable, this solution is inconsistent with a need for

active exercise upon the centrifuge. Therefore, an adaptation strategy must be developed which allows for *ad lib* head movements into and out of the plane of rotation of a short-radius centrifuge.

Recent work has demonstrated that the illusory sensations, inappropriate nystagmus, and overall motion sickness associated with head movements in a rotating environment attenuate during one hour of centrifugation, and further adapt during repeated exposures over multiple days (Young, Hecht, Lyne, Sienko, Cheung, & Kavelaars 2001). On earth, the illusory sensations experienced by a subject in a rotating environment conflict with graviceptive inputs, which indicate no change in posture relative to the gravitational vertical. The otoliths (utricle and saccule) provide the brain with information about body position with respect to gravity. Currently, it is unclear whether adaptation to yaw head movements on the SRC in the presence of a gravitational field will generalize to the microgravitic environment (Graybiel, 1997; Grigorova & Kornilova, 1996). If the context-specific adaptation requires a gravity cue, it is unlikely to transfer to microgravity, as an external gravito-inertial reference force is unavailable. The absence of gravito-inertial force (GIF) in space may even lead to an erroneous updating of the internal estimator (Glasauer and Mittelstaedt, 1998). Therefore, an optimal earth-based adaptation strategy must consider any effects due to the orientation of gravity.

1.5 Motivation

A previous study conducted on MIT's short-radius centrifuge indicated that the duration of illusory motion sensations induced by yaw head movements in the rotating

environment depend, in part, on the head's position with respect to gravity (Hecht, Kavelaars, Cheung, Young, 2001). The conflicting sensation decayed faster during head movements toward ear down than for similar head movements toward nose up (Figure 2).

H. Hecht et al. Short-radius centrifugation

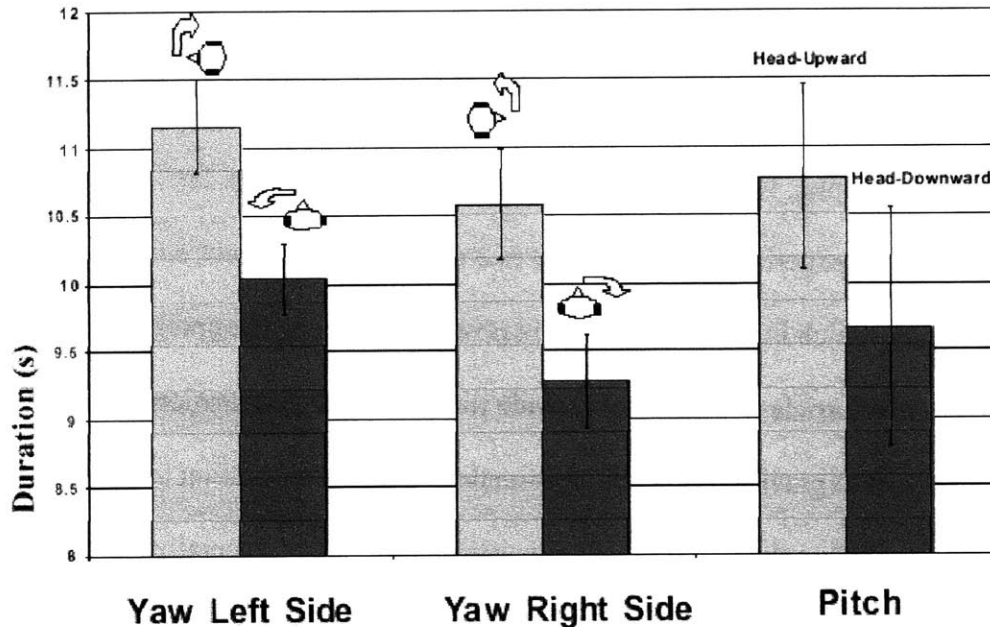


Figure 2: Illusory sensations decay faster for yaw head turns to ear down than for nose up head turns in the rotating environment. Hecht, et al (2001).

One possibility for this asymmetry is that otolithic information is modulating the overall response. Specifically, when the head is in an ear down position, Y-direction specific units are activated in the utricular macula. Alternatively, when the head is in a nose up position, X-direction specific units are activated. The differences in the durations of illusory motion sensations may be explained by a gain difference between these units, a differing canal-otolith interaction for these units, or higher level brain processing of these units.

Several other possibilities may also be causing this asymmetry. First, the velocity profile for the head turns may differ when going from right ear down (RED) to nose up (NU) than from going NU to RED. Secondly, the absolute angles of each type of head turn may also differ, leading to the observed asymmetric response. Third, the head yaw turn trajectory may also be different in each case. Finally, perhaps the relationship of the head with respect to the trunk of one's body plays a key role. For turns toward NU, the head is aligned with the body at the end of the movement, whereas, turns toward RED result in a misalignment.

This study was designed first to determine whether this asymmetry is reproducible, and if so, to discriminate between the various explanations.

1.6 Hypothesis

The principal hypothesis of this study is that otolithic information is modulating the response to angular acceleration and is the primary agent responsible for the asymmetric response observed between head movements made toward nose up versus right ear down on the SRC (Hecht, et al, 2001). Another way of stating this is that the gravity vector is an integral part of the demonstrated context-specific adaptation to the rotating environment.

1.7 Thesis Outline

Chapter 2 is constructed to equip the reader with all of the background information required to understand the nature of the investigation conducted for this thesis. It begins

with the fundamental anatomy and physiology of the vestibular system. A systems engineering approach to this system is then introduced, which includes a description of the torsion pendulum model. A literature review of the modification of angular acceleration responses by linear accelerations is then presented.

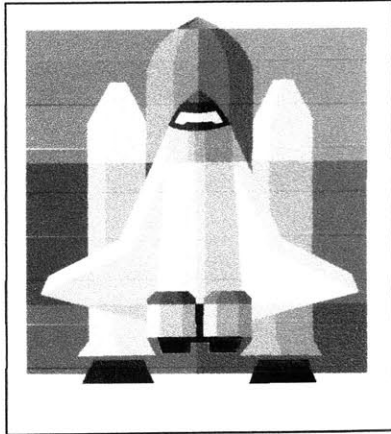
Chapter 3 focuses on the experimental methods used throughout this study. This section includes a detailed description of the rationale behind the experimental design. An account of equipment used in the experiment, as well as equipment especially designed for this study is also listed here. The chapter is concluded with the procedures and protocols utilized in this study.

Chapter 4 is concerned with detailing the data analysis techniques employed. This section contains an introduction to the measures deemed important to this study, as well as the rationale for choosing these measures. The chapter ends with the statistical analysis techniques used as well as an explanation of how outlier data points were handled.

Chapter 5 is dedicated to the significant findings of this investigation. The subjective magnitudes and durations of sensations, and normalized slow phase eye velocity as a function of head turn is presented in this section.

Chapter 6 attempts to explain the findings of the previous chapter. This section also contains a discussion of the implications of this work on future artificial gravity research.

Chapter 7 concludes the thesis by reviewing the significant results of this study and indicating future research that should be conducted.



Chapter 2

Background

2.0 Chapter Introduction

This chapter is written to provide a naïve reader with all of the background information necessary to understand the nature and results of the experiment contained in this thesis.

The experiment sought to address two questions. First, why are some head turns made in a rotating environment accompanied by longer durations of illusory motion than others?

Second, what are the pragmatic implications of this effect on centrifuge adaptation strategies, especially with regard to astronauts?

That being said, the first section offers a brief introduction to the physics of artificial gravity as well implications of short-radius centrifugation (SRC). The anatomy and physiology of the vestibular system is then explored because of the dramatic effects centrifugation has on the balance and orientation sense organs. The vestibulo-ocular reflex (VOR) was a major dependent variable in this study and thus a definition is included next. This section is followed by an engineering approach to vestibular physiology for two reasons. One is to provide better insight to the system. The other is to

build to an explanation of the velocity storage mechanism, which may be involved in an explanation of the results found in this study.

Equipped with this information, a detailed look at the stimulus imparted to participants in this study while making yaw head turns in a rotating environment can then be examined. Some of the perceptual and physiological manifestations of this stimulus are then listed. The next two sections offer a description of two mechanisms possibly responsible for the observed asymmetric response between nose up (NU) and right ear down (RED) head turns on the centrifuge. The first of these describes the gravito-inertial force (GIF) conflict resolution theory. The second concerns the modification of the response to angular accelerations by linear accelerations. The chapter concludes with a brief review of SRC adaptation research.

2.1 Artificial Gravity: Physics and Implications

The term artificial gravity is a bit of a misnomer. Gravity is not what is generated by rotating structures. Rather, these “artificial gravity” devices provide centrifugal forces of equivalent linear acceleration magnitudes as gravitational vectors. However, the nature of these two types of linear acceleration forces is very different. For example, gravitational forces fall off with the square of the distance away from an object, whereas centrifugal forces increase proportional to the distance away from the center of rotation.

Many researchers now believe that a rotating apparatus, capable of generating 1-g to several-g centrifugal forces, may be used to counter the debilitating effects of long duration exposure to the micro-g environment of space (Burton & Meeker, 1992). The linear acceleration provided by a centrifuge is equivalent to the square of the angular

velocity multiplied by the radial distance from the center of rotation ($\alpha = \omega^2 r$). Therefore, a tradeoff exists between the size of the structure and the rate of rotation. A large structure has two primary benefits. One is that the rate of rotation can be dramatically reduced. The other is that the linear acceleration gradient from the top of one's head to the bottom of one's feet can be minimized.

Unfortunately, the cost and technical challenges associated with such a large rotating mechanism prohibits its construction, at least in the near term. An alternate solution, the so called short-radius centrifuge (SRC), poses lesser technical hurdles to implementation. However, the increased rate of rotation required for an SRC to maintain a 1-g force at the rim presents some physiological challenges to astronauts using such devices. The most notable problems arise as a result of the novel vestibular system stimulation produced while making head turns into and out of the plane of rotation. Recent work indicates that adaptation to this environment is possible (Young, et al, 2001; Guedry, 1965).

2.2 Vestibular Anatomy/Physiology

The human vestibular apparatus is the principal organ that detects sensations of equilibrium. Located in the petrous portion of the temporal bone, it is composed of bony tubes and chambers called the bony labyrinth. Within this labyrinth a system of membranous tubes and chambers are

located called the membranous labyrinth. The membranous labyrinth, composed of the cochlea, three semicircular ducts, and two large otolithic chambers known as the utricle

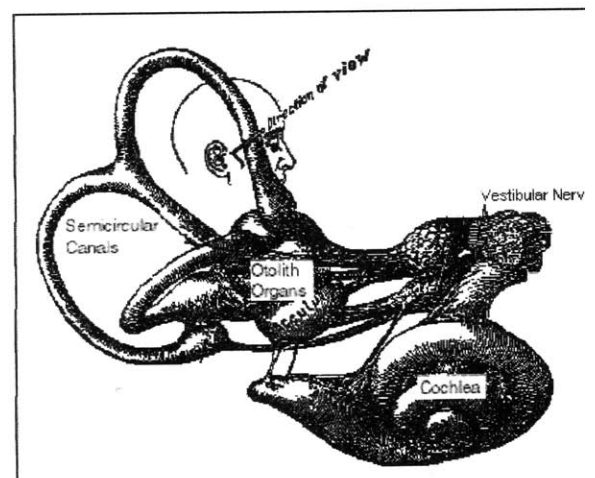


Figure 3 – Anatomy of the Inner Ear.

and saccule, is the functional portion of the apparatus (Figure 3). The cochlea is the sensory organ for hearing and has nothing to do with equilibrium. However, the utricle, saccule, and semicircular ducts are integral parts of the equilibrium mechanism (Wilson and Jones, 1979).

2.2.1 The Maculae – Detection of Head Orientation with Respect to Gravity

A sensory area, called the macula, is located on the inside surface of each utricle and saccule. The macula on the inferior surface of the utricle lies primarily in the horizontal plane for the head in an upright position (around 30 degrees pitch up with respect to earth horizontal in the upright position) and plays a key role in determining the orientation of the head with respect to the direction of gravitational force when a person is upright. The macula of the saccule is located primarily in a vertical plane, thereby serving as an important equilibrium mechanism when one is lying down (Guyton & Hall, 1996), although saccular activation can occur in all planes.

A gelatinous layer, embedded with many small calcium carbonate crystals called statoconia, cover each macula (Carlstrom, Engstrom, and Hjorth, 1953). Thousands of hair cells project cilia into the gelatinous area of each macula. These hair cells synapse with sensory endings of the vestibular nerve. The specific gravity of the statoconia is two to three times as great as the specific gravity of the surrounding fluid and tissues. In the presence of linear acceleration or gravitational forces, these statoconia will bend hair cells in the direction of the force (Gray, 1970).

2.2.2 Directional Sensitivity of the Hair Cells

Each hair cell contains 50 – 70 small cilia called stereocilia, and one large cilium called the kinocilium (Guyton and Hall, 1996). The cilia progressively decrease in length from the kinocilium side of the hair cell to the opposite side of the hair cell. The tip of each stereocilium is connected to the next longer stereocilium via a minute filamentous attachment. When the cilia bend in the direction of the kinocilium, these attachments tug one after another on the stereocilia pulling them in the outward direction (toward the kinocilium) of the cell body. This opens many small channels in the cilium membrane, allowing large quantities of positive ions to pour in from the surrounding endolymphatic fluid and cause depolarization. Hyperpolarization is caused when the cilia are bent in the opposite direction, closing many of these ion channels.

Under resting conditions, nerve fibers leading from these hair cells have continuous firing rates of around 100 impulses per second. When cilia are bent toward the kinocilium, this firing rate can increase to 300 – 400 impulses per second (Wilson and Jones, 1979). Bending of the cilia in the opposite direction will decrease the firing rate and may even silence the cell. As the spatial orientation of the head changes, the statoconia bend cilia in the direction of the gravitational or linear acceleration force.

Hair cells of the maculae are oriented in different directions such that some respond to tilt-forward, some to tilt-backward, and others to tilt-sideways stimulation (Goldberg and Fernandez, 1971). A different excitation pattern arises for each position of the head, and it is this pattern that appraises the brain of the head's orientation. The maculae of the utricles and saccules are optimized for detecting linear acceleration changes when the

head is in an upright position. A person can detect as little as a half-degree of malequilibrium when the body leans from the precise upright orientation. However, as the body is tilted further and further from upright, determination of head orientation by the vestibular sense becomes degraded (Guyton and Hall, 1996).

2.2.3 Semicircular Canals

The anterior, posterior, and lateral (horizontal) semicircular ducts are arranged roughly orthogonal to one another and represent all three planes of rotation in space. When standing upright, the lateral canals are tilted

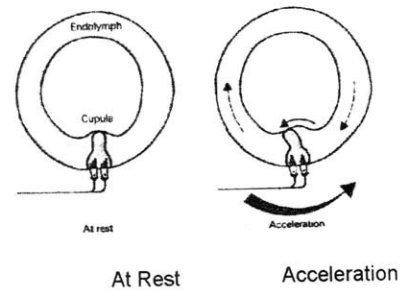
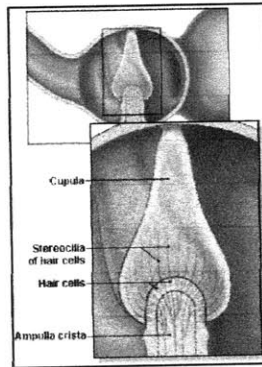


Figure 4: Detail of semicircular canal ampulla and rotational dynamics

approximately 30 degrees upward from earth horizontal. Each canal is filled with a viscous fluid called endolymph, and contains an enlargement at one of its ends called the ampulla. Fluid flow from the ducts into the ampulla excites a small crest-shaped organ within the ampulla called the crista ampullaris (Wilson and Jones, 1979). A cupula, comprised of a gelatinous mass, is located on top of each crista and projects into the ampullary space (Figure 4).

As the head rotates in space, the semicircular canals rotate with it. However, the fluid initially remains stationary due to its inertia. This relative fluid flow within the ampulla causes deflection of the cupula. Rotation of the head in one direction will cause the cupula to be bent in one direction; while opposite rotation will cause an opposite cupular deflection.

Projecting into the cupula are hundreds of cilia arising from hair cells located in the ampullary crest. All the kinocilia of these hair cells are located along one wall of the cupula. Deflection of the cupula in that direction causes depolarization, whereas deflection in the opposite direction causes hyperpolarization of the hair cells. These signals are transmitted along the vestibular nerve and apprise the brain of changes in the rate and direction of rotation of the head in the three spatial planes.

As with the hair cells of the otolith organs, semicircular canal hair cells have a tonic discharge of around 100 spikes per second (Goldberg & Fernandez, 1971). When rotation in the ipsilateral direction begins, this rate of discharge increases greatly. Under constant rotation, the excess discharge of the hair cell decays exponentially back to the resting level with a time constant of about 5 - 7 seconds in monkeys and about 7 – 10 seconds in humans. When rotation is brought to a sudden stop, the exact opposite effects occur. The cupula gets deflected in the opposite direction and hyperpolarization of the hair cell takes place. The tonic discharge rate is again attained exponentially after a period of about 30 seconds. The sensitivity of the canals to angular accelerations is on the order of 1 deg/s^2 (Wilson and Jones, 1979).

2.3 Vestibular Ocular Reflex (VOR)

Clear vision is possible only if the eye is stationary (fixed) with respect to a viewed object. The vestibulo-ocular reflex (VOR) is an important mechanism by which focused vision is made possible during head movements that are generated during everyday activities such as walking and running. For example, if the head is turned to the left, this

reflex causes the eye to move to the right (i.e. in the opposite direction of the head movement). The oppositely directed eye movement occurs at the same velocity as the head movement in light conditions, and therefore generates an eye movement which tends to keep one's line of sight fixed on the same point in visual space both during and following the movement. In darkness the gain can vary, with an average gain of about 0.7 for humans.

The VOR is a very simple central reflex. The sensory input is head velocity and the motor output is eye velocity. The head velocity signal is transmitted from the semicircular canals to the vestibular nucleus via primary vestibular afferent fibers in the eighth cranial nerve. Second order vestibular nuclei project to the appropriate pools of extraocular muscle motoneurons. This short neuronal pathway allows for very fast response times. A head movement can be detected and cause an appropriate change in eye velocity to occur in around 16 milliseconds.

2.4 Nystagmus

During short head movements, these compensatory eye movements remain well within the mechanical limits of eye rotation. However, during large amplitude head rotation, the eye can reach its effective limit of excursion long before the head movement is completed. Consequently, during this condition, an additional feature is added to the VOR: when the eye reaches an extreme position, it is rapidly flicked back to a new starting position. From this new starting position, the eye then continues a new cycle of compensatory movement. The resulting saw tooth pattern, Figure 5, of slow

compensatory/rapid resetting eye movements (slow phases and quick phases respectively) is referred to as vestibular nystagmus.

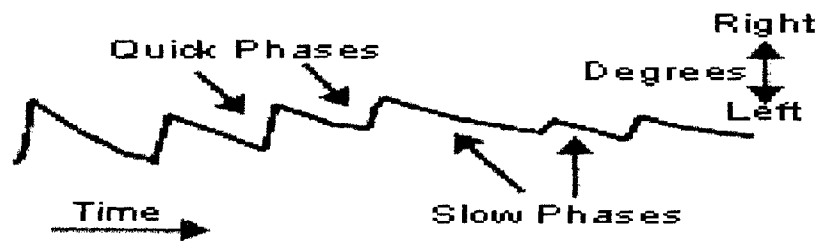


Figure 5: Illustration of slow and fast phase nystagmus.

Fortunately for vestibular researchers, nystagmus offers a fairly accurate insight into the dynamic state of the semicircular canals. By tracking eyeball motion with a mechanism such as the ISCAN eye imaging system, investigators can obtain a totally non-invasive measure of vestibular function.

2.5 Vestibular Physiology: An Engineering Approach

A great deal of modeling work has been done on the function of the vestibular system. A systems approach to physiology often provides insight not otherwise accessible. This section provides a brief review of current models of the semicircular canals, otolith organs, vestibulo-ocular reflex, and velocity storage mechanisms. Because of its importance to this study, the gravito-inertial force (GIF) conflict resolution theory is also introduced in this section.

2.5.1 Torsion Pendulum Model of the Semicircular Canals

Ernst Mach was one of the first experimenters to attempt to model the basic hydrodynamics of the canals (Mach, 1886; Mach, 2001). The problem essentially reduces

to one of second order fluid dynamics, as demonstrated in the Torsion-Pendulum Model first proposed by Steinhausen in 1931(Figure 6). This model indicates that the semicircular canals act as very fast integrating angular accelerometers. Much of the development and equations used in this and the next section are adapted from V. Wilson and G. Jones' book entitled "Mammalian Vestibular Physiology."

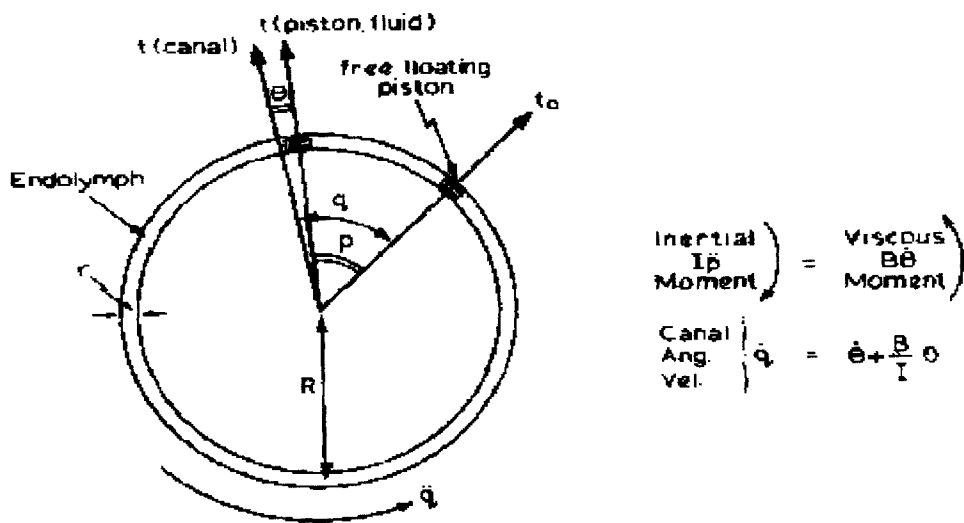


Figure 6: Simplified circular canal without cupula, illustrating the fundamental integrating function of canal hydrodynamics. V. Wilson and G. Jones (1979) p.44.

The thin circular tube of Figure 6 contains endolymph fluid of density, ρ , and viscosity, η , and has a radius of curvature R and internal radius of the tube r . After counterclockwise rotation of the whole system with an angular acceleration, \ddot{q} , for t seconds, the solid tube has turned through an angle q . Because of its mass dependent inertia, the fluid tends to lag the tube so that a free floating (frictionless) piston would have moved through a smaller angle (p) than the tube itself (q). The angular acceleration

of the fluid relative to space is therefore given by \ddot{p} , and hence a clockwise moment is generated due to the inertial forces acting on the fluid, given by the expression $I \ddot{p}$, where I is the moment of inertia of the fluid in the circular tube.

This moment leads to the generation of relative fluid flow in the tube and hence to an opposing moment due to viscous forces. This moment due to viscous forces must be strictly proportional to the rate of relative flow, expressed as $\dot{\theta}$, where θ denotes the relative angular displacement of fluid around the canal. The net moments in opposite directions must equal one another, so that

$$I \ddot{p} = B \dot{\theta}$$

where B is the moment of viscous friction per relative angular velocity of fluid flow around the canal. But since $p = q - \theta$, and assuming linearity, then

$$\ddot{p} = \ddot{q} - \ddot{\theta}$$

and hence, substituting for \ddot{p} ,

$$I(\ddot{q} - \ddot{\theta}) = B \dot{\theta}$$

Rearranging and integrating with respect to time and assuming zero initial conditions,

$$\dot{q} = \dot{\theta} + \frac{B}{I} \theta$$

We can define $T_1 = I/B$, as the time constant for the exponential function. The value of I/B has been found experimentally to be about 0.003 seconds. This very small value indicates that the integrating hydrodynamic response would be so rapid compared to the usual durations of head movements that the angular dependent velocity response could for practical purposes be considered instantaneous.

The model in Figure 7 does not account for the existence of the cupula. This can be modeled by adding a linear spring component, always tending to force the piston back to a zero position in the canal, with a force proportional to its displacement from that position. This new force turns the first-order equation of the simple torus into the following second-order equation by adding the term, $K\theta$, so that

$$I\ddot{\theta} = B\dot{\theta} + K\theta$$

where K is the spring restoring force per unit angular displacement of fluid around the circuit. As before, since $p = (q - \theta)$

$$\ddot{q} = \ddot{\theta} + \frac{B}{I}\dot{\theta} + \frac{K}{I}\theta$$

Moving from the conventional time domain to the Laplace frequency domain,

$$\ddot{q}(s) = \theta(s)(s^2 + \frac{B}{I}s + \frac{K}{I})$$

After rearranging, factoring, and noting that $\dot{q} s = \ddot{q}$, the transfer function becomes,

$$\frac{\theta}{\dot{q}}(s) = \frac{I}{K} \cdot \frac{s}{[(I/B)s+1][(B/K)s+1]}$$

This indicates that the system's response is characterized by two time constants, $T_1 = I/B$, and $T_2 = B/K$. An important step forward was made when van Egmond, et al (1949) showed experimentally that the value of T_2 is much larger than the "short" time constant. The value of T_2 for humans has been established experimentally to be on the order of 5-7 seconds. The dynamic response of this system is depicted in bode plot of Figure 7.

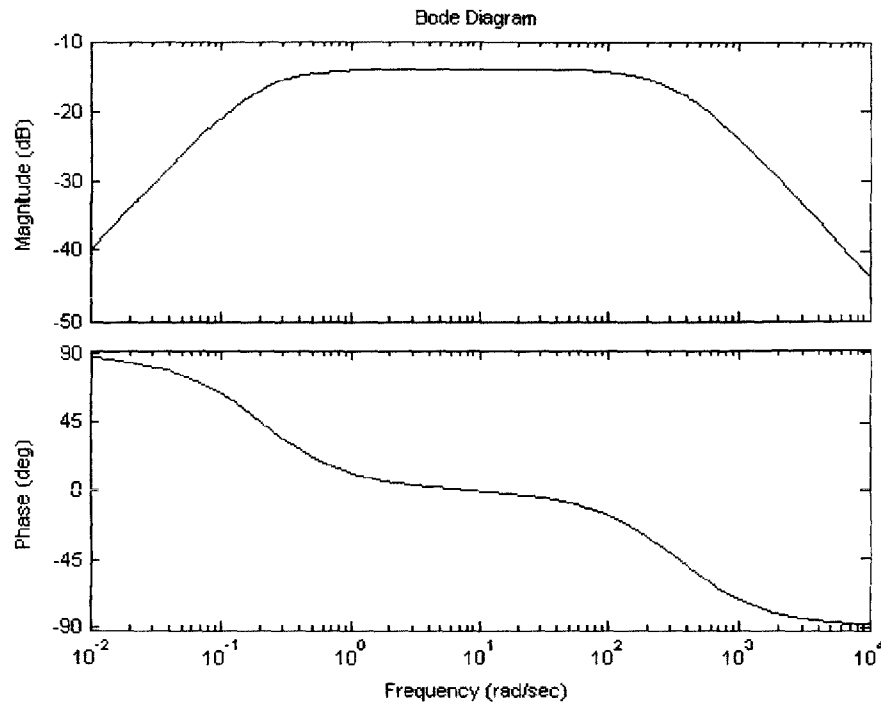


Figure 7: Bode plot for the Torsion-Pendulum model of the semicircular canals.

2.5.2 Modeling the Otolith Organs

A simplified functional arrangement of the otolith organ is diagrammed in Figure 9.

Linear acceleration of the whole system to the right (\ddot{x}) causes the otoconial mass to be left behind due to its inertia, thereby bending the cilia of the sensory hair cells to the left.

Since the otoconial mass gets left behind, its actual acceleration relative to space (\ddot{y}) will be less than that of the whole system.

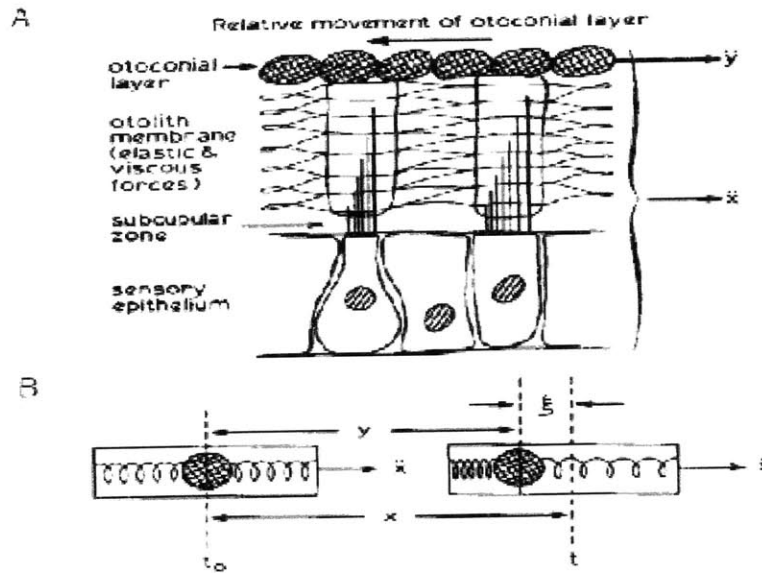


Figure 8: A: Mechanical linkage between the macula and overlying structures. B: Mechanical analogy. \dot{x} , Linear acceleration of head relative to space; \dot{y} , acceleration of otoconia relative to space; ξ , relative displacement of otoconia and macula; t_0 , position of end organ at commencement of acceleration; t , position after time t . V. Wilson and G. Jones (1979) p.71.

Figure 8B represents a mechanical model of this system. In this idealized system a body of mass M and density ρ_m is centralized between springs in a cylindrical tube of larger internal diameter than the body and containing endolymph of density ρ_e . Analogous with the canals, linear acceleration sets up a system of forces such that the sum of the leftward-acting forces equates to the sum of those acting to the right.

Acting to the left is the inertial force, $M \dot{y}$, where \dot{y} the acceleration of the body's mass, M , relative to inertial space. The resulting displacement of this mass relative to the tube ($\xi = x - y$) will generate opposing viscous ($B \dot{\xi}$) and spring ($K \xi$) forces acting to the right. In this case, however, since the otoconial mass is immersed in endolymph fluid of density ρ_e , any acceleration will also generate a buoyancy force acting in the direction of

imposed acceleration and equal to $(\rho_e/\rho_m)M\ddot{x}$, where ρ_m is the density of the otoconial mass. Equating the specific force acting to the left and the sum of all other forces acting to the right:

$$M\ddot{y} = \frac{\rho_e}{\rho_m}M\ddot{x} + B'\dot{\xi} + K'\xi$$

or since $y = (x - \xi)$,

$$(1 - \frac{\rho_e}{\rho_m})\ddot{x} = \ddot{\xi} + \frac{B'}{m}\dot{\xi} + \frac{K'}{m}\xi$$

Although very similar to the canal equation, an important difference is seen in the term $(1 - \rho_e/\rho_m)$, which would become zero if the density of the endolymph and the otoconia were identical. Numerically $\rho_e = 1.01$ (Money et al., 1971) and $\rho_m = 2.71$ (Carlstrom et al., 1953) so that a significant mechanical response is obtained. The corresponding Laplace transfer function is given by:

$$\begin{aligned} \frac{\xi}{\ddot{x}}(s) &= (1 - \frac{\rho_e}{\rho_m}) \cdot \frac{1}{s^2 + (B'/m)s + K'/m} \\ &= (1 - \frac{\rho_e}{\rho_m}) \cdot \frac{m/K'}{(T_1s + 1)(T_2s + 1)} \end{aligned}$$

where $T_1T_2 = m/K'$ and $T_1 + T_2 = B'/K'$.

2.5.3 Modeling the Vestibulo-Ocular Reflex

A model of the ideal VOR would be a simple gain term of -1. Estimated angular velocity is the input to the system and eye movements are made in the opposite direction to compensate for the perceived motion of the head. While it makes sense for the eyes to attempt to compensate directly for the perceived motion of the head, it should be recognized that this system is imperfect. To be truly accurate, an additional term which

reflects the latency of the neural processing, three-neuron reflex arc, and longer, adaptive cerebellum pathway should be incorporated. Physiological studies have estimated this time constant to be very short, on the order of 10 msec (Draper, 1998). The gain of the VOR is also not equal to -1, but can vary as a function of a number of things including the frequency of head angular velocity and distance to visual target. Natural head movements occur in the range of 0.5 to 5 Hz, with the higher frequencies occurring in the pitch plane. Paige (1983) found that in squirrel monkeys the gain of the VOR remains fairly flat over this entire frequency bandwidth at 0.86 ± 0.03 . However, below about 0.1 Hz a significant phase lead was observed approaching about 40 degrees at a frequency 0.01 Hz, consistent with a first-order, high-pass time constant of about 19 seconds. A model of these VOR characteristics developed by Paige (1983) and patterned after the Robinson (1977) model is depicted in Figure 9.

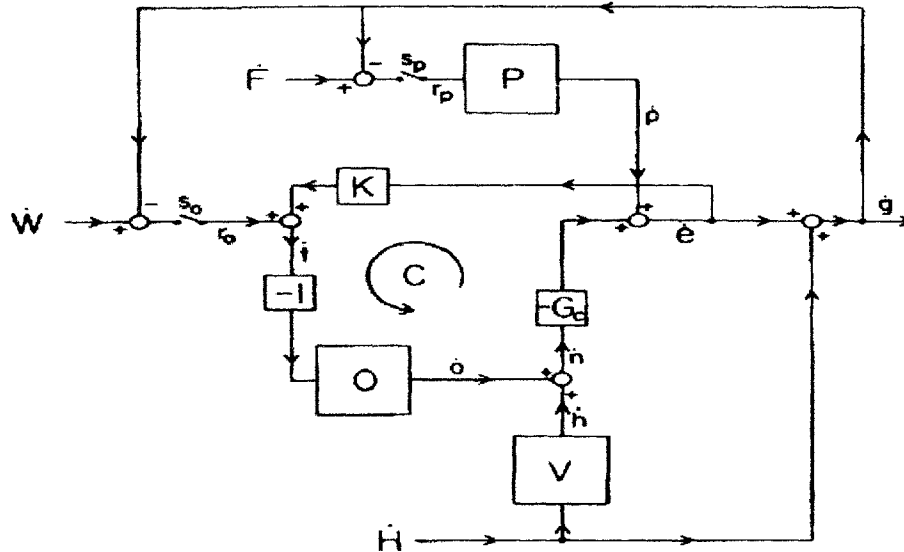


FIG. 8. Schematic model of the VOR and its interactions with visual following mechanisms. Slow-phase eye velocity in the head (\dot{e}) is influenced by three rate inputs—the velocities of the head (\dot{H}), the peripheral visual world (\dot{W}), and the foveal target (\dot{F}). The sum of \dot{e} and \dot{H} yields gaze velocity (\dot{g}), the rate of eye movement in space. Each input is processed by its own dynamic element. Head velocity (\dot{H}) is detected by the semicircular canals and processed according to the dynamic element (V), resulting in an internal estimate of head velocity (\dot{h}). The difference between foveal target (\dot{F}) and gaze (\dot{g}) velocities provides foveal image slip (r_p), which is processed by the dynamic element (P), resulting in the pursuit system's estimate of foveal slip (\dot{p}). The difference between peripheral world (\dot{W}) and gaze (\dot{g}) velocities gives peripheral-field retinal slip (r_o), which is processed through the dynamic element (O). Switches S_p and S_o are open when no contrast exists in the fovea (for S_p) or in the peripheral field (for S_o). G_o is a static gain element shared by the vestibular and peripheral field inputs. The positive feedback loop (C) operates on SPEV (\dot{e}) with a static gain element, K . The three dynamic elements, V , P , and O , are governed by the following transfer functions: $H_v(s) = (G_v(sT_v)(sT_a + 1))/(sT_v + 1)(sT_a + 1)$, where $G_v = 0.85$, $T_v = 5.7$ s, and $T_a = 80$ s; $H_p(s) = (G_p e^{-sT_d})/(sT_p + 1)$, where $G_p = 2.7$, $T_p = 0.2$ s, and $T_d = 0.01$ s; and $H_o(s) = G_o/(sT_o + 1)$, where $G_o = 1$ and $T_o = 5.2$ s and static gain elements, K and G_c , = 0.8 and 1.0, respectively.

Figure 9: Model of the VOR. Source: Paige, 1983.

2.5.4 Modeling Velocity Storage

When one is rotated with constant velocity in darkness, the slow phase velocity of per-rotational horizontal nystagmus decays with a time constant of around 20 seconds.

Vertical nystagmus decay rates are about one-half the value of horizontal decay (Young, 1983). However, as shown above, the best current estimates of the time constant of the first-order canal afferents is about 5 seconds, as measured in monkeys. Therefore, some neural mechanism must be responsible for preserving and extending the canal time constant to enable a better match to head velocity for a longer period of time. This mechanism has been referred to by several researchers as velocity storage (Raphan,

Cohen, and Matsuo, 1977); because it retains the initial rotation velocity of the head even after the canal response has dissipated (Furman & Schor, 1997).

Mathematically this can be modeled as an integrator with a gain term within a feedback loop. Some debate over whether this loop is feed-back or feed-forward has ensued over the years (Raphan, Cohen, & Matsuo, 1977; Robinson, 1977). The Robinson model suggests that an efferent copy (Young, 1971) of the canal's sense of head rotation is fed back, whereas the Raphan model suggests a central feed-forward mechanism (Figure 10). Recent investigations seem to indicate that the Raphan model is a better fit with experimental evidence. The anatomical location of the velocity storage integrator has yet to be determined. Therefore, estimates for the gain and time constant of the integrator can only be based upon experimentally obtained data. An approximate value for the gain term is around 0.7 with an integrator time constant of about 7 seconds.

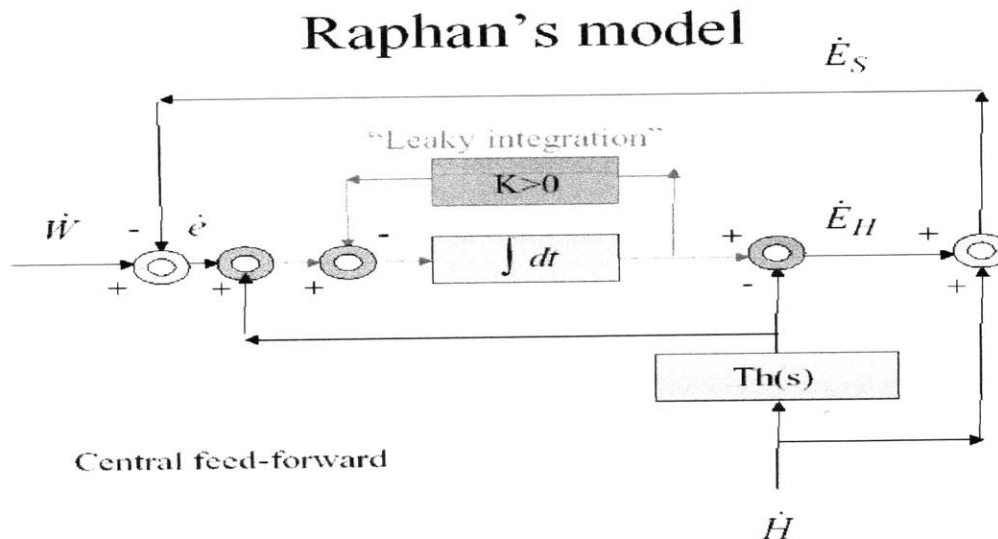


Figure 10: Raphan model of the velocity storage mechanism, where E_H is eye position in the head, E_S is eye position in space, H is head position in space, $Th(s)$ is semicircular canal dynamics, and W is the viewed image's position. All terms are first derivatives indicating velocity rather than position. Velocity storage mechanism is represented in a feedback loop by a gain term K , and integration term $\int dt$.

2.6 Stimulus Provided to the Vestibular System during SRC

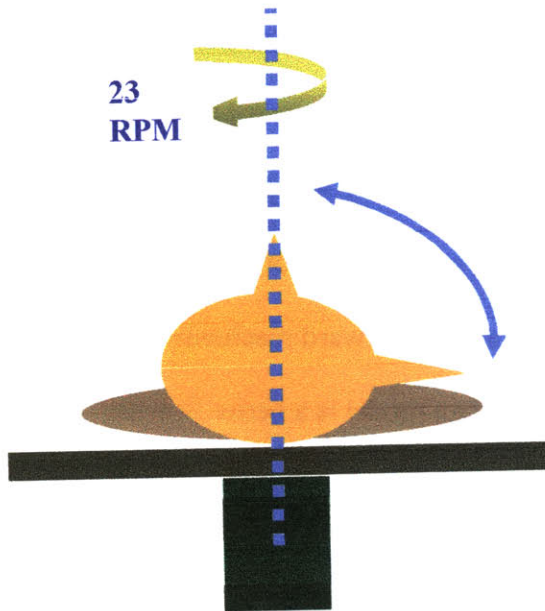


Figure 11: Experimental setup.

A number of complex stimuli can be imparted to the vestibular system by making head turns during SRC. This section only covers the unique stimulus presented to participants in this study. Namely, the result of making yaw head turns during on-axis, earth-horizontal, constant velocity, clockwise rotation aboard a 2-m centrifuge in complete darkness is explored (Figure 11). Two types of yaw head turns were

conducted; from right ear down (RED) to nose up (NU) and from NU to RED. All head turns were conducted in approximately 1 second.

The initial ramp up of the platform was conducted in a RED position. During this phase the utricles are maximally stimulated by a 1-g force in the -y-direction (the saccules have also been shown to contain some -y polarization vectors that would also be stimulated). See Figure 12 for head coordinate frame. The pitch plane of semicircular canal representation is in the plane of platform rotation. The cupulae of these canals deflect as soon as rotation begins. They continue deflecting until constant velocity rotation is attained. At

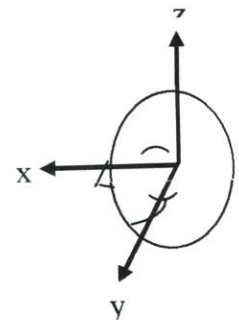


Figure 12: Right-hand coordinate frame

that instant the cupulae begin to move back toward the resting, or zero position. After about 5 seconds at constant rotation have elapsed, the cupulae have regained the datum position and afferent firing rates revert to resting levels. At the perceptual level this stimulation is experienced as a continuous pitching backward sensation until the 20 – 30 seconds at constant rotation have passed. At that time no rotary motion is sensed and participants feel as though they are stationary.

Several things happen as soon as a yaw head turn from RED to NU is executed on the rotating platform. The head turn itself results in the yaw canals being stimulated during the 1 second it takes to complete the head turn. Cupular deflection in the yaw canals will closely follow the angular velocity profile of the head turn. The pitch plane, previously in the plane of rotation, is now brought orthogonal to the plane of rotation. The inertia of the endolymph will cause a cupular deflection opposite to that of the ramp up phase. This deflection will again decay in about 5 seconds. The roll plane canals are simultaneously brought into the plane of rotation in the NU head position, resulting in a relative counterclockwise flow of the endolymph fluid within the canals equal to the magnitude of the centrifuge's angular acceleration (23 rpm). As far as it is known, roll canal dynamics mimic the dynamics of the pitch canal. Therefore, the cupulae of the roll canals will return to the zero position after 5 seconds have elapsed in this new head orientation. The otoliths, in turn, detect a change in the gravitational force vector from the -y direction to the -x-direction. Due to the anatomical orientation of the utricle, the magnitude of this force is diminished by a cosine term. Assuming an average utricle pitch angle of 30 degrees, the equivalent force directed along the -x-axis is $(1-g) \cdot \cos(30)$,

which equals 0.866-g. Perceptually this head movement should result in a sensation of one's body pitching backward accompanied by a clockwise rolling sensation.

In addition to the dominant canal response, a cross-coupled acceleration stimulus is provided to the canals during a head turn from RED to NU. Described previously by Lyne, this cross-coupled term arises as a result of making a head turn in a rotating environment. The cross product of the angular head velocity vector with the angular velocity vector of the centrifuge results in a vector torque which stimulates the pitch canals during the time it takes to complete the head turn.

A similar stimulus is provided to the vestibular system during head turns from NU to RED, with the exception that everything is reversed. The otoliths are stimulated maximally in the -y-direction at the end of the head movement. The cross-coupled term in this instance impacts the roll canals. The yaw canals indicate a head turn in the opposite direction. The pitch canals are again brought into the plane of rotation, while the roll canals are simultaneously removed from the plane of rotation. The resultant perceptual experience is one of a body pitch backward along with a roll in a counterclockwise direction.

2.7 Physical Responses to SRC Stimulus

The stimulation supplied to the vestibular system by SRC elicits a response from many of the body's physical and psychophysical systems. For everyday head turns the VOR serves a compensatory function. Head turns in the rotating environment result in semicircular canal stimulation indicating body rotations that are not expected in the rotating reference frame. This manifests itself in non-compensatory or inappropriate eye

reflex components. It also results in sensations of illusory self-motion and disorientation. Taken together these reactions can lead to symptoms of motion sickness including episodes of nausea, stomach awareness, cold sweats, salivation, and vomiting.

2.8 GIF Conflict Resolution Theory

Recent work involving the interaction of semicircular canal and otolith sensor dynamics has focused on how the vestibular system interprets the gravito-inertial force (GIF) as measured by the otoliths, i.e. how does the brain distinguish between linear accelerations and gravitational acceleration (Merfeld, Zupan, Peterka, 1999). According to Einstein's equivalence principle all linear accelerometers must measure both linear acceleration and gravity. Merfeld, et al, hypothesizes that the brain uses an internal model to aid in making this distinction. For example, a head tilt can be discriminated from a head translation if the central nervous system (CNS) simultaneously receives signals from both the otolith organs and the semicircular canals. Conversely, if only an otolith signal is received and the canals signal no rotation, the brain will interpret this as a head translation.

For ordinary head movements, these two motion sensors act in a coordinated and symbiotic manner easily interpreted by higher orders of the CNS. However, during complex vestibular stimulation this system can be deceived. Experiments have shown that eye movements can be evoked which compensate for a component of estimated linear acceleration even when no actual linear acceleration exists (Merfeld, et al, 1999). This response is consistent with internal model predictions that the nervous system can develop a non-zero estimate of linear acceleration even when no true linear acceleration is present. In the present study, pitch plane stimulation in the absence of any true body

pitch conflicts with the static (no body movement) signal arriving from the otolith organs. How the brain deals with this conflict will become of primary interest to this investigation.

2.9 Modification of the Semicircular Response by the Utricular and Saccular Maculae

Several researchers have demonstrated that the position of the head with respect to gravity is capable of modifying the response to angular accelerations (Benson, 1974). Much of this research focuses on the change in the nystagmus response engendered by angular accelerations. Especially germane to this study is work conducted in 1966 (Benson and Bodin, 1966). In this experiment subjects were rotated about their z or longitudinal body axis. Once rotation stopped the head was moved through 90 degree increments to one of four different head positions with respect to gravity (Figure 13). The time rate of post-rotational nystagmus was then compared for each of these head orientations. If the head was left in an upright position (no post-rotatory movement of the head) the time constant of decay was between 15.6 and 17.5 seconds. This time constant decreased to 9.7 seconds for a supine position, and 8.9 seconds for the right side down position following rotation. Unfortunately the authors did not state whether the time constant difference for the supine versus the right side down positions were significant.

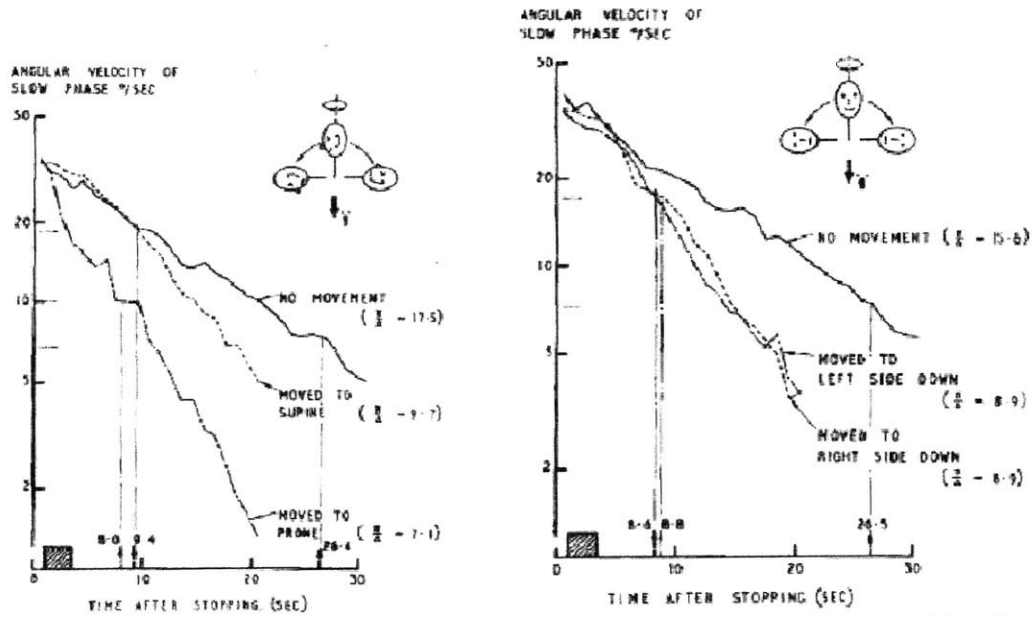


Figure 13: Effect of orientation to gravity on decay of nystagmus. Benson and Bodin (1966).

Some studies have shown that the magnitude of this suppression is related to the magnitude of linear acceleration detected by the utricle (Udo de Haes and Schöne, 1970). In this experiment subjects were rotated about a vertical axis with the head tilted forward by 30 degrees, i.e. utricles roughly orthogonal to the gravitation vector. Following rotation subjects were pitched backward through an angle ranging from 30 to 180 degrees. Maximum utricle stimulation occurred at an angle of 90 degrees, which corresponded with the largest reduction in the time rate of decay of nystagmus. However, at 180 degrees of tilt (no graviceptive stimulus) a reduction in the time constant was also observed.

The Benson study also examined how graviceptive information modified the subjective sensations of illusory motion induced by the stopping stimulus. The average times at which these sensations dissipated are marked by the vertical lines in Figure 13. It is

interesting that the subjective sensations decayed away much faster than the nystagmus, and roughly 70 percent faster than the sensations experienced when the head was left in an upright position. This same investigation found that the rate of decay of both the after-sensations and nystagmus were not reduced to the same extent for pitch and roll canal stimulation about an axis in which graviceptive content remained static as that found for yaw rotation.

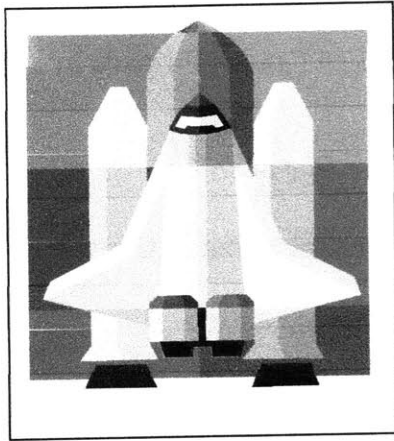
The method by which this shortening of decay rates occurs is less certain. One proposed theory is that otolith information is able to modify the adaptive time constant of the semicircular canals (Young and Oman, 1969). Another explanation is that the velocity storage mechanism of the vestibular system is modified by graviceptive inputs. Both theories work mathematically, however the manner and location of this coupling mechanism remains unclear. A recent off-vertical axis rotation (OVAR) investigation indicates that perhaps some otolith signals contain an estimate of velocity storage and others do not (Furman & Schor, 2001).

2.10 Context-Specific Adaptation

Recent work by Young, et al (2000) has demonstrated that the illusory sensations, inappropriate nystagmus, and overall motion sickness associated with head movements in a rotating environment attenuate during one hour of centrifugation, and further adapt during repeated exposures over multiple days. This adaptation appears to be context-specific as evidenced by the fact that compensation strategies employed during centrifugation are not transferred to the stationary environment. The exact nature of this context is not entirely known. Previous studies on MIT's centrifuge indicate that the

duration of illusory motion sensations induced by yaw head movements in the rotating environment depend, in part, on the head's position with respect to gravity (Aim 1, experiment 2 of the NSBRI Neurovestibular Aspects of Artificial Gravity Proposal by Young, et al, 2000).

Currently, it is unclear whether adaptation to head yaw movements on the SRC in the presence of a gravitational environment will generalize to a microgravitational environment. If the context-specific adaptation requires a gravity cue, it is unlikely to transfer to microgravity, as an external gravito-inertial reference force is unavailable. The absence of GIF in space may even lead to an erroneous updating of the internal estimator (Glasauer and Mittelstaedt, 1998). Therefore, an optimal earth-based adaptation strategy must consider any effects due to the orientation of gravity.



Chapter 3

Experimental Methods

3.1 Experimental Design

This experiment was designed to enable a unique identification of the factor responsible for the asymmetric response observed in a previous study on MIT's short-radius centrifuge between head turns ending in the nose up (NU) position versus those ending in the right ear down (RED) position. Specifically, why do yaw head turns toward NU lead to longer and stronger sensations of illusory motion? Several cogent hypotheses exist for this phenomenon, thereby requiring many separate controls in the design of this investigation.

The first possibility is that the relationship of the head with respect to one's trunk is specifying the differing response. To test the validity of this hypothesis subjects made identical yaw head turns both while lying supine and on their side. Provided the same decay of conflicting sensation phenomena observed by Hecht, et al (2001) can be reproduced here, we could say with some confidence that if the NU response in the supine condition is similar to the RED response in the lying on the side condition (also

the RED response in the supine condition similar to the NU response in the lying on side condition) that some sort of head-to-trunk sensor is modifying the overall response of head movements in the yaw plane. If the converse is true, then the role that these receptors play is essentially a marginal one at best.

Another plausible explanation is that the trajectory of the head turns may differ when going from right ear down to nose up than from going nose up to right ear down. A third explanation is that the absolute angle that the head moves through varies for RED versus NU turns. Along these same lines, the velocity profile may differ for each respective head turn. The musculature of the neck may be such that turns in one direction are easier and made quicker than turns in another direction.

To avert the above possibilities, a special head restraint device was designed and built for use in this study (Figure 16). The trajectory of head turns were controlled by restricting movement solely to the yaw rotation plane. The absolute angle of each turn was prescribed by metal stops that could be placed at ten degree increments between 0 degrees (NU) to 90 degrees (RED). The absolute angle was adjusted for each subject based upon the maximum number of degrees he/she could comfortably turn in both the supine and lying on the side conditions. The limiting case in the supine condition was head turns to RED, whereas NU head turns were more limited in the lying on the side condition. The relatively smooth rotational action of the restraint, provided for by ball bearings, made it easier to control the velocity profiles of each head turn. In addition, subjects were trained to make each turn in approximately one second. A simple roll

potentiometer was also attached to this device, which allowed for post-experiment computation of head velocity profiles as well as the total angle of each head turn.

The location of the head with respect to gravity provides the last probable explanation for the observed asymmetry between head turns toward NU versus RED. This possibility is difficult to test directly in a noninvasive manner. Therefore, the experiment was designed using a process of elimination scheme. If the asymmetry cannot be attributed to either main or cross effects of the other possible explanations, then it must be due to x versus y-direction otolith stimulation. Differing otolith gains or differing otolith-canal interactions for the x versus y-direction should appear in the eye data. This could take the form of differing amplitudes and/or decay time constants in the slow phase eye velocity for each type of head turn. If no effects are observed in the eye data, then the asymmetry is most likely due to higher central nervous system processing of the combined otolith-canal signals.

Habituation and adaptation to the rotational stimulus were not goals of this study and pains were taken to try to minimize their effect. The experiment was separated into four sections, each containing 14 head turns, with rest periods allotted between each section. In order to reduce habituation effects, head turns were performed in an alternating fashion with NU turns followed by RED turns. Two of the sections involved head turns while lying supine, and the other two sections involved head turns made while lying on one's side. In an attempt to offset the effects of habituation, these sections were ordered in such a manner that each head turn was made at the same time chronologically in the

experiment. A counterbalancing scheme was employed, whereby one half of all subjects started making head turns in the supine body position, followed by two sections of head turns in the lateral body position, and concluded with one last section of head turns in the supine body position. The other half of the subjects started with a section of head turns in the lateral body position, followed by two sections in the supine body position, and concluded with a section of head turns in the lateral body position.

Several dependent measures were taken to assess the perceived and physiological differences between NU and RED head turns. For the benefit of comparison, many of these measures needed to be consistent with prior MIT studies. For each head turn, a verbal, quantitative assessment of the perceived strength of illusory motion was recorded, as well as an estimation of the duration of these sensations. The magnitude and time rate of decay of the inappropriate, non-compensatory vertical nystagmus was also collected for each head turn. Additional dependent measures included verbal reporting of motion sickness levels, velocity and angle of each head turn, and subjective reporting of the direction of illusory motion. For 5 of the 18 subjects a subjective estimation of the visual vertical was also obtained through manipulation of a luminous line in a stationary, dark environment.

3.2 Subjects

Experimental participants were selected from within the MIT student community and were recruited via an IRB approved poster. All subjects were screened for vestibular defects through questioning and successful completion of a Romberg test. Volunteers were asked to abstain from any drugs such as alcohol, nicotine, and caffeine (including

chocolate) for at least 24 hours prior to the experiment. Subjects with heart conditions, extreme susceptibility to motion sickness, episodes of vertigo, oculomotor abnormalities, and other health concerns were excluded from the experiment. (For a complete list of medical disqualifications please refer to Appendix B).

Seventeen healthy human subjects (12 males, 5 females), ranging in age from 17 to 33 years (21.3 ± 4.9) took part in this study. The average height and weight were 171.3 ± 9.8 cm and 68.0 ± 9.2 kg, respectively. All participants were right handed, fifteen subjects were right-eye dominant and 3 subjects were left-eye dominant. Subjects were of diverse ethnicity including 9 Caucasians, 3 Hispanic-Americans, 3 Asian-Americans, 2 African-Americans, and 1 German participant.

All subjects also met the following criteria:

- Aged between 17-35 years old
- Height between 5'0" and 6'2" (152.4 cm and 188 cm)
- Weight no more than 200 lbs (90 kg)
- Some form of exercise ≥ 1 hour per day, 3 days per week
- Ability to clearly communicate experiences upon the centrifuge and understand experimental requirements
- Ability to read, comprehend, and sign the experimental consent form (see Appendix)

3.3 Equipment

The equipment used in this investigation consisted of the following: Massachusetts Institute of Technology's short-radius centrifuge, an ISCAN infrared video imaging system, a centrifuge-mounted head restraint device, a controllable one degree of freedom luminous line, and a sensation duration button.

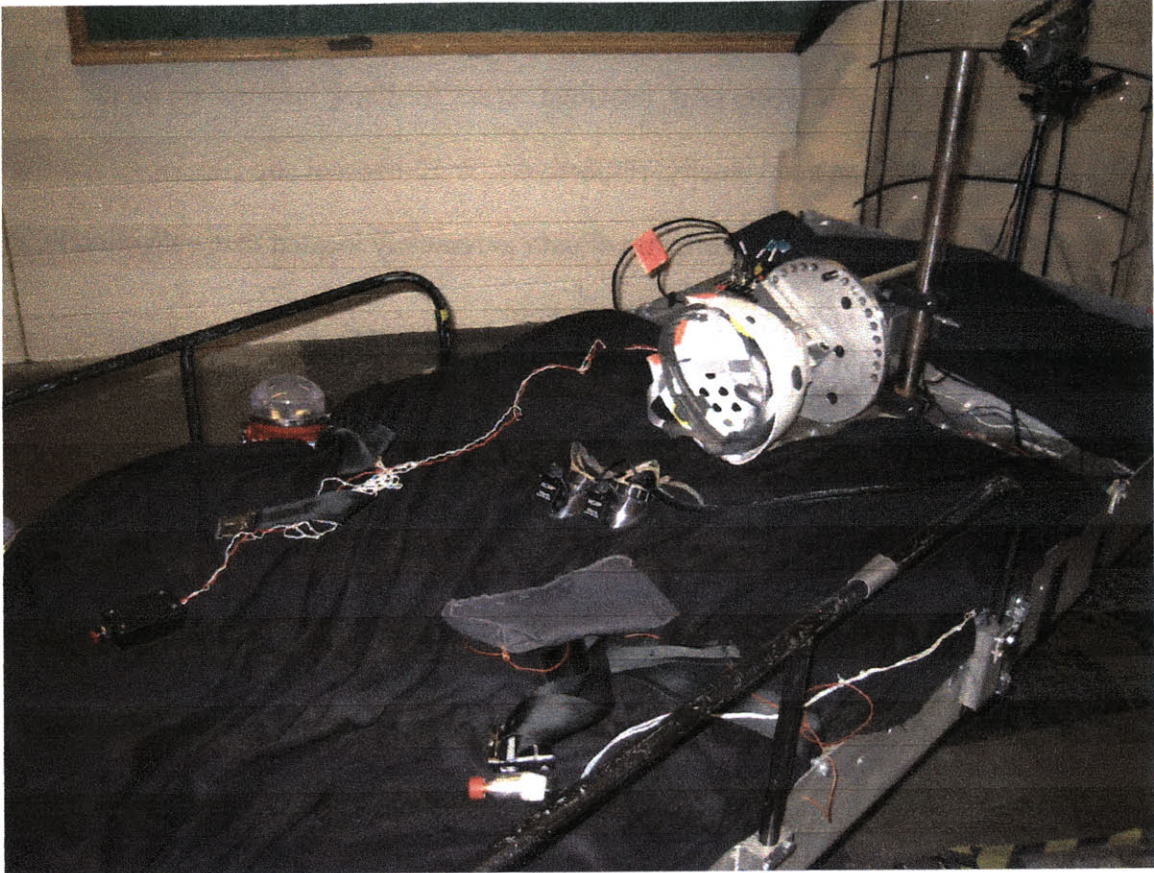


Figure 14: Short Radius Centrifuge and experimental equipment.

3.3.1 Short-Radius Centrifuge

MIT's short-radius centrifuge was first designed and constructed by Peter Diamandis in 1988. It consists of a two-meter rotating platform with adjustable foot plate such that a subject's head may be placed at the axis of rotation. The centrifuge is powered by a 1 hp Olstead Flint electric motor through a 50:1 gear reduction. A Focus 2 DC Drive motor controller used in conjunction with a LabView/ PID Control Toolset program allowed for controlled velocity profiles in both steady state and transient operation (Cheung, 2000).

An Analog Devices ADXL105 accelerometer mounted to the underside of the bed at 1.67

m from the center of rotation, and a Hewlett Packard optical encoding tachometer (256CPR) mounted to the worm gear, provided sensor feedback information on the state of the bed's acceleration and velocity, respectively. A 32-channel slip ring located at the shaft of the bed allowed for transmission of data to remotely located data collection PCs and video recording devices.

A Sony night vision camera was mounted at the head-end of the bed permitting the experimenter to observe subjects in the darkened room throughout the entire investigation. A 9-volt battery powered head restraint was also mounted at the head-end of the bed in such a manner that subjects inter-aural axis was centered directly above the centrifuge's axis of rotation. The ISCAN ocular imaging goggles powered by two onboard 12-volt/7-Ah rechargeable lead-acid batteries were also located at the head-end of the bed. A 9-volt battery powered sensation duration button was placed on the bed within arm's reach of each subject. The imaging goggles, head restraint, sensation duration button, and on-board video camera transmitted information through the slip ring. The centrifuge was also equipped with a few safety devices including a safety belt, side rails, and an emergency stop button that allows subjects to sever DC power to the bed. To counter moment arms created by subjects of varying masses, the platform has space allocated for the placement of lead weights at both the head and foot ends.

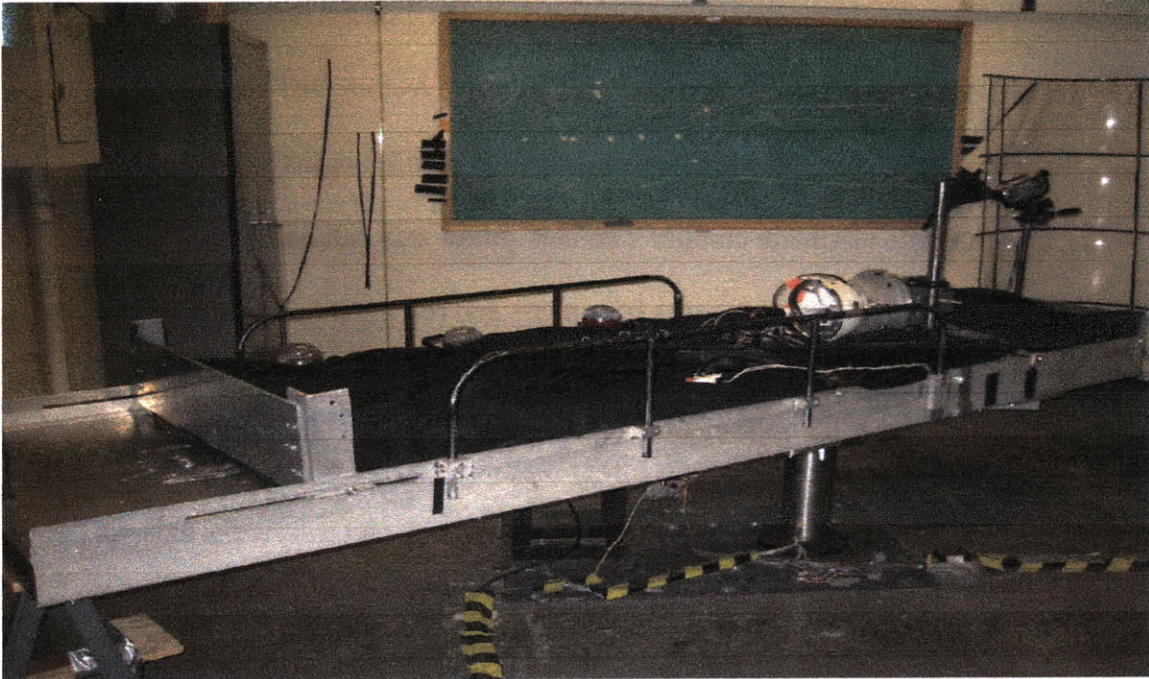


Figure 15: MIT's Short-radius Centrifuge.

A 300 MHz personal computer (AMD-K6 processor/Window's 95 OS/e-machine®) was used for ISCAN and duration button data collection. A 900 MHz personal computer (Pentium III processor/Windows 98 OS/Dell PC®) was used to control rotation of the centrifuge and for the collection of subjective data. Two video monitors were employed to view the ISCAN video images. A third monitor was used to enable observation of the subject throughout the experiment via the on-board night vision digital video camera. Two VCRs were used in the study. One was used to record the ISCAN images, and the other to record the on-board video images of each subject. A calibration stand, required for calibrating the ISCAN goggles, and device for easy attachment/detachment to the bed was also developed and utilized in this study. A hand-sewn, fabric goggle cover was also used to maintain a completely dark environment for each subject.

3.3.2 Head Restraint

As noted earlier, the unique demands of this experiment dictated that all head turns be controlled to the extent possible in terms of velocity, trajectory, and absolute angle without compromising subject comfort and safety. A device consisting of two steel shafts, an adjustable mountain climber's helmet, pillow box ball bearings, one round and one square aluminum plate, aluminum base plate, and roll potentiometer, was designed and constructed to this end.

The helmet was adjustable about a horizontal and vertical circumferential axis via two gear mechanisms located at the ears of the helmet. A chin strap was also provided, which, taken together, accommodated a wide range of head sizes. The helmet was mounted to an aluminum plate machined to match the contour of the top of the helmet. This plate, in turn, was attached to a horizontal steel shaft. This shaft, located slightly off center of the top of the helmet, was situated such that most subject's center of rotation about the z(longitudinal)-axis was in line with the shaft. This shaft was held in place through the use of two pillow box ball bearing mechanisms that restricted rotation to one plane, and was connected to a vertical steel rod via the square and round aluminum plates. The round plate had 19 separate holes drilled in it at ten degree increments ranging from 0 degrees (subject in the right ear down position) to 180 degrees (subject in the left ear down position). Two metal-stop pins could be placed in anyone of these holes, thereby restricting the absolute angle of rotation of the helmet via an additional pin affixed to the horizontal shaft.

This entire assembly could be translated vertically along the vertical steel rod to accommodate various head to platform distances. This feature became especially important because the difference in the distance from head to platform was significant between subjects lying in the supine body position versus the side body position. Given the honeycombed structure of the centrifuge platform, a large aluminum base plate was used in mounting the head restraint to the bed, distributing the torques produced by the weight of subjects' heads. A simple 1½ turn roll potentiometer was attached to the rear portion of the horizontal shaft. A 9-volt DC battery powered a 5-volt voltage regulator, whose potential difference was placed across the potentiometer. The resultant voltage signal was incorporated into the ISCAN software via a Kiethley A/D converter. The potentiometer signal facilitated post-experiment analysis of the velocity profiles for each head turn.

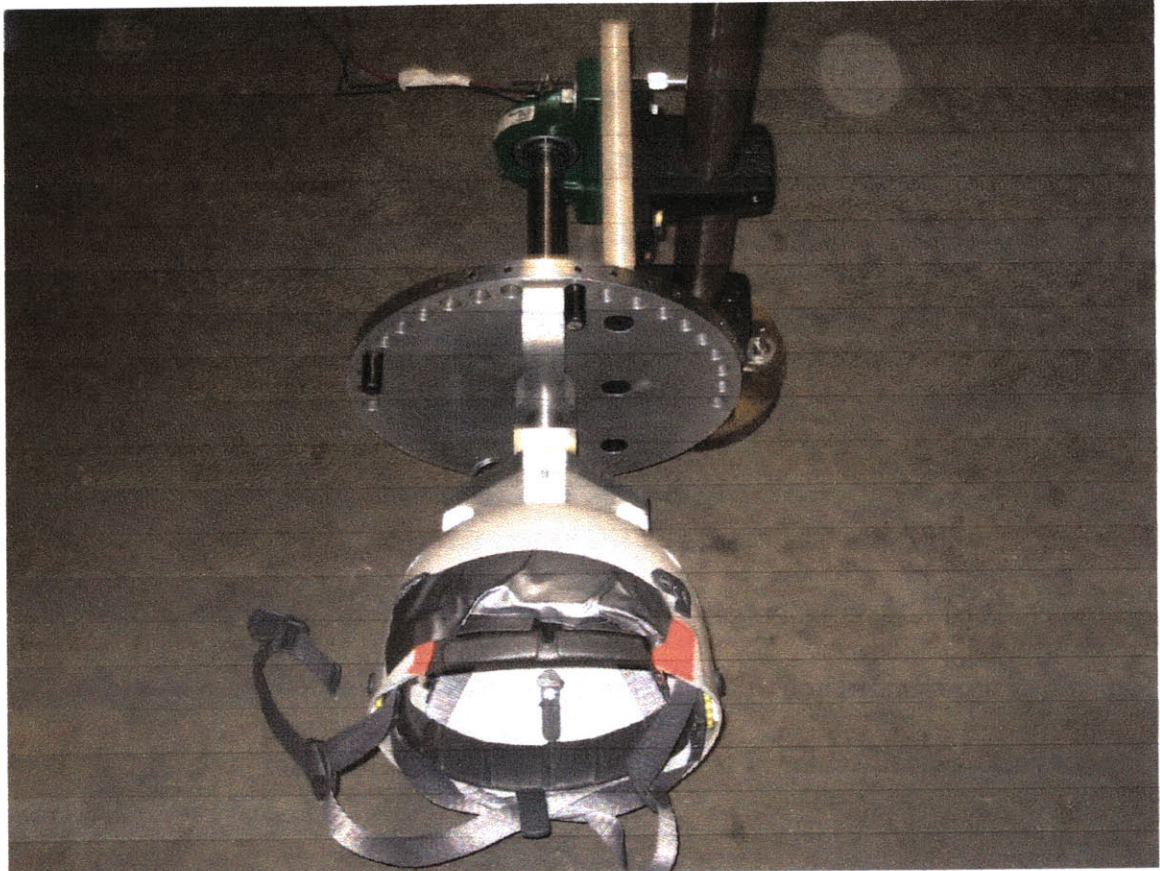


Figure 16: Head restraint device designed for this study.

3.3.3 ISCAN Video Eye Imaging Hardware and Software

An ISCAN eye imaging system (Model RK-716PCI) was used to acquire subject's pupil locations as a function of time throughout this experiment. The system's goggles are non-invasive, lightweight, and utilize infrared radiation to track the corneal reflection. Pupil location information is sampled at 60 Hz and software routines are employed to track the displacements of the reflection to within ± 0.3 degrees accuracy over a range of roughly 20 degrees in the vertical and horizontal directions. A more detailed description of the ISCAN system can be found in Sienko (2000).

3.3.4 Subjective Visual Vertical

With the help of Dylan Chavez (MIT undergraduate research opportunity program (UROP) participant in the Man-Vehicle Lab), a device was constructed to assess one's estimation of the gravitational vertical in the absence of visual orientation cues. This device consisted of a line illuminated by several red LEDs attached orthogonally to the shaft of a small, battery powered DC motor. Rotation of the luminous line could be controlled by either the experimenter or the subject. The angle of the line with respect to the gravitational vertical was determined via a roll potentiometer with a 5-volt potential drop across it. After the line was adjusted to the subject's perception of true vertical, the resultant voltage signal was measured by a digital multimeter. A calibration technique was employed that recorded the voltage level at both the Earth vertical and horizontal. A linear relationship existed for voltages between these two points, enabling accurate identification of any given angle.

3.3.5 Subjective Measures

A number of subjective measures were obtained throughout this study. These measures aided the experimenter in determining a participant's discomfort level, as well as magnitude, direction, and duration of illusory motion sensations. These measures included:

- Motion Sickness Score
- Verbal Accounts of Magnitude Estimation
- Verbal Accounts of Direction and Degrees
- Estimated Duration of Sensations

3.3.5.1 Motion Sickness Survey

Subjects were queried throughout the experiment to estimate their overall discomfort level on a scale from 0 to 20. A rating of 0 represented no discomfort or nausea symptoms and a rating of 20 represented emesis or vomiting. Motion sickness tends to have a cumulative effect, and people go from 0 to 10 much more slowly than from 10 to 20. Therefore, if at any point during the experiment a subject attained a rating of 12, they were instructed to tell this to the experimenter and to discontinue making head turns. Also, between the four separate sections of this experiment, all subjects were given a sufficient rest period to allow feelings of motion sickness to subside and ratings of 5 or below on this scale were attained.

3.3.5.2 Verbal Accounts of Magnitude Estimation

Head turns made while the bed is rotating often elicit novel sensations not encountered during stationary head turns. A scale was developed to help subjects describe how different this sensation is when compared to making everyday, normal head turns. The scale was anchored such that feelings experienced during the first head turn made in the rotating environment were assigned an arbitrary value of 10. After each subsequent head turn, subjects were asked for a subjective intensity of the illusory sensations experienced as compared with the sensations experienced during the first head turn. For instance, a turn with twice the intensity of the first one would be called a twenty, and a turn with half the intensity would be given a rating of five. If the turn felt identical to a turn made while not spinning on a centrifuge, it would have a subjective intensity of zero. It is important to note that this measure is not directly connected with perceived magnitudes and directions of illusory tilt sensations. For instance, on a given head turn a subject may feel strongly that he/she has pitched upwards by 90 degrees. On a subsequent head turn this

subject may feel as though he/she moved in the same direction with the same magnitude (90 degrees pitch upward in this example) but to a much weaker extent.

3.3.5.3 Verbal Accounts of Direction and Degrees

Subjects were asked periodically throughout the experiment to relate the direction and number of degrees of perceived motion they experienced. Three axis of rotation were defined with respect to the bed as follows:

- *Pitch* plane of rotation was defined as any motion occurring in a plane moving vertically off or into the bed. If a subject felt as though his/her head was moving into the bed it was termed a pitch downward and if the motion felt as though their head was moving vertically away from the bed it was termed a pitch downward.
- *Roll* plane of rotation was defined as any motion occurring within the plane of the bed's rotation. If a subject felt as though his/her feet were rotating toward the right it was termed a clockwise roll, and if the motion felt as though their feet were moving to the left it was termed a counterclockwise roll.
- *Yaw* plane of rotation was defined as any motion occurring in the plane in which the subject was making head turns (i.e. right ear down to nose up and nose up to right ear down). If a subject felt as though his/her right shoulder was rotating into the bed it was termed a yaw right, and if the motion felt as if their left shoulder was rotating into the bed it was termed a yaw left.

Since these planes were given in the rotating (platform) reference frame, they were used for both body conditions (supine and lateral) employed in this experiment. In addition to describing the plane of perceived motion subjects were also instructed to estimate the number of degrees through which they moved. For subjects who experienced tumbling sensations, they were asked to estimate the number of complete rotations experienced.

3.3.5.4 Estimated Duration of Sensations

A duration sensation button was built for this study by simply connecting an on/off push button to a 9-volt battery. The resultant analog voltage signal was integrated with the ISCAN software through a Kiethley A/D converter board. All experimenters signaled the initiation of a head movement using a simple countdown. Once the countdown was completed, subjects were instructed to begin making their head turn while simultaneously pressing the sensation duration button. This button was then held down for the entirety of a subject's perception of any illusory, strange, or tumbling motions. Subjects were advised to release the button once these sensations subsided and they again felt completely stationary.

3.4 Experimental Procedure

All subjects participated in four sessions of centrifugation, each lasting approximately 15 minutes. Two of these sessions involved lying in a supine body position on the SRC, and the other two had subjects lying on their right side. Fourteen separate yaw head turns were made during centrifugation for each individual session. Reflexive eye components and several subjective measures were recorded for each head turn. Depending on instruction and instrumentation time, the entire experiment lasted anywhere from 90 to 120 minutes,

Experimental protocols and procedures were explained to each subject prior to participation. Subjects were asked to abstain from alcohol and caffeine for the 24 hours preceding the experiment and to be free from all medically disqualifying conditions. All subjects were advised that a possible side effect of participation in the study would be symptoms of motion sickness, and that they were free to terminate the experiment at any

time. Subjects who expressed an extreme susceptibility to motion sickness were excluded from the study. A signed, written consent form (see Appendix A) was obtained from all participants.

Each subject was asked to provide the following demographic data: age, race, gender, handedness, eye dominance, virtual reality experience, and general level of health on the day of the study. The height and weight of each subject was recorded to enable proper placement of the centrifuge foot plate and counterbalancing weights. A resting blood pressure measurement was obtained in both the standing and supine position. A Romberg test was then administered to discount any gross vestibular defects.

In order to aid in the description of self-motion, the roll, pitch, and yaw planes of rotation were explained to all participants. Subjects were then instructed on the use of the magnitude duration button and the reporting of magnitude estimates for each head turn. Subjects' understanding of the 0–20 motion sickness scale was also verified prior to centrifugation. The final step prior to instrumentation, was a clear explanation of the safety features of the SRC and the proper use of the emergency stop button.

Five subjects underwent testing to ascertain their estimates of the subjective visual vertical. Prior to centrifugation, these participants were positioned on their right side such that the gravitational vector was aligned with their inter-aural (y-axis) in a completely darkened environment. With the LEDs turned off, the experimenter displaced a line located about 0.5 m in front of the subject's nose from the gravitational vertical by a

minimum of 20 degrees toward or away from the subject's head. The line was then illuminated via a set of LEDs and subjects were instructed to rotate the line in the bed pitch plane until it was in agreement with their perception of Earth vertical. Five such trials occurred for each of these participants, and a mean estimate was calculated.

All subjects were instructed to don the ISCAN imaging goggles and appropriate adjustments were made to ensure comfort of fit and centered eye video image. Subjects were then positioned on the centrifuge in a supine body position and placed their head inside of the helmet located at the center of the bed's axis of rotation. The helmet was adjusted until no slip was observed between the head and the helmet when conducting head turns. The absolute angle of excursion that each subject could comfortably turn through was then determined. While still in the supine position, subjects were asked to turn their head as far as was comfortable to the right ear down position. This angle was noted to within the nearest ten degree increment and a metal stop was placed in the restraint at this location. Subjects were then positioned on their right side, and the same determination was made for head turns toward nose up. A second metal stop was placed at this location; thereby setting the absolute angle for which all subsequent head turns would be performed.

At this point in the investigation subjects were repositioned in the supine position to enable calibration of the eye imaging goggles via a stand that attached to the side of the centrifuge. The stand consisted of a cross suspended 71 cm above the subject's head. The cross contained five separate dots, one of which was centered directly above the midpoint

between the subject's eyes. The other four dots represented viewing angles separated by ± 10 degrees in the horizontal direction and ± 10 degrees in the vertical direction from the center dot. Calibration was completed through the use of ISCAN's Raw Eye Movement Data Acquisition software.

Subjects were then placed in the body position, either supine or right shoulder down, in which they would begin rotation. The safety belt was fastened and foot plate adjusted until it was flush with the soles of the subject's feet. Next, the use and location of the emergency stop switch for the centrifuge was demonstrated. All participants then conducted several practice head turns to ensure they were made in approximately one second for both nose up and right ear down turns. This also afforded an opportunity to become familiar with the proper use of the sensation duration button. Subjects were again instructed to depress this button at the beginning of each head turn and to release it as soon as all novel or illusory perceptions of motion abated. Once the experimenter was satisfied that all turns were being executed properly, the cloth cover was placed over the ISCAN goggles. The bed's support structure was then released and counterbalancing weights were added or removed as necessary. The centrifuge was manually spun once around to guarantee unimpeded rotation within the room, prior to turning off all of the lights.

Two experimenters were required to conduct this study. One experimenter was responsible for all communication with the subject while on the centrifuge including: indication of when and in what direction each head turn should be made, querying the

subject for the various subjective measures, and monitoring the subject's level of motion sickness symptoms throughout the study. This experimenter also operated the ISCAN software, which collected all of the eye position and head turn data. The other experimenter was responsible for the safe operation of the centrifuge. This person also recorded all of the subjective dependent measures in a Microsoft Excel spreadsheet and documented the investigation timeline. For a detailed list of experimental protocols and activities please refer to Appendix C.

The experiment consisted of 20 distinct phases, all conducted in the dark, as depicted in Figure 16. Phases 1 and 2 occurred while the bed was stationary. In phase 1, the subject remained in the right ear down position for 30 seconds while baseline eye location information was recorded. In phase 2, the subject made three sets of directed, yaw head movements. Each head turn was initiated by a simple countdown from the experimenter, such as "3, 2, 1 turn". The subject would then make a head turn in the appropriate direction, either from right ear down (RED) to nose up (NU) or from NU to RED, and then hold that position until instructed to make the next head turn.












	Pre-Rotation	Ramp Up	Per-Rotation	Ramp Down	Rest Period	Post-Rotation				
Centrifuge Velocity	0 rpm	25 secs	23 rpm	25 secs		0 rpm				
Head Position	  		  			  				
Phase(s)	1	2	3, 8, 12, 16	4	5, 9, 13, 17	6,10, 14, 18	7,11, 15	19	20	
Motion Sickness	↑		↑	↑	↑		↑	↑	↑	
Verbal Reports				⊗	⊗				⊗	
Eye & Duration Data	← All Head Turns →									

Figure 17: Protocol

During phase 3 the centrifuge was ramped up in a clockwise direction from 0 to 23 revolutions per minute in 25 seconds. This provided an angular acceleration of 6 deg/s^2 . The subject remained in the RED orientation throughout this phase while eye positional information was recorded. The centrifuge continued to rotate at 23 rpm for phases 4 and 5. In phase 4, the subject remained RED for the first 30 seconds of constant velocity rotation, while per-rotation baseline data was gathered.

Seven complete sets of directed head turns (7 toward NU and 7 toward RED) were conducted during phase 5. For the very first turn in this phase, subjects were instructed to assign a magnitude estimation value of 10 to the overall strength of the illusory motion sensations experienced. The experiences on this first turn were used as a reference for all subsequent magnitude estimates, and the importance of remembering this feeling was made clear to all subjects. For every head turn in this phase: pupil displacement, head

turn velocity, and duration of sensation information were measured and recorded. After head turn numbers 3, 4, 7, 8, 11, and 12 were completed, subjects were asked to estimate the direction and number of degrees of any perceived self-motion. Motion sickness ratings on the 0 – 20 scale were obtained after the 6th and 12th head turns in this phase. In phase 6, the subject remained in the RED position while the bed was linearly decelerated from 23 to 0 rpm in 25 seconds.

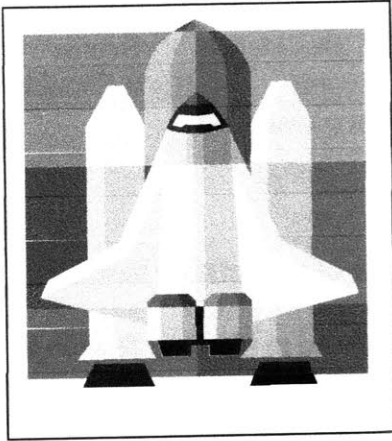
Phase 7 allowed a rest period sufficient to return motion sickness levels to a value of 5 or less. Subjects were allowed to disembark from the centrifuge, drink water, and move around if necessary. Approximately 75 percent of all subjects remained on the centrifuge during this period and simply rested there for around three to several minutes. Once the subject was ready to continue with the study, they were placed on the centrifuge in the body position other than that in which they started the experiment. For instance, if phases 1 through 6 were conducted in the supine body position, the subject was placed on his/her right shoulder at this time. The subject would remain in this body orientation for phases 8 through 15. Prior to commencement of phase 16, the subject would again be positioned in the supine position until completion the experiment. The converse was true for subjects starting in the right shoulder down position. One-half of all subjects began this study in the supine position, and the other half began in the right shoulder down position. This counterbalancing schema, as depicted in Table 1, ensured that all subjects performed head turns at the same point chronologically in the experiment and aided in reduction of adaptation effects.

Percentage of Subjects	Phase			
	1-6	8-10	12-14	16-20
50%	Supine	Right Shoulder	Right Shoulder	Supine
50%	Right Shoulder	Supine	Supine	Right Shoulder

Table 1: Subjects' body positions for various experimental phases.

With the exception of the changing body position and absence of per-rotation baseline data collection, phases 8 - 10, 12 - 14, and 16 - 18 were conducted in identical fashion to phases 3 - 6. Following the centrifuge ramp-down in phase 18, subjects remained RED for 30 seconds of post-rotation data collection in the dark. This was followed by the final phase of the experiment, in which 3 more sets of directed head turns were made with the bed stationary and the subject still in the dark.

Upon completion of phase 20, subjects were asked to remain on the centrifuge while experimenters locked it into its support structure. The subject was then aided in the removal of all instrumentation. After obtaining a supine, resting blood pressure measurement, the subject was assisted off the centrifuge and a standing blood pressure measurement taken. The participant was then questioned to certify subjective ratings given during the experiment were consistent with those recorded by the experimenter.



Chapter 4

Analysis

Techniques

4.1 Eye Data

As described in the experimental methods section, eye position data was obtained using ISCAN's Raw Eye Movement Data Acquisition software. Calibrated eye data was also recorded with this software and was obtained using the previously detailed calibration technique. This data was stored in an ASCII format and was processed using various Matlab m-file routines. The majority of these routines were written by David Balkwill (Balkwill, 1992). Significant modifications were subsequently made to this set of programs by Carol Cheung, Kathleen Sienko, and David Phillips. The author also contributed a set of modifications tailored to meet the unique demands of this experiment. A complete listing of these program files is located in Appendix F.

This software performed three main functions. The first was to remove noise from the positional data through the use of order statistical filtering. Secondly, eye velocity information was acquired from the positional data via differentiation. The third major function was to remove the fast phases from this velocity to yield strictly slow phase eye

velocity (SPV) information. The means by which this was accomplished has been described at length by both Sienko and Balkwill and, therefore, will not be reproduced here.

An additional function of these programs was to automatically fit exponential curves to areas of nystagmus within the SPV data. This was accomplished by first locating the duration button information. Recall that each subject was instructed to push a button at the beginning of every head turn and to keep it depressed until all illusory sensations of motion subsided. This signal was fed into the ISCAN system and provided a means of pinpointing the time at which nystagmus was expected to appear in the SPV profile. For each curve fit obtained from a Matlab program, a value of the amplitude, A , and time constant of decay, τ , was returned according to the following exponential equation: SPV curve fit = $\pm Ae^{-(t/\tau)}$. An F-test value was also returned as a measure of the goodness of the exponential fit to the SPV data.

This data was then examined to determine whether or not a manual inspection of the curve fit was warranted. These conditions included: a non-significant F-test value, outlier amplitude or time constant point, or an area of nystagmus that was skipped due to missing duration button data. An F-test value less than 3 indicated non-significance. Amplitude was considered out of physiological range if it exceeded a value of 150. This value was determined from the stimulus to the canals in this experiment according to the following equation: stimulus amplitude = $\sin(\theta)*138$, where θ represented the angle of the head turn in radians and 138 was the angular velocity of the bed in degrees/second. The value of 150 was chosen because it represents a gain (response/stimulus_{max}=138) of

about 1.1, which is around the expected physiological maximum. Any time constant value less than 2 seconds or greater than 20 seconds was considered an outlier. An omitted data point was determined by simply counting the number of data points in the file and comparing it with the expected number of points. A separate Matlab file was employed to manually refit a curve in the first three conditions, or to look at the head turn data to locate nystagmus in the last condition.

Primarily left vertical eye movements were examined in this study. Right vertical movements were examined only for cases where left eye data was either missing or too noisy to obtain statistically significant fits. Eye velocity information was processed only for the phases of interest, namely 5, 9, 13, and 17. There were 14 head turns (or data points) per phase, resulting in 56 data points per subject. Figure 18 illustrates typical data obtained for each head turn, and Figure 19 depicts the best curve fit for the SPV accompanied by this particular head turn.

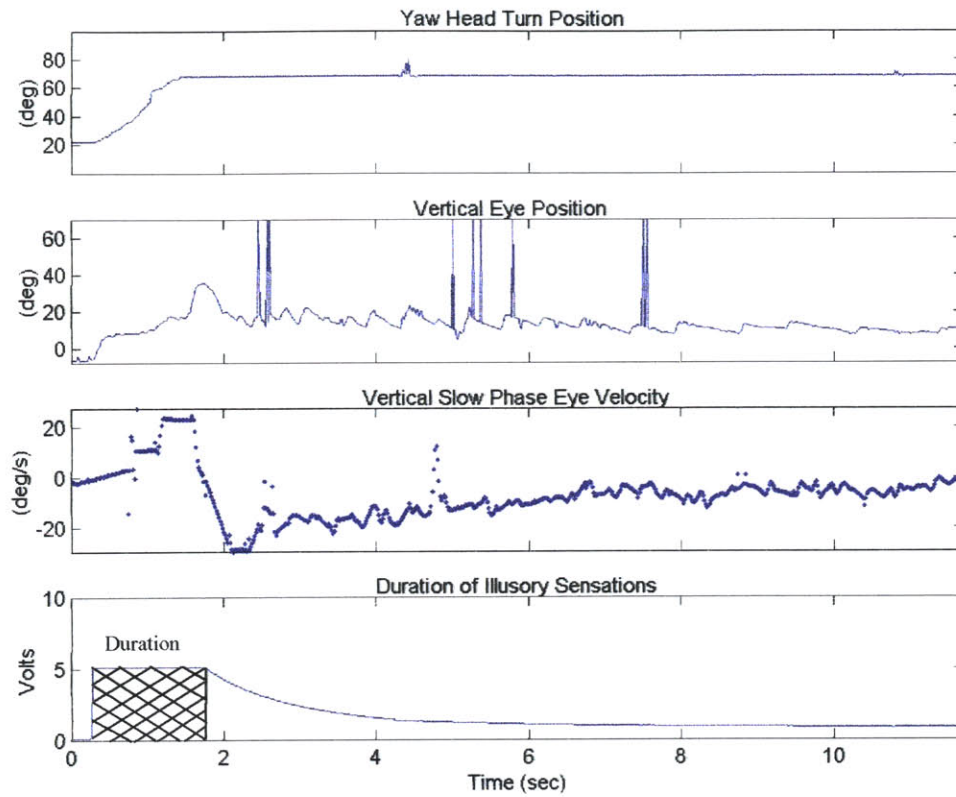


Figure 18: Data collected from subject 13, phase 9, head turn number 12. From top to bottom: head position during yaw movement, eye position, SPV, and subject's estimate of the duration of illusory motion sensations.

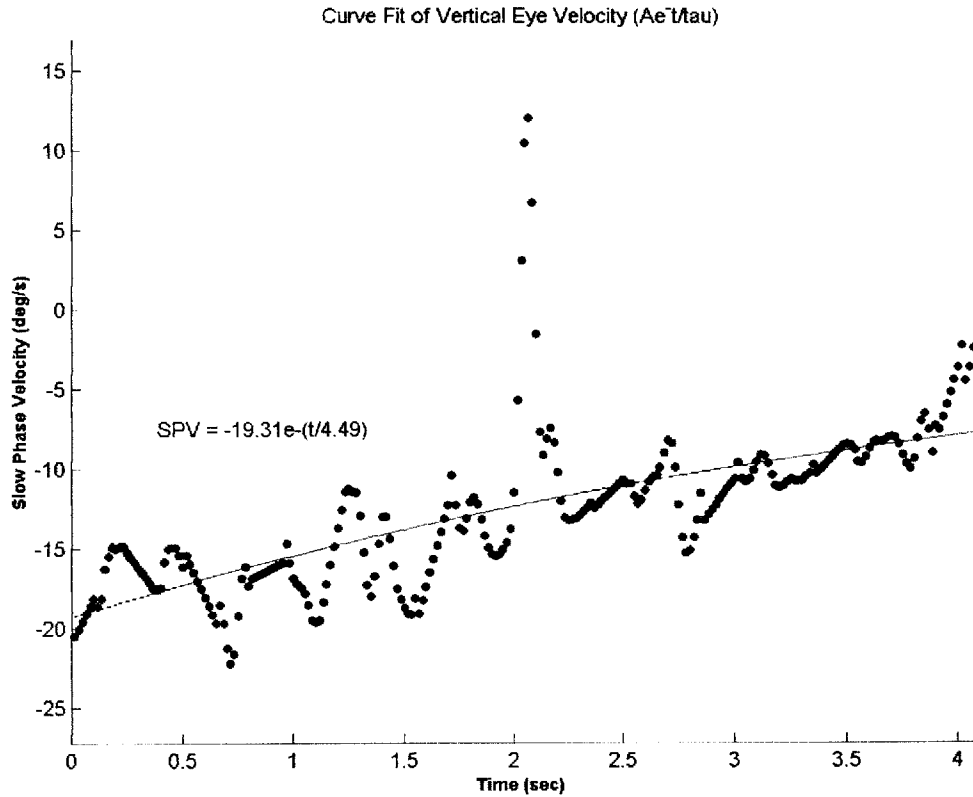


Figure 19: Exponentially decaying curve fit for the SPV depicted in Figure X. Amplitude equal to -19.31 with a time constant of 4.49 seconds.

4.2 Normalized SPV

Participants in this study made head turns through an angle that they could comfortably and consistently perform. This angle was held constant within subject, but varied across subjects. In order to make statistical across subject comparisons, a normalizing parameter was introduced. Normalized SPV (or NSPV) was calculated by dividing the eye velocity amplitude response by the amplitude of the stimulus induced during a head turn on the centrifuge. This is a reasonable normalization because it represents the gain (output/input) of the VOR system, which should be more or less the same for all subjects. As previously mentioned, the stimulus was calculated by the product of the sine of the angle of the head turn and the angular velocity of the bed. More formally:

$$NSPV = \frac{EyeVelocityAmplitude}{\sin(HeadAngle * \frac{\pi}{180}) * 138}$$

4.3 Head Movements

Head positional data was measured via a roll potentiometer attached to the axis of rotation of the head restraint device. The resultant voltage signal was transmitted to the ISCAN Data Acquisition Software through the centrifuge's slip rings. At the beginning of the experiment, both the NU and RED down angle relative to fixed space (0 degrees representing earth vertical and 90 degrees representing earth horizontal) through which all subsequent head turns were made was noted and recorded manually. An average turn velocity was calculated using Matlab software according to the following equation:

$$V_{avg} = \frac{\angle RED - \angle NU}{t_{end} - t_{start}}$$

where t_{end} the time at the end of the head turn and t_{start} was the time at which the head turn began. Velocity profiles were obtained by differentiating the positional data.

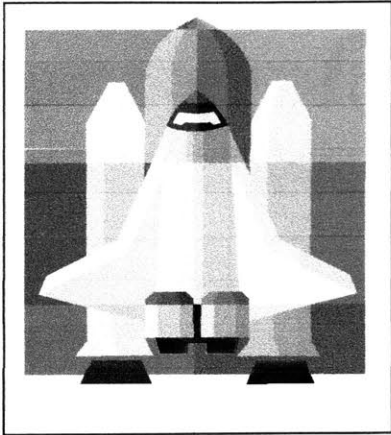
4.4 Missing Data Points

A complete set of subjective magnitude and direction measures were obtained for all subjects. Table X depicts the number of data points that were missed for the other four important dependent measures. All measures that were excluded from analysis (red numbers in the table) were attributed to equipment failure. The remaining data points were missed for a variety of reasons, including operator error, noise, outlier point, or subject inattentiveness. In an effort to retain the maximum number of subjects for

statistical analysis these points were replaced with the average of the two nearest, like data points. For example if the eye amplitude data for the third RED head turn was missing, the average of the first and third RED amplitude points within that same phase were used to replace that value. If the first or last data point within a phase were missing, the one nearest like value was substituted instead of averaging points across a given phase. The advantage of this method is that it preserves any time or order effects that may have been in the data.

Table 2: Missing dependent variable data points. Grayed boxes denote variables that were not statistically analyzed. Items in black indicate the number of points replaced using averaging schema.

Subject	Duration Button	Average Head Velocity	Eye Amplitude	Time Rate of SPV Decay
1		56		1
4	2	1	1	2
5	14			3
6				4
8				
9				3
10			1	5
11				5
12	28	28	28	28
13	12			
14				6
16			2	
17				3
18				1
19	11			3
20	2	2	3	1
21				5
<i>Totals</i>	69	87	33	70
<i>Percentage of Measurements</i>	7.2	9.1	3.5	7.4



Chapter 5

Results

5.1 Head Movements

The average velocity of all head movements made in this experiment was analyzed using SYSTAT (Version 10) General Linear Model univariate repeated measures ANOVA.

Two subjects (1 and 12) had to be excluded from this analysis because some of their data points were missing. The other fifteen subjects (8 who started in the supine body position and 7 in the right shoulder down position) were investigated. A significant effect of head position on head turn velocity was found. Those turns made to the nose up (NU) position were made faster, 75.0 deg/s, than those made to the right ear down (RED) position, 70.8 deg/s, ($F(14,1) = 7.681$, $p < 0.02$). Although it was significantly different, the magnitude (4.2 deg/s) of this difference was small.

The interaction effect between head turn direction and body position on head turn velocity was significant, ($F(14,1) = 10.9$, $p = 0.005$). Subjects in right shoulder down body position showed no difference in turn velocity between NU and RED head turns, whereas in supine position (Figure 20), NU were significantly faster than RED head turns.

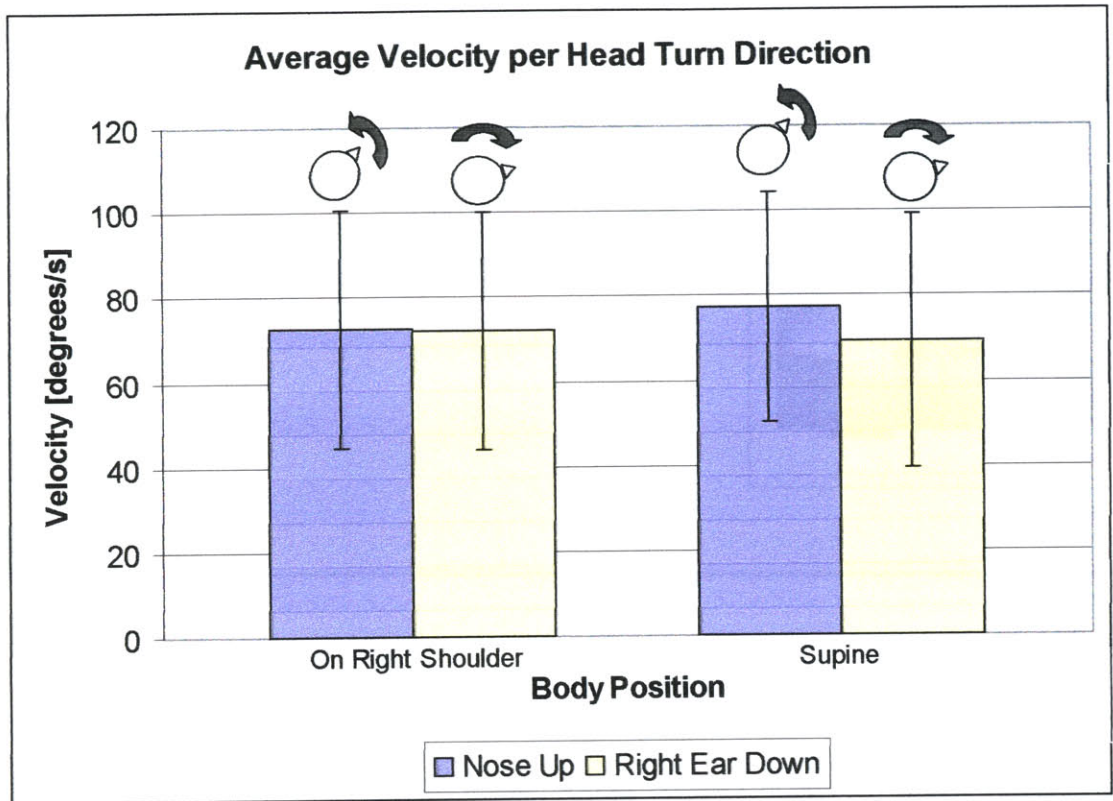


Figure 20: Average head turn velocity for supine versus right shoulder down body positions.

A third cross-effect on head turn velocity, $p < 0.05$, was seen between subject head turn direction and whether the turn was made in the first or second phase of head turns for a given body position. Head turns toward NU tended to slow down from the first to second set of turns, whereas no such significant average velocity difference was seen for turns toward RED. These effects were represented in a significant ($p < .05$) multivariate cross effect of body position, head turn direction, and repetition number.

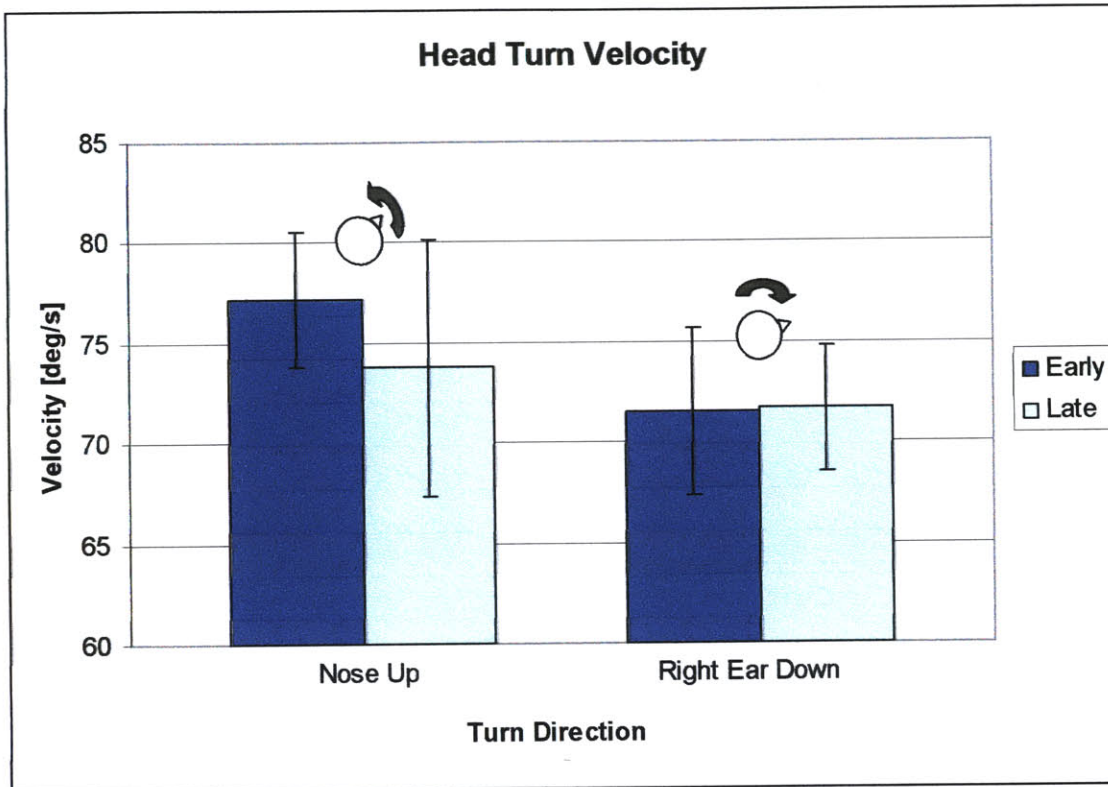


Figure 21: Average turn velocity as a function of whether it occurred in the early or late set of turns for a particular body position.

5.2 Subjective Magnitude Estimates

Subjective magnitude estimates of illusory sensations experienced while making head turns on the centrifuge were analyzed for 17 subjects (9 starting in supine position and 8 in right shoulder down position). A General Linear Model repeated measures ANOVA found that magnitude estimates for NU head turns were significantly larger ($F(16,1) = 24.504, p < 0.001$) than for head turns toward RED irrespective of the subject's body position (Figure 22). In fact, no significant effect of body position was observed.

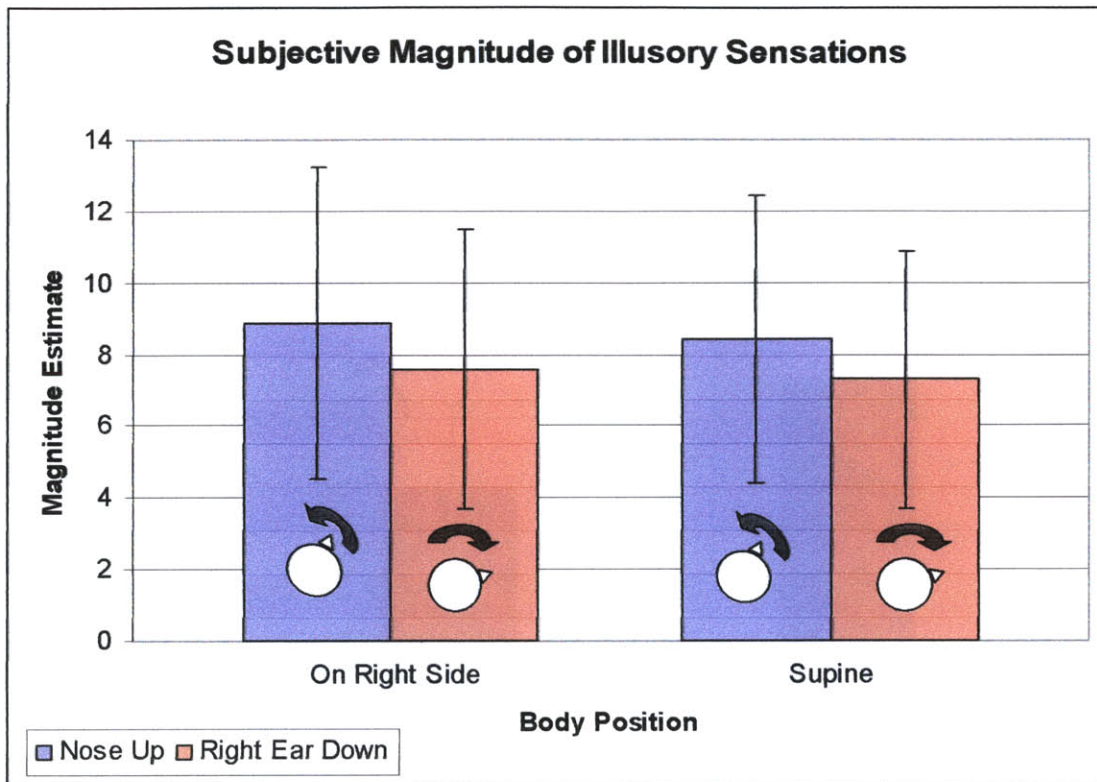


Figure 22: Subjective magnitude estimates of illusory motion for head turns toward nose up and toward right ear down. NU vs. RED differences were significant for both body positions.

There was significant habituation seen in the magnitude estimates as a function of repetition number ($F(16,1) = 3.677, p = 0.002$). As Figure 23 indicates, magnitude estimates were largest for the first few repetitions, and smallest for the last few repetitions within a given phase. Adaptation appeared to carry over between phases for magnitude estimates, as evidenced by a significant Phase x Repetition x Head Position ($F(16,1) = 3.08, p < 0.01$) effect as illustrated in Figure 24. There is a difference between NU and RED head turns. These time trends were represented in a significant multivariate effect of repetition ($F(16,1) = 3.496, p < 0.05$).

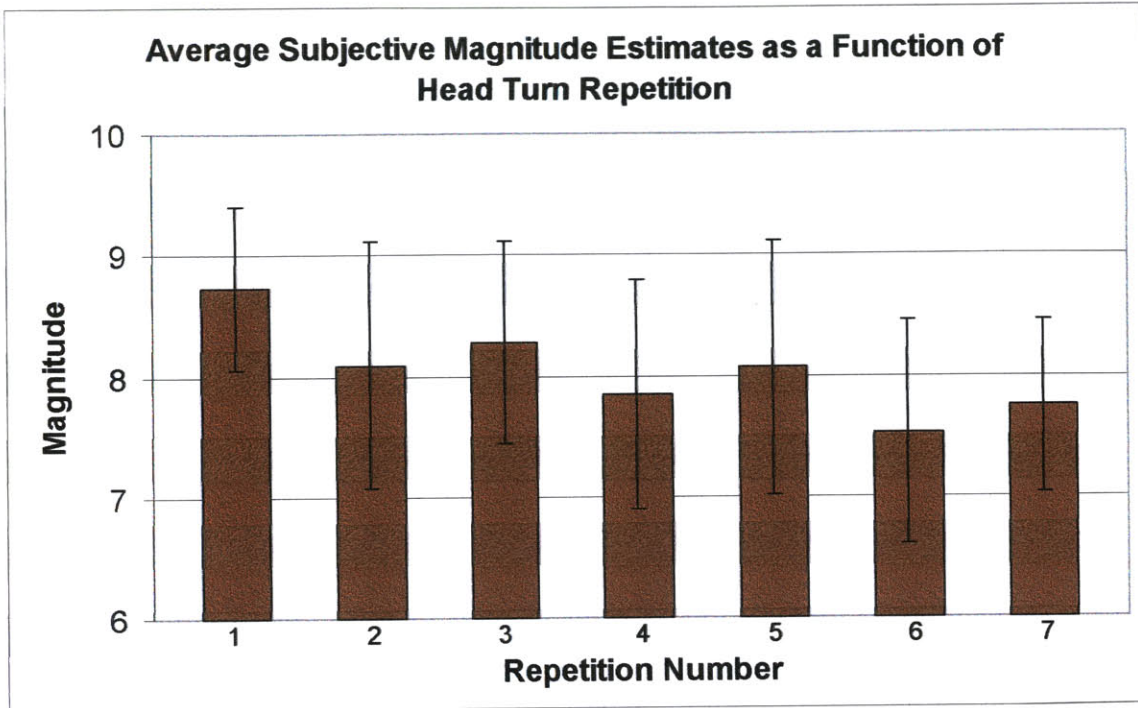


Figure 23: Magnitude estimates habituate as a function of head turn repetition.

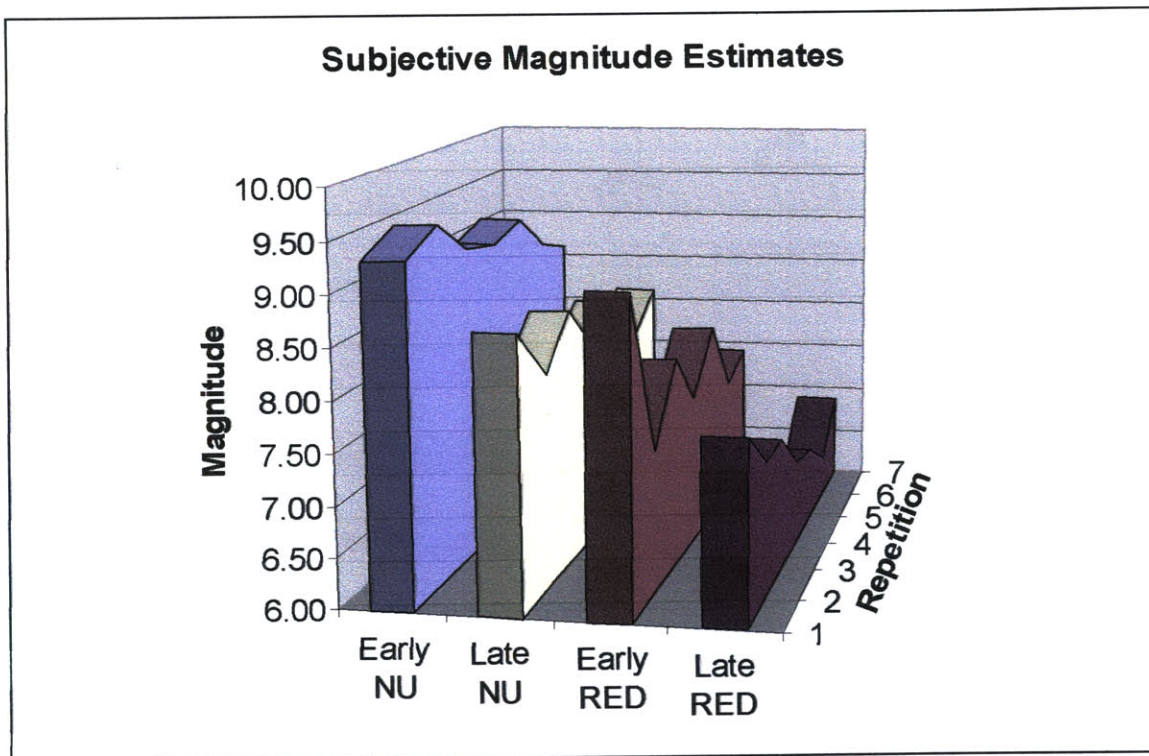


Figure 24: Magnitude estimates habituate over repetitions, and adapt across phases.

5.3 Duration of Illusory Sensations

Duration of novel pitch or roll sensations experienced while making yaw head turns on the centrifuge were analyzed for 13 subjects (7 starting in the supine position and 6 in the right shoulder down position). Some subjects were excluded primarily because of equipment failures. The General Linear Model repeated measures ANOVA showed significant main effects of head turn direction on duration ($F(12,1) = 4.962, p < 0.05$) and phase ($F(12,1) = 8.755, p < 0.02$). As with magnitude estimates, the duration of illusory motion sensations were longer for head turns toward NU than for those toward RED. Again, no significant effect on body position was seen (Figure 25). The durations were longer in the early phase head turns, and again appear to adapt across phases as illustrated in Figure 26.

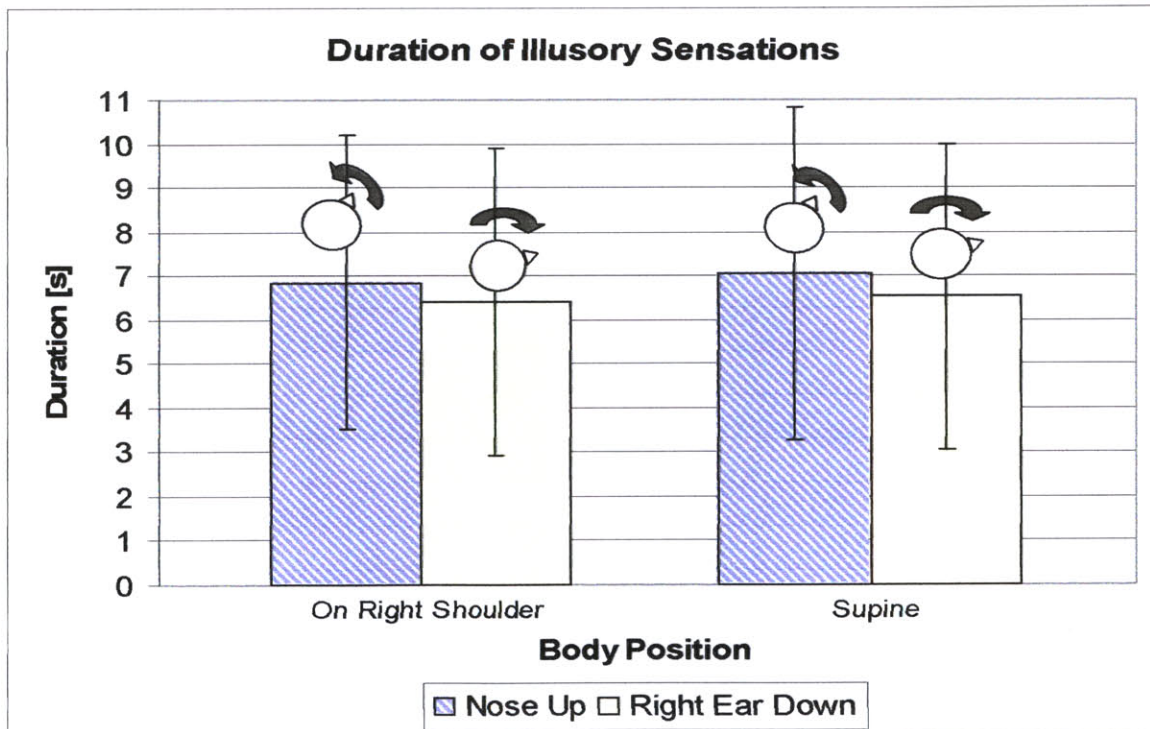


Figure 25: Longer illusory sensations were experienced for NU than for RED head turns. No significant effect of body position was observed.

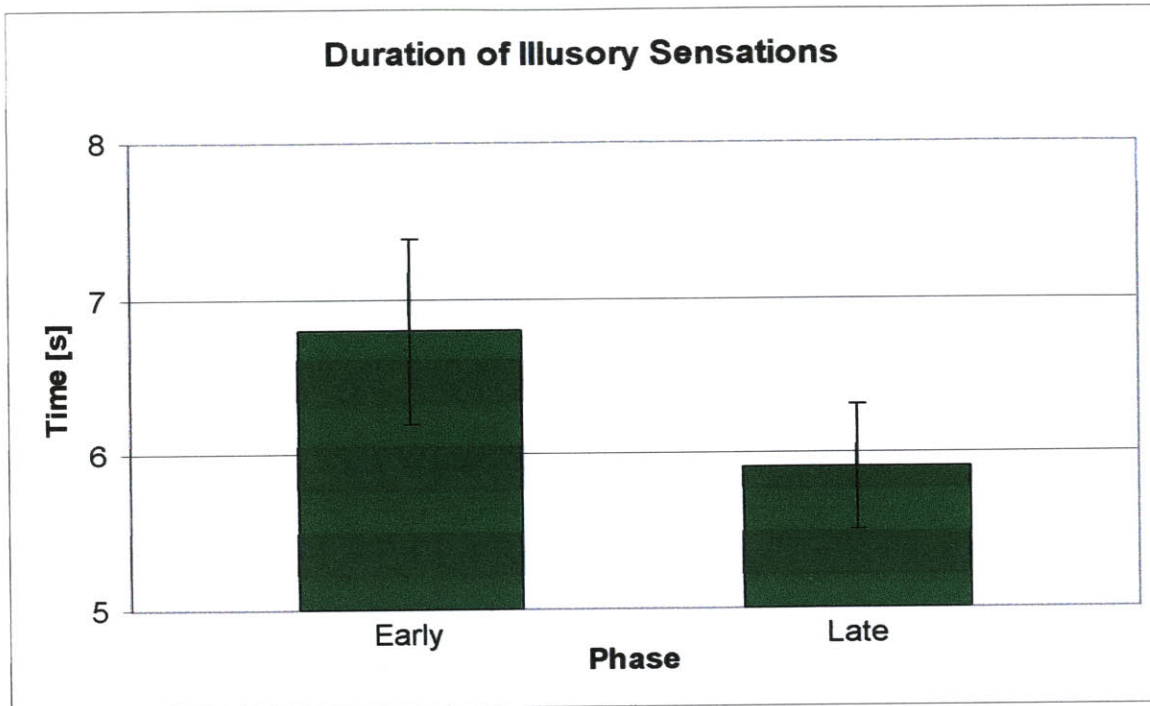


Figure 26: Duration of illusory sensations is significantly shorter in the later than in the earlier phase for a given body position.

5.4 Normalized Slow Phase Eye Velocity (NSPV)

Repeated measures ANOVA found no significant effects of the major independent variables on normalized slow phase eye velocity (NSPV). One subject was excluded from the analysis due to equipment failure. The average NSPV for turns toward NU was 0.300, which differs little from the average ($=0.305$) for turns toward RED. Neither habituation across repetition, nor adaptation across phase was evident for slow phase eye velocity. Figure 27 also shows that no significant difference existed for head turn direction as a function of body position.

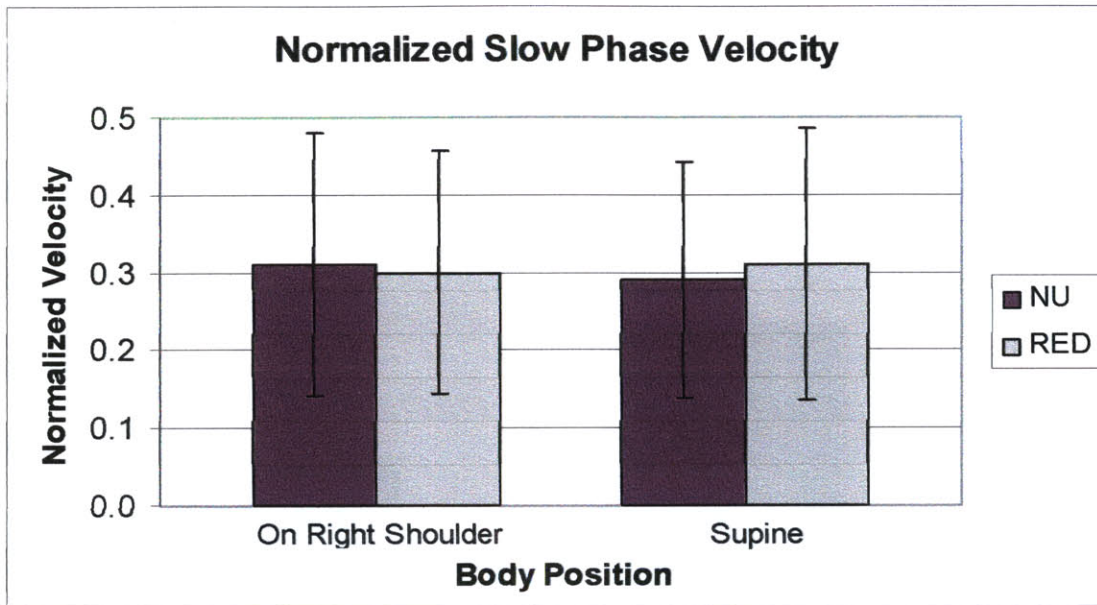


Figure 27: NSPV for head turn direction was not significantly different in either body orientation.

No main effects on the time constant of vertical slow phase velocity were found. A multivariate effect on time constant of Phase x Rep was found to be significant ($p=0.046$). The average time constant was 5.34 seconds. (A histogram of all values is shown below.)

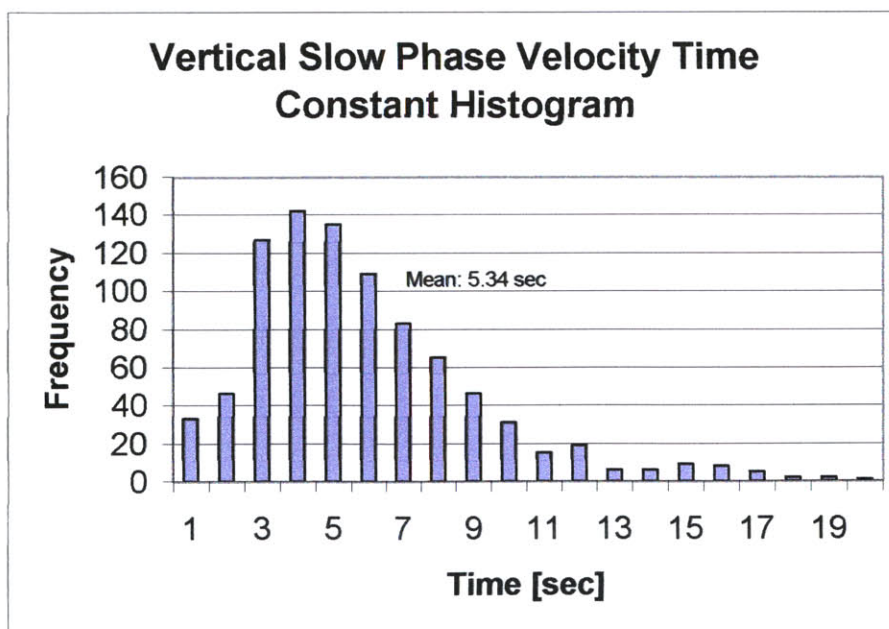


Figure 28: Histogram of time constant of decay of nystagmus.

5.5 Subjective Visual Vertical (SVV)

It is well known that the subjective vertical is influenced by tilting of the head relative to gravity. Either an Aubert or a Müller effect can be observed. According to Mittelstaedt (1988), the idiotropic vector (defined by the subject's own longitudinal z-axis) could explain this apparent disparity. The Aubert effect is triggered by giving too much weight to the idiotropic vector, i.e. to the egocentric reference, whereas the Müller effect would result from a smaller idiotropic vector, i.e. giving more weight to an exocentric (gravitational) reference.

Due to continuing mechanical and technical problems with the luminous line device used to measure estimates of the subjective visual vertical, data was only obtained for 5 of the study's subjects. Table 3 summarizes these results. All subjects showed an Aubert (A) effect, and one subject nearly aligned the luminous line parallel to the idiotropic vector.

Table 3: Results from SVV testing.

Subject	Mean 'A' Effect [degrees from vertical]
9	18.92
10	81.71
11	14.50
12	14.94
13	32.15

5.6 Subjective Descriptions of Self-motion

Based upon subjects' descriptions of self-motion, three distinct categories emerged. All of these categories are related to the amount of gravito-inertial force (GIF) conflict

between *perceived* motion and the macular afferent signals. For example, a body rolling sensation results in no GIF conflict between the semicircular canals and the otoliths for either the RED or NU turn directions. The perception is that one is simply rotating about an earth gravity-axis. Pitch and yaw sensations do, however, result in a GIF conflict for both NU and RED turn directions. For instance, during a turn to the NU position, one may feel as though his/her body pitched up 90 degrees from the supine position. If the canal afferent signal is to be believed, the brain would anticipate that the maculae would indicate a GIF in the $-z$ -body axis. However, since the subject had not in actuality pitched up, but remained supine in the NU head position, the otoliths are indicating a GIF in the $-x$ -body axis. The brain must then resolve this discrepancy, which will be referred to from now on as a GIF conflict.

The three GIF conflict groups are as follows:

- Group 1: Large GIF conflict in NU head turns and very little for RED turns.
- Group 2: Similar GIF conflict in both NU and RED head turns.
- Group 3: Large GIF conflict in RED head turns and very little for NU turns.

The average perceived motion for each of these groups is portrayed in the graphs below.

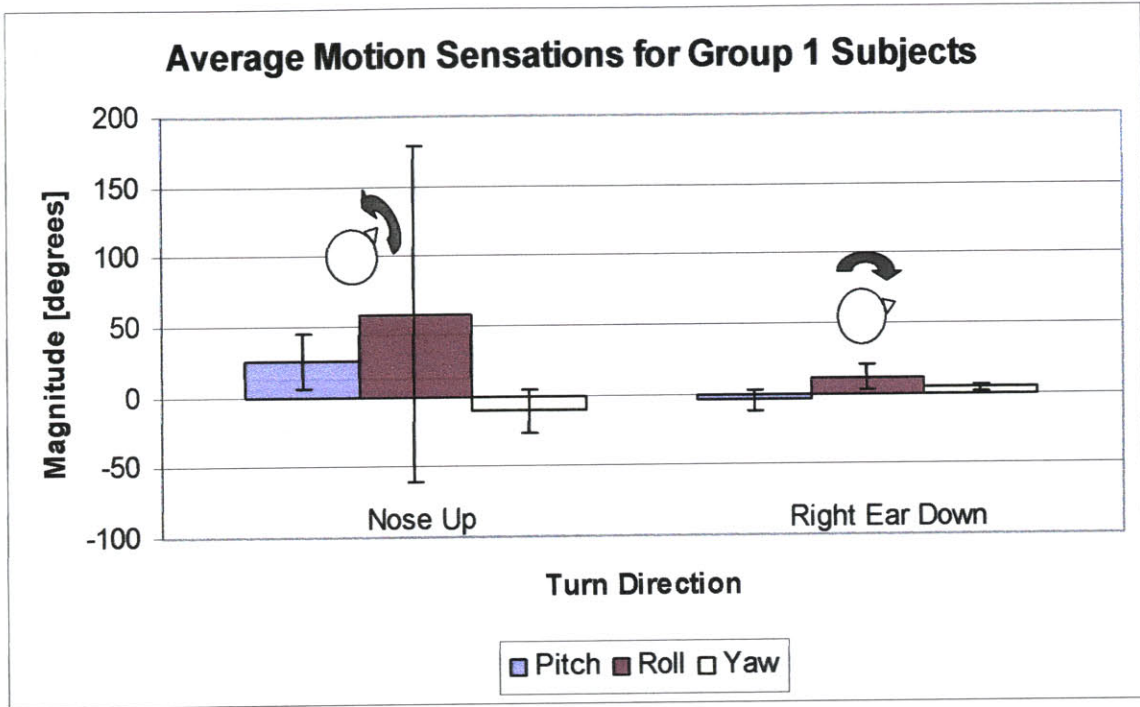


Figure 29: Group 1 average self-motion; magnitude and direction.

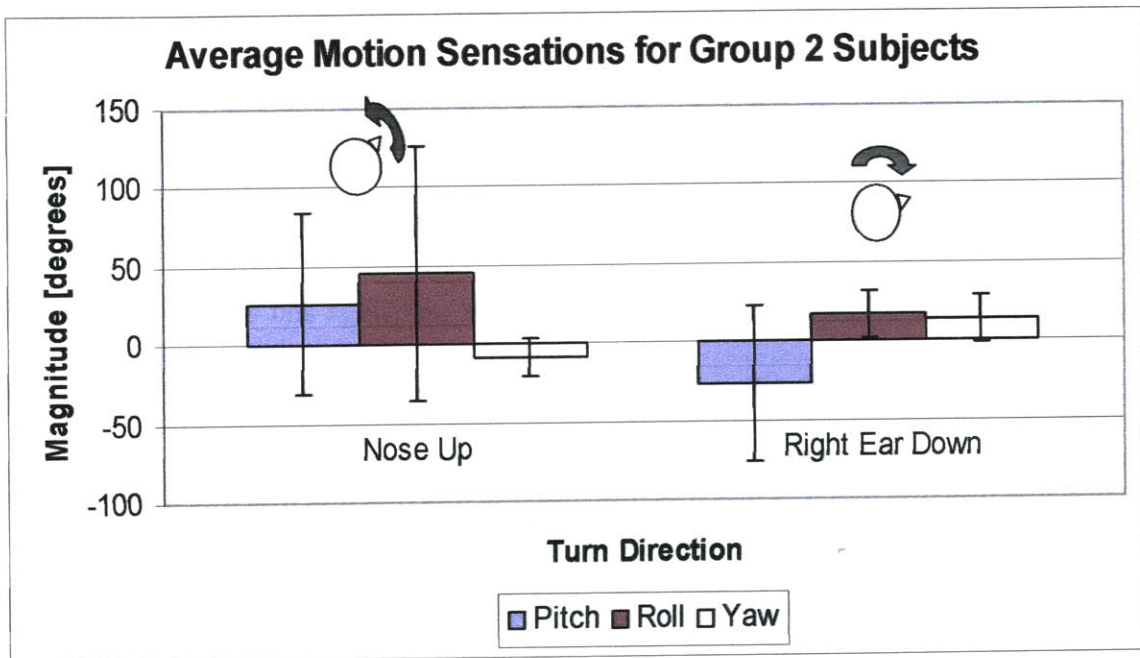


Figure 30: Group 2 average self-motion; magnitude and direction.

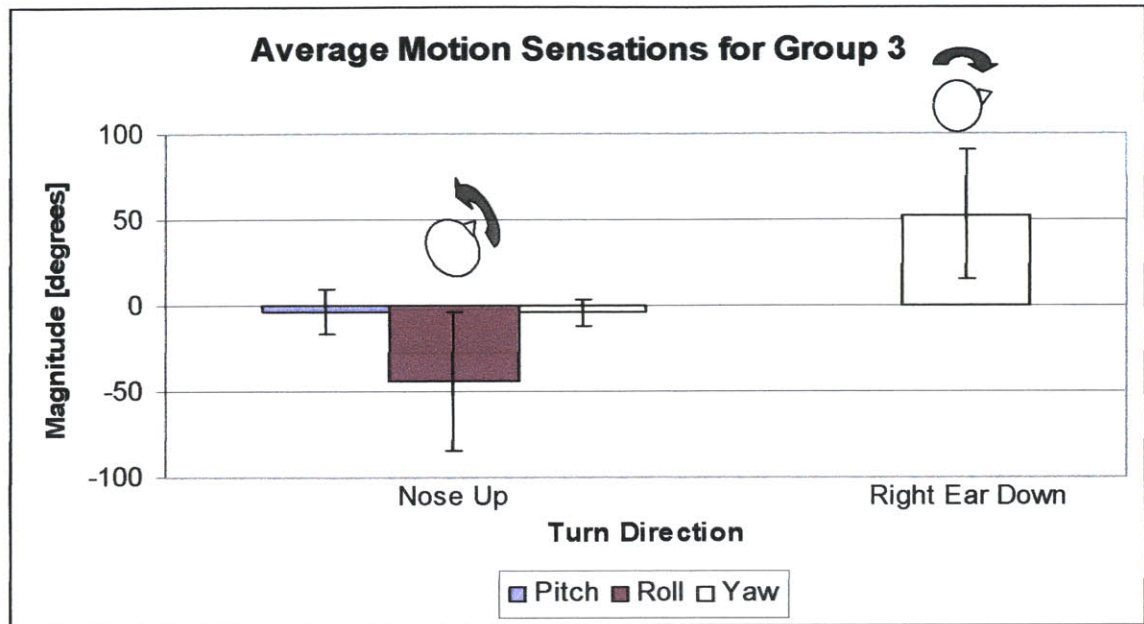


Figure 31: Group 3 average self-motion; magnitude and direction.

As these graphs illustrate, Group 1 subjects reported very little perceived pitch and yaw sensations for RED head turns, leading to a very small GIF conflict. The opposite is true for the NU head turns. Group 2 had roughly the same GIF conflict for both types of head turns, and group 3 had a relatively larger GIF conflict during RED turns. Groups 1, 2, and 3 contained 5, 7, and 1 subjects respectively. Three subjects (“tumblers”) experienced tumbling sensations while making head turns on the centrifuge and were categorized separately due to the difficulty in determining the overall GIF conflict. One subject was excluded altogether because of incomplete duration button information.

A General Linear Model repeated measures ANOVA was used to analyze effects on duration and magnitude estimates for Group 1 and Group 2 subjects. The magnitude estimates for NU turns were significantly higher than those for RED turns ($F(4,1) = 62.477, p = 0.001$). Similarly, duration estimates for NU were significantly longer than

for RED head turns ($F(3,1) = 391.909$, $p < 0.001$). For Group 2 subjects, magnitude estimates for NU turns were larger than RED estimates ($F(6,1) = 6.716$, $p = 0.041$). Duration estimates, however, were not found to be significantly different between the two types of head turns. Tables 4 and 5 summarize the averages and differences in the averages for subjective magnitude and duration of illusory sensation estimates based on this classification.

Table 4: Average subjective magnitude estimates for head turns toward NU and RED.

Head Turn Direction	Group 1	Group 2	Group 3	Tumblers
Nose Up	8.11	8.38	6.07	11.78
Right Ear Down	6.35	7.57	5.82	9.79
<i>Difference</i>	<i>1.76</i>	<i>0.81</i>	<i>0.25</i>	<i>1.99</i>

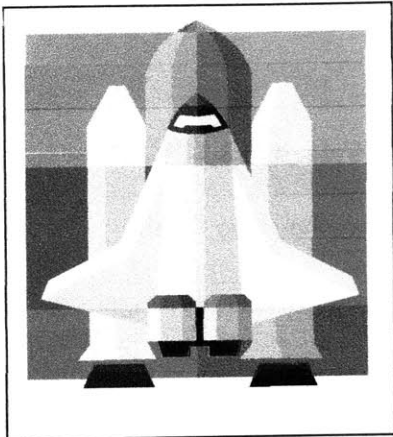
Table 5: Average subjective duration estimates for head turns toward NU and RED.

Head Turn Direction	Group 1	Group 2	Group 3	Tumblers
Nose Up	7.68	3.82	8.00	10.77
Right Ear Down	6.21	3.61	8.10	10.97
<i>Difference</i>	<i>1.47</i>	<i>0.20</i>	<i>-0.10</i>	<i>-0.20</i>

A Kruskal-Wallis test was performed for Groups 1 and 2 to determine effects on duration and magnitude. The difference in magnitude estimates for NU versus RED head turns of Group 1 was twice as large as Group 2 (χ^2 approximation = 29.114 with 1 df), and seven times that of Group 3. The tumblers had the largest overall magnitude difference.

The difference in duration estimates were largest for Group 1, almost even for Group 2, and Group 3 actually perceived RED head turn sensations to last longer than NU turns. Group 1 difference in duration estimates were significantly longer than that of Group 2 (χ^2 approximation = 30.139 with 1 df). The tumblers also had longer RED sensation duration estimates. Group 1 had significantly longer duration estimates than those of

Group 2 for both NU (χ^2 approximation = 197.493 with 1 df) and RED turns (χ^2 approximation = 150.966 with 1 df). Magnitude estimates were not found to be significantly different for the two groups for either NU or RED head turns.



Chapter 6

Discussion

6.0 Main Findings

The results of this study confirm a previous finding by Hecht, et al, (2001) that the conflicting sensations associated with yaw head turns during horizontal centrifugation decay faster for RED than for NU head turns. Subjects in this study reported larger magnitude and longer duration estimates of illusory motion for head turns made toward NU not only in a supine body position, but also in a right side down orientation. This asymmetry was not reflected in the eye velocity data, pointing to a significant dissociation between one's perceptual and physiological experiences.

The subjective difference may be explained by several competing hypotheses. Through a process of elimination, the current study identifies graviceptive information as the likeliest responsible agent. The exact mechanism by which this happens is less clear. The goal of the rest of this chapter is to discuss why some hypotheses can be rejected, and to explore more thoroughly the possible means by which graviceptive information may be driving this asymmetric response. The chapter concludes with a look at some of the

pragmatic consequences of this finding as it relates to astronaut SRC adaptation strategies.

6.1 Semicircular Canals and Normalized Slow Phase Eye Velocity (NSPV)

An asymmetric semicircular canal response offers a possible explanation for the differences in subjective duration and magnitude estimates found in this investigation. The strongest argument against this possibility is provided by the normalized slow phase eye velocity (NSPV) data. The pitch plane of the semicircular canals is solely responsible for the inappropriate vertical eye movements made during head turns on the centrifuge. For turns toward NU, this canal is brought out of the plane of rotation causing a deceleration of the endolymph. Most subjects experience this as a pitching up sensation accompanied by slow phase eye movements in the up or positive z-axis. The exact opposite is true for RED turns. Endolymph is accelerated resulting in a pitch back sensation with slow phases in the down or negative z-axis. If the pitch canal responded differently for fluid acceleration versus deceleration it should be reflected in the eye velocity data, and could then be identified as an agent responsible for the asymmetric subjective responses. However, no significant effect on NSPV was found for head turns toward NU or RED. In fact, the averages were nearly identical (0.300 for NU and 0.305 for RED).

The roll canal is also involved in yaw head turns on the centrifuge. When endolymph is accelerated in the pitch canal during a head turn it is simultaneously being decelerated in the roll canal and vice versa. Roll canal stimulation results in torsional eye movements. It is possible that an asymmetry in the roll canal is directly responsible for this study's

findings. Unfortunately, the system used for measuring eye movements was incapable of determining torsional displacements. One could speculate that since the pitch canal showed no evidence of an asymmetry that the likelihood of the roll canal containing a variable response is marginal. Also several of the participants in this study reported no roll component in their subjective assessments of motion. In addition, some researchers have determined that torsional eye movements are not a good indicant of roll canal afferent activity. However, this explanation cannot be strictly ruled out.

Another interesting NSPV finding was that no significant habituation or adaptation of the VOR gain occurred in this investigation. One of the primary drivers of VOR adaptation is visual slip of images on the retina. All the participants in this study remained in complete darkness during centrifugation. This absence of retinal slip must, therefore, be the main reason that no adaptation was observed. This finding is in good agreement with prior investigations (Clément, Wood, Lathan, Peterka, & Reschke, 1999) and recent work at MIT (Brown, 2002). Melvill Jones also found no adaptation of the vestibulo-ocular reflex (VOR) occurring across three days for subjects undergoing rotation in the dark (Melvill Jones, 1977).

6.2 Neck Proprioceptors

The vestibular system detects the orientation and movements only of the head (Guyton and Hall, 1996). It is essential that the nervous centers also receive appropriate information relating the orientation of the head with respect to the body. This information is transmitted from proprioceptors of the neck and body directly to the vestibular nuclei of the brain stem and indirectly by way of the cerebellum. When a head turn is made,

impulses from neck proprioceptors keep the vestibular apparatus from giving a person a sense of malequilibrium. This is accomplished by sending signals that exactly oppose the signals transmitted from the vestibular system.

It is entirely plausible that this mechanism is responsible for the differing subjective responses for NU and RED head turns made on the centrifuge. This investigation was designed, in part, to prove or refute this explanation. For the supine body position, NU head turns leave the head aligned with the body axis and RED turns result in a non-aligned head to body relationship. The converse is true for the right shoulder down body position. If this aligned / not aligned condition is responsible for the asymmetric response then NU head turns in the supine body orientation should be similar in subjective magnitude and duration to RED turns in the right shoulder down body orientation. This explanation can be disregarded because the contrary result was found. NU head turns had significantly longer durations and larger magnitude estimates regardless of the subject's body orientation.

6.3 Head Turn Properties

Several measures were taken in this study to maintain an equal velocity for all head turns. Despite these efforts, significant velocity differences existed between NU and RED head turns. This difference only occurred during head turns made in the supine body position, where turns toward NU were made an average of 8 deg/s faster than turns toward RED. Since significant effects on magnitude and duration existed between these head turns for both body positions, it is improbable that velocity is causing the effects.

The small magnitude of the velocity difference is also contraindicative. As pointed out by Lyne, the velocity at which a head turn is executed only contributes to the cross-coupled term of the overall stimulus to the semicircular canals, which is probably insignificant compared to the stimulus evoked by moving the canals into and out of the plane of centrifuge rotation. For this cross-coupled term, the canal response begins and ends in approximately the same amount of time it takes to conduct the head turn.

Using the average turn angle in this study of 54 degrees, NU head turns made in the supine position were conducted in an average time of 0.70 seconds, whereas RED turns took an average 0.78 seconds to complete. By comparison, the dominant stimulus caused by moving the canals in and out of the plane of centrifuge rotation causes cupula deflection to last on the order of 10 to 20 seconds. Therefore, the cross-coupled term contributes around 4 percent of the overall canal stimulus. A 0.08 second difference in this term contributes at best, 0.5 percent to the overall stimulus.

The finding by Hecht, et al, (2001) could have been attributed to the velocity profile and/or trajectory of the yaw head turns. Effort was taken in this investigation to control for both of these possibilities. A head restraint device was used to restrict turn trajectories to just the yaw plane of rotation. Velocity profiles were not controlled directly but repeatable turns were facilitated by the relatively smooth rotation action of this device. In addition, subjects were trained to use a similar velocity profile for both NU and RED head turns. Therefore, differing head turn trajectories can be strictly ruled out, and differing velocity profiles marginalized as possible explanations for the difference between NU and RED turns in this study.

6.4 Perception of Angular Rotation

A tendency to interpret angular self-motion induced by NU head turns more strongly than RED turns is another possible explanation of the results found in this study. Some evidence exists in the visually induced circularvection literature to support this hypothesis. Previous reports have shown thatvection magnitude is larger for yaw rotation than for pitch, which in turn is larger than for roll (Howard, Cheung, & Landoldt, 1988). Another study found that illusory self-inclination is larger for backward rotation of the visual scene about the subject's y-axis (inducing a pitch forward sensation) compared to backward-inducing pitch motion (Young, Oman, Dichgans, 1975).

Models of the canal response to the stimulation derived from making yaw head turns while rotating on the centrifuge in the current study would predict that both a rolling and pitching sensation should be evoked for both NU and RED head turns. For a turn toward NU, a pitch forward sensation accompanied by a clockwise rolling sensation should be present. Turns to RED should present an experience of pitching backward and rolling in a counterclockwise direction. If the results obtained from visually induced angular motion converges with vestibularly induced angular motion as recent research indicates (Sharp, Blair, Etkin, Tzanetos, 1995; Smith 1997) then NU head turns on the centrifuge (inducing a pitch forward sensation) would elicit stronger or more provocative responses.

Two problems exist with this hypothesis. One is that the literature is inconsistent with regard to the actual sensitivity and threshold values of the subjective estimates of angular velocity due to pitch and roll canal stimulation (Guedry, 1974). This is due, in large part, to the inherent noisiness of the measure and variability of recording techniques employed

by different researchers. Another cause for concern is that the novelty and complexity of the stimulus used in this study often yielded conflicting reports of self-motion. Both within and across subject reports were sometimes inconsistent. Finally, motion reports also were not in perfect agreement with model predictions. For example, several subjects reported feeling full body yaw when the only stimulus provided to this canal occurred as a result of the 1 second head turn. Other subjects experienced little or no pitch sensations as a result of making head turns on the centrifuge.

6.5 Graviceptive Information

Partial or complete elimination of the above hypotheses leave graviceptive information as the sole difference existing between head turns toward NU versus RED. The mechanism by which this information affects the results of this study could take many forms. The otolith organs are the primary means of detecting gravito-inertial force. The existence of anatomical or physiological asymmetries at this level offers one possible explanation. A second option is that some type of otolith-semicircular canal interaction is occurring at a physiological level. Perceptual processing and interpretation of the collective vestibular signals offers a third possibility. The following few sections are dedicated to exploring and discriminating between these hypotheses.

6.5.1 Otolith Asymmetries

Shear Force

When a yaw head turn was made in this experiment from NU to RED, the detection of the gravito-inertial force (GIF) vector changed from the subject's naso-occipital (-x-axis) to the inter-aural (-y-axis). Geometrically, the utricles are inclined approximately 30

degrees upward from true horizontal. Therefore, for a supine, NU head position the shear force acting on the utricle is modified by a cosine function with respect to inclination angle from the vertical. Specifically, the shear force in this orientation is 0.866-g directed in the $-x$ direction. Conversely, the utricles are maximally stimulated (1-g force) in the $-y$ direction for the RED position. It is possible that the difference between these force magnitudes is sufficient to drive the asymmetric subjective responses observed between these two types of head turns.

The otolith organs are responsible for indicating that no angular body rotations have occurred as a result of conducting a head turn on the centrifuge. Therefore, it seems reasonable to expect that the ability of the otoliths to suppress illusory motion will improve proportionally with the strength the signal detected. Indeed, Udo de Haes and Schöne (1970) showed that the rate of decay of post-rotational nystagmus was fastest when the utricles were brought into a plane of maximal stimulation.

Three arguments can be made to counter this hypothesis. The first is that only two of the participants in this study made RED head turns in which the position of the utricle was brought into the plane of maximal stimulation. Shear force in the y direction is a sine function of the angle from true vertical. The average RED resting angle in this study was approximately 72 degrees, reducing the average maximal shear force to 0.95-g. The second argument involves the distribution of polarization vectors within the utricle. Shear force responses may vary as a function of the number of neuronal units activated in a particular orientation. Randomly sampled polarization vectors in the squirrel monkey

suggest that an asymmetry exists for the distribution of these vectors within the utricle (Fernandez & Goldberg, 1976). However, if the same asymmetry existed in each utricle, the combined signal should cancel out. Without intimate knowledge of the distribution of these polarization vectors it is difficult to confirm this geometrical argument. The third, and perhaps most convincing, argument against this hypothesis is that any shear force differences should have appeared in the eye data. Shorter slow phase eye velocity decay rates should be associated with larger shear forces. The data indicates no difference in the decay rates for yaw turns toward NU versus RED.

An interesting follow-up study would be to conduct this same experiment with subjects' heads tilted 30 degrees pitch forward. This would ensure that the magnitude of the shear force acting in both the x and y-directions were equivalent. If the asymmetry disappeared in such an experiment it would provide decisive evidence that the differing shear forces used in the current study were responsible for the observed response disparity.

X versus Y Gain

The existence of a gain asymmetry at the physiological or psychophysical level could also account for the perceived difference in NU versus RED head turns. The problem again is that little is known about physiological gain differences of the otolith afferents in humans. What is known from squirrel monkeys indicates that little difference exists between either the resting discharge rates or sensitivities of polarization vectors in the x or y directions (Fernandez & Goldberg, 1976). Subjective estimates of linear acceleration threshold or sensitivity differences about the x and y axis encounter many of the same

issues previously discussed in the determination of subjective rotation. The problem is further compounded by the fact that the utricles measure both translational and gravitational linear accelerations. One study reports slightly larger sensitivity to tilt in roll than in pitch during sub-threshold movements in these axes (Otakeo, Matthews, Folio, Previc, and Lessard, 2002). If true, this effect alone or combined with the shear force differences in x versus y directions, could account for the findings in this study.

6.5.2 Otolith-Canal Interaction

Several researchers have demonstrated the otolith system's capability of modifying the nystagmus response to angular accelerations (Benson and Bodin, 1966; Benson, 1974; Merfeld, 1999). Experimental evidence has shown that the post-rotational position of the head with respect to gravity is able to modify the time rate of decay of slow phase eye velocity (SPV). The exact mechanism of this process is unclear, but it is thought that duration of nystagmus is shortened either through a modification of the adaptation time constant of the semicircular canals or through a 'dumping' of velocity storage information. Velocity storage ordinarily prolongs the response to constant velocity rotation by keeping a record of previous rotation information. This information decays over time, thereby acting like a 'leaky' integrator.

A similar 'dumping' mechanism may be at work in this experiment. If this were the case, the time constant of SPV decay would be different for head turns toward NU versus RED. No significant effects on time constant were discovered, however. This time

constant also did not demonstrate any significant habituation or adaptation effects throughout the experiment.

6.5.3 CNS Processing of Otolith-Canal Interactions

One possible source remains to aid in an explanation of the results derived from this study. The inferior vestibular nucleus receives signals from both the semicircular canals and the otoliths and in turn sends signals into both the cerebellum and the reticular formation of the brain stem. From here these signals are passed upward to the cerebral cortex to apprise the psyche of the spatial orientation and equilibrium status of the body. Since the differences in NU versus RED head turns on the centrifuge appeared primarily in the subjective measures of magnitude and duration, it seems appropriate that subjective processing centers of the brain are specifying this difference. The unanswered question is why?

A speculative answer may be found in the GIF conflict resolution theory. This theory, in part, states that when a conflict between the brain's estimate of GIF and the end organ's measurement of GIF exists, a longer or perhaps more involved process for resolving this discrepancy is invoked (Zupan, Peterka, & Merfeld, 2000). For example, when a subject made head turns toward NU on the centrifuge, the dominant sensation evoked was one of a body pitch upwards. For purposes of illustration, let's say this pitch sensation had a magnitude of 90 degrees. Based upon the pitch canal information, the brain would estimate that the GIF is located in the long-body $-z$ -axis. Conflict arises because no actual pitch occurred, and the maculae are detecting the GIF in the naso-occipital $-x$ -axis. For RED head turns, the dominant subjective sensation of movement was one of body

roll. This sensation presents no conflict with the GIF, as one is simply rolling about an axis coplanar with earth gravity. The larger GIF error induced by NU head turns may be responsible for making this type of turn a more provocative one.

6.5.3.1 Subjective Descriptions of Illusory Motion

Seven of the subjects in this study experienced sensations similar to model predictions, i.e. a combination of pitch and roll sensations for both NU and RED head turns. For five of the participants in this study, the response of the pitch canal tended to subjectively mask or dominate the response of the roll canal during RED head turns. Pitch canal stimulation was responsible for a sense of body-pitch up for NU turns, and for a sense of body-roll for RED head turns with respect to the platform of the centrifuge. The opposite is true for roll canal stimulation. For whatever reason, these subjects reported very little pitch motion associated with head turns toward RED.

Of the remaining subjects, three of them experienced tumbling sensations while making yaw head turns on the centrifuge. Two of these subjects regularly reported a feeling of completing two full rotations about the roll-axis for RED turns and about the pitch-axis for NU turns. The other subject felt at most one complete rotation of *both* roll and pitch for each type of head turn. The one subject not yet categorized, felt primarily rolling motion for NU turns, and a strong sense of yaw motion for RED turns. Plots of the average motion sensations experienced by all subjects can be found in Appendix D.

6.5.3.2 Subject Grouping by Amount of GIF Conflict

An attempt was made to categorize the participants of this study according to the amount of GIF conflict present based upon their verbal descriptions of self-motion. These groups were presented in Chapter 5 along with graphical representations of the average perceived motion for each grouping. Recall that these groups were:

Group 1: Large GIF conflict in NU head turns and very little for RED turns (5 subjects).

Group 2: Similar GIF conflict in both NU and RED head turns (7 subjects).

Group 3: Large GIF conflict in RED head turns and very little for NU turns (1 subject).

Group 4: Tumblers (3 subjects)

A subject was placed in Group 1 if the sum of the average perceived motion in the pitch and yaw planes for NU head turns was at least twice the magnitude of the sum of perceived pitch and yaw motion for RED turns. Only one subject in this group was somewhat close to this minimum criterion, while the others had greater than four times the magnitude of perceived motion for NU turns than for RED.

If the sum of the average perceived motion in the pitch and yaw planes for RED turns were at least twice the magnitude of NU turns, they were assigned to Group 3. Only one of the participants in this study exhibited this characteristic. Group 4 was reserved for subjects whose average magnitude of perceived motion in any plane for both NU and RED turns exceeded 360 degrees. All other subjects were assigned to Group 2.

Had it not been for the tumbling sensation, two of the Group 4 subjects would have been ideal Group 1 members, and the other would have fit nicely into Group 2. A separate classification for these subjects was created for three reasons. One reason is that it is more difficult to ascertain the exact nature of the GIF conflict. For instance, the conflict

would reach a maximum at every odd multiple of 180 degrees of rotation and would disappear entirely for every multiple of 360 degrees. Another reason is that these subjects may contain a very weak internal estimate of the gravitational vertical. Testing of the subjective visual vertical in one of these subjects revealed an average error in the estimate of earth vertical by 82 degrees (nearly earth horizontal, along the body axis) toward the head while lying right shoulder down. A final reason for separating these individuals is that their subjective measures of magnitude and duration were interesting in its own right. All of these subjects reported much higher magnitude estimates for NU turns than for RED. Paradoxically, they reported that the duration of illusory sensations lasted longer for RED turns.

6.5.3.3 Analysis of GIF Conflict Groups

As illustrated in Chapter 5, significant differences for the subjective measures of duration and magnitude estimates existed between Groups 1 and 2. If the magnitude of GIF conflict is specifying the asymmetry between NU and RED head turns we should expect that Group 1 subjects would have larger differences in their estimates of magnitude and duration between these two types of head turns. This is exactly what was found. The differences in magnitude and duration estimates for NU versus RED head turns were significantly larger in Group 1 than in Group 2. In fact, almost no difference in duration estimates existed for Group 2 subjects. Group 3 contained only one subject rendering a statistical analysis untenable. However, it is interesting to note that this subject had longer duration estimates for RED head turns as this theory would predict.

6.5.3.4 Possible Concerns with GIF Conflict Theory

The GIF conflict resolution theory appears to provide a reasonable explanation for the asymmetry observed during yaw head turns on the centrifuge, however, several caveats warrant mentioning. First, this explanation only takes into account the subjective descriptions of motions experienced by subjects. Both the roll and pitch semicircular canals are involved during yaw head turns on the centrifuge. The fact that roughly 30% of the participants in this study described motion attributed solely to pitch canal stimulation for RED turns, while interesting, does not explain why roll canal stimulation was not perceived by these subjects. One explanation is that the subjective reports were in error. The stimuli presented in this study are so novel and complex that subjects may have had difficulty verbalizing their experiences, although subjects reported that the accuracy of their assessments improved after the first few head turns. The other possibility is that some interesting ensemble processing of the canal afferent signals is occurring at the level of the psyche.

A second reason for concern is that the verbal accounts of self-motion are a somewhat noisy measure as evidenced by the difficulty some subjects had in accurately describing both the magnitude and direction of illusory motion. Third, this explanation does not match the data perfectly. For instance, those subjects placed in Group 2 should have perceived no difference between NU and RED head turns. While this was the case for duration estimates, these subjects still reported significantly higher magnitude estimates for NU head turns. Another point is that this theory would predict shorter duration estimates for RED turns in Group 1 (very little GIF conflict) than those of Group 2. The

data shows that Group 1 had duration estimates nearly twice as long as Group 2 for the same RED head turns.

6.6 Pragmatic Aspects of this Study

The results of this investigation indicate that earth's gravitational field plays a key role in interpretation of the stimulus induced by making yaw head turns in a rotating environment. A recent study involving angular VOR gain adaptation also confirms this hypothesis (Yakushin, Raphan, and Cohen, 2000). In this investigation, monkey's aVOR gain was adapted during centrifugation in one of three different head positions with respect to gravity. Transference of this adaptation did not occur when the animal was subsequently centrifuged in the other two head positions, but was retained in the originally adapted head position. Since the canal input was the same in all three head positions, the authors contend that the head's position with respect to gravity is specifying the context for adaptation. They also suggest that this context is stored somewhere in the central vestibular system where otolith-canal signals converge.

Based on this evidence, problems may arise for astronauts pre-adapted to artificial gravity on earth when making head turns in a rotating environment on orbit. The difference between the earth-based expected stimulus and the actual stimulus while on orbit may unnecessarily complicate the adaptation process. Indeed, the absence of gravity in space may even lead to an erroneous updating of the internal estimator (Glasauer and Mittelstaedt, 1998). The danger is that a new adaptation strategy to the rotating environment in weightlessness would not occur at all. The other possibility is that the

time course of obtaining a new strategy will frustrate and discourage astronauts to the point where they no longer use the artificial gravity device, thereby negating all of its beneficial effects.

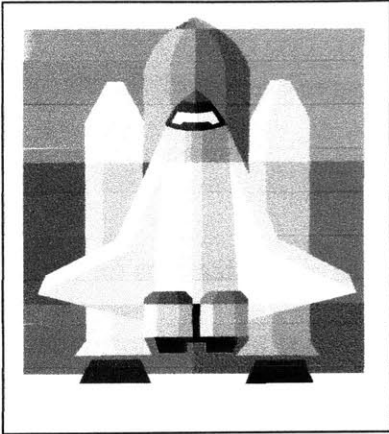
6.5 Recommendations

More work is required to determine exactly how gravity specifies the context in which adaptation to the rotating environment occurs. The current investigation has narrowed the list of possibilities, but has not determined the specific mechanism. A simple follow-up study would be to perform this same experiment with subjects' heads tilted 30 degrees forward to place the principal plane of the utricular maculae in the yaw head rotation plane. This would help determine whether or not the magnitude of the shear force acting on the otoliths is of primary importance. Better angular and linear acceleration threshold studies could also be carried out to establish whether any true directional asymmetries exist.

The adaptation transference investigation conducted by Yakushin, et al, (2000) should be performed on human subjects. In such an experiment both the perceptual and physiological aspects of whether adaptation depends upon a gravity cue could be further probed. A human centrifuge aboard the International Space Station would be beneficial for a number of reasons. In regard to this investigation, it could also be used to determine whether earth-based adaptation to the rotating environment effectively transfers to the weightless environment.

The GIF conflict resolution theory offered an intriguing explanation for the findings of this study. However, better experiments could be designed to specifically explore the

nature of this theory. A simplification of the canal stimulus, i.e. restricting illusory motion to one plane, would allow for more accurate descriptions of self-motion. The theory could be refuted or confirmed by presenting two such stimuli to each subject; one in which a GIF conflict arises, and one in which no conflict is present.



Chapter 7

Conclusion

Seventeen subjects participated in this study designed to further investigate a previously discovered asymmetry in the response to nose up versus ear down head turns made in a rotating environment. The major dependent variables included the amplitude and time rate of decay of vertical nystagmus, along with the subjective analog of these measures, namely, the magnitude and duration of illusory sensations associated with head movements aboard the centrifuge. The main finding is that head turns made toward the nose up position proved more powerful in terms of subjective reports of duration and magnitude than similar turns made toward a right ear down position. This result was not reflected in the eye data, suggesting a disassociation between physical and psychophysical experiences.

Several hypotheses have been proposed to account for this asymmetry. The results of this experiment indicate that it is the relationship of the head with respect to gravity that is specifying the difference. The exact role this graviceptive information plays is not entirely clear. An intriguing explanation is that the brain's interpretation of the interaction

between otolith and canal signals may be responsible. These signals are easier to process when they are in accord with one another. Conflicting signals may invoke an error resolution program resulting in a more confusing and provocative experience for the subject.

From a practical perspective, the results of this investigation have implications for the design of protocols used to adapt astronauts, to the cross-coupled stimuli of short-radius centrifugation. Recent work suggests that this adaptation is context specific. Since gravity appears to be a key component of this context, any earth-based adaptation achieved may be difficult to transfer to the weightless environment of space.

Future studies should be performed to determine the exact mechanism gravity plays in adaptation to the rotating environment.

References

- Balkwill, M.D. (1992). *Changes in Human Horizontal Angular VOR after the Spacelab SLS-1 mission*. Unpublished S.M. Thesis, Massachusetts Institute of Technology.
- Benson, A.J. (1974). *Modification of the response to angular accelerations by linear accelerations*. In: Kornluber HH, (ed.) *Handbook of Sensory Physiology*, Vol VI/2: Vestibular System. Springer Verlag New York, p.281-320.
- Benson, A.J., Bodin, M.A.(1966a). Comparison of the effect of the direction of the gravitational acceleration on post-rotational responses in yaw, pitch, and roll. *Aerospace Medicine*, 37, 889-897.
- Benson, A.J., Bodin, M.A.(1966b). Interaction of linear and angular accelerations on vestibular receptors in man. *Aerospace Medicine*, 37, 144-154.
- Brown, E. (2002). *Artificial Gravity: The role of visual inputs in adaptation to short-radius centrifugation*. Unpublished SM Thesis, Massachusetts Institute of Technology.
- Burton, RR & Meeker, LJ (1992). *Physiologic validation of a short-arm centrifuge for space application*. *Aviation Space, and Environmental Medicine*, 63 (6), 476-481.
- Burton, R.R. & Meeker, L.J. (1997). Taking gravity into space. *Journal of Gravitational Physiology*, 4(2), 17-20.
- Burton, R.R. (1994). Artificial gravity in spaceflight. *Journal of Gravitational Physiology*, 1(1), 15-18.
- Caiozzo, V. J. Baker, M.J., Herrick, R.E., Tao, M., and K. M. Baldwin. (1994). Effect of spaceflight on skeletal muscle: mechanical properties and myosin isoform content of a slow muscle. *Journal of Applied Physiology*. 76, 1764-1773.
- Carlstrom, D., Engstrom, H., and Hjorth, S. (1953). Electronmicroscopic and x-ray diffraction studies of statoconia. *Laryngoscope* 63, 1052-1057.
- Cheung, C.C. (2000). *Regulator control of a short-radius centrifuge and subjective responses to head movements in a rotating environment*. Unpublished S.M. Thesis, Massachusetts Institute of Technology.
- Churchill, S.E. (1997). *Fundamentals of Space Life Sciences*. Malabar, FL: Krieger Pub Co.
- Clément, G., Wood, S.J., Lathan, C. E., Peterka, R. J., & Reschke, M. F. (1999). Effects of body orientation and rotation axis on pitch visual-vestibular interaction. *Journal of Vestibular Research*, 9, 1-11.

- Cramer, D. & Graybiel, A. Some physiological aspects of artificial gravity. *The Role of Vestibular Organs in Space Exploration*, 73-83.
- Diamandis, P.H. (1988). *The artificial gravity sleeper: A deconditioning countermeasure for long duration space habituation*. Unpublished S.M. Thesis, Massachusetts Institute of Technology.
- Diamandis, P.H. (1997). *Countermeasures and artificial gravity*. In S.E. Churchill (Ed.), *Fundamentals of space life sciences*. Malabar, FL: Krieger.
- Draper MH (1998). *The Adaptive Effects of Virtual Interfaces: Vestibulo-Ocular Reflex and Simulator Sickness*. Doctoral Dissertation, University of Washington.
- Fernandez, C. & Goldberg, J.M. (1976). Physiology of peripheral neurons innervating otolith organs of the squirrel monkey. I. Response to static tilts and to long-duration centrifugal force. *Journal of Neurophysiology*, 39, pp 970-984.
- Furman, J.M. & Schor, R.H. (2001). Semicircular canal-otolith interaction during off-vertical axis rotation in humans. *Journal of the Association for Research in Otolaryngology*. 2/1, 22-30.
- Furman, J.M. & Schor, R.H. (1997). The influence of otolithic stimulation on the velocity storage system. ARO Midwinter Research Meeting, p.127 (abstracts).
- Glasauer, S., & Mittelstaedt, H. (1998). Perception of spatial orientation in microgravity. *Brain Research Reviews*, 28, 185-193.
- Glasauer, S. & Merfeld, D. (1997). Modelling three-dimensional vestibular responses during complex motion stimulation. In *Three-dimensional kinematics of eye, head and limb movements*, M. Fetter, T. Haslwanter and H. Misslisch (Eds.), Harwood academic publishers, Amsterdam, 387-98.
- Goldberg JM & Fernandez C (1971). Physiology of peripheral neurons innervating semicircular canals of the squirrel monkey. I. Resting discharge and response to constant angular accelerations. *Journal of Neurophysiology*, 34 (4), 635-60.
- Gray, H. (1970). The organs of the senses. In C.M. Goss (Ed.), *Gray's anatomy* (28th ed.) (pp. 1091-1098). Philadelphia: Lea & Febiger.
- Graybiel A. (1997). "Some Physiological Effects of Alternation Between Zero Gravity and One Gravity." *Space Manufacturing Facilities (Space Colonies): Proceedings of the Princeton / AIAA / NASA Conference, May 7-9, 1975, pages 137-149*. Edited by Jerry Grey. American Institute of Aeronautics and Astronautics.

Grigorova, V. & Kornilova, L. (1996). Microgravity effect on the vestibulo-ocular reflex is dependent on otolith and vision contributions. *Aviation, Space and Environmental Medicine*, 67, 947-54.

Guedry, F.E. (1965). Habituation to complex vestibular stimulation in man: transfer and retention of effects from twelve days of rotation at 10 r.p.m. *Perceptual and Motor Skills*, 21, 459-481. (Monograph Supplement 1-V21).

Guedry, F.E. (1974). *Psychophysics of vestibular sensation*. In Editors: H. Autrum, R. Jung, W.R. Loewenstein, D.M. MacKay, & H.L. Teuber (Eds.), *Handbook of Sensory Physiology*, 1(pp. 18-103). New York: Springer Verlag.

Gurovsky, N.N., Gzenko, O.G., Adamovich, B.A., Ilyin, E.A., Genin, A.M., Korolkov, V.I., Shipov, A.A., Kotovskaya, A.R., Kondratyeva, V.A., Serova, L.V., & Kondratyev, Yu.I. (1980). Study of physiological effects of weightlessness and artificial gravity in the flight of the biosatellite Cosmos-936. *Acta Astronautica*, 7, 113-121.

Guyton, A. C., & Hall, J.E. (1996). In: Textbook of medical physiology, W. B. Saunders: Philadelphia. edition 9.

Hecht, H., Kavelaars, J., Cheung, C. & Young, L.R. (2001). Artificial gravity: Orientation illusions and heart rate changes during short radius centrifugation. *Journal of Vestibular Research* Volume 11, Number 2/2001, pp. 115-127.

Howard IP, Cheung BSK, Landoldt J (1988). Influence of vection axis and body posture on visually-induced self rotation. *Advisory Group for Aerospace Research and Development* 433:15-1 to 15-8.

Koizuka, I., Schor, R.H., Furman, J.M. (1996). Influence of otolith organs, semicircular canals, and neck afferents on postrotatory nystagmus. *Journal of Vestibular Research*. 6(5), 319-329.

Kotovskaya, A.R., Galle, R.R., & Shipov, A.A. (1981). Soviet research on artificial gravity. *Kosmicheskaya Biologiya I Aviakosmicheskaya*, 2, 71-79.

Lyne, L. (2000) *Artificial gravity: Evaluation of subjective adaptation of head movements during short-radius centrifugation*. Unpublished S.M. Thesis, Massachusetts Institute of Technology.

Mach, E. (2001). *Fundamentals of the Theory of Movement Perception*. (Translated and Annotated by Young, L.R., Henn, V., and Scherberger, H.). Kluwer Academic / Plenum Publishers. New York.

Mach, E. (1886). *Beitrage zur Analyse der Empfindungen*. Jena: Fisher. English translation by C.M. Williams, revised and supplemented by Sydney Waterlow, 1959. New York: Dover.

Mast, F. & Jarchow, T. (1996). Perceived body position and the visual horizontal. *Brain Research Bulletin*. 40(5), 393-398.

Meiry, J.L. (1965). *The vestibular system and human dynamic space orientation*. Unpublished S.M. Thesis, Massachusetts Institute of Technology.

Melvill Jones, G. (1977). Plasticity in the adult vestibulo-ocular arc. *Phil. Trans. R. Soc. Lond. B*. 278, 319-334.

Merfeld DM, Young LR, Oman CM, Shelhamer MJ (1993). A multidimensional model of the effect of gravity on the spatial orientation of the monkey. *Journal of Vestibular Research*, 3, 141-161.

Merfeld DM (1995). Modeling the vestibulo-ocular reflex of the squirrel monkey during eccentric rotation and roll tilt. *Exp Brain Res*, 106: 123-134.

Merfeld DM, Zupan L, Peterka RJ (1999). Humans use internal models to estimate gravity and linear acceleration. *Nature*, 398: 615-618.

Mittelstaedt, H (1988). *The information processing structure of the subjective visual vertical. A cybernetic bridge between its psychophysics and its neurobiology*. In: Marko H.; Hauske, G.; Struppler, A., eds. *Processing structures for perception and action*. Weinheim: VCH-Verlagsgesellschaft; pp. 217-263.

Otakeno, S., Matthews, R.S.J., Folio, L., Previc, F., & Lessard, C.S. (2002). The effects of visual scenes on roll and pitch thresholds in pilots versus nonpilots. *Aviation, Space and Environmental Medicine*. 73, 98-101.

Paige, G. (1983). Vestibuloocular reflex and its interactions with visual following mechanisms in the squirrel monkey. I. Response characteristics in normal animals. *Journal of Neurophysiology*. Vol 49. No 1. pp. 134-151.

Raphan, T., Cohen, B., & Henn, V. (1981). Effects of gravity on rotatory nystagmus in monkeys. *Ann. N.Y. Acad. Sci.* 545, 29-50.

Raphan, T., Cohen, B., & Matsuo, V. (1977). A velocity storage mechanism responsible for optokinetic nystagmus (OKN) optokinetic after-nystagmus (OKAN) and vestibular nystagmus. In: Baker, R. Brthoz, A., (eds) *Control of Gaze by Brainstem Neurons*. Elsevier/North Holland Biomedical Press Amsterdam. Pp 37-47.

Robinson, D.A. (1977). Vestibular and optokinetic symbiosis: An example of explaining by modeling. *Control of Gaze by Brainstem Neurons. Development in Neurosciences*. Vol 1. edited by Barker and Berthos. Elsevier/North-Holland Biomedical Press.

- Sharp PE, Blair HT, Etkin D, Tzanetos DB (1995). Influences of vestibular and visual-motion information on the spatial firing patterns of hippocampal place cells. *Journal of Neuroscience*. 15:173–189
- Shelhamer, M, Robinson, DA, & Tan, HS (1992). Context-specific adaptation of the gain of the vestibulo-ocular reflex in humans. *Journal of Vestibular Research*, 2, 89-96.
- Shenkman, B. S. & Kozlovskaya, I.B. (2000) “*Results of studies on the effects of spaceflight factors on human physiological systems and psychological status, and suggestions of future collaborative activities between the NSBRI and the IBMP.*” NSBRI Institute for Biomedical Problems, Section 3: Muscles.
- Shipov, A.A., Kotovskaya, A.R., & Galle, R.R. (1981). Biomedical aspects of artificial gravity, R.R., Institute of Biomedical Problems, USSR Ministry of Health, Moscow, USSR, *Acta Astronautica*, 8(9-10), 1117-1121.
- Sienko, K.H. (2000): *Artificial Gravity: Adaptation of the vestibulo-ocular reflex to head movements during short radius centrifugation*. Unpublished S.M. Thesis, Massachusetts Institute of Technology.
- Smith, P.F. (1997). Vestibular-hippocampal interactions. *Hippocampus* 7:465–471
- Steinhausen, W. (1931). Über den Nachweis der Bewegung der Cupula in der intakten Bogengangsampulle des Labyrinthes bei der natürlichen rotatorischen und calorischen Reizung. *Pflugers Arch. Ges. Physiol.* 228, 322-328.
- Stone, R.W. (1970). *An overview of artificial gravity* [NASA SP-314] (pp. 23-33). Pensacola, FL: Naval Aerospace Medical Research Laboratory. Rpt. In Fifth Symposium on the Role of the Vestibular Organs in Space Exploration, Washington, DC.
- Udo de Haes, H. A. & Schöne, H. (1970). The effectiveness of the statolith organs in human spatial orientation. *Acta Otolaryngologica*, 69, 25-31.
- Van de Vegte J (1994). *Feedback Control Systems: 3rd Edition*. Englewood Cliffs, NJ: Prentice-Hall, Inc.;
- Van Egmond, A. A. J., Groen, J. J., and Jongkees, L. B. W. (1949). The mechanics of the semicircular canals. *Journal of Physiology*. 110, 1-17.
- Wall, C. 3rd (1987). Eye movements induced by gravitational force and by angular acceleration: their relationship. *Acta Oto-Laryngologica*, 104, 1-6.
- Wilson V, and Jones GM (1979), *Mammalian Vestibular Physiology*. New York, NY: Plenum Press.

- Welch, R.B., Bridgeman, B., Williams, J.A., & Semmler, R. (1998). Dual adaptation and adaptive generalization of the human vestibulo-ocular reflex. *Perception and Psychophysics*, 60(8), 1415-1425.
- Yakushin, S.B., Raphan, T. Cohen, B. (2000). Context-specific adaptation of the vertical vestibuloocular reflex with regard to gravity. *Journal of Neurophysiology*. 84, 3067-3071.
- Young, L. R., Hecht, H., Lyne, L., Sienko, K., Cheung, C., & Kavelaars, J. (2001). Artificial gravity: Head movements during short-radius centrifugation. *Acta Astronautica*, 49, 215-226.
- Young, L. R. (1999). *Artificial gravity considerations for a Mars exploration mission*. In B. J. M. Hess & B. Cohen (Eds.), *Otolith Function in Spatial Orientation and Movement*. New York: New York Academy of Sciences. 871, 367-378.
- Young, L. R. (1983). *Perception of the body in space: mechanisms*. In J. M. Brookhart, V. B. Mountcastle and H. W. Magoun. *Handbook of Physiology: The nervous system III*. Bethesda, MD: American Physiological Society. 1023-1066.
- Young, L.R., Oman, C.M., and Dichgans, J.M. (1975). Influence of head orientation on visually induced pitch and roll sensation. *Aviation, Space, and Environmental Medicine*. 46(3), 264-268.
- Young, L.R. (1971). in *Control of Eye Movements* (Bach-y-Rita, P. and Collins, C.C., eds.) pp. 429-443. Academic Press, New York.
- Young, L. R., & Oman, C. M. (1970). *Modeling adaptation in the human semicircular canal response to rotation*. Transactions of The New York Academy of Sciences, Series II, 32(4), 489-494.
- Zupan, L.H., Peterka, R.J., & Merfeld, D.M. (2000). Neural processing of gravito-inertial cues in humans. I. Influence of the semicircular canals following post-rotatory tilt. *Journal of Neurophysiology*. 84, 2001-2015.

APPENDIX A: Consent Form

MASSACHUSETTS INSTITUTE OF TECHNOLOGY
MAN-VEHICLE LABORATORY
CONTEXT-SPECIFIC ADAPTATION OF OCULOMOTOR RESPONSES TO CENTRIFUGATION
CONSENT FORM

I have been asked to participate in a study on adaptation to movement in a rotating environment. I understand that participation is voluntary and that I may end my participation at any time for any reason. I understand that I should not participate in this study if I have any medical heart conditions, respiratory conditions, if I have any medical conditions which would be triggered if I develop motion sickness, if I am under the influence of alcohol, caffeine, anti-depressants, or sedatives, if I have suffered in the past from a serious head injury (concussion), or if there is any possibility that I may be pregnant. My participation as a subject on the MIT Artificial Gravity Simulator (AGS) involves either the testing of equipment or actual experimental trials.

Prior to rotation on the AGS, I will be oriented to the rotator and data acquisition instrumentation. I understand that my height, weight, heart rate, blood pressure, and general medical history may be measured and recorded. During the experiment I will lie in either the supine, the prone position, or on the side on the rotator bed. If I am in the prone or side position my head will be supported by a pivoting, cushioned headrest. The headrest will allow me to make a free range of head movements to the left and the right, and I will be in full control of my head movements at all times. If I experience any discomfort from head movements while in either the prone or the supine position, I am free to discontinue the movements at any time. During the experiment, I will also wear eye imaging goggles, angular rate sensors, and - in some conditions - a heart rate monitor. How these devices will feel has been described to me. I agree to participate in possible stationary monitoring periods before and/or after rotation.

My rotation on the AGS will not exceed the following parameters:

- -acceleration no greater than 1 rpm/s
- -G level at my feet no greater than 1.5 G
- -time of rotation not exceeding 2 hours

I understand that these parameters are well within the safe limits for short-radius rotation. I can terminate rotation at any time by pressing the emergency stop button, the use of which has been demonstrated to me.

I understand that during rotation I may develop a headache or feel pressure in my legs caused by a fluid shift due to centrifugation. I may also experience nausea or motion sickness, especially as a result of the required head movements. The experimenter may terminate the experiment if I report a pre-determined degree of motion sickness symptoms. In addition, I understand that my heart rate may increase due to the rotation speed; this is no greater than that sustained

during aerobic exercise, and will be measured before and after the experiment.

I understand that serious injury could result from falling off the AGS while it is rotating. I will be loosely restrained at by a safety belt, which is to be worn around the waist/chest at all times while the AGS is rotating. The restraint must be fastened in order for the AGS to rotate. If the restraint is unlatched, the AGS will stop automatically. In addition, the AGS is equipped with strong side railings similar to those on a hospital bed, and it is covered by a steel-framed canopy. I will be continuously monitored by at least one experimenter in the same room, and I will be equipped with a 2-way headset communication system connected to the observing experimenter. The investigator can also see me through a video camera mounted on the AGS, and in this way determine the nature of any problems that arise.

During and after the experiment I will be asked to report my subjective experience (how I feel, how I think I perceive my head movements, etc.), both verbally and by using computer animations. In addition, I will be asked to report a motion sickness rating both during and at half-hour intervals after the experiment, until I go to bed. This data will be recorded anonymously.

If I am a participant in experimental trials, I tentatively agree to return for additional trials (at most 10) requested by the experimenter. I understand that a possible protocol for an actual trial will consist of a short period of supine rest in the dark, followed by a period of head movements (ranging from 90 degrees to the left, to vertical, to 90 degrees to the right) in the dark, followed by a period of similar head movements in the light, and that this trial could be repeated many times. During these head movements, my head will move at approximately a speed of 0.25 meters per second.

In the unlikely event of physical injury resulting from participation in this research, I understand that medical treatment will be available from the MIT Medical Department, including first aid emergency treatment and follow-up care as needed, and that my insurance carrier may be billed for the cost of such treatment. However, no compensation can be provided for medical care apart from the foregoing. I further understand that making such medical treatment available, or providing it, does not imply that such injury is the investigator's fault. I also understand that by my participation in this study I am not waiving any of my legal rights (further information may be obtained by calling the Institute's Insurance and Legal Affairs Office at 253-2822).

Monetary compensation for those who are not members of the Man-Vehicle Laboratory will be \$10 per hour. Subjects from the Man-Vehicle Lab will be taken on a voluntary basis and will not be paid.

I understand that I may also contact the Chairman of the Committee on the Use of Humans as Experimental Subjects, Leigh Firn, M.D. (MIT E23-389, 253-6787), if I feel I have been treated unfairly as a subject.

I have been informed as to the nature of and the purpose of this experiment and the risks involved, and agree to participate in the experiment. In case I experience any discomfort, I am free to discontinue the head-movements any time I wish to do so.

Subject

Date

Experimenter

Date

APPENDIX B: Medical Disqualifications

- Experiences with the rotating centrifuge or other rotating devices in a research environment
- Frequent or severe headaches
- Dizziness or fainting spells
- Paralysis
- Epilepsy
- Disturbances in consciousness
- Loss of control of nervous system functions
- Neuritis
- Loss of memory or amnesia
- Lazy eye
- Cross looking of the eyes
- Cylindrical eye lenses
- Reduced eye movements
- Astigmatisms
- Ear, nose and throat trouble
- Hearing loss
- Chronic or frequent colds
- Head injury
- Asthma
- Shortness of breath
- Pain or pressure in the chest
- Medication (check for sedatives, anti-dizziness, anti-depressants, birth prevention medication is allowed)
- Substance dependence or abuse (includes alcohol, and drugs like sedatives, anxiolytics cocaine, marijuana, opiodes, amphetamines, hallucinogens or other psychoactive drugs or chemicals)
- Diagnosis of psychosis, bipolar disorder or severe personality disorders
- Heart problems (check for Angina pectoris, coronary heart disease, myocardial infarction in the past, cardiac valve replacement, pacemaker.
- High or low blood pressure
- Recent loss or gain of weight
- Moderate car, train, sea or air sickness
- Thyroid trouble
- Inability to perform certain motions
- Inability to assume certain positions

APPENDIX C: Experimental Protocols

0. Recruiting subjects

- recruiting ads – general description of experiment and compensation
- first response email – thanks and check health requirements, height limitations (5'2"-6'0"), weight limitation: 200 lb
- second response email – set schedule and provide info on clothing, diet below

1. The day before the experiment

- remind participant of
 - o scheduled appointment
 - o no drugs including pain killers, caffeine
 - o wear long sleeves, pants, and closed-toe shoes
 - o no large meal before the run

2. Before the subject arrives

2.1 Room

- remove potential stationary obstruction: closet, chairs, tripods, etc.
- remove/secure potentially hazardous moving objects in lab: nothing on top of closet, lamps, etc.
- cabinet doors shut and locked
- remove or secure all loose items from sink next to centrifuge

2.2 Centrifuge

- centrifuge arrested and supported
- check if foot plate and counterweights are secure
- check if on-board equipment (batteries, camera, cables, etc.) is firmly attached
- connect appropriate accessories to slip ring BNC plate

2.3 Controls

- turn both computers on
- turn on TVs and VCRs
- label and insert videotapes
- check if all centrifuge controls are in off position !!!
- check if dial is set to 0
- plug in power cord (wall socket)
- power on tach (prevents bed from spinning when off)
- test duration switch and kill switch
- check that ISCAN is properly configured

BED
CHANNELS
0 –
1 –
2 –
3 –

2.4 Preparation of subject

- prepare data collection sheet
- give summary of experiment
- advise of potential hazards and side-effects
- test for normal vision (follow the finger)
- Rhomberg test
- sign consent form
- practice 90 deg head turn in 1 sec
- familiarize with body pitch, roll, and yaw using inflatable astronaut and reenactment
- alert to the potentially disturbing effects without biasing them what to feel
- walk through protocol and give time estimate of whole experiment
- ask for general health rating (Extremely good, Slightly better than normal, normal, Slightly worse than normal, Extremely poor)
- take down subject's weight, height, birthday, sports involvement, prior VR experience, eye and hand dominance
- mount ISCAN and check alignment on monitors
- attach head restraint to bed
- place participant **centered** on bed and adjust foot plate
- fit subject into head restraint
- attach goniometer to head restraint
- take supine blood pressure
- fasten safety belt
- power on video camera (lens cover off!)
- power on ISCAN and head tracker
- remove all moving objects from bed, also check for stray binder clips
- explain light switch
- explain panic kill switch
- provide nausea bag
- explain pitch duration switch
- practice head turns again with pitch switch
- power on control unit
- put up "Experiment in progress" sign and lock door

3. Run experiment

- calibrate ISCAN, ask participant not to adjust goggles even if they should itch
- calibrate goniometer
- place cover over goggles
- remove support and balance centrifuge
- make clearance check by rotating bed manually (1 complete revolution)
- synchronize watches and clocks
- switch off room lights
- fasten rope at end of work area to prevent accidental intrusion into centrifuge space when operating
- instruct subject when to make head turns

3.1 Controls

- double check that dial = 0, all centrifuge controls in off position
- power on control unit
- use manual or automated controls to start the bed

3.2 Collect data

- operate ISCAN to save each phase of data
- prompt and record head turns, subjective motion sickness data, pitch magnitude and direction, and comments as below:

*Experimental Note:

Phases 5 and 9 below will be counterbalanced across all subjects. This means that one half of all subjects will be presented with the experimental protocol in the order depicted below. The other half of the subjects will be presented with an identical protocol with the exception that phases 5 and 9 are interchanged. In addition, a subjective vertical assessment will be performed on each subject while positioned on his or her side with the bed remaining stationary. This assessment will be made during phase 7 in the protocol listed below. For all experiments where phases 5 and 9 are interchanged, the subjective vertical assessment will be made during phase 1.

Phase 1: Pre-rotation baseline data collection with head stationary

RED in the dark, centrifuge stationary, ISCAN collecting

BASELINE MOTION SICKNESS SCORE

30 seconds of baseline eye reflex data with the head stationary

Phase 2: Pre-rotation baseline data collection with head movements

RED in the dark, with the centrifuge stationary, ISCAN collecting

3 sets of yaw head turns (30 sec separation)

Baseline eye reflex and pitch duration data collection during the head turns.

MOTION SICKNESS SCORE following the 3rd turn

Phase 3: Ramp-up to 23-rpm with head stationary

RED in the dark, while the centrifuge ramps up to 23rpm, ISCAN collecting

MOTION SICKNESS SCORE at steady state speed

Phase 4: Pre-adaptation with head stationary

30 seconds of RED baseline eye reflex data with the head stationary in the dark, centrifuge at constant velocity, ISCAN collecting

Phase 5: Controlled head movements (subject in supine position)

centrifuge at constant velocity, ISCAN collecting

15 sets of yaw head turns (30 sec separation) with pitch duration, and **magnitude estimation reporting** for all 15 turns.

Subjective comments on illusory tilt direction and degrees following head turns 5 & 6, 11 & 12, 17 & 18, 23 & 24, 29 & 30

MOTION SICKNESS SCORE following every 3 sets of head turns

--

Phase 6: Ramp-down to 0-rpm with head stationary

RED in the dark, while the centrifuge ramps down to 0 rpm
30 sec ISCAN collecting during deceleration for 30 seconds
MOTION SICKNESS SCORE at stop

Phase 7: Rest Period

Minimum 6-minute break, subject taken out of head restraint, room lights turned on.

MOTION SICKNESS SCORE at beginning of break, after 3 minutes, and at end of break. Subject repositioned into head restraint at the end of break.

Phase 8: Ramp-up to 23-rpm with head stationary

RED in the dark, while the centrifuge ramps up to 23rpm, ISCAN collecting
MOTION SICKNESS SCORE at steady state speed

Phase 9: Controlled head movements (subject lying on right side)

centrifuge at constant velocity, ISCAN collecting

15 sets of yaw head turns (30 sec separation) with pitch duration, and **magnitude estimation reporting** for all 15 turns.

Subjective comments on illusory tilt direction and degrees following head turns 5 & 6, 11 & 12, 17 & 18, 23 & 24, 29 & 30

MOTION SICKNESS SCORE following every 3 sets of head turns

Phase 10: Ramp-down to 0-rpm with head stationary

RED in the dark, while the centrifuge ramps down to 0 rpm
30 sec ISCAN collecting during deceleration for 30 seconds
MOTION SICKNESS SCORE at stop

Phase 11: Post-rotation with head stationary

RED in the dark, centrifuge stationary, ISCAN collecting
30 seconds of baseline eye reflex data with the head stationary

Phase 12: Post-rotation with head movements

RED in the dark, with the centrifuge stationary, ISCAN collecting
3 sets of yaw head turns (30 sec separation) with pitch duration, and **magnitude estimation reporting** for all 6 turns.

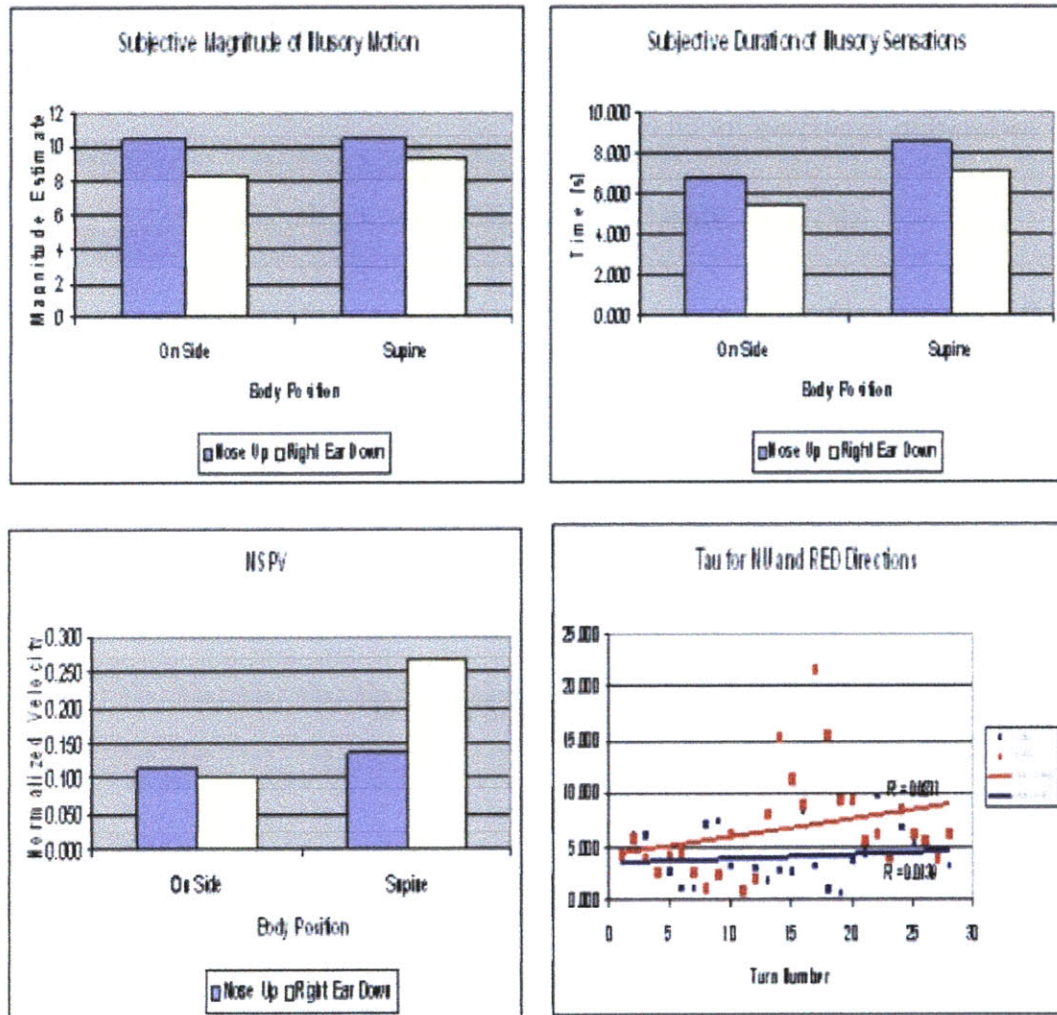
MOTION SICKNESS SCORE following the last head turn

4. After the experiment

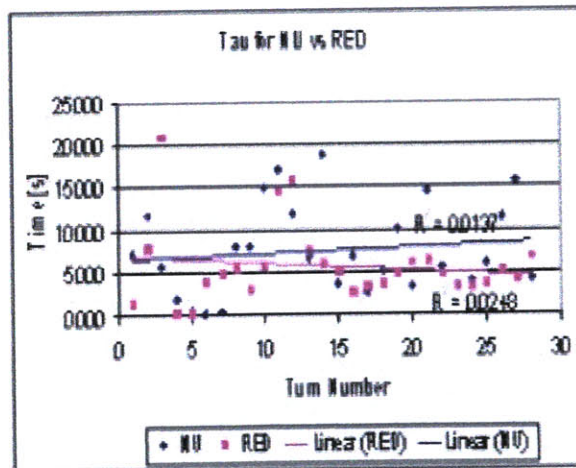
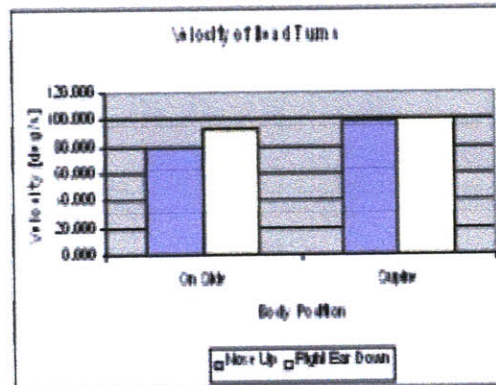
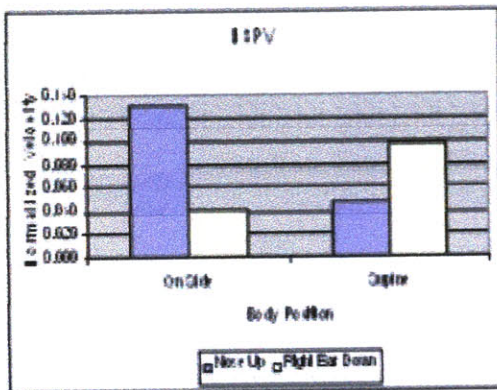
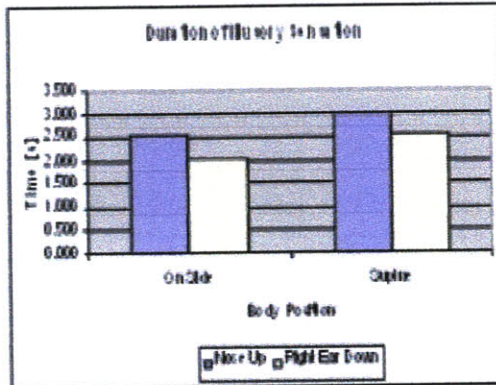
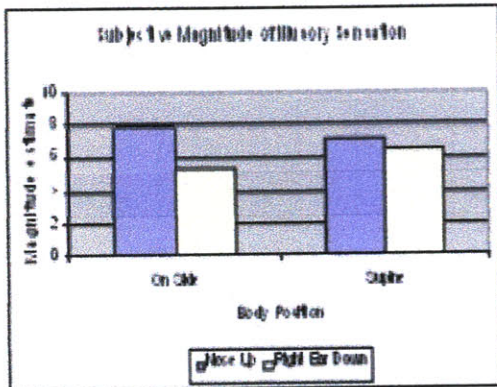
- save ISCAN data as an ASCII file
- ask subject not to move until bed is supported
- power off control unit
- remove rope
- secure bed, add weights to foot end
- power off tach (prevents bed from spinning)
- take supine blood pressure
- power off ISCAN and disconnect batteries
- power off monitoring video camera, VCR
- power off head tracker
- take off ISCAN and assist subject out of head restraint
- disconnect on-board batteries
- unplug power cord from wall
- assess Pensacola MS (where applicable)
- help participant sit up, make sure he or she is not nauseous, offer some water, then slowly help off the bed
- check for after-effects
- take standing blood pressure
- administer post-centrifuge questionnaire
- ask for any other comments the subject would like to make
- have participant sign reimbursement sheet
- provide participant with take-home MS questionnaire (need time to baseline!)
- take down "Experiment in progress" sign
- check videotape label and file as necessary

APPENDIX D: Individual Subject Data

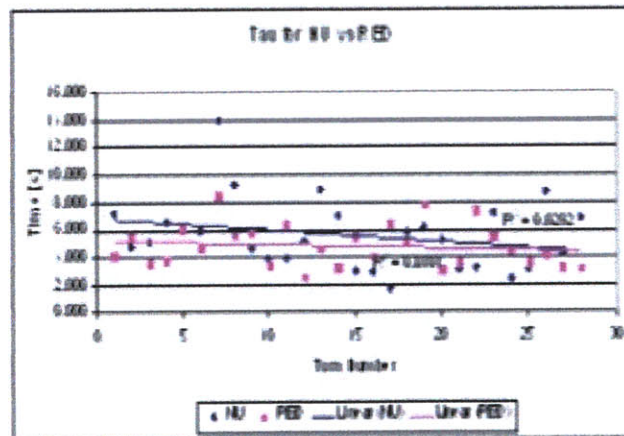
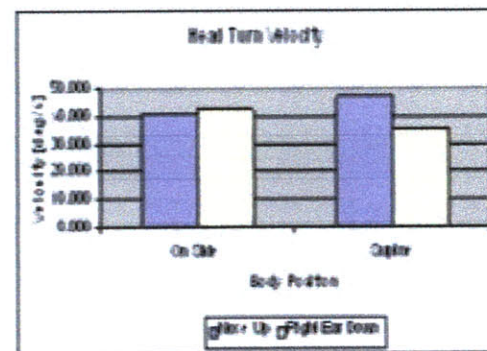
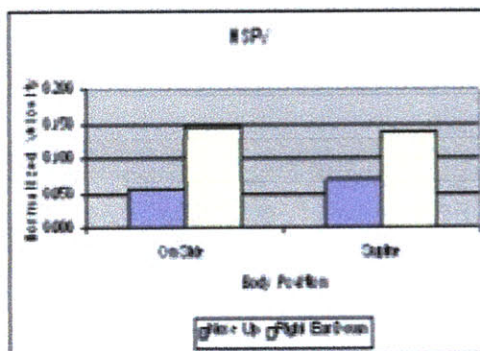
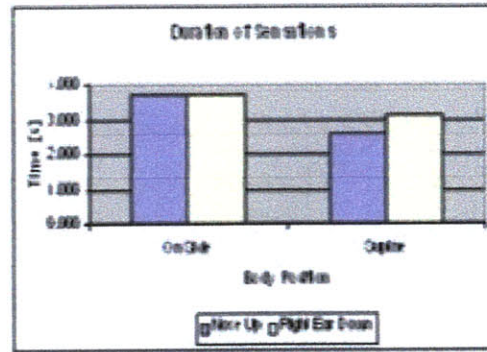
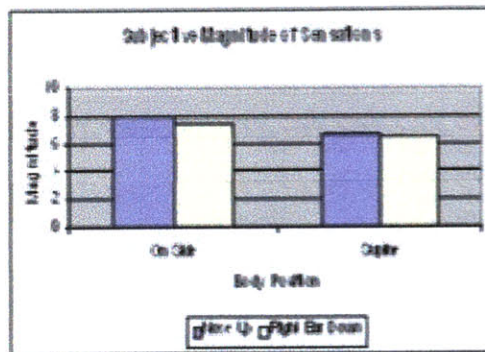
Subject 1



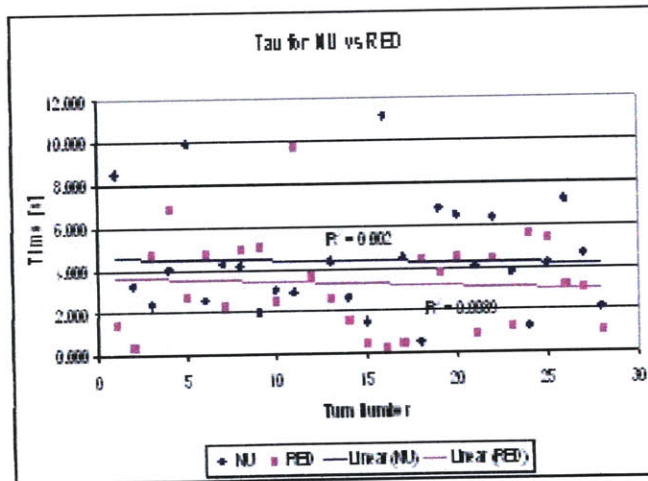
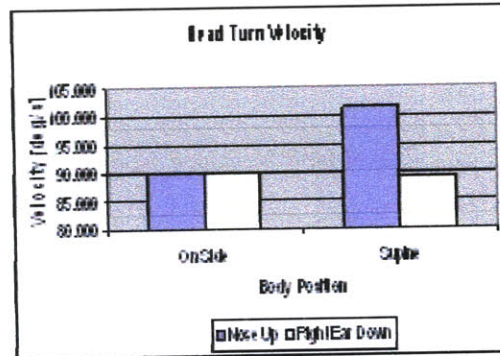
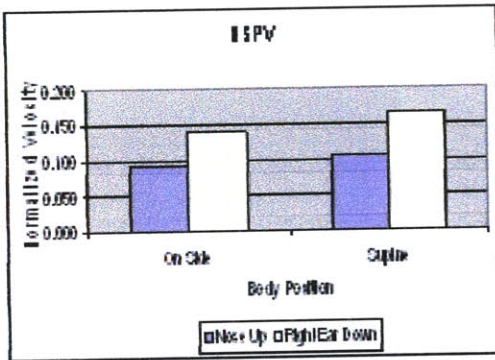
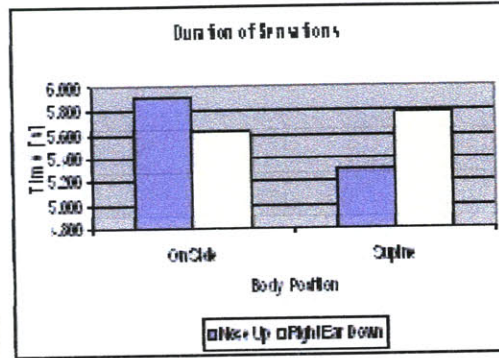
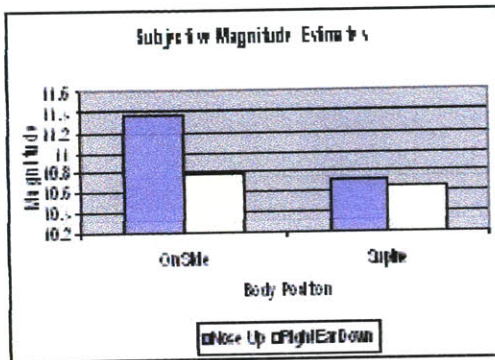
Subject 4



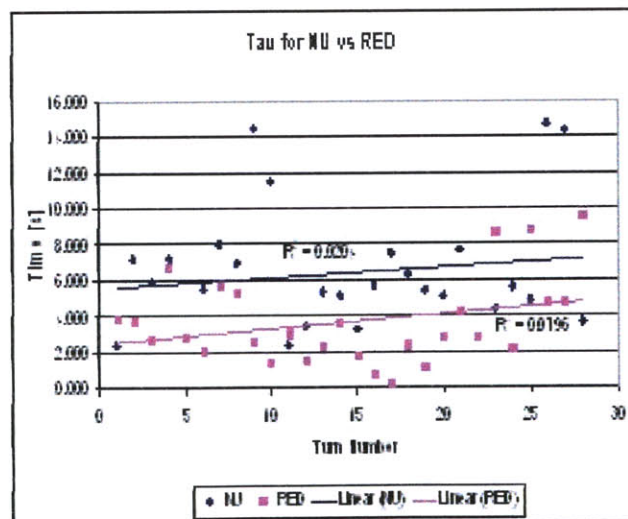
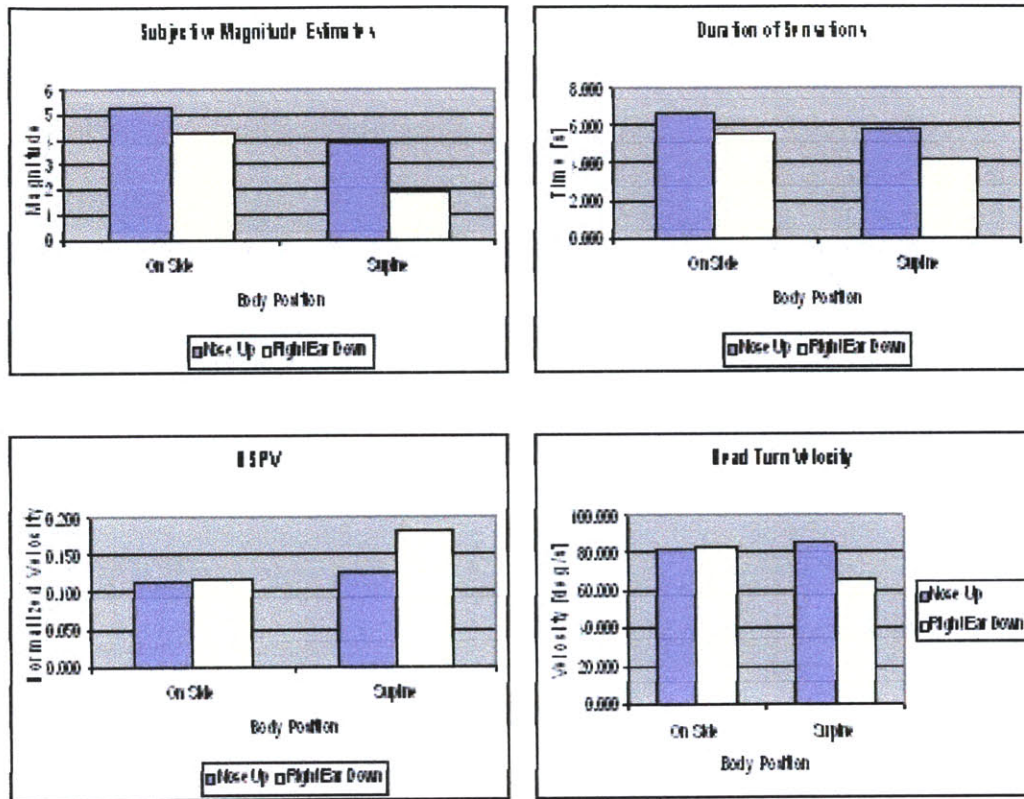
Subject 5



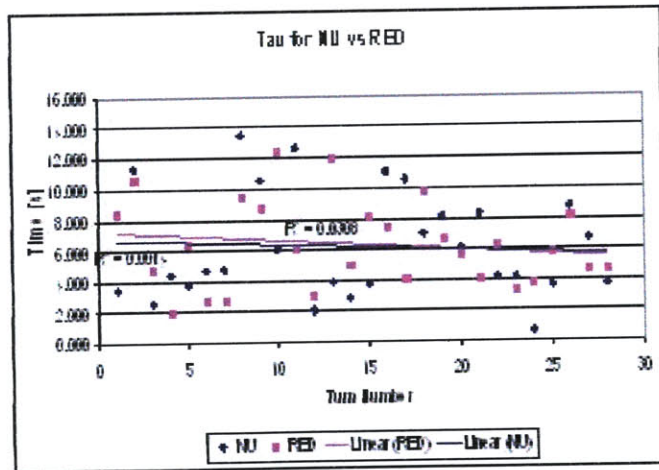
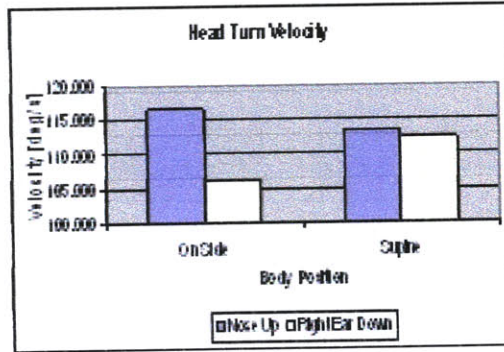
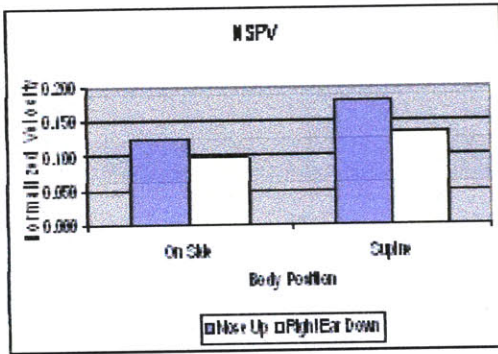
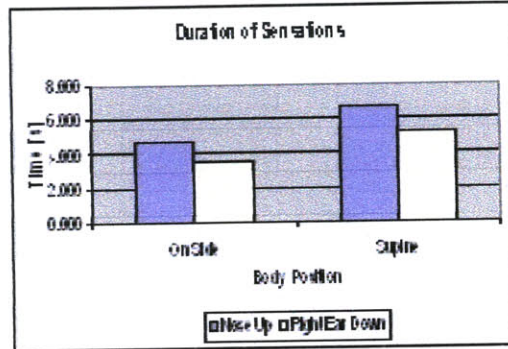
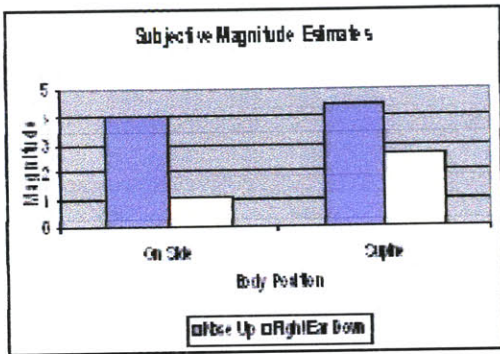
Subject 6



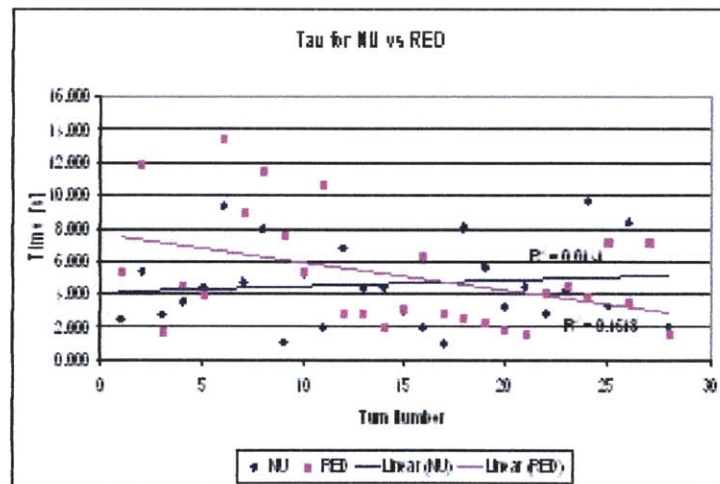
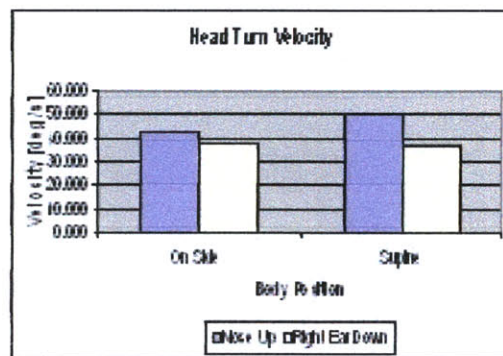
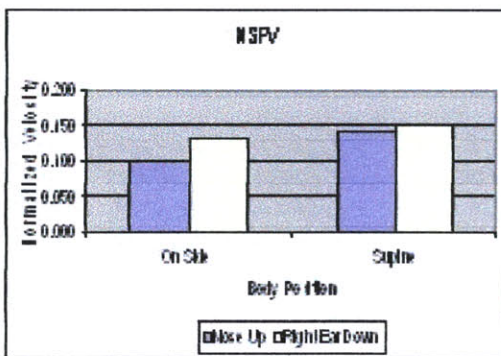
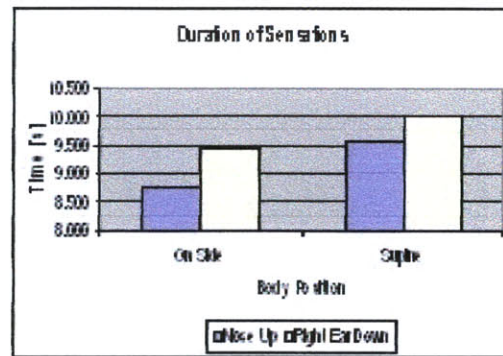
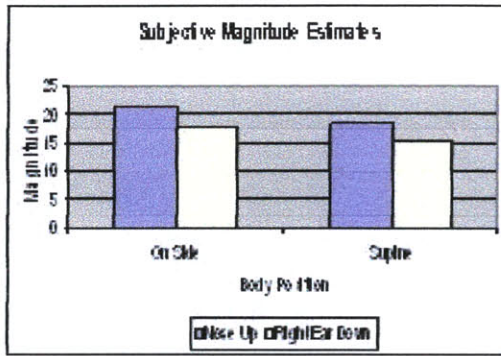
Subject 8



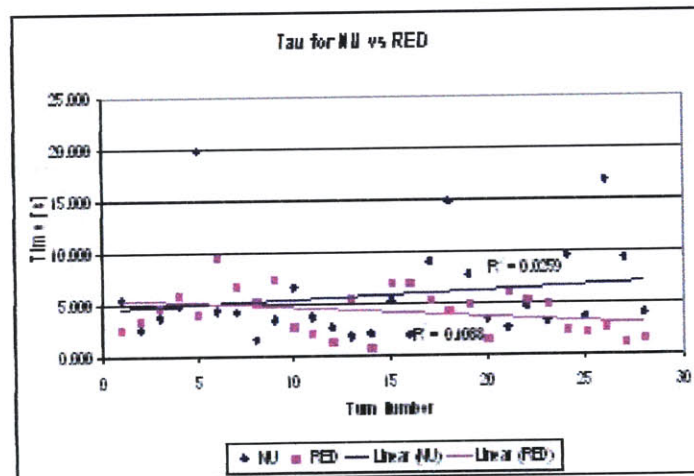
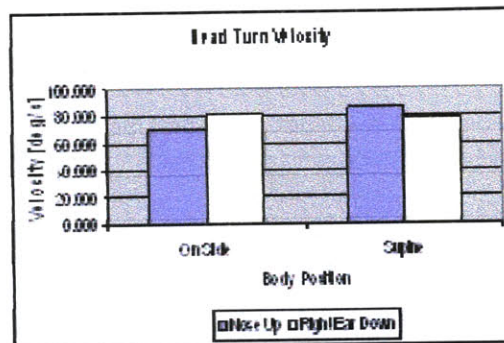
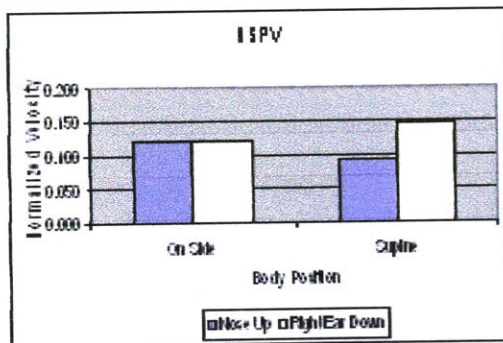
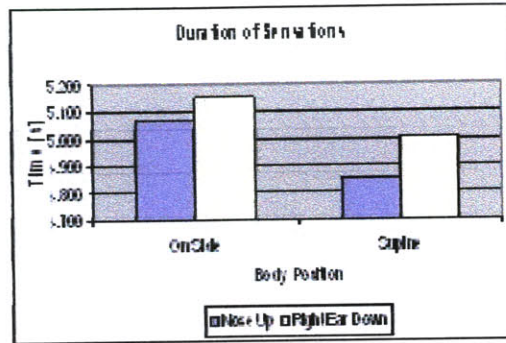
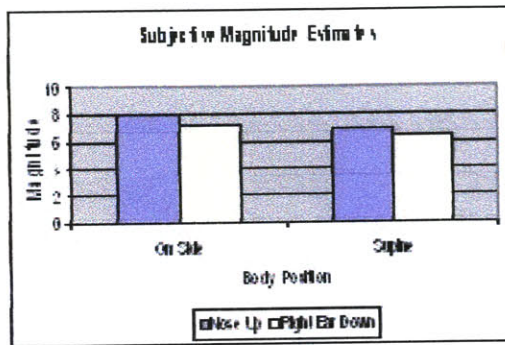
Subject 9



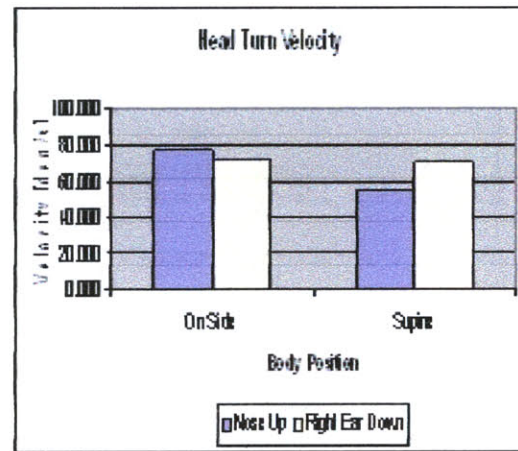
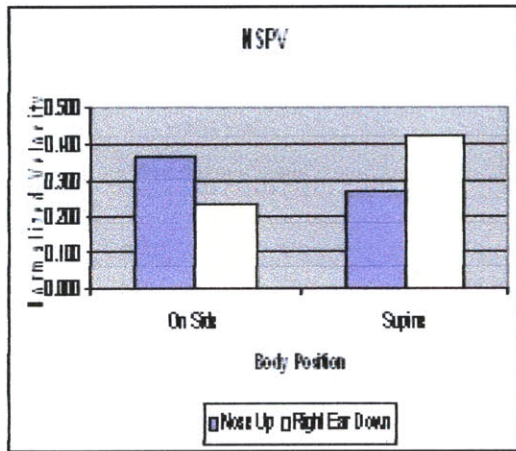
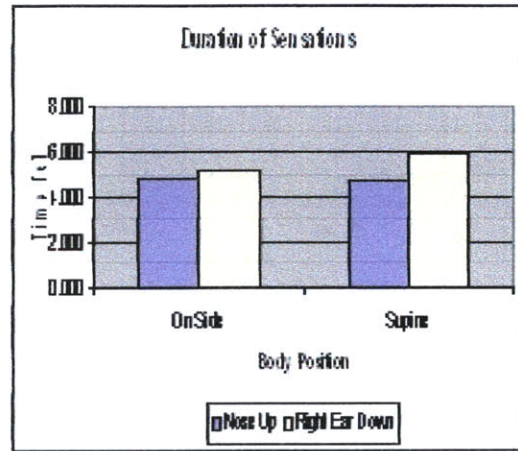
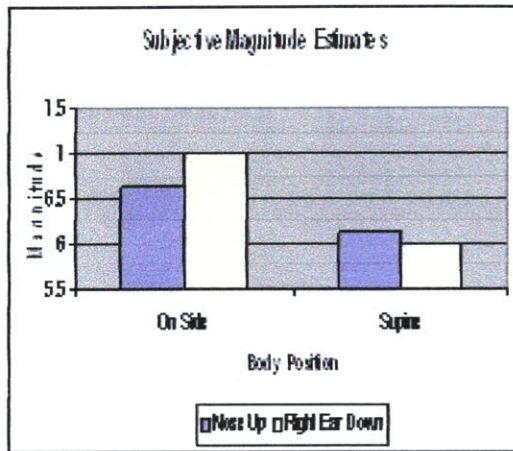
Subject 10



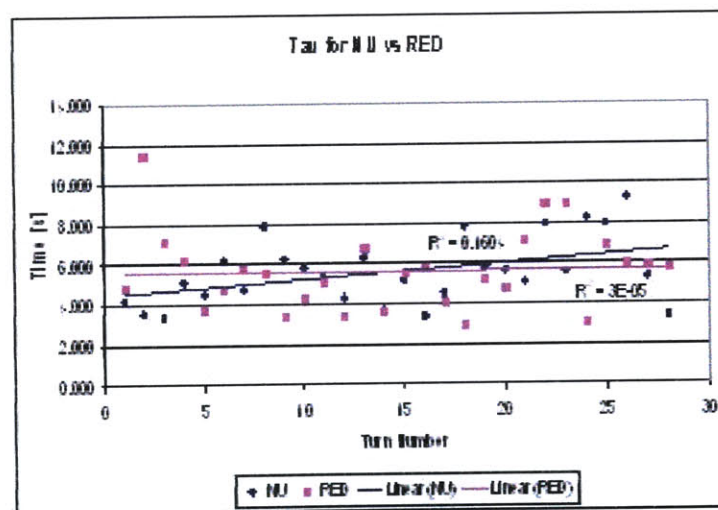
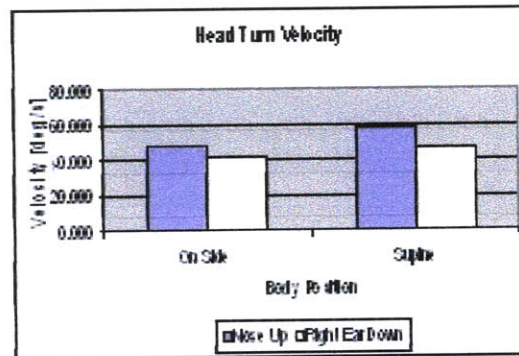
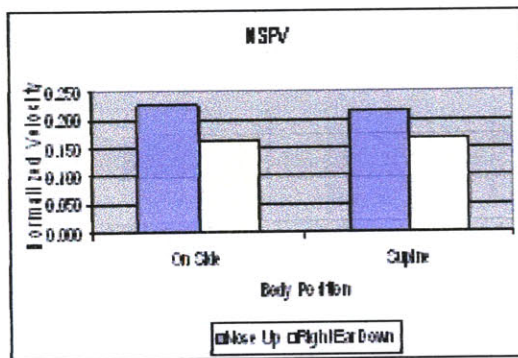
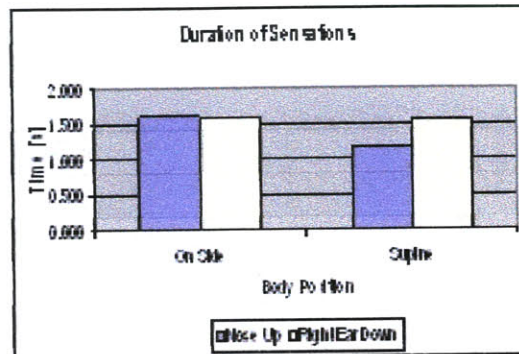
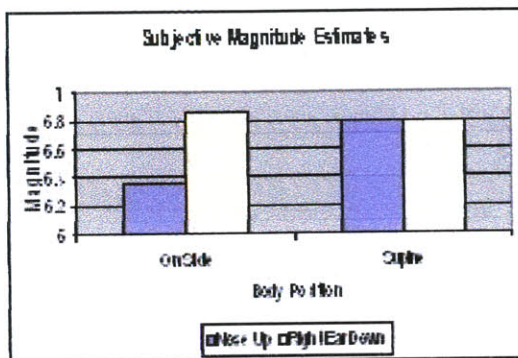
Subject 11



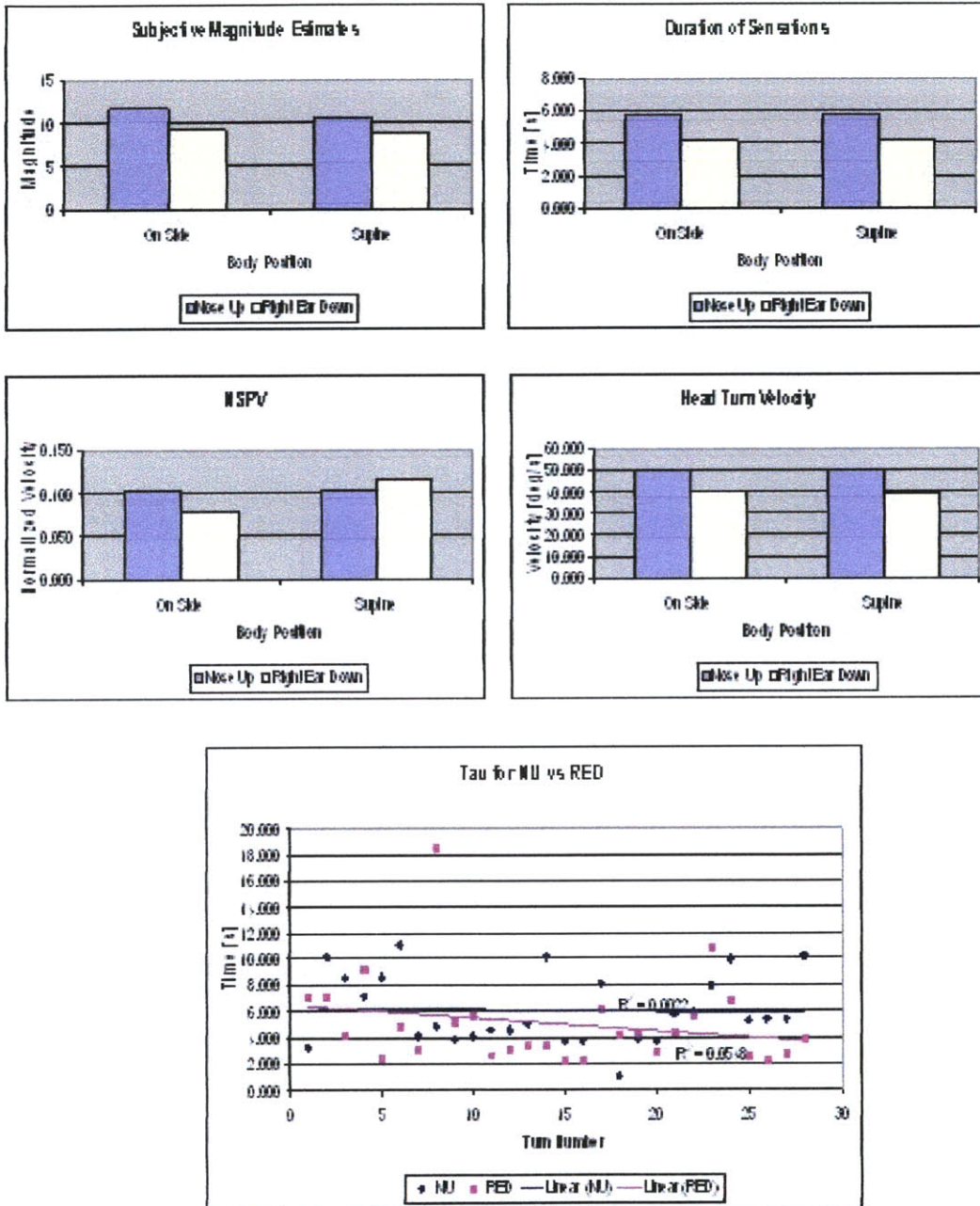
Subject 12



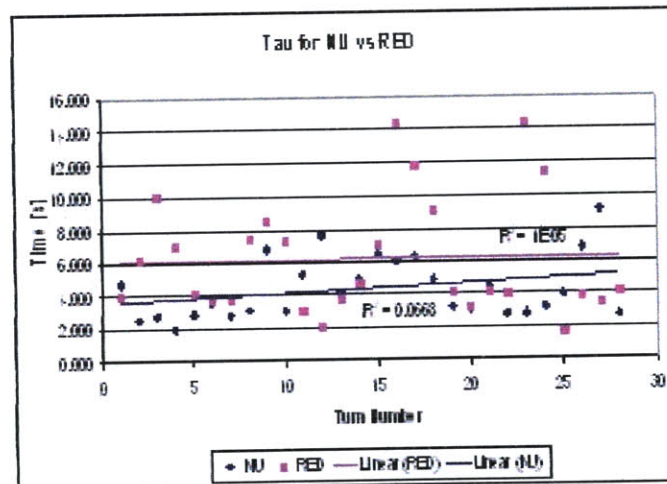
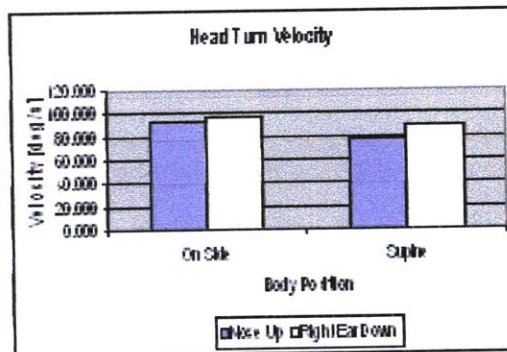
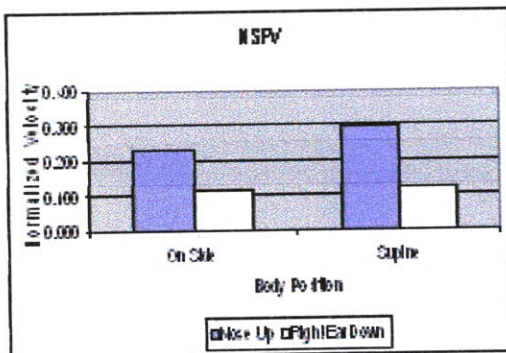
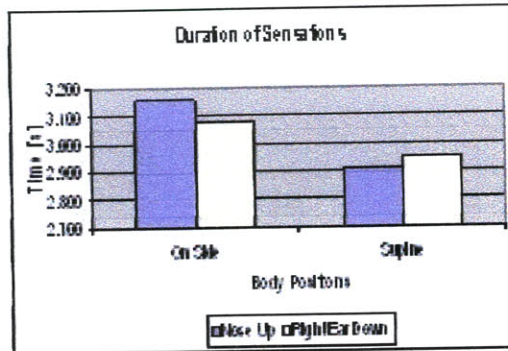
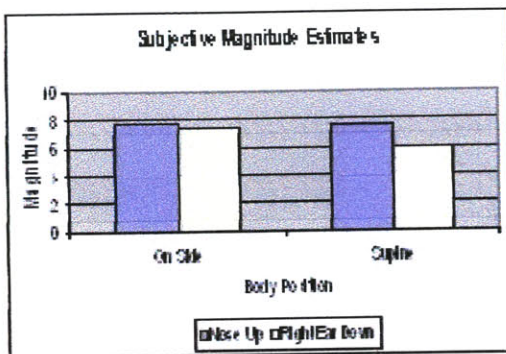
Subject 13



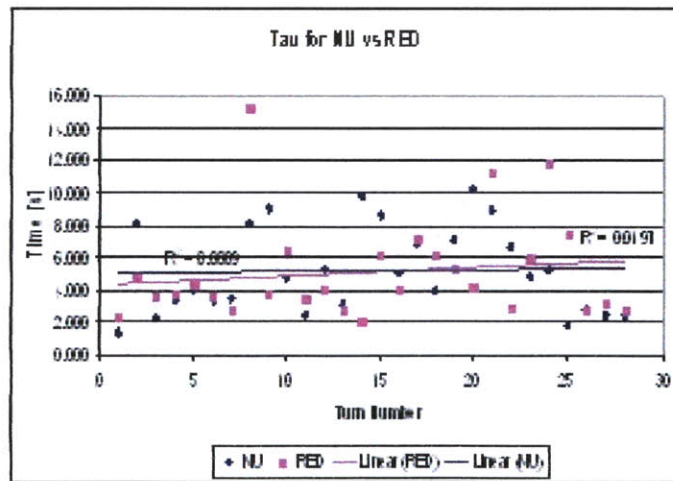
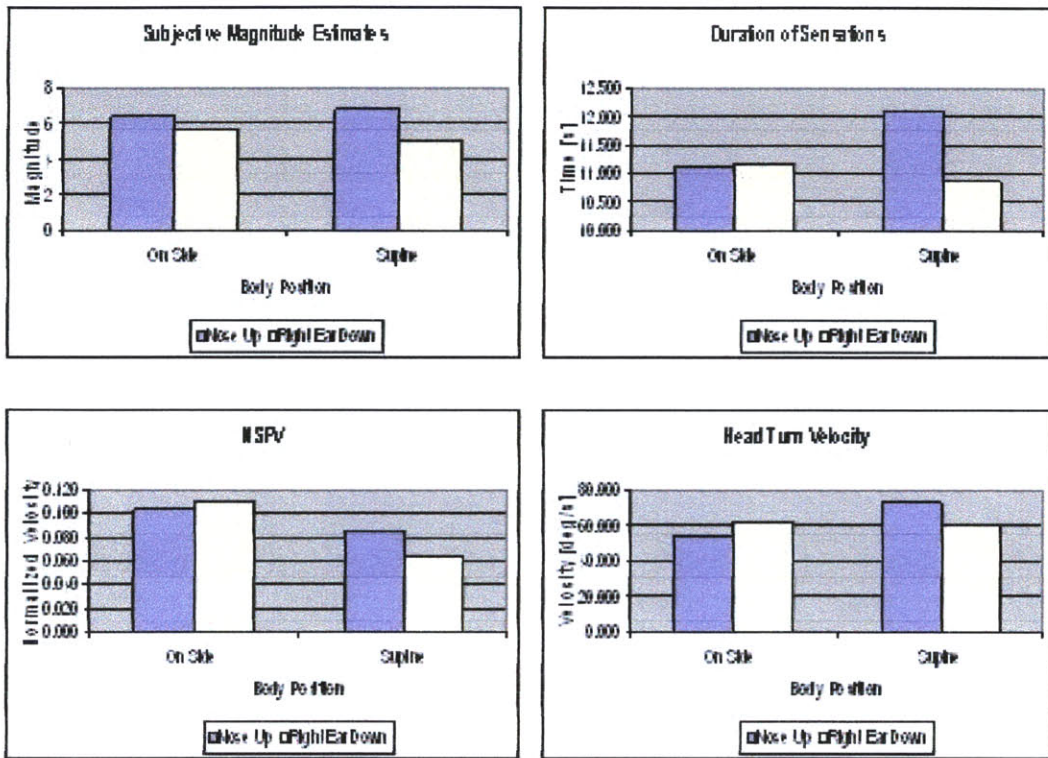
Subject 14



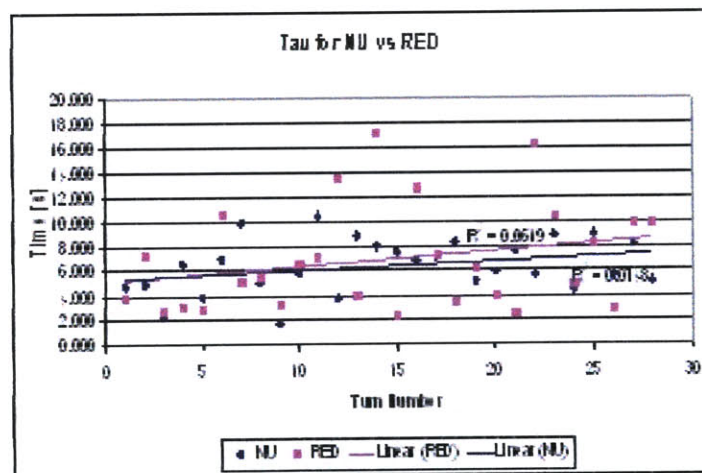
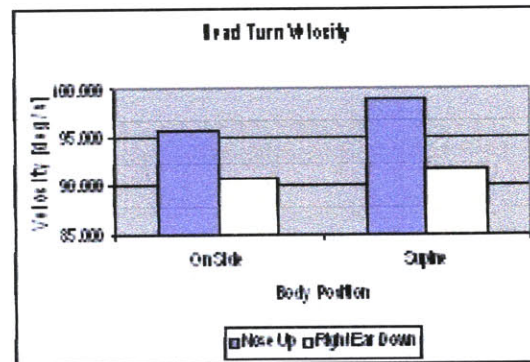
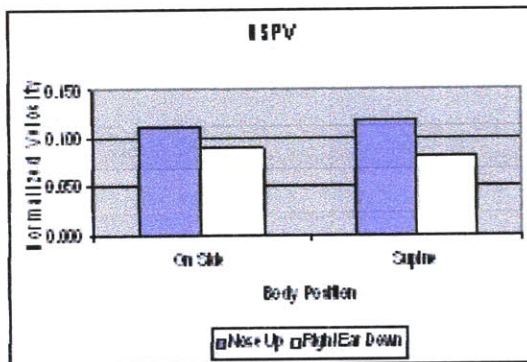
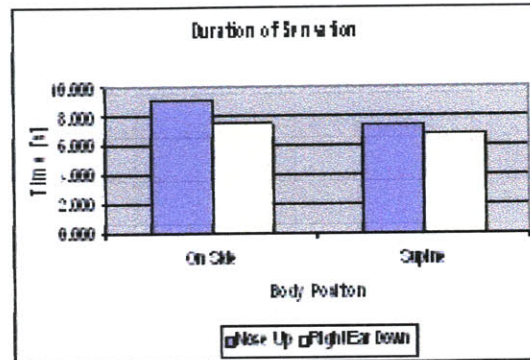
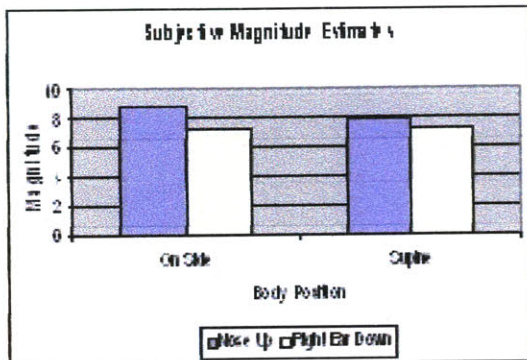
Subject 16



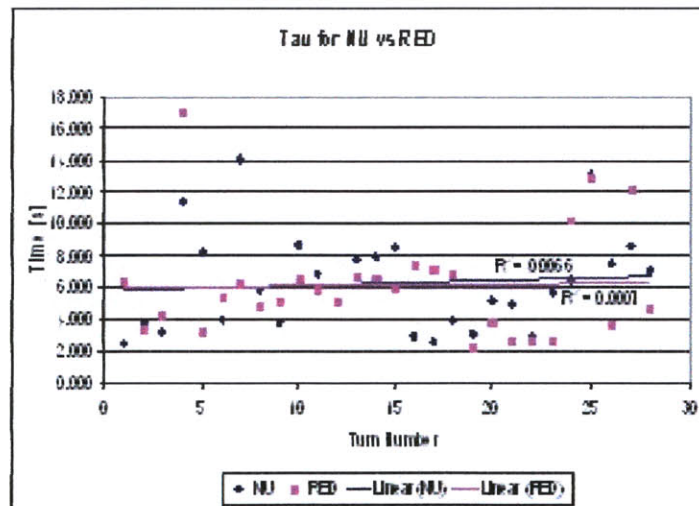
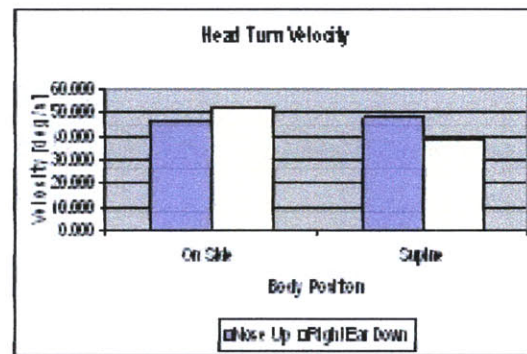
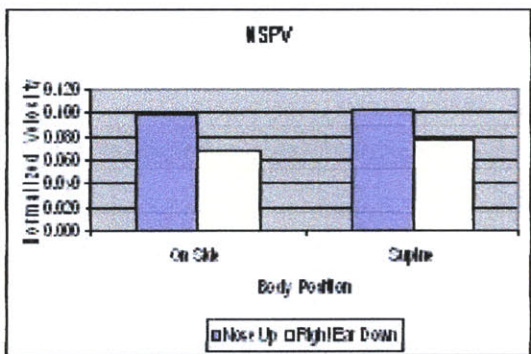
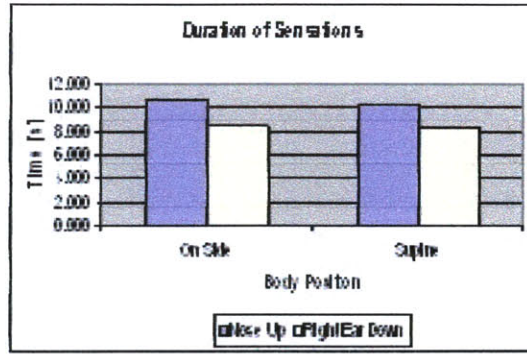
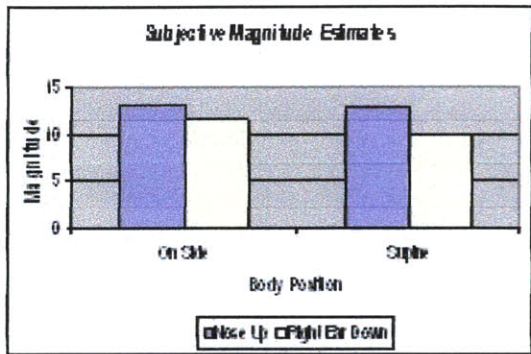
Subject 17



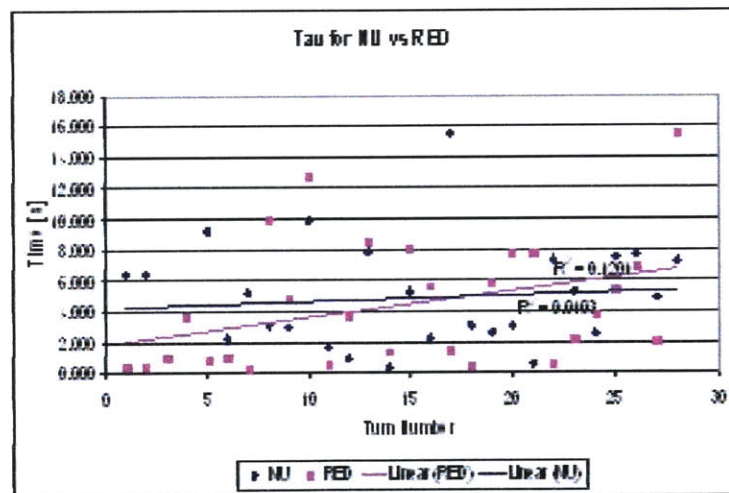
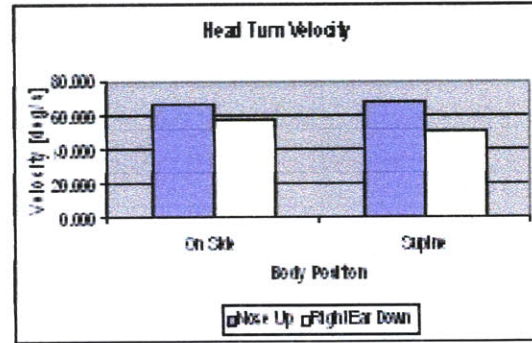
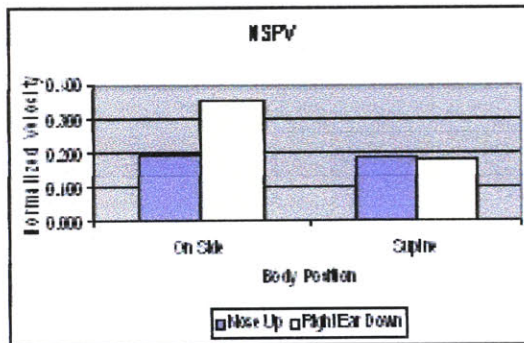
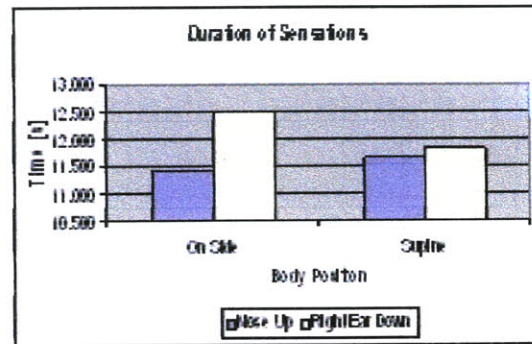
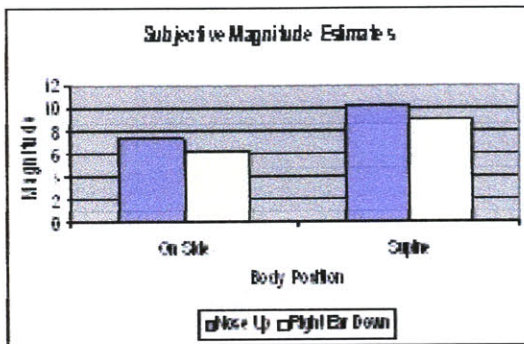
Subject 18



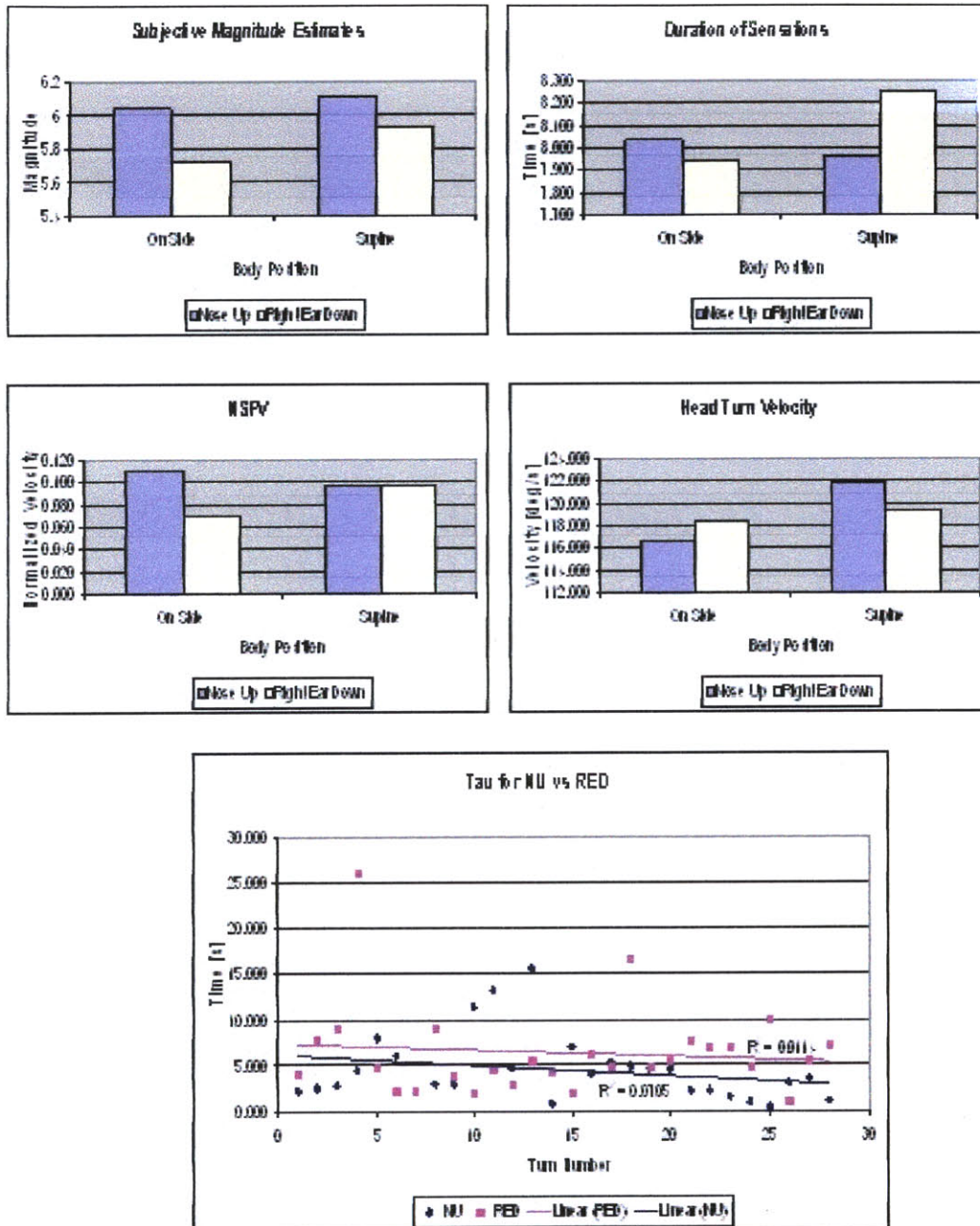
Subject 19



Subject 20



Subject 21



APPENDIX E: Raw Data

Subject	BodyPosGroup (Lateral, Supine)=(0,1)	POST 1 (0,1) = Lat, Sup	HdAng group	Gender	VR Experience None=1,Some=2,Lots =3	Hand (L,R)	Eye Dom (L,R)
1	0	1	60	M	3	R	R
1	0	1	60	M	3	R	R
1	0	1	60	M	3	R	R
1	0	1	60	M	3	R	R
1	0	1	60	M	3	R	R
1	0	1	60	M	3	R	R
1	0	1	60	M	3	R	R
1	0	1	60	M	3	R	R
1	0	1	60	M	3	R	R
1	0	1	60	M	3	R	R
1	0	1	60	M	3	R	R
1	0	1	60	M	3	R	R
1	0	1	60	M	3	R	R
1	0	1	60	M	3	R	R
1	0	1	60	M	3	R	R
1	0	1	60	M	3	R	R
1	0	1	60	M	3	R	R
1	0	1	60	M	3	R	R
1	0	1	60	M	3	R	R
1	0	1	60	M	3	R	R
1	0	1	60	M	3	R	R
1	1	1	60	M	3	R	R
1	1	1	60	M	3	R	R
1	1	1	60	M	3	R	R
1	1	1	60	M	3	R	R
1	1	1	60	M	3	R	R
1	1	1	60	M	3	R	R
1	1	1	60	M	3	R	R
1	1	1	60	M	3	R	R
1	1	1	60	M	3	R	R
1	1	1	60	M	3	R	R
1	1	1	60	M	3	R	R
1	1	1	60	M	3	R	R
1	1	1	60	M	3	R	R
1	1	1	60	M	3	R	R
1	1	1	60	M	3	R	R
1	1	1	60	M	3	R	R
1	1	1	60	M	3	R	R

1	1	1	60	M	3	R	R
1	1	1	60	M	3	R	R
1	1	1	60	M	3	R	R
1	1	1	60	M	3	R	R
1	1	1	60	M	3	R	R
1	1	1	60	M	3	R	R
1	1	1	60	M	3	R	R
1	1	1	60	M	3	R	R
1	1	1	60	M	3	R	R
1	1	1	60	M	3	R	R
4	0	1	70	F	1	R	R
4	0	1	70	F	1	R	R
4	0	1	70	F	1	R	R
4	0	1	70	F	1	R	R
4	0	1	70	F	1	R	R
4	0	1	70	F	1	R	R
4	0	1	70	F	1	R	R
4	0	1	70	F	1	R	R
4	0	1	70	F	1	R	R
4	0	1	70	F	1	R	R
4	0	1	70	F	1	R	R
4	0	1	70	F	1	R	R
4	0	1	70	F	1	R	R
4	0	1	70	F	1	R	R
4	0	1	70	F	1	R	R
4	0	1	70	F	1	R	R
4	0	1	70	F	1	R	R
4	0	1	70	F	1	R	R
4	0	1	70	F	1	R	R
4	0	1	70	F	1	R	R
4	0	1	70	F	1	R	R
4	0	1	70	F	1	R	R
4	0	1	70	F	1	R	R
4	0	1	70	F	1	R	R
4	0	1	70	F	1	R	R
4	0	1	70	F	1	R	R
4	1	1	70	F	1	R	R
4	1	1	70	F	1	R	R
4	1	1	70	F	1	R	R
4	1	1	70	F	1	R	R
4	1	1	70	F	1	R	R
4	1	1	70	F	1	R	R
4	1	1	70	F	1	R	R
4	1	1	70	F	1	R	R

4	1	1	70	F	1	R	R
4	1	1	70	F	1	R	R
4	1	1	70	F	1	R	R
4	1	1	70	F	1	R	R
4	1	1	70	F	1	R	R
4	1	1	70	F	1	R	R
4	1	1	70	F	1	R	R
4	1	1	70	F	1	R	R
4	1	1	70	F	1	R	R
4	1	1	70	F	1	R	R
4	1	1	70	F	1	R	R
4	1	1	70	F	1	R	R
4	1	1	70	F	1	R	R
4	1	1	70	F	1	R	R
4	1	1	70	F	1	R	R
4	1	1	70	F	1	R	R
4	1	1	70	F	1	R	R
4	1	1	70	F	1	R	R
4	1	1	70	F	1	R	R
5	0	0	50	M	2	R	R
5	0	0	50	M	2	R	R
5	0	0	50	M	2	R	R
5	0	0	50	M	2	R	R
5	0	0	50	M	2	R	R
5	0	0	50	M	2	R	R
5	0	0	50	M	2	R	R
5	0	0	50	M	2	R	R
5	0	0	50	M	2	R	R
5	0	0	50	M	2	R	R
5	0	0	50	M	2	R	R
5	0	0	50	M	2	R	R
5	0	0	50	M	2	R	R
5	0	0	50	M	2	R	R
5	0	0	50	M	2	R	R
5	0	0	50	M	2	R	R
5	0	0	50	M	2	R	R
5	0	0	50	M	2	R	R
5	0	0	50	M	2	R	R
5	0	0	50	M	2	R	R
5	0	0	50	M	2	R	R
5	0	0	50	M	2	R	R
5	0	0	50	M	2	R	R
5	0	0	50	M	2	R	R
5	0	0	50	M	2	R	R

5	0	0	50	M	2	R	R
5	1	0	50	M	2	R	R
5	1	0	50	M	2	R	R
5	1	0	50	M	2	R	R
5	1	0	50	M	2	R	R
5	1	0	50	M	2	R	R
5	1	0	50	M	2	R	R
5	1	0	50	M	2	R	R
5	1	0	50	M	2	R	R
5	1	0	50	M	2	R	R
5	1	0	50	M	2	R	R
5	1	0	50	M	2	R	R
5	1	0	50	M	2	R	R
5	1	0	50	M	2	R	R
5	1	0	50	M	2	R	R
5	1	0	50	M	2	R	R
5	1	0	50	M	2	R	R
5	1	0	50	M	2	R	R
5	1	0	50	M	2	R	R
5	1	0	50	M	2	R	R
5	1	0	50	M	2	R	R
5	1	0	50	M	2	R	R
6	0	1	60	M	1	R	R
6	0	1	60	M	1	R	R
6	0	1	60	M	1	R	R
6	0	1	60	M	1	R	R
6	0	1	60	M	1	R	R
6	0	1	60	M	1	R	R
6	0	1	60	M	1	R	R
6	0	1	60	M	1	R	R
6	0	1	60	M	1	R	R
6	0	1	60	M	1	R	R
6	0	1	60	M	1	R	R
6	0	1	60	M	1	R	R
6	0	1	60	M	1	R	R
6	0	1	60	M	1	R	R
6	0	1	60	M	1	R	R
6	0	1	60	M	1	R	R
6	0	1	60	M	1	R	R
6	0	1	60	M	1	R	R
6	0	1	60	M	1	R	R
6	0	1	60	M	1	R	R

6	0	1	60	M	1	R	R
6	0	1	60	M	1	R	R
6	0	1	60	M	1	R	R
6	0	1	60	M	1	R	R
6	0	1	60	M	1	R	R
6	0	1	60	M	1	R	R
6	0	1	60	M	1	R	R
6	0	1	60	M	1	R	R
6	0	1	60	M	1	R	R
6	1	1	60	M	1	R	R
6	1	1	60	M	1	R	R

6	1	1	60	M	1	R	R
6	1	1	60	M	1	R	R
6	1	1	60	M	1	R	R
6	1	1	60	M	1	R	R
6	1	1	60	M	1	R	R
6	1	1	60	M	1	R	R
6	1	1	60	M	1	R	R
6	1	1	60	M	1	R	R
6	1	1	60	M	1	R	R
6	1	1	60	M	1	R	R
6	1	1	60	M	1	R	R
6	1	1	60	M	1	R	R
6	1	1	60	M	1	R	R
6	1	1	60	M	1	R	R
6	1	1	60	M	1	R	R
6	1	1	60	M	1	R	R
6	1	1	60	M	1	R	R
6	1	1	60	M	1	R	R
6	1	1	60	M	1	R	R
6	1	1	60	M	1	R	R
6	1	1	60	M	1	R	R
6	1	1	60	M	1	R	R
6	1	1	60	M	1	R	R
6	1	1	60	M	1	R	R
6	1	1	60	M	1	R	R
8	0	0	70	M	2	R	R
8	0	0	70	M	2	R	R
8	0	0	70	M	2	R	R
8	0	0	70	M	2	R	R
8	0	0	70	M	2	R	R
8	0	0	70	M	2	R	R
8	0	0	70	M	2	R	R
8	0	0	70	M	2	R	R
8	0	0	70	M	2	R	R
8	0	0	70	M	2	R	R
8	0	0	70	M	2	R	R
8	0	0	70	M	2	R	R
8	0	0	70	M	2	R	R
8	0	0	70	M	2	R	R
8	0	0	70	M	2	R	R
8	0	0	70	M	2	R	R
8	0	0	70	M	2	R	R
8	0	0	70	M	2	R	R
8	0	0	70	M	2	R	R
8	0	0	70	M	2	R	R
8	0	0	70	M	2	R	R
8	0	0	70	M	2	R	R
8	0	0	70	M	2	R	R
8	0	0	70	M	2	R	R

8	0	0	70	M	2	R	R
8	0	0	70	M	2	R	R
8	0	0	70	M	2	R	R
8	0	0	70	M	2	R	R
8	0	0	70	M	2	R	R
8	0	0	70	M	2	R	R
8	0	0	70	M	2	R	R
8	0	0	70	M	2	R	R
8	0	0	70	M	2	R	R
8	0	0	70	M	2	R	R
8	0	0	70	M	2	R	R
8	0	0	70	M	2	R	R
8	0	0	70	M	2	R	R
8	0	0	70	M	2	R	R
8	0	0	70	M	2	R	R
8	0	0	70	M	2	R	R

8	0	0	70	M	2	R	R
8	0	0	70	M	2	R	R
8	0	0	70	M	2	R	R
8	0	0	70	M	2	R	R
8	1	0	70	M	2	R	R
8	1	0	70	M	2	R	R
8	1	0	70	M	2	R	R
8	1	0	70	M	2	R	R
8	1	0	70	M	2	R	R
8	1	0	70	M	2	R	R
8	1	0	70	M	2	R	R
8	1	0	70	M	2	R	R
8	1	0	70	M	2	R	R
8	1	0	70	M	2	R	R
8	1	0	70	M	2	R	R
8	1	0	70	M	2	R	R
8	1	0	70	M	2	R	R
8	1	0	70	M	2	R	R
8	1	0	70	M	2	R	R
8	1	0	70	M	2	R	R
8	1	0	70	M	2	R	R
8	1	0	70	M	2	R	R
8	1	0	70	M	2	R	R
8	1	0	70	M	2	R	R
8	1	0	70	M	2	R	R
8	1	0	70	M	2	R	R
8	1	0	70	M	2	R	R
8	1	0	70	M	2	R	R
8	1	0	70	M	2	R	R
8	1	0	70	M	2	R	R
8	1	0	70	M	2	R	R
8	1	0	70	M	2	R	R
8	1	0	70	M	2	R	R
8	1	0	70	M	2	R	R

9	0	1	70	F	1	R	R
9	0	1	70	F	1	R	R
9	0	1	70	F	1	R	R
9	0	1	70	F	1	R	R
9	0	1	70	F	1	R	R
9	0	1	70	F	1	R	R
9	0	1	70	F	1	R	R
9	0	1	70	F	1	R	R
9	0	1	70	F	1	R	R
9	0	1	70	F	1	R	R
9	0	1	70	F	1	R	R
9	0	1	70	F	1	R	R
9	0	1	70	F	1	R	R
9	0	1	70	F	1	R	R
9	0	1	70	F	1	R	R
9	0	1	70	F	1	R	R

9	0	1	70	F	1	R	R
9	0	1	70	F	1	R	R
9	0	1	70	F	1	R	R
9	0	1	70	F	1	R	R
9	0	1	70	F	1	R	R
9	0	1	70	F	1	R	R
9	0	1	70	F	1	R	R
9	0	1	70	F	1	R	R
9	0	1	70	F	1	R	R
9	1	1	70	F	1	R	R
9	1	1	70	F	1	R	R
9	1	1	70	F	1	R	R
9	1	1	70	F	1	R	R
9	1	1	70	F	1	R	R
9	1	1	70	F	1	R	R
9	1	1	70	F	1	R	R
9	1	1	70	F	1	R	R
9	1	1	70	F	1	R	R
9	1	1	70	F	1	R	R
9	1	1	70	F	1	R	R
9	1	1	70	F	1	R	R
9	1	1	70	F	1	R	R
9	1	1	70	F	1	R	R
9	1	1	70	F	1	R	R
9	1	1	70	F	1	R	R
9	1	1	70	F	1	R	R
9	1	1	70	F	1	R	R
9	1	1	70	F	1	R	R
9	1	1	70	F	1	R	R
9	1	1	70	F	1	R	R

10	1	1	40	M	1	R	R
10	1	1	40	M	1	R R	R R
10	1	1	40	M	1	R R R	R R R
10	1	1	40	M	1	R R R	R R R
10	1	1	40	M	1	R R R	R R R
10	1	1	40	M	1	R R	R R
10	1	1	40	M	1	R R	R R
10	1	1	40	M	1	R R	R R
10	1	1	40	M	1	R R	R R
10	1	1	40	M	1	R R	R R
10	1	1	40	M	1	R R	R R
10	1	1	40	M	1	R R	R R
10	1	1	40	M	1	R R	R R
10	1	1	40	M	1	R R	R R
10	1	1	40	M	1	R R	R R
10	1	1	40	M	1	R R	R R
10	1	1	40	M	1	R R	R R
10	1	1	40	M	1	R R	R R
10	1	1	40	M	1	R R	R R
10	1	1	40	M	1	R R	R R
10	1	1	40	M	1	R R	R R
10	1	1	40	M	1	R R	R R
10	1	1	40	M	1	R R	R R
11	0	0	50	M	1	R	L
11	0	0	50	M	1	R	L L
11	0	0	50	M	1	R	L L
11	0	0	50	M	1	R	L L
11	0	0	50	M	1	R	L L
11	0	0	50	M	1	R	L L
11	0	0	50	M	1	R	L L
11	0	0	50	M	1	R	L L
11	0	0	50	M	1	R	L L
11	0	0	50	M	1	R	L L
11	0	0	50	M	1	R	L L
11	0	0	50	M	1	R	L L
11	0	0	50	M	1	R	L L
11	0	0	50	M	1	R	L L
11	0	0	50	M	1	R	L L
11	0	0	50	M	1	R	L L
11	0	0	50	M	1	R	L L
11	0	0	50	M	1	R	L L
11	0	0	50	M	1	R	L L
11	0	0	50	M	1	R	L L
11	0	0	50	M	1	R	L L
11	0	0	50	M	1	R	L L
11	0	0	50	M	1	R	L L
11	0	0	50	M	1	R	L L
11	0	0	50	M	1	R	L L
11	1	0	50	M	1	R	L

11	1	0	50	M	1	R	L
11	1	0	50	M	1	R	L
11	1	0	50	M	1	R	L
11	1	0	50	M	1	R	L
11	1	0	50	M	1	R	L
11	1	0	50	M	1	R	L
11	1	0	50	M	1	R	L
11	1	0	50	M	1	R	L
11	1	0	50	M	1	R	L
11	1	0	50	M	1	R	L
11	1	0	50	M	1	R	L
11	1	0	50	M	1	R	L
11	1	0	50	M	1	R	L
11	1	0	50	M	1	R	L
11	1	0	50	M	1	R	L
11	1	0	50	M	1	R	L
11	1	0	50	M	1	R	L
11	1	0	50	M	1	R	L
11	1	0	50	M	1	R	L
11	1	0	50	M	1	R	L
11	1	0	50	M	1	R	L
11	1	0	50	M	1	R	L

12	0	0	60	M	1	R	R
12	0	0	60	M	1	R	R
12	0	0	60	M	1	R	R
12	0	0	60	M	1	R	R
12	0	0	60	M	1	R	R
12	0	0	60	M	1	R	R
12	0	0	60	M	1	R	R
12	0	0	60	M	1	R	R
12	0	0	60	M	1	R	R
12	0	0	60	M	1	R	R
12	0	0	60	M	1	R	R
12	0	0	60	M	1	R	R
12	0	0	60	M	1	R	R
12	0	0	60	M	1	R	R
12	0	0	60	M	1	R	R
12	0	0	60	M	1	R	R
12	0	0	60	M	1	R	R
12	0	0	60	M	1	R	R
12	0	0	60	M	1	R	R
12	0	0	60	M	1	R	R

12	0	0	60	M	1	R	R
12	0	0	60	M	1	R	R
12	0	0	60	M	1	R	R
12	0	0	60	M	1	R	R
12	0	0	60	M	1	R	R
12	0	0	60	M	1	R	R
12	0	0	60	M	1	R	R
12	0	0	60	M	1	R	R
12	1	0	60	M	1	R	R
12	1	0	60	M	1	R	R
12	1	0	60	M	1	R	R
12	1	0	60	M	1	R	R
12	1	0	60	M	1	R	R
12	1	0	60	M	1	R	R
12	1	0	60	M	1	R	R
12	1	0	60	M	1	R	R
12	1	0	60	M	1	R	R
12	1	0	60	M	1	R	R
12	1	0	60	M	1	R	R
12	1	0	60	M	1	R	R
12	1	0	60	M	1	R	R
12	1	0	60	M	1	R	R
12	1	0	60	M	1	R	R
12	1	0	60	M	1	R	R
12	1	0	60	M	1	R	R
12	1	0	60	M	1	R	R
12	1	0	60	M	1	R	R
12	1	0	60	M	1	R	R
12	1	0	60	M	1	R	R
12	1	0	60	M	1	R	R

12	1	0	60	M	1	R	R
12	1	0	60	M	1	R	R
12	1	0	60	M	1	R	R
12	1	0	60	M	1	R	R
12	1	0	60	M	1	R	R
13	0	1	50	M	2	R	R
13	0	1	50	M	2	R	R
13	0	1	50	M	2	R	R
13	0	1	50	M	2	R	R
13	0	1	50	M	2	R	R
13	0	1	50	M	2	R	R
13	0	1	50	M	2	R	R
13	0	1	50	M	2	R	R
13	0	1	50	M	2	R	R
13	0	1	50	M	2	R	R
13	0	1	50	M	2	R	R
13	0	1	50	M	2	R	R

13	0	1	50	M	2	R	R
13	0	1	50	M	2	R	R
13	0	1	50	M	2	R	R
13	0	1	50	M	2	R	R
13	0	1	50	M	2	R	R
13	0	1	50	M	2	R	R
13	0	1	50	M	2	R	R
13	0	1	50	M	2	R	R
13	0	1	50	M	2	R	R
13	0	1	50	M	2	R	R
13	0	1	50	M	2	R	R
13	0	1	50	M	2	R	R
13	0	1	50	M	2	R	R
13	0	1	50	M	2	R	R
13	0	1	50	M	2	R	R
13	0	1	50	M	2	R	R
13	0	1	50	M	2	R	R
13	1	1	50	M	2	R	R
13	1	1	50	M	2	R	R
13	1	1	50	M	2	R	R
13	1	1	50	M	2	R	R
13	1	1	50	M	2	R	R
13	1	1	50	M	2	R	R
13	1	1	50	M	2	R	R
13	1	1	50	M	2	R	R
13	1	1	50	M	2	R	R
13	1	1	50	M	2	R	R
13	1	1	50	M	2	R	R
13	1	1	50	M	2	R	R
13	1	1	50	M	2	R	R
13	1	1	50	M	2	R	R
13	1	1	50	M	2	R	R
13	1	1	50	M	2	R	R
13	1	1	50	M	2	R	R
14	0	1	50	M	1	R	R
14	0	1	50	M	1	R	R

13	1	1	50	M	2	R	R
13	1	1	50	M	2	R	R
13	1	1	50	M	2	R	R
13	1	1	50	M	2	R	R
13	1	1	50	M	2	R	R
13	1	1	50	M	2	R	R
13	1	1	50	M	2	R	R
13	1	1	50	M	2	R	R
13	1	1	50	M	2	R	R
13	1	1	50	M	2	R	R
13	1	1	50	M	2	R	R
13	1	1	50	M	2	R	R
13	1	1	50	M	2	R	R
13	1	1	50	M	2	R	R
13	1	1	50	M	2	R	R
14	0	1	50	M	1	R	R
14	0	1	50	M	1	R	R

14	0	1	50	M	1	R	R
14	0	1	50	M	1	R	R
14	0	1	50	M	1	R	R
14	0	1	50	M	1	R	R
14	0	1	50	M	1	R	R
14	0	1	50	M	1	R	R
14	0	1	50	M	1	R	R
14	0	1	50	M	1	R	R
14	0	1	50	M	1	R	R
14	0	1	50	M	1	R	R
14	0	1	50	M	1	R	R
14	0	1	50	M	1	R	R
14	0	1	50	M	1	R	R
14	0	1	50	M	1	R	R
14	0	1	50	M	1	R	R
14	0	1	50	M	1	R	R
14	0	1	50	M	1	R	R
14	0	1	50	M	1	R	R
14	0	1	50	M	1	R	R
14	0	1	50	M	1	R	R
14	0	1	50	M	1	R	R
14	0	1	50	M	1	R	R
14	0	1	50	M	1	R	R
14	0	1	50	M	1	R	R
14	1	1	50	M	1	R	R
14	1	1	50	M	1	R	R
14	1	1	50	M	1	R	R
14	1	1	50	M	1	R	R
14	1	1	50	M	1	R	R
14	1	1	50	M	1	R	R
14	1	1	50	M	1	R	R
14	1	1	50	M	1	R	R
14	1	1	50	M	1	R	R
14	1	1	50	M	1	R	R
14	1	1	50	M	1	R	R

14	1	1	50	M	1	R	R
14	1	1	50	M	1	R	R
14	1	1	50	M	1	R	R
14	1	1	50	M	1	R	R
14	1	1	50	M	1	R	R
14	1	1	50	M	1	R	R
14	1	1	50	M	1	R	R
14	1	1	50	M	1	R	R
14	1	1	50	M	1	R	R
14	1	1	50	M	1	R	R
14	1	1	50	M	1	R	R
14	1	1	50	M	1	R	R
14	1	1	50	M	1	R	R
14	1	1	50	M	1	R	R
14	1	1	50	M	1	R	R
14	1	1	50	M	1	R	R
14	1	1	50	M	1	R	R

14	1	1	50	M	1	R	R
14	1	1	50	M	1	R	R
14	1	1	50	M	1	R	R
14	1	1	50	M	1	R	R
14	1	1	50	M	1	R	R
14	1	1	50	M	1	R	R
14	1	1	50	M	1	R	R
14	1	1	50	M	1	R	R
15	0	1	50	M	2	R	R
15	0	1	50	M	2	R	R
15	0	1	50	M	2	R	R
15	0	1	50	M	2	R	R
15	0	1	50	M	2	R	R
15	0	1	50	M	2	R	R
15	0	1	50	M	2	R	R
15	0	1	50	M	2	R	R
15	0	1	50	M	2	R	R
15	0	1	50	M	2	R	R
15	0	1	50	M	2	R	R
15	0	1	50	M	2	R	R
15	0	1	50	M	2	R	R
15	0	1	50	M	2	R	R
15	0	1	50	M	2	R	R
15	0	1	50	M	2	R	R
15	0	1	50	M	2	R	R
15	0	1	50	M	2	R	R
15	0	1	50	M	2	R	R
15	0	1	50	M	2	R	R
15	0	1	50	M	2	R	R
15	0	1	50	M	2	R	R
15	0	1	50	M	2	R	R
15	0	1	50	M	2	R	R
15	0	1	50	M	2	R	R
15	0	1	50	M	2	R	R
15	0	1	50	M	2	R	R
15	0	1	50	M	2	R	R
15	0	1	50	M	2	R	R
15	0	1	50	M	2	R	R
15	0	1	50	M	2	R	R
15	0	1	50	M	2	R	R
15	0	1	50	M	2	R	R
15	0	1	50	M	2	R	R
15	1	1	50	M	2	R	R
15	1	1	50	M	2	R	R
15	1	1	50	M	2	R	R
15	1	1	50	M	2	R	R
15	1	1	50	M	2	R	R
15	1	1	50	M	2	R	R
15	1	1	50	M	2	R	R
15	1	1	50	M	2	R	R

18	0	0	50	M	2	R	L
18	0	0	50	M	2	R R	L L
18	0	0	50	M	2	R R	L L
18	0	0	50	M	2	R R	L L
18	0	0	50	M	2	R R	L L
18	0	0	50	M	2	R R	L L
18	0	0	50	M	2	R R	L L
18	0	0	50	M	2	R R	L L
18	0	0	50	M	2	R R	L L
18	0	0	50	M	2	R R	L L
18	0	0	50	M	2	R R	L L
18	0	0	50	M	2	R R	L L
18	0	0	50	M	2	R R	L L
18	0	0	50	M	2	R R	L L
18	1	0	50	M	2	R R	L L
18	1	0	50	M	2	R R	L L
18	1	0	50	M	2	R R	L L
18	1	0	50	M	2	R R	L L
18	1	0	50	M	2	R R	L L
18	1	0	50	M	2	R R	L L
18	1	0	50	M	2	R R	L L
18	1	0	50	M	2	R R	L L
18	1	0	50	M	2	R R	L L
18	1	0	50	M	2	R R	L L
18	1	0	50	M	2	R R	L L
18	1	0	50	M	2	R R	L L
18	1	0	50	M	2	R R	L L
18	1	0	50	M	2	R R	L L
18	1	0	50	M	2	R R	L L
18	1	0	50	M	2	R R	L L
18	1	0	50	M	2	R R	L L
18	1	0	50	M	2	R R	L L
18	1	0	50	M	2	R R	L L
18	1	0	50	M	2	R R	L L
18	1	0	50	M	2	R R	L L
18	1	0	50	M	2	R R	L L
18	1	0	50	M	2	R R	L L
18	1	0	50	M	2	R R	L L
18	1	0	50	M	2	R R	L L
19	0	1	50	M	1	R R	R R
19	0	1	50	M	1	R R	R R
19	0	1	50	M	1	R R	R R
19	0	1	50	M	1	R R	R R
19	0	1	50	M	1	R R	R R
19	0	1	50	M	1	R R	R R
19	0	1	50	M	1	R R	R R
19	0	1	50	M	1	R R	R R
19	0	1	50	M	1	R R	R R
19	0	1	50	M	1	R R	R R

19	0	1	50	M	1	R	R
19	0	1	50	M	1	R	R
19	0	1	50	M	1	R	R
19	0	1	50	M	1	R	R
19	0	1	50	M	1	R	R
19	0	1	50	M	1	R	R
19	0	1	50	M	1	R	R
19	0	1	50	M	1	R	R
19	0	1	50	M	1	R	R
19	0	1	50	M	1	R	R
19	0	1	50	M	1	R	R
19	0	1	50	M	1	R	R
19	0	1	50	M	1	R	R
19	0	1	50	M	1	R	R
19	0	1	50	M	1	R	R
19	0	1	50	M	1	R	R
19	1	1	50	M	1	R	R
19	1	1	50	M	1	R	R
19	1	1	50	M	1	R	R
19	1	1	50	M	1	R	R
19	1	1	50	M	1	R	R
19	1	1	50	M	1	R	R
19	1	1	50	M	1	R	R
19	1	1	50	M	1	R	R
19	1	1	50	M	1	R	R
19	1	1	50	M	1	R	R
19	1	1	50	M	1	R	R
19	1	1	50	M	1	R	R
19	1	1	50	M	1	R	R
19	1	1	50	M	1	R	R
19	1	1	50	M	1	R	R
19	1	1	50	M	1	R	R
19	1	1	50	M	1	R	R
19	1	1	50	M	1	R	R
19	1	1	50	M	1	R	R
19	1	1	50	M	1	R	R
19	1	1	50	M	1	R	R

21	1	0	40	M	2	R	L
21	1	0	40	M	2	R	L
21	1	0	40	M	2	R	L
21	1	0	40	M	2	R	L
21	1	0	40	M	2	R	L
21	1	0	40	M	2	R	L
21	1	0	40	M	2	R	L
21	1	0	40	M	2	R	L
21	1	0	40	M	2	R	L
21	1	0	40	M	2	R	L
21	1	0	40	M	2	R	L
21	1	0	40	M	2	R	L
21	1	0	40	M	2	R	L
21	1	0	40	M	2	R	L
21	1	0	40	M	2	R	L
21	1	0	40	M	2	R	L
21	1	0	40	M	2	R	L
21	1	0	40	M	2	R	L
21	1	0	40	M	2	R	L
21	1	0	40	M	2	R	L

SVV Mean	Final HP (NU, Red)	Phase (1..4)	HeadTurn # 1..14	Magnit. of Sensation	Pitch [°] Up(+)	Roll [°] CW(+)	Yaw [°] Right(+)	Duration of Illusion
	NU	2	1	9				7.033
	RED	2	2	11				7.200
	NU	2	3	10	0	0	-20	6.600
	RED	2	4	11	0	-220	0	8.600
	NU	2	5	12				8.567
	RED	2	6	12				9.567
	NU	2	7	13	0	0	-90	8.867
	RED	2	8	8	0	40	0	6.050
	NU	2	9	11				6.700
	RED	2	10	11				5.067
	NU	2	11	10	0	0	-30	8.433
	RED	2	12	7	0	0	10	4.200
	NU	2	13	9				5.650
	RED	2	14	8				2.683
	NU	3	1	12				9.500
	RED	3	2	8				6.267
	NU	3	3	11	0	0	-40	6.917
	RED	3	4	6	0	20	20	3.717
	NU	3	5	11				5.733
	RED	3	6	7				5.650
	NU	3	7	10	0	0	-30	5.650
	RED	3	8	8	0	20	0	6.300
	NU	3	9	9				5.267
	RED	3	10	8				5.683
	NU	3	11	10	0	0	-40	5.867
	RED	3	12	6	0	20	0	2.333
	NU	3	13	9				4.917
	RED	3	14	5				2.400
	NU	1	1	10				16.333

RED	1	2	10				7.833
NU	1	3	9	0	0	-40	10.517
RED	1	4	10	0	360	0	15.017
NU	1	5	12				13.150
RED	1	6	7				5.683
NU	1	7	11	0	-20	-60	11.117
RED	1	8	8	0	30	30	10.367
NU	1	9	10				10.383
RED	1	10	9				7.867
NU	1	11	11	0	0	-50	7.600
RED	1	12	9	0	-180	0	9.567
NU	1	13	9				5.867
RED	1	14	10				6.883
NU	4	1	13				7.917
RED	4	2	10				5.783
NU	4	3	8	0	0	-20	2.133
RED	4	4	10	0	60	10	5.283
NU	4	5	10				4.300
RED	4	6	9				5.833
NU	4	7	11	0	10	-30	6.900
RED	4	8	9	0	20	0	5.517
NU	4	9	12				6.383
RED	4	10	11				5.450
NU	4	11	10	0	0	0	8.400
RED	4	12	8	0	40	10	3.083
NU	4	13	11				7.983
RED	4	14	10				4.867
NU	2	1	5				6.067
RED	2	2	5				1.750
NU	2	3	10	-90	0	-30	3.958
RED	2	4	5	-90	0	0	2.467
NU	2	5	10				1.850
RED	2	6	5				1.717
NU	2	7	10	-45	0	70	2.617
RED	2	8	5	-30	0	0	2.217
NU	2	9	10				2.067
RED	2	10	5				1.567
NU	2	11	10	-30	0	-45	2.383
RED	2	12	5	-20	0	45	1.433
NU	2	13	5				1.850
RED	2	14	5				2.333
NU	3	1	10				1.717
RED	3	2	10				2.217
NU	3	3	10	0	0	-45	1.717
RED	3	4	5	-30	0	0	1.083
NU	3	5	5				3.367
RED	3	6	5				3.333
NU	3	7	5	0	0	45	2.267
RED	3	8	5	-45		-15	2.267
NU	3	9	10				2.383

RED	3	10	5				2.317
NU	3	11	5	0	0	-45	1.783
RED	3	12	5	0	0	0	1.933
NU	3	13	5				1.867
RED	3	14	5				2.300
NU	1	1	10				4.883
RED	1	2	10				6.983
NU	1	3	20	-90	0	0	6.083
RED	1	4	10	0	0	30	4.600
NU	1	5	5				5.433
RED	1	6	5				1.733
NU	1	7	5	0	0	-15	1.867
RED	1	8	5	0	0	0	2.067
NU	1	9	5				2.500
RED	1	10	5				2.617
NU	1	11	5	-45	0	-15	1.867
RED	1	12	5	-45	0	0	1.450
NU	1	13	5				6.433
RED	1	14	5				3.983
NU	4	1	10				2.233
RED	4	2	10				1.433
NU	4	3	5	0	0	15	2.000
RED	4	4	5	-45	0	-15	1.450
NU	4	5	10				1.950
RED	4	6	5				1.550
NU	4	7	5	0	0	-30	2.450
RED	4	8	5	-45	0	20	1.333
NU	4	9	5				1.567
RED	4	10	5				2.083
NU	4	11	5	0	0	20	1.550
RED	4	12	5	-30	0	-10	2.333
NU	4	13	5				1.583
RED	4	14	10				2.450
NU	1	1	10				
RED	1	2	9				
NU	1	3	9	20	0	0	
RED	1	4	6	-10	0	0	
NU	1	5	8				
RED	1	6	7				
NU	1	7	7	25	0	-10	
RED	1	8	7	-20	0	20	
NU	1	9	9				
RED	1	10	8				
NU	1	11	7	30	0	-10	
RED	1	12	6	-10	0	20	
NU	1	13	8				
RED	1	14	8				
NU	4	1	8				3.650
RED	4	2	8				3.933
NU	4	3	8	25	0	-15	3.933

RED	4	4	9	-30	0	15	4.550
NU	4	5	8				3.517
RED	4	6	8				3.417
NU	4	7	8	20	0	-10	4.050
RED	4	8	7	-20	-5	0	3.683
NU	4	9	7				3.767
RED	4	10	7				3.350
NU	4	11	8	20	0	-10	3.767
RED	4	12	8	-15	0	5	3.533
NU	4	13	7				3.417
RED	4	14	7				3.550
NU	2	1	8				2.867
RED	2	2	8				3.267
NU	2	3	8	25	0	0	3.650
RED	2	4	7	-15	0	0	2.550
NU	2	5	8				2.833
RED	2	6	9				3.050
NU	2	7	6	15	0	0	2.150
RED	2	8	7	-15	0	5	3.133
NU	2	9	5				1.917
RED	2	10	2				3.433
NU	2	11	4	5	0	0	2.050
RED	2	12	6	-15	0	0	2.300
NU	2	13	6				1.950
RED	2	14	6				3.000
NU	3	1	8				2.783
RED	3	2	8				2.950
NU	3	3	8	30	0	-10	2.817
RED	3	4	7	-20	0	10	3.033
NU	3	5	7				1.867
RED	3	6	7				3.550
NU	3	7	6	20	0	-10	3.333
RED	3	8	6	-10	-5	10	3.250
NU	3	9	7				2.483
RED	3	10	6				3.817
NU	3	11	7	35	0	-5	3.150
RED	3	12	7	-20	0	5	2.767
NU	3	13	6				2.467
RED	3	14	6				3.883
NU	2	1	9				5.883
RED	2	2	9				7.300
NU	2	3	10	60	0	0	5.967
RED	2	4	9	0	60	0	8.500
NU	2	5	10				5.783
RED	2	6	11				5.017
NU	2	7	12	0	0	-60	5.183
RED	2	8	13	0	70	0	4.867
NU	2	9	13				6.317
RED	2	10	13				5.750
NU	2	11	12	50	0	0	5.683

RED	2	12	12	0	60	0	5.600
NU	2	13	11				5.367
RED	2	14	11				5.767
NU	3	1	10				5.083
RED	3	2	9				4.950
NU	3	3	10	0	50	0	6.383
RED	3	4	10	0	0	60	6.100
NU	3	5	12				7.367
RED	3	6	11				8.267
NU	3	7	12	0	60	0	5.433
RED	3	8	13	0	0	50	4.950
NU	3	9	14				7.083
RED	3	10	9				0.017
NU	3	11	11	40	0	0	5.133
RED	3	12	10	0	50	0	5.433
NU	3	13	13				5.983
RED	3	14	11				6.183
NU	1	1	10				3.633
RED	1	2	10				5.550
NU	1	3	8	40	0	0	4.633
RED	1	4	8	0	0	50	3.800
NU	1	5	11				4.283
RED	1	6	11				3.900
NU	1	7	9	60	0	0	3.233
RED	1	8	10	0	0	60	4.000
NU	1	9	12				5.000
RED	1	10	11				5.367
NU	1	11	11	70	10	0	5.517
RED	1	12	12	0	0	80	6.133
NU	1	13	14				9.133
RED	1	14	13				9.250
NU	4	1	12				5.933
RED	4	2	9				5.017
NU	4	3	10	0	50	0	5.117
RED	4	4	10	0	0	40	4.867
NU	4	5	13				6.033
RED	4	6	8				6.617
NU	4	7	10	50	0	0	4.983
RED	4	8	11	0	0	60	6.583
NU	4	9	9				5.483
RED	4	10	11				6.467
NU	4	11	10	40	0	0	5.400
RED	4	12	13	0	70	0	6.117
NU	4	13	11				5.683
RED	4	14	12				7.167
NU	1	1	10				8.767
RED	1	2	10				12.217
NU	1	3	9	20	0	-25	21.517
RED	1	4	8	0	0	20	10.783
NU	1	5	9				6.383

RED	1	6	8				6.500
NU	1	7	8	20	0	-20	7.517
RED	1	8	7	-10	0	0	6.017
NU	1	9	9				8.250
RED	1	10	6				4.650
NU	1	11	7	10	0	-10	6.367
RED	1	12	6	-7	0	10	5.933
NU	1	13	7				5.750
RED	1	14	6				6.283
NU	4	1	3				4.083
RED	4	2	3				4.417
NU	4	3	3	10	0	-10	5.567
RED	4	4	1	-10	0	0	4.417
NU	4	5	2				3.817
RED	4	6	2				4.983
NU	4	7	1	0	10	0	3.917
RED	4	8	1	0	0	0	2.117
NU	4	9	2				3.933
RED	4	10	1				4.550
NU	4	11	2	10	10	0	4.183
RED	4	12	0	0	0	0	4.300
NU	4	13	2				3.367
RED	4	14	1				1.983
NU	2	1	4				4.017
RED	2	2	6				5.817
NU	2	3	4	20	-20	-10	4.800
RED	2	4	0	0	0	0	3.700
NU	2	5	3				4.000
RED	2	6	2				4.283
NU	2	7	6	20	0	-10	7.783
RED	2	8	3	0	20	0	3.800
NU	2	9	5				7.917
RED	2	10	2				4.717
NU	2	11	5	30	0	-30	7.367
RED	2	12	2	0	10	0	6.233
NU	2	13	4				7.467
RED	2	14	2				4.383
NU	3	1	3				4.267
RED	3	2	2				2.683
NU	3	3	3	20	0	-10	3.317
RED	3	4	2	-10	10	0	2.983
NU	3	5	3				5.317
RED	3	6	2				5.717
NU	3	7	3	20	-10	-10	5.767
RED	3	8	1	0	-10	0	3.767
NU	3	9	5				5.883
RED	3	10	1				3.850
NU	3	11	3	20	0	-10	7.150
RED	3	12	1	-10	10	0	2.167
NU	3	13	3				5.550

	RED	3	14	1				4.050
18.92	NU	2	1	5				3.983
18.92	RED	2	2	3				3.517
18.92	NU	2	3	3	0	90	0	6.317
18.92	RED	2	4	2	0	0	2	3.283
18.92	NU	2	5	5				6.417
18.92	RED	2	6	2				2.583
18.92	NU	2	7	2	0	90	0	1.117
18.92	RED	2	8	2	0	0	10	5.617
18.92	NU	2	9	4				4.417
18.92	RED	2	10	1				4.950
18.92	NU	2	11	3	5	360	0	7.733
18.92	RED	2	12	1	0	0	2	3.367
18.92	NU	2	13	4				5.767
18.92	RED	2	14	0				2.383
18.92	NU	3	1	6				5.633
18.92	RED	3	2	1				3.100
18.92	NU	3	3	4	5	540	0	6.483
18.92	RED	3	4	1	0	0	2	5.450
18.92	NU	3	5	5				3.333
18.92	RED	3	6	1				2.767
18.92	NU	3	7	5	0	15	0	5.850
18.92	RED	3	8	1	0	0	3	3.683
18.92	NU	3	9	4				3.117
18.92	RED	3	10	0				3.000
18.92	NU	3	11	3	0	15	0	1.717
18.92	RED	3	12	0	0	0	2	2.650
18.92	NU	3	13	3				4.967
18.92	RED	3	14	0				3.000
18.92	NU	1	1	10				1.400
18.92	RED	1	2	12				7.833
18.92	NU	1	3	8	540	0	-15	14.050
18.92	RED	1	4	5	0	0	15	14.517
18.92	NU	1	5	5				12.133
18.92	RED	1	6	5				8.200
18.92	NU	1	7	6	0	1080	0	11.550
18.92	RED	1	8	3	0	0	15	6.650
18.92	NU	1	9	5				8.217
18.92	RED	1	10	3				2.783
18.92	NU	1	11	4	0	720	0	10.367
18.92	RED	1	12	3	0	0	5	4.717
18.92	NU	1	13	5				8.683
18.92	RED	1	14	2				4.567
18.92	NU	4	1	3				3.117
18.92	RED	4	2	2				2.917
18.92	NU	4	3	3	0	360	-5	6.383
18.92	RED	4	4	1	0	0	15	5.450
18.92	NU	4	5	3				3.617
18.92	RED	4	6	1				3.533
18.92	NU	4	7	3	0	-180	-5	4.067

18.92	RED	4	8	0				2.900
18.92	NU	4	9	2				3.633
18.92	RED	4	10	0				3.383
18.92	NU	4	11	2	0	180	-3	4.217
18.92	RED	4	12	0	0	0	5	3.417
18.92	NU	4	13	2				2.317
18.92	RED	4	14	0				2.533
81.71	NU	2	1	20				8.317
81.71	RED	2	2	20				9.733
81.71	NU	2	3	20	-20	720	0	9.200
81.71	RED	2	4	15	-20	-720	0	12.500
81.71	NU	2	5	25				11.217
81.71	RED	2	6	15				11.133
81.71	NU	2	7	20	0	720	0	9.217
81.71	RED	2	8	15	-45	-360	0	8.783
81.71	NU	2	9	20				8.867
81.71	RED	2	10	20				10.100
81.71	NU	2	11	20	-20	720	0	8.700
81.71	RED	2	12	15	-45	-540	0	9.483
81.71	NU	2	13	20				7.817
81.71	RED	2	14	15				10.033
81.71	NU	3	1	20				3.033
81.71	RED	3	2	15				8.800
81.71	NU	3	3	20	0	720	-20	7.717
81.71	RED	3	4	20	-720	0	0	8.283
81.71	NU	3	5	25				8.217
81.71	RED	3	6	25				7.733
81.71	NU	3	7	20	0	720	-45	6.350
81.71	RED	3	8	20	-720	0	0	5.650
81.71	NU	3	9	25				10.550
81.71	RED	3	10	15				7.283
81.71	NU	3	11	20	45	720	0	12.367
81.71	RED	3	12	15	-20	360	0	13.850
81.71	NU	3	13	25				10.700
81.71	RED	3	14	20				9.317
81.71	NU	1	1	10				1.283
81.71	RED	1	2	10				5.050
81.71	NU	1	3	12	360	0	0	10.267
81.71	RED	1	4	10	-360	0	0	7.350
81.71	NU	1	5	18				6.933
81.71	RED	1	6	18				9.483
81.71	NU	1	7	20	720	20	0	10.533
81.71	RED	1	8	15	-360	0	0	9.750
81.71	NU	1	9	20				10.117
81.71	RED	1	10	15				14.267
81.71	NU	1	11	20	720	0	0	13.533
81.71	RED	1	12	15	-360	0	0	8.833
81.71	NU	1	13	20				13.150
81.71	RED	1	14	15				10.567
81.71	NU	4	1	20				10.083

81.71	RED	4	2	20				14.167
81.71	NU	4	3	20	720	30	0	10.633
81.71	RED	4	4	20	-720	-20	0	10.567
81.71	NU	4	5	20				9.683
81.71	RED	4	6	15				6.717
81.71	NU	4	7	20	720	0	0	9.100
81.71	RED	4	8	15	-540	0	0	11.450
81.71	NU	4	9	20				10.167
81.71	RED	4	10	15				9.567
81.71	NU	4	11	20	720	45	0	10.283
81.71	RED	4	12	15	-540	0	-20	11.517
81.71	NU	4	13	20				8.600
81.71	RED	4	14	15				10.633
14.5	NU	1	1	10				6.100
14.5	RED	1	2	8				5.083
14.5	NU	1	3	8	0	360	0	5.600
14.5	RED	1	4	7	-180	0	0	4.267
14.5	NU	1	5	7				2.483
14.5	RED	1	6	7				2.433
14.5	NU	1	7	10	0	540	0	6.700
14.5	RED	1	8	8	-180	0	0	4.950
14.5	NU	1	9	10				5.683
14.5	RED	1	10	9				5.767
14.5	NU	1	11	7	0	180	0	2.800
14.5	RED	1	12	9	530	0	0	6.850
14.5	NU	1	13	8				5.117
14.5	RED	1	14	8				6.533
14.5	NU	4	1	6				4.450
14.5	RED	4	2	8				5.617
14.5	NU	4	3	8	0	360	0	5.750
14.5	RED	4	4	9	0	180	0	7.033
14.5	NU	4	5	7				4.900
14.5	RED	4	6	9				5.717
14.5	NU	4	7	8	0	540	0	4.767
14.5	RED	4	8	6	0	180	0	4.683
14.5	NU	4	9	8				5.317
14.5	RED	4	10	7				3.933
14.5	NU	4	11	7	0	360	0	5.883
14.5	RED	4	12	5	-180	0	0	4.883
14.5	NU	4	13	8				5.433
14.5	RED	4	14	1				4.383
14.5	NU	2	1	6				4.033
14.5	RED	2	2	8				4.883
14.5	NU	2	3	8	360	0	0	5.517
14.5	RED	2	4	8	-360	0	0	5.217
14.5	NU	2	5	8				6.050
14.5	RED	2	6	7				5.417
14.5	NU	2	7	8	180	0	0	5.800
14.5	RED	2	8	9	-360	0	0	4.817
14.5	NU	2	9	7				4.517

14.5	RED	2	10	9				4.400
14.5	NU	2	11	8	540	0	0	4.900
14.5	RED	2	12	9	-360	0	0	5.933
14.5	NU	2	13	7				5.350
14.5	RED	2	14	5				5.200
14.5	NU	3	1	6				4.417
14.5	RED	3	2	8				6.483
14.5	NU	3	3	8	360	0	0	5.600
14.5	RED	3	4	9	-360	0	0	7.067
14.5	NU	3	5	8				5.600
14.5	RED	3	6	7				4.350
14.5	NU	3	7	8	180	180	0	4.700
14.5	RED	3	8	1	0	0	0	3.433
14.5	NU	3	9	6				3.350
14.5	RED	3	10	4				3.533
14.5	NU	3	11	4	180	0	0	4.567
14.5	RED	3	12	2	-180	0	0	4.783
14.5	NU	3	13	3				3.567
14.5	RED	3	14	4				4.533
14.94	NU	1	1	10				5.767
14.94	RED	1	2	8				3.900
14.94	NU	1	3	8	0	540	0	4.350
14.94	RED	1	4	8	-30	540	0	6.117
14.94	NU	1	5	7				5.017
14.94	RED	1	6	8				7.767
14.94	NU	1	7	6	0	360	0	4.817
14.94	RED	1	8	7	0	540	0	5.533
14.94	NU	1	9	7				4.733
14.94	RED	1	10	8				5.300
14.94	NU	1	11	7	50	180	0	4.400
14.94	RED	1	12	8	0	-180	0	3.683
14.94	NU	1	13	7				4.617
14.94	RED	1	14	8				4.067
14.94	NU	4	1	7				
14.94	RED	4	2	7				
14.94	NU	4	3	6	-20	180	0	
14.94	RED	4	4	7	0	180	40	
14.94	NU	4	5	6				
14.94	RED	4	6	5				
14.94	NU	4	7	8	0	540	0	
14.94	RED	4	8	7	0	360	0	
14.94	NU	4	9	6				
14.94	RED	4	10	4				
14.94	NU	4	11	4	0	90	0	
14.94	RED	4	12	6	0	360	0	
14.94	NU	4	13	4				
14.94	RED	4	14	7				
14.94	NU	2	1	7				5.150
14.94	RED	2	2	8				6.300
14.94	NU	2	3	8	45	540	0	1.083

14.94	RED	2	4	7	0	540	0	6.600
14.94	NU	2	5	6				6.917
14.94	RED	2	6	7				4.550
14.94	NU	2	7	8	-20	720	0	5.117
14.94	RED	2	8	8	-90	360	0	7.567
14.94	NU	2	9	6				4.817
14.94	RED	2	10	7				5.050
14.94	NU	2	11	6	0	180	0	4.683
14.94	RED	2	12	4	-20	0	0	6.333
14.94	NU	2	13	6				5.067
14.94	RED	2	14	7				5.083
14.94	NU	3	1	7				
14.94	RED	3	2	4				
14.94	NU	3	3	6	0	360	0	
14.94	RED	3	4	4	0	90	0	
14.94	NU	3	5	5				
14.94	RED	3	6	7				
14.94	NU	3	7	6	0	180	0	
14.94	RED	3	8	7	-30	270	0	
14.94	NU	3	9	5				
14.94	RED	3	10	6				
14.94	NU	3	11	5	0	180	0	
14.94	RED	3	12	2	-20	0	0	
14.94	NU	3	13	5				
14.94	RED	3	14	6				
32.15	NU	2	1	8				1.700
32.15	RED	2	2	11				2.033
32.15	NU	2	3	9	0	360	-10	2.000
32.15	RED	2	4	8	-15	360	0	0.883
32.15	NU	2	5	6				0.450
32.15	RED	2	6	5				1.533
32.15	NU	2	7	7	0	0	-10	1.483
32.15	RED	2	8	6	-10	0	0	1.567
32.15	NU	2	9	5				2.000
32.15	RED	2	10	5				1.867
32.15	NU	2	11	6	5	0	0	1.733
32.15	RED	2	12	7	-10	0	0	1.633
32.15	NU	2	13	7				1.850
32.15	RED	2	14	7				1.650
32.15	NU	3	1	8				1.400
32.15	RED	3	2	9				1.533
32.15	NU	3	3	7	0	0	10	2.000
32.15	RED	3	4	6	0	0	-5	
32.15	NU	3	5	5				1.700
32.15	RED	3	6	6				
32.15	NU	3	7	5	5	0	0	1.533
32.15	RED	3	8	6	0	0	5	
32.15	NU	3	9	4				
32.15	RED	3	10	5				
32.15	NU	3	11	6	5	0	0	

32.15	RED	3	12	7	0	0	10	
32.15	NU	3	13	6				
32.15	RED	3	14	8				
32.15	NU	1	1	10				1.333
32.15	RED	1	2	10				1.117
32.15	NU	1	3	10	40	360	0	1.167
32.15	RED	1	4	0	0	0	0	1.117
32.15	NU	1	5	0				0.350
32.15	RED	1	6	3				1.117
32.15	NU	1	7	4	10	0	-10	0.233
32.15	RED	1	8	4	0	0	10	0.600
32.15	NU	1	9	5				0.650
32.15	RED	1	10	7				1.100
32.15	NU	1	11	6	10	0	0	1.517
32.15	RED	1	12	5	0	0	15	2.067
32.15	NU	1	13	6				1.517
32.15	RED	1	14	9				1.850
32.15	NU	4	1	7				1.333
32.15	RED	4	2	8				1.733
32.15	NU	4	3	7	0	0	10	1.333
32.15	RED	4	4	7	0	0	5	1.833
32.15	NU	4	5	10				1.367
32.15	RED	4	6	8				1.817
32.15	NU	4	7	5	5	0	0	1.333
32.15	RED	4	8	6	-5	0	0	1.867
32.15	NU	4	9	7				1.300
32.15	RED	4	10	9				1.833
32.15	NU	4	11	8	0	0	3	1.317
32.15	RED	4	12	8	0	0	5	1.683
32.15	NU	4	13	10				1.550
32.15	RED	4	14	11				2.033
	NU	2	1	11				5.500
	RED	2	2	13				5.333
	NU	2	3	12	-10	0	-45	6.767
	RED	2	4	9.5	0	0	22.5	5.583
	NU	2	5	12				4.250
	RED	2	6	8				3.233
	NU	2	7	12	0	-32.5	-20	6.217
	RED	2	8	10.5	-5	0	15	4.150
	NU	2	9	13				8.333
	RED	2	10	9				3.733
	NU	2	11	12.5	-10	60	10	5.850
	RED	2	12	8.5	0	0	6	4.417
	NU	2	13	13				7.150
	RED	2	14	9				3.933
	NU	3	1	10				5.817
	RED	3	2	7				2.850
	NU	3	3	11	0	0	-20	4.917
	RED	3	4	9	-7.5	15	0	5.483
	NU	3	5	11.5				6.983

RED	3	6	9				3.317
NU	3	7	13	0	-20	0	6.783
RED	3	8	10	-5	0	10	3.367
NU	3	9	12				5.567
RED	3	10	11				6.017
NU	3	11	11	5	0	-7.5	3.783
RED	3	12	7	0	0	5	3.400
NU	3	13	10.5				3.233
RED	3	14	8				2.950
NU	1	1	10				1.850
RED	1	2	8				5.467
NU	1	3	8	0	900	0	7.600
RED	1	4	6	0	5	10	2.817
NU	1	5	10				5.217
RED	1	6	8				4.800
NU	1	7	7.5	0	0	-25	4.983
RED	1	8	8	-10	10	15	3.950
NU	1	9	7				2.967
RED	1	10	10				6.650
NU	1	11	11.5	2	-100	0	8.383
RED	1	12	10				3.717
NU	1	13	10				5.700
RED	1	14	8				9.067
NU	4	1	9.5				3.183
RED	4	2	10				4.300
NU	4	3	10	0	-35	0	3.867
RED	4	4	9	0	6	0	3.233
NU	4	5	12				6.483
RED	4	6	9				2.767
NU	4	7	11.5	-5	5	-5	4.633
RED	4	8	9	0	0	7.5	3.050
NU	4	9	13				10.217
RED	4	10	10				3.133
NU	4	11	13	-17.5	0	10	8.400
RED	4	12	8.5	-5	0	0	3.383
NU	4	13	14				6.800
RED	4	14	9				3.250
NU	2	1	8				3.483
RED	2	2	13				4.033
NU	2	3	7	35	10	0	3.483
RED	2	4	12	0	15	20	4.033
NU	2	5	11				3.417
RED	2	6	11				3.783
NU	2	7	11	20	10	5	4.250
RED	2	8	12	10	30	10	3.633
NU	2	9	13				3.483
RED	2	10	12				4.233
NU	2	11	12	25	-10	-5	2.850
RED	2	12	10	10	20	15	3.500
NU	2	13	12				3.450

RED	2	14	13				4.383
NU	4	1	13				4.433
RED	4	2	12				3.217
NU	4	3	13	20	10	15	3.667
RED	4	4	12	10	30	15	4.167
NU	4	5	14				4.117
RED	4	6	12				3.433
NU	4	7	13	15	12	5	3.117
RED	4	8	14	10	-10	-5	5.683
NU	4	9	13				5.917
RED	4	10	14				5.083
NU	4	11	15	10	-10	-10	5.667
RED	4	12	13	15	20	10	3.567
NU	4	13	16				4.717
RED	4	14	15				3.917
NU	1	1	10				2.083
RED	1	2	12				5.050
NU	1	3	9	45	0	0	2.400
RED	1	4	12	-10	45	0	3.267
NU	1	5	10				3.267
RED	1	6	13				2.017
NU	1	7	7	20	-20	-10	1.983
RED	1	8	11	15	30	10	1.917
NU	1	9	11				4.050
RED	1	10	8				3.800
NU	1	11	9	20	5	0	2.933
RED	1	12	10	30	0	10	3.650
NU	1	13	9				3.617
RED	1	14	11				3.233
NU	3	1	12				3.350
RED	3	2	13				3.033
NU	3	3	11	20	10	0	2.817
RED	3	4	12	-5	15	10	2.700
NU	3	5	14				2.367
RED	3	6	13				3.867
NU	3	7	11	15	-10	-10	2.233
RED	3	8	13	10	15	10	3.717
NU	3	9	15				3.833
RED	3	10	15				4.767
NU	3	11	13	20	-10	-10	2.983
RED	3	12	13	5	20	5	4.167
NU	3	13	15				4.000
RED	3	14	14				4.400
NU	1	1	10				3.833
RED	1	2	10				2.767
NU	1	3	10	0	0	-90	3.433
RED	1	4	10	0	0	90	2.967
NU	1	5	11				3.300
RED	1	6	11				3.883
NU	1	7	9	0	-45	0	3.667

RED	1	8	7	0	0	20	2.267
NU	1	9	11				2.267
RED	1	10	10				3.017
NU	1	11	8	0	-45	0	3.617
RED	1	12	7	0	20	0	2.983
NU	1	13	10				2.633
RED	1	14	11				3.100
NU	4	1	10				3.617
RED	4	2	8				2.650
NU	4	3	6	0	-45	0	3.400
RED	4	4	5	0	90	0	3.100
NU	4	5	5				3.400
RED	4	6	5				4.083
NU	4	7	5	0	-45	0	3.400
RED	4	8	5	0	0	90	4.083
NU	4	9	4				2.100
RED	4	10	5				2.233
NU	4	11	5	0	0	-90	2.933
RED	4	12	5	0	60	0	2.500
NU	4	13	5				2.600
RED	4	14	5				3.500
NU	2	1	10				3.583
RED	2	2	6				3.333
NU	2	3	6	0	0	-25	3.200
RED	2	4	6	0	70	0	3.783
NU	2	5	10				3.783
RED	2	6	9				3.967
NU	2	7	8	0	0	-180	3.817
RED	2	8	4	0	45	0	3.183
NU	2	9	9				3.150
RED	2	10	6				2.767
NU	2	11	8	0	-90	0	2.867
RED	2	12	8	0	90	0	4.550
NU	2	13	8				1.583
RED	2	14	8				2.217
NU	3	1	10				2.783
RED	3	2	8				2.783
NU	3	3	6	0	0	-25	2.850
RED	3	4	4	0	0	25	1.883
NU	3	5	6				2.000
RED	3	6	5				2.200
NU	3	7	5	0	-45	0	2.283
RED	3	8	5	0	0	45	2.650
NU	3	9	7				2.867
RED	3	10	5				2.000
NU	3	11	5	0	-90	0	3.017
RED	3	12	5	0	0	180	3.350
NU	3	13	8				2.950
RED	3	14	5				2.650
NU	2	1	8				10.050

RED	2	2	9				12.933
NU	2	3	9	1080	0	0	12.567
RED	2	4	8	0	1080	0	12.083
NU	2	5	9				12.983
RED	2	6	8				13.033
NU	2	7	8	900	0	0	14.250
RED	2	8	7	0	900	0	14.233
NU	2	9	7				13.050
RED	2	10	6				11.717
NU	2	11	8	900	0	0	13.917
RED	2	12	6	0	720	0	12.333
NU	2	13	8				13.833
RED	2	14	6				11.583
NU	3	1	5				9.083
RED	3	2	4				9.217
NU	3	3	5	720	0	0	9.017
RED	3	4	5	0	720	0	11.767
NU	3	5	5				8.600
RED	3	6	4				8.283
NU	3	7	4.5	540	0	0	8.467
RED	3	8	4	0	540	0	8.600
NU	3	9	4				9.317
RED	3	10	4				10.083
NU	3	11	4.5	540	0	0	9.917
RED	3	12	4	0	630	0	11.517
NU	3	13	4.5				10.467
RED	3	14	4				9.067
NU	1	1	10				17.817
RED	1	2	8.5				13.817
NU	1	3	10	900	0	-35	16.283
RED	1	4	8	0	1080	0	15.550
NU	1	5	10				18.367
RED	1	6	8				14.450
NU	1	7	11.5	1080	0	-7.5	20.183
RED	1	8	7	0	990	0	17.000
NU	1	9	10				17.400
RED	1	10	7				13.917
NU	1	11	9	900	0	0	15.817
RED	1	12	6	0	720	0	10.950
NU	1	13	9				14.600
RED	1	14	6				11.950
NU	4	1	3				6.867
RED	4	2	3				4.433
NU	4	3	4	540	0	0	5.500
RED	4	4	3	0	540	0	8.517
NU	4	5	4				7.583
RED	4	6	3				7.467
NU	4	7	4	540	0	0	6.433
RED	4	8	3	0	540	0	8.867
NU	4	9	3.5				8.000

RED	4	10	3				8.100
NU	4	11	3.25	450	0	0	7.800
RED	4	12	3	0	540	0	9.117
NU	4	13	3				6.783
RED	4	14	3				7.833
NU	1	1	10				1.550
RED	1	2	10				1.583
NU	1	3	13	90	0	0	14.533
RED	1	4	10	-40	30	0	7.583
NU	1	5	9				11.350
RED	1	6	8				9.717
NU	1	7	10	40	0	0	10.033
RED	1	8	8	-20	30	0	8.717
NU	1	9	9				10.400
RED	1	10	7				8.300
NU	1	11	9	40	0	0	8.417
RED	1	12	5	-30	20	0	5.517
NU	1	13	8				8.100
RED	1	14	6				5.933
NU	4	1	10				5.917
RED	4	2	8				8.600
NU	4	3	9	40	0	0	7.167
RED	4	4	7	-30	10	0	9.250
NU	4	5	8				8.767
RED	4	6	7				8.967
NU	4	7	7	40	0	0	9.317
RED	4	8	7	-30	0	0	7.500
NU	4	9	8				9.217
RED	4	10	7				10.183
NU	4	11	7	45	0	0	13.750
RED	4	12	6	-20	10	0	7.033
NU	4	13	7				8.700
RED	4	14	6				5.683
NU	2	1	10				6.933
RED	2	2	8				7.883
NU	2	3	9	45	0	0	7.967
RED	2	4	8	-10	30	0	9.333
NU	2	5	8				7.000
RED	2	6	7				4.750
NU	2	7	7	30	0	0	7.017
RED	2	8	7	-10	20	0	5.683
NU	2	9	8				7.367
RED	2	10	8				7.133
NU	2	11	7	35	0	0	6.717
RED	2	12	7	0	30	0	6.883
NU	2	13	7				5.883
RED	2	14	6				5.783
NU	3	1	8				5.083
RED	3	2	7				5.733
NU	3	3	8	40	0	0	6.350

RED	3	4	8	0	30	0	6.533
NU	3	5	7				7.417
RED	3	6	6				7.333
NU	3	7	8	45	0	0	9.583
RED	3	8	7	-5	30	0	6.983
NU	3	9	9				7.333
RED	3	10	8				6.983
NU	3	11	8	45	0	0	8.917
RED	3	12	7	-10	10	0	7.150
NU	3	13	7				10.450
RED	3	14	7				7.200
NU	2	1	8				7.683
RED	2	2	7				1.767
NU	2	3	10	15	20	0	9.250
RED	2	4	10	0	20	0	11.100
NU	2	5	12				9.700
RED	2	6	13				13.483
NU	2	7	15	10	30	0	14.667
RED	2	8	14	0	30	0	10.400
NU	2	9	15				10.433
RED	2	10	14				8.183
NU	2	11	16	20	40	0	12.250
RED	2	12	10	0	10	0	6.783
NU	2	13	11				9.133
RED	2	14	10				7.633
NU	3	1	12				10.983
RED	3	2	12				9.250
NU	3	3	13	20	0	-15	9.700
RED	3	4	12	0	20	0	5.300
NU	3	5	14				10.650
RED	3	6	12				7.083
NU	3	7	14	20	35	0	11.683
RED	3	8	12	0	20	0	9.067
NU	3	9	13				11.350
RED	3	10	12				10.133
NU	3	11	15	35	40	0	11.433
RED	3	12	11	0	15	0	6.267
NU	3	13	16				11.100
RED	3	14	12				11.433
NU	1	1	10				2.117
RED	1	2	10				
NU	1	3	10	0	0	-30	
RED	1	4	8	23	20	0	
NU	1	5	10				0.133
RED	1	6	11				
NU	1	7	12	20	30	0	
RED	1	8	7	-20	0	0	
NU	1	9	12				12.100
RED	1	10	12				
NU	1	11	13	23	20	0	

RED	1	12	10	-10	0	0	
NU	1	13	13				
RED	1	14	5				
NU	4	1	14				12.017
RED	4	2	11				6.200
NU	4	3	14	40	0	0	13.200
RED	4	4	13	0	20	10	12.433
NU	4	5	14				14.383
RED	4	6	13				10.650
NU	4	7	15	20	30	10	15.533
RED	4	8	12	0	0	15	14.050
NU	4	9	14				11.617
RED	4	10	8				4.050
NU	4	11	14	20	30	0	9.883
RED	4	12	12	0	20	0	7.450
NU	4	13	14				12.133
RED	4	14	8				3.600
NU	1	1	10				14.000
RED	1	2	10				13.850
NU	1	3	8	70	-45	0	14.000
RED	1	4	2	-90	1800	0	13.850
NU	1	5	9				11.217
RED	1	6	8				13.833
NU	1	7	6	720	0	0	12.133
RED	1	8	6	0	720	0	12.600
NU	1	9	9				10.850
RED	1	10	7				12.800
NU	1	11	5	35	-50	0	13.050
RED	1	12	4	-10	60	0	12.983
NU	1	13	5				11.733
RED	1	14	6				16.733
NU	4	1	6				8.600
RED	4	2	7				10.367
NU	4	3	7	900	0	0	10.883
RED	4	4	5	0	900	0	11.400
NU	4	5	8				11.417
RED	4	6	6				12.883
NU	4	7	7	720	0	0	11.200
RED	4	8	5	0	1080	0	9.517
NU	4	9	8				8.133
RED	4	10	6				12.517
NU	4	11	8	900	0	0	9.533
RED	4	12	7	0	1080	0	8.433
NU	4	13	7				12.933
RED	4	14	9				13.033
NU	2	1	10				11.150
RED	2	2	8				11.683
NU	2	3	11	900	0	0	12.133
RED	2	4	9	0	720	0	10.967
NU	2	5	11				11.050

RED	2	6	9				12.000
NU	2	7	10	1440	0	0	10.650
RED	2	8	9	0	1080	45	14.067
NU	2	9	12				13.883
RED	2	10	10				12.567
NU	2	11	11	1440	0	0	13.183
RED	2	12	8	0	720	45	12.333
NU	2	13	10				12.867
RED	2	14	10				11.467
NU	3	1	8				8.833
RED	3	2	8				10.650
NU	3	3	9	540	0	0	10.217
RED	3	4	8	0	720	90	11.750
NU	3	5	10				11.183
RED	3	6	10				12.833
NU	3	7	10	1260	0	0	11.867
RED	3	8	8	0	1260	45	10.567
NU	3	9	9				12.100
RED	3	10	11				14.000
NU	3	11	11	1260	0	0	11.683
RED	3	12	9	0	900	50	10.167
NU	3	13	11				12.333
RED	3	14	9				10.417
NU	1	1	10				11.050
RED	1	2	9				10.033
NU	1	3	9	0	-90	0	10.717
RED	1	4	7	0	0	90	9.367
NU	1	5	7				7.617
RED	1	6	6				8.200
NU	1	7	7	-45	-90	0	9.917
RED	1	8	5	0	0	80	7.517
NU	1	9	7				6.950
RED	1	10	5				5.917
NU	1	11	6	0	-90	0	8.100
RED	1	12	5	0	0	90	7.733
NU	1	13	6				8.167
RED	1	14	5				7.950
NU	4	1	6				5.300
RED	4	2	6.5				7.283
NU	4	3	4	0	-5	-5	6.483
RED	4	4	6	0	0	20	7.633
NU	4	5	5				7.983
RED	4	6	6				7.367
NU	4	7	5	0	-10	-10	8.500
RED	4	8	5	0	0	15	8.617
NU	4	9	5				7.283
RED	4	10	4				7.450
NU	4	11	3	0	0	-10	6.750
RED	4	12	5.5	0	0	15	8.967
NU	4	13	4.5				7.683

RED	4	14	5				7.067
NU	2	1	9				9.817
RED	2	2	7				7.150
NU	2	3	8	0	-80	0	9.483
RED	2	4	6	0	0	90	11.450
NU	2	5	8				8.183
RED	2	6	7				9.300
NU	2	7	7	0	-80	-15	10.400
RED	2	8	5	0	0	90	8.033
NU	2	9	5				7.750
RED	2	10	6				8.483
NU	2	11	5	0	-5	15	8.900
RED	2	12	5	0	0	90	9.367
NU	2	13	6.5				7.883
RED	2	14	6				7.500
NU	3	1	5				4.500
RED	3	2	7				7.883
NU	3	3	5	0	-10	-10	6.333
RED	3	4	6.5	0	0	20	7.383
NU	3	5	6				6.167
RED	3	6	6				8.333
NU	3	7	4	0	-10	-10	7.333
RED	3	8	6	0	0	20	7.200
NU	3	9	6				7.050
RED	3	10	6.5				7.533
NU	3	11	5	0	-60	-2	9.300
RED	3	12	5	0	0	15	8.550
NU	3	13	6				8.350
RED	3	14	4				7.383

EYE	τ -eye	Cum Eye		AVG Head Vel	Head Turn Time	MS/Peak	MS
Amp	movement	POS	NSPV	Deg/sec	[sec]	Pensacola	(0-20)
68.2654	4.625	147.764	0.571			8	
-45.4649	4.212	-66.830	-0.380			8	
31.1283	6.072	74.113	0.260			8	
-29.9543	5.771	-43.800	-0.251			8	
30.4499	6.146	8.273	0.255			8	
-33.3768	3.847	-24.908	-0.279			8	7
42.6279	2.766	67.885	0.357			8	
-29.4068	2.483	-2.859	-0.246			8	
30.0724	2.733	33.456	0.252			8	
-29.4369	4.050	-29.716	-0.246			8	
33.3327	1.261	18.388	0.279			8	
-39.8231	4.474	-38.137	-0.333			8	8
32.3027	1.200	10.273	0.270			8	
-29.1522	2.633	-26.872	-0.244			8	
28.2535	7.127	44.363	0.236			8	

-25.6751	1.181	-7.049	-0.215			8	
40.3915	7.555	43.084	0.338			8	
-30.2324	2.452	-18.159	-0.253			8	
34.1685	3.231	6.290	0.286			8	
-41.3933	6.345	-68.462	-0.346			8	6
30.7168	0.769	12.535	0.257			8	
-56.3932	1.002	-55.094	-0.472			8	
23.602	1.330	0.809	0.197			8	
-33.2909	1.999	-23.486	-0.279			8	
31.2792	1.892	28.568	0.262			8	
-28.9358	8.114	-36.793	-0.242			8	8
43.6216	2.826	48.890	0.365			8	
-32.6002	15.246	-24.479	-0.273			8	
28.6723	2.740	31.198	0.240			8	
-46.6879	11.439	-209.594	-0.391			8	
25.1158	8.381	37.500	0.210			8	
-38.9048	8.990	-173.828	-0.326			8	
27.5754	3.282	32.714	0.231			8	
-48.2919	21.588	-265.532	-0.404			8	4
38.7539	0.968	26.660	0.324			8	
-52.3798	15.477	-220.134	-0.438			8	
35.8632	0.728	12.767	0.300			8	
-53.7373	9.316	-158.900	-0.450			8	
37.7392	3.745	44.256	0.316			8	
-50.1007	9.400	-121.501	-0.419			8	6
27.6761	4.384	8.255	0.232			8	
-42.8222	5.595	-146.791	-0.358			8	
46.131	9.803	53.637	0.386			8	
-56.2222	6.359	-192.914	-0.470			8	
64.0757	4.235	99.339	0.536			8	
-56.6772	4.089	-138.667	-0.474			8	
48.1116	6.818	52.673	0.403			8	
-62.8283	8.502	-194.009	-0.526			8	6
48.2538	5.247	143.981	0.404			8	
-97.3779	6.115	-176.286	-0.815			8	
48.7624	4.936	48.043	0.408			8	
-81.4149	5.528	-264.563	-0.681			8	
40.7406	4.425	49.503	0.341			8	
-56.742	3.971	-119.210	-0.475			8	8
62.7023	3.244	121.846	0.525			8	
-55.4141	6.358	-161.018	-0.464			8	
15.205	7.347	10.622	0.117	76.364	0.917	5	
-26.9516	1.700	-14.863	-0.208	105.001	0.667	5	
21.271	11.672	15.791	0.164	67.742	1.033	5	
-31.9724	8.090	-51.589	-0.247	76.364	0.917	5	
13.6266	5.857	11.984	0.105	60.000	1.167	5	
-28.5669	21.020	-47.119	-0.220	82.353	0.850	5	0
27.4985	2.016	11.808	0.212	76.364	0.917	5	
-16.289	0.298	-2.832	-0.126	100.000	0.700	5	
40.0717	0.698	16.975	0.309	100.000	0.700	5	

-29.8982	0.401	-7.823	-0.231	89.362	0.783	5	
22.0284	0.229	7.430	0.170	87.500	0.800	5	
-27.8216	4.021	-11.156	-0.215	79.245	0.883	5	0
15.8618	0.475	70.674	0.122	95.455	0.733	5	
-14.1537	4.939	-22.720	-0.109	89.362	0.783	5	
31.1554	8.187	14.571	0.240	95.455	0.733	5	
-14.0701	5.449	-6.445	-0.109	67.742	1.033	5	
31.1554	8.187	14.571	0.240	95.455	0.733	5	
-14.28	3.210	-6.211	-0.110	85.714	0.817	5	
13.3871	15.044	10.259	0.103	76.364	0.917	5	
-9.1353	5.722	-5.173	-0.070	97.674	0.717	5	0
13.6303	17.140	14.364	0.105	85.714	0.817	5	
-25.0622	14.600	-18.020	-0.193	116.667	0.600	5	
43.1422	11.971	10.474	0.333	63.636	1.100	5	
-20.3591	16.055	-21.515	-0.157	95.455	0.733	5	
23.1428	6.802	6.584	0.178	63.636	1.100	5	
-38.4451	7.682	-3.930	-0.296	120.000	0.583	5	0
57.9947	18.876	13.121	0.447	76.364	0.917	5	
-7.7425	6.082	-5.838	-0.060	82.353	0.850	5	
30.9349	3.601	43.481	0.239	95.459	0.733	5	
-34.3146	5.310	-93.966	-0.265	76.361	0.917	5	
25.3183	6.999	62.114	0.195	123.522	0.567	5	
-28.1932	2.843	-95.267	-0.217	104.995	0.667	5	
28.9684	2.609	16.480	0.223	110.532	0.633	5	
-99.8997	3.264	-41.542	-0.770	120.007	0.583	5	0
18.174	5.325	15.498	0.140	82.353	0.850	5	
-18.7414	3.674	-94.624	-0.145	100.000	0.700	5	
6.659	10.018	33.486	0.051	87.500	0.800	5	
-23.6754	4.770	-24.458	-0.183	95.459	0.733	5	
33.0108	3.448	18.938	0.255	127.273	0.550	5	
-31.5227	6.353	-15.669	-0.243	79.248	0.883	5	1
25.5514	14.614	39.237	0.197	100.000	0.700	5	
-34.2044	6.435	-50.429	-0.264	85.711	0.817	5	
71.8594	5.608	41.615	0.554	91.300	0.767	144.6761	
-39.9555	4.738	-58.864	-0.308	110.532	0.633	454.5564	
31.8396	3.336	2.358	0.246	63.636	1.100	1.0221	
-31.7096	3.396	-31.263	-0.245	120.007	0.583	44.3696	
20.9034	3.976	4.845	0.161	79.248	0.883	3.4597	
-34.6844	3.409	-14.735	-0.267	93.333	0.750	0.1893	0
26.8049	6.169	16.889	0.207	107.692	0.650	1.1508	
-23.9066	3.639	-7.947	-0.184	116.667	0.600	0.0667	
29.4569	11.666	28.326	0.227	84.003	0.833	-2.1589	
-33.892	5.360	-45.946	-0.261	100.000	0.700	11.5677	
19.8394	15.713	23.439	0.153	104.995	0.667	-40.1315	
-45.1525	4.315	-8.485	-0.348	104.995	0.667	60.0182	0
32.2511	4.287	14.293	0.249	127.273	0.550	78.7793	
-33.9904	6.930	-50.974	-0.262	113.507	0.617	114.2169	
65.2213	7.216	10.117	0.617	46.155	1.083	1	
-46.6122	4.084	-43.479	-0.441	83.333	0.600	1	
32.2905	4.747	13.391	0.305	52.632	0.950	1	

-60.9204	5.495	-20.206	-0.576	39.473	1.267	1	
35.6735	5.048	21.025	0.337	48.389	1.033	1	
-52.884	3.555	-92.612	-0.500	65.215	0.767	1	0
37.08	6.537	17.615	0.351	35.714	1.400	1	
-50.4728	3.671	-76.319	-0.477	35.293	1.417	1	
39.5628	6.236	20.639	0.374	41.095	1.217	1	
-44.6699	6.069	-86.533	-0.423	36.584	1.367	1	
45.594	5.936	23.663	0.431	46.874	1.067	1	
-50.4862	4.693	-111.371	-0.478	36.584	1.367	1	0
37.5792	13.908	15.297	0.355	41.095	1.217	1	
-38.7302	8.465	-76.448	-0.366	40.000	1.250	1	
33.447	9.297	39.722	0.316	44.775	1.117	1	
-37.1872	5.594	-37.429	-0.352	35.714	1.400	1	
35.5104	4.597	30.865	0.336	36.584	1.367	1	
-31.516	5.782	-20.380	-0.298	31.580	1.583	1	
28.2527	3.926	39.974	0.267	42.255	1.183	1	
-37.8031	3.410	-39.597	-0.358	34.090	1.467	1	0
29.582	3.941	30.301	0.280	34.885	1.433	1	
-37.6477	6.463	-49.902	-0.356	35.714	1.400	1	
39.3376	5.190	32.388	0.372	34.885	1.433	1	
-29.0888	2.507	-46.409	-0.275	40.000	1.250	1	
29.7193	8.853	21.853	0.281	36.584	1.367	1	
-32.5843	4.579	-25.338	-0.308	41.095	1.217	1	0
37.7616	7.022	27.121	0.357	34.885	1.433	1	
-36.7867	3.189	-38.238	-0.348	38.462	1.300	1	
30.3739	2.941	18.173	0.287	50.849	0.983	1	
-47.7579	5.440	-65.670	-0.452	28.847	1.733	1	
29.2242	2.941	18.173	0.276	34.483	1.450	1	
-41.8483	4.000	-79.069	-0.396	32.966	1.517	1	
43.6883	1.625	18.127	0.413	40.000	1.250	1	
-44.2627	6.352	-95.639	-0.419	28.847	1.733	1	0
30.4223	5.722	30.984	0.288	48.389	1.033	1	
-41.9595	5.101	-78.315	-0.397	36.584	1.367	1	
31.0197	6.123	18.352	0.293	44.775	1.117	1	
-44.4577	7.780	-87.502	-0.421	28.847	1.733	1	
14.5881	5.131	16.332	0.138	42.255	1.183	1	
-34.886	3.064	-50.977	-0.330	35.714	1.400	1	1
40.398	3.047	40.844	0.382	53.573	0.933	1	
-42.1495	3.513	-55.902	-0.399	32.258	1.550	1	
26.5571	3.209	14.838	0.251	51.722	0.967	1	
-29.3061	7.346	-29.689	-0.277	37.501	1.333	1	
30.7592	7.220	33.339	0.291	46.874	1.067	1	
-38.5022	5.428	-67.522	-0.364	41.095	1.217	1	
51.261	2.390	31.770	0.485	53.573	0.933	1	
-41.8236	4.527	-43.878	-0.396	32.258	1.550	1	1
33.7652	3.165	19.433	0.319	46.874	1.067	1	
-37.1547	3.576	-41.109	-0.351	48.389	1.033	1	
27.5739	8.645	15.197	0.261	56.606	0.883	1	
-37.7699	3.996	-40.300	-0.357	35.714	1.400	1	
33.0353	4.281	27.719	0.312	46.874	1.067	1	

-33.932	3.192	-25.075	-0.321	41.095	1.217	1	1
28.8678	6.831	9.765	0.273	43.478	1.150	1	
-46.4734	3.163	-31.304	-0.440	37.501	1.333	1	
25.9425	8.553	9.742	0.217	81.822	0.733	0	
-29.6638	1.428	-25.539	-0.248	75.000	0.800	0	
25.4566	3.269	8.203	0.213	89.996	0.667	0	
-27.8242	0.410	-19.638	-0.233	89.996	0.667	0	
33.4794	2.385	21.796	0.280	102.863	0.583	0	
-47.6683	4.807	-35.388	-0.399	100.000	0.600	0	0
27.6636	4.058	18.960	0.231	85.714	0.700	0	
-32.4925	6.902	-35.219	-0.272	89.996	0.667	0	
33.7648	9.928	51.116	0.283	92.308	0.650	0	
-39.554	2.713	-35.556	-0.331	89.996	0.667	0	
28.0697	2.596	17.282	0.235	94.742	0.633	0	
-29.6959	4.742	-40.804	-0.248	78.257	0.767	0	0
41.1249	4.291	35.390	0.344	102.863	0.583	0	
-39.703	2.295	-36.963	-0.332	94.742	0.633	0	
34.5135	4.151	27.904	0.289	60.000	1.000	0	
-41.6806	4.979	-42.630	-0.349	73.466	0.817	0	
48.627	1.985	36.686	0.407	78.257	0.767	0	
-30.3013	5.158	-77.086	-0.254	73.466	0.817	0	
45.9214	3.026	55.104	0.384	76.599	0.783	0	
-48.7871	2.544	-34.424	-0.408	102.863	0.583	0	0
47.2817	2.897	30.013	0.396	105.876	0.567	0	
-25.2778	9.819	-22.072	-0.212	94.742	0.633	0	
65.8582	3.707	84.279	0.551	116.122	0.517	0	
-58.7865	3.628	-56.230	-0.492	109.091	0.550	0	
37.4328	4.349	17.327	0.313	83.717	0.717	0	
-39.634	2.642	-35.980	-0.332	94.742	0.633	0	0
36.789	2.614	45.206	0.308	89.996	0.667	0	
-60.4194	1.603	-37.040	-0.506	89.996	0.667	0	
28.2731	1.497	22.710	0.237	89.996	0.667	0	
-28.8207	0.503	-4.548	-0.241	94.742	0.633	0	
70.6782	11.180	25.279	0.591	109.091	0.550	0	
-40.8285	0.325	-15.333	-0.342	81.822	0.733	0	
44.6908	4.482	43.651	0.374	116.122	0.517	0	
-39.6735	0.452	-22.110	-0.332	102.863	0.583	0	0
49.8693	0.528	14.184	0.417	116.122	0.517	0	
-57.9681	4.517	-38.119	-0.485	94.742	0.633	0	
34.7359	6.827	40.337	0.291	116.122	0.517	0	
-26.0198	3.811	-29.045	-0.218	109.091	0.550	0	
21.4851	6.488	20.408	0.180	143.988	0.417	0	
-29.6238	4.575	-33.000	-0.248	102.863	0.583	0	0
50.8854	4.026	46.806	0.426	105.876	0.567	0	
-41.0902	0.914	-16.012	-0.344	85.714	0.700	0	
30.4883	6.360	39.724	0.255	67.927	0.883	0	
-53.4827	4.493	-53.240	-0.448	65.452	0.917	0	
68.9007	3.789	27.115	0.577	89.996	0.667	0	
-34.6261	1.229	-11.845	-0.290	85.714	0.700	0	
38.2908	1.218	14.507	0.320	109.091	0.550	0	

-62.4831	5.577	-52.591	-0.523	75.000	0.800	0	0
39.6538	4.199	34.873	0.332	76.599	0.783	0	
-36.9942	5.423	-42.589	-0.310	89.996	0.667	0	
50.6881	7.180	55.239	0.424	92.308	0.650	0	
-48.4831	3.127	-59.648	-0.406	78.257	0.767	0	
57.2178	4.651	45.943	0.479	102.863	0.583	0	
-46.4676	3.098	-64.323	-0.389	102.863	0.583	0	0
60.7067	2.122	36.647	0.508	81.822	0.733	0	
-39.2147	1.017	-26.158	-0.328	81.822	0.733	0	
31.4324	2.383	20.325	0.242	91.300	0.767	6	
-46.3469	3.852	-34.125	-0.357	87.500	0.800	6	
32.6618	7.217	36.664	0.252	110.532	0.633	6	
-28.4769	3.768	-17.122	-0.220	79.248	0.883	6	
34.7525	5.945	51.552	0.268	116.667	0.600	6	
-25.7633	2.700	-38.776	-0.199	107.692	0.650	6	2
40.6093	7.172	57.025	0.313	113.507	0.617	6	
-32.2572	6.698	-34.699	-0.249	100.000	0.700	6	
51.2878	2.801	71.657	0.396	110.532	0.633	6	
-27.0647	2.784	-50.993	-0.209	95.459	0.733	6	
45.9997	5.541	49.282	0.355	95.459	0.733	6	
-40.17	2.042	-49.449	-0.310	100.000	0.700	6	2
33.9788	7.987	56.116	0.262	85.711	0.817	6	
-24.8112	5.709	-49.548	-0.191	82.353	0.850	6	
28.7038	6.964	143.350	0.221	75.003	0.933	6	
-26.7072	5.306	-39.582	-0.206	87.500	0.800	6	
25.8459	14.480	30.324	0.199	70.000	1.000	6	
-50.0752	2.540	-32.492	-0.386	70.000	1.000	6	
28.1716	11.493	24.812	0.217	56.000	1.250	6	
-23.461	1.424	-42.322	-0.181	79.248	0.883	6	1
43.2942	2.388	19.938	0.334	63.636	1.100	6	
-29.2149	3.074	-30.001	-0.225	82.353	0.850	6	
31.3557	3.439	103.309	0.242	51.218	1.367	6	
-32.4013	1.556	-35.812	-0.250	73.684	0.950	6	
42.682	5.329	58.352	0.329	63.636	1.100	6	
-37.5785	2.315	-41.445	-0.290	53.163	1.317	6	1
26.0277	5.122	75.891	0.201	54.547	1.283	6	
-33.3546	3.609	-31.153	-0.257	70.000	1.000	6	
34.7182	3.285	65.865	0.268	100.000	0.700	6	
-31.9057	1.855	-26.275	-0.246	76.361	0.917	6	
18.3052	5.658	120.854	0.141	65.623	1.067	6	
-74.9854	0.800	-59.028	-0.578	63.636	1.100	6	
31.6466	7.529	44.801	0.244	100.000	0.700	6	
-59.8015	0.253	-23.950	-0.461	79.248	0.883	6	2
61.5287	6.338	45.434	0.474	91.300	0.767	6	
-21.7382	2.423	-43.796	-0.168	76.361	0.917	6	
34.8625	5.430	41.933	0.269	82.353	0.850	6	
-40.4626	1.176	-25.540	-0.312	63.636	1.100	6	
28.6726	5.097	100.543	0.221	84.003	0.833	6	
-30.4699	2.820	-30.215	-0.235	65.623	1.067	6	6
31.6062	7.662	122.595	0.244	79.248	0.883	6	

-21.7009	4.270	-63.785	-0.167	87.500	0.800	6	
29.5092	2.795	30.783	0.228	93.333	0.750	6	
-58.8717	2.866	-32.163	-0.454	67.744	1.033	6	
25.5462	4.438	26.802	0.197	95.459	0.733	6	
-23.6033	8.735	-41.258	-0.182	65.623	1.067	6	
37.8145	5.579	41.383	0.292	91.300	0.767	6	
-25.9608	2.178	-24.549	-0.200	59.157	1.183	6	2
29.1007	4.860	94.173	0.224	73.684	0.950	6	
-35.5598	8.806	-43.411	-0.274	59.998	1.167	6	
27.9471	14.756	25.995	0.216	79.248	0.883	6	
-37.0776	4.837	-43.683	-0.286	48.838	1.433	6	
32.5606	14.354	64.034	0.251	82.353	0.850	6	
-25.9792	4.788	-37.848	-0.200	65.623	1.067	6	3
32.3125	3.655	79.308	0.249	82.353	0.850	6	
-25.8413	9.573	-21.406	-0.199	53.846	1.300	6	
39.9703	3.466	67.406	0.308	100.000	0.700	1	
-34.3449	8.489	-126.903	-0.265	95.459	0.733	1	
30.6906	11.331	24.487	0.237	127.273	0.550	1	
-37.3231	10.628	-43.373	-0.288	104.995	0.667	1	
27.7849	2.605	68.594	0.214	135.475	0.517	1	
-27.0983	4.823	-33.966	-0.209	144.838	0.483	1	1
35.1592	4.413	80.372	0.271	127.273	0.550	1	
-40.1095	2.105	-19.151	-0.309	127.273	0.550	1	
30.7818	3.761	48.438	0.237	144.838	0.483	1	
-29.6557	6.399	-50.119	-0.229	120.007	0.583	1	
18.7418	4.658	104.998	0.145	127.273	0.550	1	
-28.6315	2.782	-31.137	-0.221	135.475	0.517	1	0
70.6931	4.747	68.950	0.545	135.475	0.517	1	
-47.4487	2.782	-31.137	-0.366	93.333	0.750	1	
28.0992	13.460	64.418	0.217	104.995	0.667	1	
-73.4054	9.543	-79.987	-0.566	100.000	0.700	1	
30.0487	10.548	91.866	0.232	104.995	0.667	1	
-62.7312	8.730	-66.965	-0.484	91.300	0.767	1	
50.9576	6.014	60.791	0.393	100.000	0.700	1	
-42.1956	12.405	-72.302	-0.325	93.333	0.750	1	0
34.3653	12.638	72.309	0.265	127.273	0.550	1	
-60.3794	6.134	-69.552	-0.466	95.459	0.733	1	
62.0512	2.115	49.708	0.479	89.366	0.783	1	
-67.7652	3.065	-98.456	-0.523	70.000	1.000	1	
65.861	3.897	32.490	0.508	95.459	0.733	1	
-25.6219	11.940	-20.088	-0.198	95.459	0.733	1	0
39.6824	2.837	41.441	0.306	110.532	0.633	1	
-30.0896	5.003	-47.684	-0.232	120.007	0.583	1	
64.126	3.717	95.081	0.495	48.838	1.433	1	
-35.8438	8.099	-81.819	-0.276	135.475	0.517	1	
33.6105	11.107	135.684	0.259	116.667	0.600	1	
-27.7756	7.455	-86.385	-0.214	100.000	0.700	1	
38.1354	10.560	43.252	0.294	120.007	0.583	1	
-34.3152	4.058	-45.183	-0.265	85.711	0.817	1	1
38.9651	6.964	46.629	0.300	120.007	0.583	1	

-35.0245	9.740	-46.440	-0.270	91.300	0.767	1	
39.7143	8.165	52.532	0.306	100.000	0.700	1	
-39.6274	6.704	-63.645	-0.306	127.273	0.550	1	
26.9418	6.073	85.459	0.208	135.475	0.517	1	
-28.1765	5.689	-55.530	-0.217	120.007	0.583	1	
28.9326	8.330	34.740	0.223	110.532	0.633	1	
-25.4349	4.061	-78.440	-0.196	120.007	0.583	1	
30.4942	4.151	102.871	0.235	113.507	0.617	1	
-26.1642	6.303	-36.999	-0.202	120.007	0.583	1	
30.1506	4.151	102.871	0.233	127.273	0.550	1	
-42.1791	3.269	-99.654	-0.325	107.692	0.650	1	
69.9178	0.673	56.776	0.539	120.007	0.583	1	
-27.8356	3.801	-49.542	-0.215	87.500	0.800	1	0
28.9105	3.647	84.517	0.223	144.838	0.483	1	
-33.8137	5.875	-103.088	-0.261	135.475	0.517	1	
30.6933	8.748	32.031	0.237	89.366	0.783	1	
-30.4182	8.180	-132.044	-0.235	104.995	0.667	1	
31.2745	6.643	125.707	0.241	127.273	0.550	1	
-31.2449	4.647	-70.574	-0.241	120.007	0.583	1	0
40.7519	3.742	76.164	0.314	113.507	0.617	1	
-29.3462	4.647	-70.574	-0.226	116.667	0.600	1	
33.8976	2.452	19.422	0.382	54.548	0.733	9	
-40.84	5.342	-33.515	-0.460	47.059	0.850	9	
32.51045	5.349	45.519	0.367	45.285	0.883	9	
-44.7344	11.893	-36.176	-0.504	54.548	0.733	9	
31.1233	2.738	13.253	0.351	64.861	0.617	9	
-48.6288	1.712	-38.603	-0.548	38.711	1.033	9	5
31.6155	3.573	25.720	0.356	43.635	0.917	9	
-28.3855	4.578	-36.904	-0.320	32.876	1.217	9	
40.1258	4.408	38.187	0.452	45.285	0.883	9	
-35.2602	3.922	-20.796	-0.398	37.499	1.067	9	
34.6458	9.391	25.284	0.391	47.059	0.850	9	
-33.0389	13.444	-29.871	-0.372	32.876	1.217	9	7
86.643	4.710	23.849	0.977	41.378	0.967	9	
-38.3209	8.928	-47.481	-0.432	37.499	1.067	9	
35.0604	7.963	16.216	0.395	37.499	1.067	9	
-32.5121	11.411	-40.341	-0.367	47.059	0.850	9	
31.7598	1.036	25.801	0.358	37.499	1.067	9	
-26.7567	7.522	-23.435	-0.302	33.804	1.183	9	
23.8269	5.230	19.664	0.269	35.295	1.133	9	
-22.4954	5.394	-21.388	-0.254	35.820	1.117	9	8
53.0658	1.970	17.253	0.598	29.268	1.367	9	
-30.124	10.713	-13.061	-0.340	32.876	1.217	9	
19.9499	6.765	27.277	0.225	40.679	0.983	9	
-27.9684	2.885	-37.243	-0.315	42.859	0.933	9	
30.4796	4.427	33.523	0.344	35.295	1.133	9	
-24.2835	2.883	-37.367	-0.274	21.819	1.833	9	9
28.2485	4.378	23.936	0.318	32.876	1.217	9	
-45.4331	2.011	-84.404	-0.512	32.000	1.250	9	
34.0119	2.987	24.386	0.383	57.143	0.700	9	

-45.3007	3.063	-47.304	-0.511	28.571	1.400	9	
75.5482	2.005	29.157	0.852	61.538	0.650	9	
-48.9402	6.270	-52.270	-0.552	40.000	1.000	9	
45.5888	1.023	33.927	0.514	50.000	0.800	9	
-42.3385	2.882	-29.588	-0.477	38.711	1.033	9	8
30.9702	8.010	23.922	0.349	59.997	0.667	9	
-44.2264	2.544	-46.784	-0.499	40.679	0.983	9	
64.282	5.635	31.769	0.725	47.059	0.850	9	
-58.4256	2.207	-63.980	-0.659	31.170	1.283	9	
66.3504	3.260	39.616	0.748	43.635	0.917	9	
-57.1509	1.925	-44.011	-0.644	40.000	1.000	9	7
47.5183	4.489	42.950	0.536	38.711	1.033	9	
-45.283	1.644	-24.041	-0.510	33.333	1.200	9	
46.3202	2.787	58.305	0.522	47.059	0.850	9	
-39.5635	4.186	-30.038	-0.446	42.105	0.950	9	
29.6004	4.198	15.094	0.334	43.635	0.917	9	
-25.7732	4.567	-25.677	-0.291	32.876	1.217	9	
30.5259	9.696	29.902	0.344	68.575	0.583	9	
-44.8346	3.819	-14.021	-0.505	35.820	1.117	9	8
34.1581	3.318	15.579	0.385	51.066	0.783	9	
-29.2927	7.172	-26.796	-0.330	45.285	0.883	9	
31.2473	8.394	35.586	0.352	37.499	1.067	9	
-27.608	3.561	-32.621	-0.311	25.806	1.550	9	
28.1472	7.190	21.695	0.317	42.105	0.950	9	
-27.4881	7.165	-33.780	-0.310	38.711	1.033	9	7
31.0341	2.016	34.101	0.350	57.143	0.700	9	
-25.158	1.636	-19.575	-0.284	40.000	1.000	9	
66.9302	5.512	134.994	0.633	78.952	0.633	4	
-48.894	2.651	-58.034	-0.463	78.952	0.633	4	
34.7582	2.647	11.248	0.329	81.077	0.617	4	
-34.9172	3.512	-39.466	-0.330	83.333	0.600	4	
54.6039	3.730	30.914	0.517	83.333	0.600	4	
-48.6103	4.678	-32.043	-0.460	125.000	0.400	4	1
44.0043	4.813	50.580	0.416	63.833	0.783	4	
-17.2179	5.844	-24.620	-0.163	96.768	0.517	4	
31.1498	19.816	31.126	0.295	85.719	0.583	4	
-49.6057	4.104	-54.152	-0.469	96.768	0.517	4	
43.2124	4.362	23.171	0.409	58.824	0.850	4	
-43.1991	9.371	-73.301	-0.409	78.952	0.633	4	1
50.9732	4.305	32.133	0.482	96.768	0.517	4	
-39.9736	6.737	-63.726	-0.378	71.429	0.700	4	
49.4489	1.580	30.223	0.468	81.077	0.617	4	
-31.8006	5.307	-25.713	-0.301	76.923	0.650	4	
38.9553	3.523	29.600	0.368	69.764	0.717	4	
-35.4575	7.361	-26.368	-0.335	96.768	0.517	4	
42.7875	6.657	59.111	0.405	68.185	0.733	4	
-35.6807	2.911	-24.344	-0.338	56.606	0.883	4	4
33.6367	3.707	29.482	0.318	58.824	0.850	4	
-45.9384	2.124	-25.139	-0.435	74.996	0.667	4	
92.1792	2.786	34.262	0.872	54.543	0.917	4	

-39.6119	1.337	-25.935	-0.375	68.185	0.733	4	
39.2495	1.864	39.043	0.371	65.215	0.767	4	
-38.2676	5.551	-44.802	-0.362	71.429	0.700	4	3
116.4061	2.104	37.362	1.101	54.543	0.917	4	
-							
126.9717	0.719	-18.307	-1.201	50.000	1.000	4	
40.8352	5.273	34.075	0.386	90.909	0.550	4	
-28.7735	6.988	-45.699	-0.272	61.222	0.817	4	
30.0086	2.007	42.510	0.284	90.909	0.550	4	
-35.8333	7.037	-46.448	-0.339	63.833	0.783	4	
84.615	9.004	86.612	0.800	90.909	0.550	4	
-44.8086	5.307	-32.215	-0.424	74.996	0.667	4	1
42.3091	14.771	37.152	0.400	96.768	0.517	4	
-28.3	4.423	-35.369	-0.268	71.429	0.700	4	
48.7769	7.811	46.726	0.461	85.719	0.583	4	
-28.9644	4.952	-32.233	-0.274	78.952	0.633	4	
36.6995	3.545	14.318	0.347	74.996	0.667	4	
-50.0229	1.649	-36.024	-0.473	71.429	0.700	4	1
29.0675	2.678	6.342	0.275	85.719	0.583	4	
-40.5631	6.261	-53.781	-0.384	83.333	0.600	4	
30.9101	4.680	25.727	0.292	83.333	0.600	4	
-38.8603	5.338	-57.397	-0.368	157.878	0.317	4	
26.2129	3.289	15.189	0.248	74.996	0.667	4	
-27.2007	4.878	-20.926	-0.257	50.000	1.000	4	
27.8414	9.505	36.649	0.263	76.923	0.650	4	
-							
172.1991	2.345	-36.684	-1.629	76.923	0.650	4	3
28.5619	3.651	30.908	0.270	74.996	0.667	4	
-33.6656	2.161	-32.690	-0.318	81.077	0.617	4	
32.3835	16.721	92.303	0.306	103.455	0.483	4	
-28.456	2.598	-30.567	-0.269	58.824	0.850	4	
25.9956	9.241	44.596	0.246	96.768	0.517	4	
-12.3952	1.273	-41.685	-0.117	78.952	0.633	4	2
38.8004	4.019	39.805	0.367	74.996	0.667	4	
-18.1549	1.572	-55.830	-0.172	90.909	0.550	4	
24.4313	1.168	135.764	0.204	97.292	0.617	2	
-23.683	1.844	-97.918	-0.198	75.000	0.800	2	
16.4032	0.711	5.164	0.137	89.996	0.667	2	
-33.0295	2.993	-39.706	-0.276	67.927	0.883	2	
30.6272	0.455	9.638	0.256	70.588	0.850	2	
-32.4347	2.680	-17.100	-0.271	83.717	0.717	2	1
24.9058	1.613	11.228	0.208	85.714	0.700	2	
-24.2983	1.784	-24.353	-0.203	64.288	0.933	2	
39.1065	3.738	12.376	0.327	34.616	1.733	2	
-57.7476	0.303	-1.914	-0.483	78.257	0.767	2	
19.1535	2.755	343.230	0.160	100.000	0.600	2	
-51.0039	1.654	-55.492	-0.427	76.599	0.783	2	1
27.6133	2.713	56.067	0.231	63.158	0.950	2	
-19.4486	1.248	-85.067	-0.163	52.174	1.150	2	
			0.000			2	
			0.000			2	

			0.000			2	
			0.000			2	
			0.000			2	
			0.000			2	1
			0.000			2	
			0.000			2	
			0.000			2	
			0.000			2	
			0.000			2	
			0.000			2	2
			0.000			2	
			0.000			2	
27.6487	4.056	9.278	0.231	37.896	1.583	2	
-23.6966	2.182	-30.293	-0.198	63.158	0.950	2	
50.0644	1.430	110.462	0.419	89.996	0.667	2	
-27.4755	1.761	-140.584	-0.230	94.742	0.633	2	
16.7912		59.357	0.140	54.545	1.100	2	
-43.3129	8.819	-89.459	-0.362	94.742	0.633	2	2
42.334	0.841	25.727	0.354	59.014	1.017	2	
-36.9465	2.632	-95.515	-0.309	63.158	0.950	2	
25.9681	0.133	4.785	0.217	39.560	1.517	2	
-38.3226	1.011	-33.442	-0.321	60.000	1.000	2	
45.2355	0.139	6.936	0.379	52.174	1.150	2	
-42.5341	1.054	-60.413	-0.356	62.067	0.967	2	2
30.2201	1.570	36.458	0.253	49.314	1.217	2	
-23.4589	1.258	-145.814	-0.196	52.943	1.133	2	
			0.000			2	
			0.000			2	
			0.000			2	
			0.000			2	
			0.000			2	
			0.000			2	1
			0.000			2	
			0.000			2	
			0.000			2	
			0.000			2	
			0.000			2	1
			0.000			2	
			0.000			2	
16.2345	4.163	99.505	0.154	43.478	1.150	4	
-26.8141	4.880	-111.321	-0.254	31.580	1.583	4	
59.031	3.569	142.532	0.558	40.000	1.250	4	
-28.237	11.520	-53.508	-0.267	38.962	1.283	4	
21.244	3.412	62.854	0.201	56.606	0.883	4	
-17.2333	7.130	-53.659	-0.163	44.119	1.133	4	0
14.314	5.162	63.240	0.135	50.000	1.000	4	
-15.4787	6.317	-62.641	-0.146	35.714	1.400	4	
12.402	4.526	44.011	0.117	65.215	0.767	4	
-20.687	3.791	-72.808	-0.196	38.462	1.300	4	

24.8566	6.205	204.301	0.235	48.389	1.033	4	
-22.202	4.794	-93.213	-0.210	42.255	1.183	4	1
10.9199	4.721	121.980	0.103	46.874	1.067	4	
-13.6907	5.837	-62.444	-0.130	30.927	1.617	4	
25.633	7.909	97.368	0.242	51.722	0.967	4	
-25.787	5.587	-92.919	-0.244	51.722	0.967	4	
30.1594	6.280	147.730	0.285	28.301	1.767	4	
-21.656	3.421	-64.195	-0.205	50.000	1.000	4	
24.006	5.832	85.020	0.227	56.606	0.883	4	
-24.2492	4.355	-70.328	-0.229	42.255	1.183	4	1
27.5983	5.350	122.718	0.261	42.255	1.183	4	
-9.7526	5.068	-64.754	-0.092	43.478	1.150	4	
27.3894	4.337	36.219	0.259	56.606	0.883	4	
-23.6898	3.438	-64.553	-0.224	43.478	1.150	4	
9.9959	6.382	45.591	0.095	42.856	1.167	4	
-16.8998	6.809	-54.623	-0.160	44.775	1.117	4	2
29.7842	3.696	86.803	0.282	46.874	1.067	4	
-7.2593	3.668	-42.800	-0.069	44.119	1.133	4	
30.914	5.239	137.943	0.292	44.119	1.133	4	
-19.440	5.640	-91.024	-0.184	46.874	1.067	4	
14.318	3.365	41.958	0.135	46.874	1.067	4	
-10.532	5.823	-42.773	-0.100	51.722	0.967	4	
15.7032	4.507	95.951	0.149	43.478	1.150	4	
-38.300	4.028	-141.392	-0.362	50.000	1.000	4	0
27.271	7.819	153.878	0.258	45.455	1.100	4	
-17.038	2.965	-38.589	-0.161	30.303	1.650	4	
27.051	5.756	128.304	0.256	45.455	1.100	4	
-22.5997	5.182	-101.302	-0.214	40.000	1.250	4	
31.698	5.683	202.439	0.300	56.606	0.883	4	
-19.2715	4.830	-61.519	-0.182	36.584	1.367	4	0
10.3464	5.084	131.522	0.098	46.155	1.083	4	
-27.577	7.121	-148.156	-0.261	46.874	1.067	4	
25.5804	7.953	70.655	0.242	68.185	0.733	4	
-28.219	8.895	-59.253	-0.267	50.000	1.000	4	
17.118	5.594	90.422	0.162	71.429	0.700	4	
-27.6719	8.934	-72.191	-0.262	50.000	1.000	4	
40.4776	8.274	101.372	0.383	66.667	0.750	4	
-24.0257	3.054	-46.614	-0.227	68.185	0.733	4	2
18.457	7.974	105.184	0.175	71.429	0.700	4	
-18.6778	6.990	-71.038	-0.177	46.874	1.067	4	
21.4175	9.276	104.086	0.203	71.429	0.700	4	
-17.8553	6.006	-37.040	-0.169	44.119	1.133	4	
16.5037	5.335	96.032	0.156	68.185	0.733	4	
-13.7227	5.866	-77.529	-0.130	51.722	0.967	4	3
23.1986	3.402	44.401	0.219	68.185	0.733	4	
-38.5633	5.816	-75.780	-0.365	48.389	1.033	4	
51.3313	3.288	87.768	0.486	56.606	0.883	4.5	
-26.5444	7.166	-26.167	-0.251	35.714	1.400	4.5	
22.6785	10.124	37.292	0.215	54.543	0.917	4.5	
-19.9456	7.166	-26.167	-0.189	31.250	1.600	4.5	

27.7885	8.650	40.190	0.263	46.874	1.067	4.5	
-24.8733	4.215	-28.371	-0.235	30.927	1.617	4.5	1.5
23.4129	7.176	43.089	0.221	50.000	1.000	4.5	
-25.3941	9.200	-35.226	-0.240	37.974	1.317	4.5	
15.6238	8.607	47.773	0.148	48.389	1.033	4.5	
-20.0817	2.366	-26.455	-0.190	39.473	1.267	4.5	
13.0003	11.103	57.233	0.123	35.714	1.400	4.5	
-17.3472	4.871	-20.738	-0.164	36.584	1.367	4.5	3
18.1835	4.097	31.371	0.172	40.000	1.250	4.5	
-20.9631	3.062	-28.570	-0.198	48.389	1.033	4.5	
17.2386	4.890	27.046	0.163	56.606	0.883	4.5	
-5.4209	18.503	-29.598	-0.051	40.000	1.250	4.5	
15.2864	3.815	62.814	0.145	41.095	1.217	4.5	
-25.8126	5.268	-22.833	-0.244	45.455	1.100	4.5	
18.6042	4.094	30.635	0.176	44.775	1.117	4.5	
-27.8745	5.672	-23.810	-0.264	46.155	1.083	4.5	3.5
15.8604	4.575	56.319	0.150	54.543	0.917	4.5	
-17.4132	2.687	-16.000	-0.165	48.389	1.033	4.5	
18.5609	4.590	19.939	0.176	56.606	0.883	4.5	
-18.6074	3.080	-28.506	-0.176	41.095	1.217	4.5	
27.946	5.080	35.929	0.264	43.478	1.150	4.5	
-24.4376	3.324	-59.579	-0.231	40.000	1.250	4.5	4.5
9.282	10.161	46.881	0.088	71.429	0.700	4.5	
-15.8358	3.472	-30.883	-0.150	45.455	1.100	4.5	
8.7873	3.708	15.702	0.083	44.119	1.133	4.5	
-4.9142	2.250	-60.781	-0.046	35.714	1.400	4.5	
7.4993	3.708	15.702	0.071	46.874	1.067	4.5	
-13.899	2.294	-60.034	-0.131	27.778	1.800	4.5	
20.2685	8.157	54.603	0.192	42.255	1.183	4.5	
-15.1251	6.152	-28.341	-0.143	32.258	1.550	4.5	2
29.6648	1.092	26.820	0.281	26.087	1.917	4.5	
-27.3621	4.192	-49.479	-0.259	26.549	1.883	4.5	
20.4567	3.971	50.487	0.194	35.714	1.400	4.5	
-6.3421	4.374	-32.038	-0.060	26.087	1.917	4.5	
23.2999	3.707	69.770	0.220	40.000	1.250	4.5	
-27.3219	2.996	-44.866	-0.258	23.256	2.150	4.5	2
17.525	5.701	70.440	0.166	38.962	1.283	4.5	
-7.998	4.410	-27.953	-0.076	37.974	1.317	4.5	
7.0955	5.902	28.338	0.067	50.849	0.983	4.5	
-34.2366	5.745	-21.265	-0.324	45.455	1.100	4.5	
29.0267	7.936	35.820	0.275	58.824	0.850	4.5	
-24.1477	10.897	-33.205	-0.228	40.000	1.250	4.5	
28.1405	9.970	43.303	0.266	74.996	0.667	4.5	
-13.2413	6.762	-31.863	-0.125	41.095	1.217	4.5	2.5
20.9518	5.311	28.807	0.198	54.543	0.917	4.5	
-20.8062	2.626	-30.521	-0.197	48.389	1.033	4.5	
11.2001	5.342	28.557	0.106	68.185	0.733	4.5	
-8.8156	2.188	-24.858	-0.083	52.632	0.950	4.5	
14.0035	5.374	28.307	0.132	56.606	0.883	4.5	
-13.5106	2.733	-17.101	-0.128	50.000	1.000	4.5	3

22.7057	10.270	23.160	0.215	54.543	0.917	4.5	
-34.6931	3.916	-27.217	-0.328	60.002	0.833	4.5	
			0.000	54.543	0.917	7	
			0.000	65.215	0.767	7	
	2.978	68.026	0.000	54.543	0.917	7	
	5.641	-89.720	0.000	65.215	0.767	7	
	0.401	10.018	0.000	53.573	0.933	7	
	2.346	-25.987	0.000	78.952	0.633	7	1
	12.295	64.136	0.000	58.824	0.850	7	
	6.032	-82.477	0.000	78.952	0.633	7	
	10.208	119.695	0.000	71.429	0.700	7	
	6.122	-40.278	0.000	54.543	0.917	7	
	16.682	187.724	0.000	63.833	0.783	7	
	6.162	-96.105	0.000	74.996	0.667	7	5
	12.014	115.612	0.000	63.833	0.783	7	
	4.027	-15.801	0.000	53.573	0.933	7	
	5.459	49.061	0.000	56.606	0.883	7	
	6.119	-16.842	0.000	58.824	0.850	7	
	6.706	37.993	0.000	58.824	0.850	7	
	0.243	-4.251	0.000	74.996	0.667	7	
	3.028	47.739	0.000	68.185	0.733	7	
	4.521	-50.200	0.000	66.667	0.750	7	6
	6.269	134.539	0.000	61.222	0.817	7	
	3.797	-30.597	0.000	52.632	0.950	7	
	8.802	102.496	0.000	68.185	0.733	7	
	4.799	-51.176	0.000	58.824	0.850	7	
	5.469	140.957	0.000	63.833	0.783	7	
	6.757	-64.417	0.000	58.824	0.850	7	7
	6.305	57.340	0.000	58.824	0.850	7	
	4.505	-38.445	0.000	50.000	1.000	7	
	3.575	63.338	0.000	56.606	0.883	7	
	5.377	-73.666	0.000	33.709	1.483	7	
	3.749	87.260	0.000	74.996	0.667	7	
	2.698	-58.178	0.000	50.849	0.983	7	
	5.807	29.212	0.000	65.215	0.767	7	
	3.279	-70.151	0.000	42.255	1.183	7	1
	3.870	77.434	0.000	58.824	0.850	7	
	4.479	-46.654	0.000	51.722	0.967	7	
	2.714	50.940	0.000	76.923	0.650	7	
	5.611	-37.867	0.000	50.000	1.000	7	
	9.483	73.134	0.000	68.185	0.733	7	
	4.778	-52.363	0.000	43.478	1.150	7	1
	1.151	27.329	0.000	61.222	0.817	7	
	5.079	-39.966	0.000	48.389	1.033	7	
	9.612	53.454	0.000	68.185	0.733	7	
	9.452	-30.005	0.000	51.722	0.967	7	
	3.232	33.448	0.000	63.833	0.783	7	
	1.804	-6.312	0.000	63.833	0.783	7	
	25.430	64.634	0.000	96.768	0.517	7	
	0.914	-11.802	0.000	53.573	0.933	7	6

	6.010	53.435	0.000	74.996	0.667	7	
	5.207	-29.817	0.000	71.429	0.700	7	
	6.470	57.670	0.000	96.768	0.517	7	7
	1.958	-2.308	0.000	81.077	0.617	7	
	2.282	32.540	0.000	74.996	0.667	7	
	3.715	-12.059	0.000	42.255	1.183	7	6
	3.635	20.143	0.000	78.952	0.633	7	
	0.311	-3.413	0.000	58.824	0.850	7	
49.4287	4.782	35.949	0.557	100.000	0.400	0	
-42.5003	4.043	-31.630	-0.479	88.889	0.450	0	
31.0726	2.560	27.538	0.350	104.357	0.383	0	
-65.1439	6.146	-19.173	-0.734	85.708	0.467	0	
70.5126	2.824	33.832	0.795	92.315	0.433	0	
-71.5997	10.004	-73.355	-0.807	82.764	0.483	0	0
77.5537	1.952	34.392	0.874	85.708	0.467	0	
-							
115.5439	7.062	-57.766	-1.303	133.333	0.300	0	
48.4793	2.846	41.377	0.547	109.081	0.367	0	
-66.3771	4.120	-42.177	-0.748	109.081	0.367	0	
78.8957	3.495	60.296	0.889	82.764	0.483	0	
-63.573	3.781	-48.934	-0.717	120.012	0.333	0	0
69.0794	2.808	62.146	0.779	92.315	0.433	0	
-39.3474	3.781	-48.934	-0.444	92.315	0.433	0	
71.5634	3.119	109.891	0.807	92.315	0.433	0	
-41.6533	7.477	-25.492	-0.470	88.889	0.450	0	
47.3242	6.832	42.438	0.534	92.315	0.433	0	
-							
35.13525	8.511	-28.707	-0.396	109.081	0.367	0	
27.4163	3.013	109.522	0.309	109.081	0.367	0	
-28.6172	7.273	-33.916	-0.323	77.414	0.517	0	0
21.7635	5.288	35.433	0.245	77.414	0.517	0	
-42.6431	3.106	-34.410	-0.481	92.315	0.433	0	
23.2476	7.620	44.944	0.262	100.000	0.400	0	
-33.3727	2.071	-23.355	-0.376	80.000	0.500	0	
46.7925	4.181	159.398	0.528	77.414	0.517	0	
-28.3776	3.737	-38.472	-0.320	92.315	0.433	0	0
33.9699	4.938	133.166	0.383	100.000	0.400	0	
-30.7025	4.775	-28.861	-0.346	82.764	0.483	0	
60.1464	6.485	138.497	0.678	100.000	0.400	0	
-86.1836	6.972	-87.522	-0.972	72.727	0.550	0	
72.279	6.042	98.720	0.815	68.575	0.583	0	
-96.8145	14.474	-41.611	-1.091	88.889	0.450	0	
29.8307	6.319	91.400	0.336	77.414	0.517	0	
-55.8898	11.804	-36.357	-0.630	88.889	0.450	0	0
16.8922	4.941	82.956	0.190	64.861	0.617	0	
-31.1481	9.134	-31.102	-0.351	82.764	0.483	0	
58.8655	3.195	65.642	0.664	72.727	0.550	0	
-61.5962	4.179	-42.769	-0.694	92.315	0.433	0	
50.9909	3.141	70.241	0.575	72.727	0.550	0	
-58.3864	3.176	-38.373	-0.658	100.000	0.400	0	0
26.3401	4.396	69.703	0.297	64.861	0.617	0	

-40.9612	4.159	-44.204	-0.462	92.315	0.433	0	
17.4331	2.813	75.198	0.197	88.889	0.450	0	
-13.7661	4.048	-33.328	-0.155	85.708	0.467	0	
11.7441	2.763	97.406	0.132	77.414	0.517	0	
-32.8113	14.474	-41.611	-0.370	82.764	0.483	0	
33.0735	3.188	65.869	0.373	77.414	0.517	0	
-30.0092	11.482	-56.843	-0.338	77.414	0.517	0	0
34.0735	3.932	131.940	0.384	77.414	0.517	0	
-26.7137	1.687	-30.603	-0.301	72.727	0.550	0	
20.4331	6.830	168.091	0.230	82.764	0.483	0	
-51.407	3.865	-52.126	-0.580	109.081	0.367	0	
40.8788	9.111	130.522	0.461	77.414	0.517	0	
-33.4884	3.530	-17.635	-0.378	82.764	0.483	0	0
43.7899	2.669	109.287	0.494	82.764	0.483	0	
-32.6262	4.159	-44.204	-0.368	109.081	0.367	0	
29.5164	1.384	49.610	0.247	46.754	1.283	0	
-31.764	2.360	-66.339	-0.266	47.367	1.267	0	
25.3987	8.102	17.868	0.213	54.545	1.100	0	
-7.622	4.851	-28.142	-0.064	73.466	0.817	0	
28.0029	2.274	34.720	0.234	56.248	1.067	0	
-10.798	3.572	-32.981	-0.090	70.588	0.850	0	0
19.2651	3.391	40.310	0.161	62.067	0.967	0	
-11.6621	3.742	-32.349	-0.098	65.452	0.917	0	
17.277	4.031	57.136	0.145	41.861	1.433	0	
-9.1571	4.355	-72.170	-0.077	58.066	1.033	0	
20.9626	3.408	45.910	0.175	58.066	1.033	0	
-21.1898	3.674	-26.331	-0.177	81.822	0.733	0	0
9.357	3.448	27.893	0.078	54.545	1.100	0	
-9.055	2.810	-23.202	-0.076	52.943	1.133	0	
16.7318	8.152	35.352	0.140	62.067	0.967	0	
-17.5366	15.212	-60.169	-0.147	89.996	0.667	0	
53.4239	9.086	51.645	0.447	50.706	1.183	0	
-41.6816	3.736	-46.757	-0.349	56.248	1.067	0	
56.6258	4.767	14.188	0.474	70.588	0.850	0	
-20.7016	6.459	-53.682	-0.173	67.927	0.883	0	0
70.3791	2.438	61.866	0.589	50.706	1.183	0	
-41.4847	3.446	-25.329	-0.347	60.000	1.000	0	
40.4814	5.207	17.392	0.339	45.568	1.317	0	
-41.1605	3.995	-30.314	-0.344	52.943	1.133	0	
22.1342	3.112	19.573	0.185	53.730	1.117	0	
-38.4453	2.737	-36.785	-0.322	49.314	1.217	0	0
20.1347	9.844	40.011	0.168	58.066	1.033	0	
-43.167	2.067	-47.894	-0.361	48.000	1.250	0	
20.7932	8.658	41.818	0.174	64.109	0.936	0	
-59.1267	6.101	-34.327	-0.495	52.174	1.150	0	
14.5444	5.076	54.817	0.122	65.452	0.917	0	
-19.9496	4.098	-25.701	-0.167	62.067	0.967	0	
20.093	6.884	32.974	0.168	76.599	0.783	0	
-14.7711	7.122	-30.663	-0.124	62.067	0.967	0	0
7.736	4.009	28.450	0.065	81.822	0.733	0	

-28.3073	6.187	-28.180	-0.237	48.000	1.250	0	
22.6093	7.147	33.467	0.189	62.067	0.967	0	
-5.8971	5.252	-25.698	-0.049	75.000	0.800	0	
7.592	10.284	38.484	0.064	62.067	0.967	0	
-35.5319	4.116	-21.847	-0.297	60.000	1.000	0	0
20.6802	8.994	23.003	0.173	81.822	0.733	0	
-17.1424	11.380	-24.778	-0.143	64.288	0.933	0	
23.4461	6.680	32.466	0.196	73.466	0.817	0	
-30.9729	2.837	-33.923	-0.259	75.000	0.800	0	
19.8631	4.834	13.535	0.166	102.863	0.583	0	
-22.6857	6.012	-32.828	-0.190	62.067	0.967	0	
6.679	5.209	25.633	0.056	85.714	0.700	0	
-34.6163	11.879	-23.192	-0.290	54.545	1.100	0	0
9.4967	1.854	69.792	0.079	67.927	0.883	0	
-26.0308	7.431	-20.172	-0.218	70.588	0.850	0	
7.3661	2.835	15.116	0.062	70.588	0.850	0	
-10.8719	2.731	-33.190	-0.091	52.174	1.150	0	
8.3718	2.495	30.010	0.070	60.000	1.000	0	
-47.7121	3.135	-30.178	-0.399	52.174	1.150	0	0
36.4642	2.495	30.010	0.305	70.588	0.850	0	
-16.9527	2.736	-14.844	-0.142	65.452	0.917	0	
35.2764	4.754	78.408	0.334	90.909	0.550	1	
-23.0503	3.695	-47.591	-0.218	63.833	0.783	1	
34.2091	4.846	63.345	0.324	103.455	0.483	1	
-20.7307	7.218	-45.724	-0.196	81.077	0.617	1	
42.4937	2.428	26.251	0.402	103.455	0.483	1	
-22.4212	2.717	-12.766	-0.212	90.909	0.550	1	0
22.3227	6.570	59.002	0.211	103.455	0.483	1	
-47.3663	3.078	-30.094	-0.448	83.333	0.600	1	
29.2376	3.912	21.637	0.277	85.719	0.583	1	
-26.8407	2.988	-32.974	-0.254	81.077	0.617	1	
15.9247	6.901	29.310	0.151	90.909	0.550	1	
-25.3769	10.603	-54.397	-0.240	90.909	0.550	1	1
11.0085	9.890	36.984	0.104	88.230	0.567	1	
-38.6812	5.081	-48.572	-0.366	85.719	0.583	1	
16.1534	5.004	32.605	0.153	97.014	0.515	1	
-42.5816	5.460	-49.143	-0.403	96.768	0.517	1	
60.3819	1.664	37.510	0.571	90.909	0.550	1	
-29.2331	3.346	-32.798	-0.277	90.909	0.550	1	
25.9281	5.852	41.783	0.245	96.768	0.517	1	
-37.7523	6.565	-31.122	-0.357	115.393	0.433	1	1
42.1349	10.402	38.370	0.399	103.455	0.483	1	
-23.3186	7.154	-16.391	-0.221	115.393	0.433	1	
26.7807	3.736	75.503	0.253	96.768	0.517	1	
-45.3437	13.520	-36.460	-0.429	90.909	0.550	1	
12.6957	8.855	24.247	0.120	90.909	0.550	1	
-35.5762	3.936	-44.418	-0.337	88.230	0.567	1	1
37.6132	7.937	31.413	0.356	96.768	0.517	1	
-26.3525	17.310	-44.090	-0.249	96.768	0.517	1	
23.8547	7.551	67.093	0.226	85.719	0.583	1	

-22.0278	2.441	-17.506	-0.208	74.996	0.667	1	
20.9638	6.866	42.559	0.198	103.455	0.483	1	
-23.185	12.701	-51.315	-0.219	90.909	0.550	1	
25.3664	7.151	31.166	0.240	96.768	0.517	1	
-30.4506	7.294	-31.261	-0.288	103.455	0.483	1	0
17.6993	8.267	48.376	0.167	96.768	0.517	1	
-16.984	3.412	-49.791	-0.161	96.768	0.517	1	
11.4245	5.146	45.780	0.108	115.393	0.433	1	
-16.055	6.242	-46.817	-0.152	90.909	0.550	1	
21.0028	5.922	57.678	0.199	107.135	0.467	1	
-25.2743	4.014	-26.332	-0.239	85.719	0.583	1	0
60.3354	7.615	67.551	0.571	125.000	0.400	1	
-22.8578	2.607	-11.318	-0.216	103.455	0.483	1	
44.3766	5.652	48.707	0.420	90.909	0.550	1	
-15.0566	16.282	-27.513	-0.142	74.996	0.667	1	
21.962	8.897	50.386	0.208	90.909	0.550	1	
-14.2738	10.497	-41.408	-0.135	90.909	0.550	1	
26.0929	4.436	73.736	0.247	125.000	0.400	1	
-29.5468	4.963	-34.880	-0.279	96.768	0.517	1	0
20.0925	8.953	42.842	0.190	88.230	0.567	1	
-25.6692	8.250	-32.511	-0.243	103.455	0.483	1	
28.0359	5.574	94.901	0.265	51.722	0.967	1	
-28.5479	2.808	-30.985	-0.270	115.393	0.433	1	
24.6495	8.140	29.923	0.233	111.111	0.450	1	
-25.4489	9.857	-34.149	-0.241	83.333	0.600	1	0
25.1417	5.068	43.930	0.238	96.768	0.517	1	
-24.2947	9.857	-34.149	-0.230	71.429	0.700	1	
45.4563	2.457	37.736	0.430	50.000	1.000	8	
-10.7128	6.457	-36.035	-0.101	48.389	1.033	8	
7.510	3.766	23.767	0.071	54.543	0.917	8	
-31.0267	3.407	-21.408	-0.293	28.301	1.767	8	
11.4339	3.208	29.389	0.108	42.255	1.183	8	
-21.5832	4.268	-29.352	-0.204	30.927	1.617	8	1
24.7397	11.365	27.157	0.234	29.999	1.667	8	
-20.2747	16.999	-23.272	-0.192	38.462	1.300	8	
16.6561	8.187	26.863	0.158	40.000	1.250	8	
-34.6111	3.208	-35.854	-0.327	42.255	1.183	8	
31.7198	3.969	37.734	0.300	46.155	1.083	8	
-22.4403	5.318	-22.640	-0.212	46.874	1.067	8	2
16.9432	14.060	53.632	0.160	38.962	1.283	8	
-20.3895	6.268	-24.731	-0.193	44.775	1.117	8	
32.9577	5.839	29.190	0.312	44.119	1.133	8	
-57.1748	4.812	-37.774	-0.541	69.764	0.717	8	
22.2944	3.754	51.418	0.211	50.000	1.000	8	
-20.6658	5.112	-16.902	-0.195	111.111	0.450	8	
3.3979	8.662	72.290	0.032	52.632	0.950	8	
-32.1009	6.557	-42.479	-0.304	42.255	1.183	8	3
7.1276	6.844	51.111	0.067	56.606	0.883	8	
-23.5028	5.816	-31.106	-0.222	43.478	1.150	8	
22.5892	5.026	29.932	0.214	45.455	1.100	8	

-22.3938	5.075	-19.734	-0.212	54.543	0.917	8	
32.9124	7.710	37.708	0.311	44.119	1.133	8	
-25.9898	6.708	-17.047	-0.246	68.185	0.733	8	4
22.2657	7.922	65.742	0.211	48.389	1.033	8	
-24.955	6.556	-25.599	-0.236	65.215	0.767	8	
39.8486	8.476	43.297	0.377	34.885	1.433	8	
-26.0253	5.903	-28.595	-0.246	20.548	2.433	8	
20.8227	2.943	44.973	0.197	44.119	1.133	8	
-26.2702	7.397	-29.033	-0.249	30.303	1.650	8	
8.4706	2.537	34.686	0.080	48.389	1.033	8	
-21.0599	7.107	-27.650	-0.199	41.095	1.217	8	0
27.4903	3.982	65.558	0.260	48.389	1.033	8	
-26.756	6.817	-26.268	-0.253	44.119	1.133	8	
23.2912	3.125	27.203	0.220	56.606	0.883	8	
-22.03	2.169	-19.413	-0.208	26.549	1.883	8	
21.1176	5.147	30.414	0.200	50.000	1.000	8	
-24.6853	3.853	-36.754	-0.234	28.847	1.733	8	0
26.6844	4.858	48.250	0.252	45.455	1.100	8	
-15.7713	2.601	-42.194	-0.149	32.258	1.550	8	
23.2306	2.902	26.704	0.220	40.000	1.250	8	
-18.362	2.534	-25.551	-0.174	45.455	1.100	8	
24.7698	5.667	37.572	0.234	50.000	1.000	8	
-26.25	2.676	-19.129	-0.248	48.389	1.033	8	
22.9105	6.426	29.436	0.217	53.573	0.933	8	
-23.5258	10.182	-25.218	-0.223	38.962	1.283	8	3
19.4488	13.061	53.203	0.184	41.095	1.217	8	
-21.9733	12.890	-28.582	-0.208	50.849	0.983	8	
21.9253	7.489	39.565	0.207	54.543	0.917	8	
-27.5857	3.704	-21.620	-0.261	52.632	0.950	8	
17.3787	8.557	32.692	0.164	61.222	0.817	8	
-28.4898	12.195	-35.057	-0.269	34.885	1.433	8	8
18.0962	7.012	28.909	0.171	45.455	1.100	8	
-26.089	4.646	-27.494	-0.247	45.455	1.100	8	
6.601	6.382	27.986	0.062	57.690	0.867	6	
-26.5885	0.403	-34.816	-0.252	57.326	0.872	6	
6.601	6.382	27.986	0.062	96.768	0.517	6	
-26.5885	0.403	-34.816	-0.252	60.002	0.833	6	
10.7472	0.912	18.786	0.102	81.077	0.617	6	
-23.2756	1.000	-31.218	-0.220	54.543	0.917	6	0
16.956	3.658	52.636	0.160	37.974	1.317	6	
-15.1629	3.673	-18.637	-0.143	58.824	0.850	6	
20.9373	9.222	43.318	0.198	61.222	0.817	6	
-17.585	0.829	-33.547	-0.166	50.000	1.000	6	
5.5334	2.247	64.351	0.052	50.000	1.000	6	
-22.8482	0.999	-35.397	-0.216	61.222	0.817	6	1
15.551	5.177	59.488	0.147	53.573	0.933	6	
-18.4868	0.297	-36.409	-0.175	61.222	0.817	6	
13.6707	3.077	23.385	0.129	85.719	0.583	6	
-42.907	9.982	-19.456	-0.406	54.543	0.917	6	
50.6329	2.988	41.307	0.479	54.543	0.917	6	

-33.1175	4.904	-28.889	-0.313	61.222	0.817	6	
17.0898	9.859	40.877	0.162	85.719	0.583	6	
-23.328	12.787	-32.346	-0.221	61.222	0.817	6	2
60.5146	1.634	53.828	0.572	85.719	0.583	6	
-26.0347	0.592	-26.535	-0.246	55.556	0.900	6	
61.2322	0.927	43.479	0.579	65.215	0.767	6	
-26.0268	3.565	-51.075	-0.246	52.632	0.950	6	
21.0596	7.864	42.791	0.199	45.455	1.100	6	
-24.2904	8.418	-48.412	-0.230	65.215	0.767	6	1.5
58.9283	0.355	20.990	0.557	76.923	0.650	6	
-47.3576	1.393	-31.763	-0.448	56.606	0.883	6	
25.7295	5.319	66.569	0.243	90.909	0.550	6	
-15.3919	8.036	-41.587	-0.146	35.714	1.400	6	
9.1628	2.247	51.667	0.087	63.833	0.783	6	
-10.3778	5.612	-31.564	-0.098	45.455	1.100	6	
18.0176	15.515	62.173	0.170	58.824	0.850	6	
-19.050	1.437	-26.845	-0.180	50.000	1.000	6	3.5
22.0844	3.035	40.041	0.209	66.667	0.750	6	
-50.4087	0.464	-22.511	-0.477	41.095	1.217	6	
22.35	2.649	55.123	0.211	58.824	0.850	6	
-38.7179	5.893	-35.937	-0.366	56.606	0.883	6	
59.8894	3.013	93.882	0.567	96.768	0.517	6	
-26.4906	7.781	-28.996	-0.251	53.573	0.933	6	4
22.9685	0.640	39.585	0.217	51.722	0.967	6	
-28.9739	7.781	-28.996	-0.274	40.000	1.250	6	
10.3657	7.304	37.428	0.098	71.429	0.700	6	
-21.0972	0.603	-31.831	-0.200	45.455	1.100	6	
24.2963	5.287	50.619	0.230	65.215	0.767	6	
-22.5641	2.153	-31.340	-0.213	41.095	1.217	6	
27.062	2.531	63.760	0.256	76.923	0.650	6	
-32.9853	3.802	-55.083	-0.312	52.632	0.950	6	3
32.3104	7.535	28.217	0.306	81.077	0.617	6	
-32.2798	5.349	-32.965	-0.305	78.952	0.633	6	
37.9389	7.658	78.463	0.359	56.606	0.883	6	
-36.9459	6.909	-43.093	-0.349	56.606	0.883	6	
94.9086	4.875	50.030	0.898	50.000	1.000	6	
-19.7729	1.960	-84.113	-0.187	53.573	0.933	6	2
67.4141	7.283	51.669	0.638	68.185	0.733	6	
-22.9331	15.574	-77.915	-0.217	62.500	0.800	6	
20.3756	2.304	48.319	0.230	133.333	0.300	2	
-24.4936	4.036	-23.025	-0.276	109.081	0.367	2	
25.3094	2.560	39.798	0.285	160.000	0.250	2	
-29.46	7.922	-26.868	-0.332	141.193	0.283	2	
28.636	2.817	31.276	0.323	141.193	0.283	2	
-30.2415	9.110	-29.397	-0.341	133.333	0.300	2	0
17.0164	4.477	35.387	0.192	133.333	0.300	2	
-18.3409	26.128	-28.298	-0.207	109.081	0.367	2	
26.643	8.053	35.166	0.300	133.333	0.300	2	
-24.3022	4.709	-17.699	-0.274	100.000	0.400	2	
32.6904	6.043	28.547	0.369	160.000	0.250	2	

-21.0378	2.191	-12.799	-0.237	133.333	0.300	2	0
22.1572	2.221	31.546	0.250	120.012	0.333	2	
-33.0491	2.191	-12.799	-0.373	120.120	0.333	2	
47.8606	2.976	9.569	0.540	133.333	0.300	2	
-14.3806	9.165	-30.947	-0.162	126.302	0.317	2	
23.6568	2.976	9.569	0.267	77.414	0.517	2	
-6.2355	3.873	-28.985	-0.070	109.081	0.367	2	
26.3064	11.349	25.800	0.297	68.575	0.583	2	
-14.6361	2.042	-10.161	-0.165	120.012	0.333	2	1
24.3866	13.126	6.658	0.275	59.997	0.667	2	
-21.5372	4.691	-33.140	-0.243	120.012	0.333	2	
25.9634	4.670	13.680	0.293	92.315	0.433	2	
-31.1023	2.993	-14.301	-0.351	120.012	0.333	2	
33.617	15.564	31.532	0.379	120.012	0.333	2	
-24.4825	5.674	-27.580	-0.276	95.992	0.417	2	0
27.2415	0.905	19.842	0.307	100.000	0.400	2	
-9.4784	4.368	-17.399	-0.107	120.012	0.333	2	
30.2731	7.027	31.332	0.341	133.333	0.300	2	
-23.8939	2.033	-67.127	-0.269	133.333	0.300	2	
50.5337	4.026	30.409	0.570	120.012	0.333	2	
-28.7594	6.160	-23.745	-0.324	141.193	0.283	2	
40.2224	5.265	37.352	0.453	160.000	0.250	2	
-15.4068	4.839	-44.678	-0.174	120.012	0.333	2	0
22.6064	4.946	28.878	0.255	109.081	0.367	2	
-44.3151	16.481	-53.040	-0.500	141.193	0.283	2	
19.5184	4.628	20.404	0.220	141.193	0.283	2	
-10.338	4.875	-34.660	-0.117	133.333	0.300	2	
12.816	4.667	22.504	0.144	120.012	0.333	2	
-22.6803	5.410	-36.379	-0.256	100.000	0.400	2	0
14.5983	2.278	26.789	0.165	95.992	0.417	2	
-42.4571	7.667	-32.480	-0.479	149.981	0.267	2	
26.6315	2.236	12.215	0.300	126.302	0.317	2	
-15.0136	6.947	-12.879	-0.169	120.012	0.333	2	
14.9476	1.600	7.413	0.169	100.000	0.400	2	
-11.6084	6.947	-12.879	-0.131	100.000	0.400	2	
30.0456	1.029	10.458	0.339	120.012	0.333	2	
-22.4276	4.728	-23.208	-0.253	109.081	0.367	2	0
15.5388	0.393	7.979	0.175	120.012	0.333	2	
-27.8996	9.967	-23.148	-0.315	95.992	0.417	2	
14.6596	3.063	14.585	0.165	120.012	0.333	2	
-19.0456	1.095	-6.205	-0.215	109.081	0.367	2	
32.0901	3.520	23.342	0.362	141.193	0.283	2	
-25.5796	5.446	-29.824	-0.288	109.081	0.367	2	1
12.1113	1.055	7.256	0.137	100.000	0.400	2	
-38.9438	7.124	-14.362	-0.439	109.081	0.367	2	

APPENDIX F: Matlab Source Code

batch_bed.m

```
close all
clear all

init_bed

batch_mode = TRUE;

% get research data folder name
get_PC_bed_path

% get list of patients to be processed
get_patient_list

[num_patients,n] = size(patient_list);

for patnum=1:num_patients,

    file_name = patient_list(patnum,:);
    idx = find(abs(file_name) >= 32);          % printable non-blank characters
    file_name = file_name(idx);

    idx = find(file_name == '.');
    if (isempty(idx)),
        root_file = file_name;
    else
        root_file = file_name(1:(idx(1)-1));
    end

    convert_bed_file

    for rn=1:num_runs,
        if (rn < 10),
            run_code = [root_file, '_run0', int2str(rn)];
        else
            run_code = [root_file, '_run', int2str(rn)];
        end
        run_file = [data_path, run_code, '.mat'];

        fprintf(['\nProcessing ', run_code, ' ...']);
        load(run_file);

        batch_bed_file

    end
end
```

batch_bed_anal.m

```
close all
clear all

init_bed

batch_mode = TRUE;

% get research data folder name
get_PC_bed_path

% get list of patients to be processed
get_patient_list
```

```

[num_patients,n] = size(patient_list);

for patnum=1:num_patients,

    file_name = patient_list(patnum,:);
    idx = find(abs(file_name) > 32);           % printable non-blank characters
    file_name = file_name(idx);

    idx = find(file_name == '.');
    if (isempty(idx)),
        root_file = file_name;
    else
        root_file = file_name(1:(idx(1)-1));
    end

    convert_bed_file

for rn=1:num_runs,
    if (rn < 10),
        run_code = [root_file, '_run0', int2str(rn)];
    else
        run_code = [root_file, '_run', int2str(rn)];
    end

    run_file = [data_path, run_code, '.mat'];

    fprintf(['\nProcessing ', run_code, '...']);
    load(run_file);

    batch_bed_file

end

for phase=1:1:4,
    if (phase==1),
        run_code = [root_file, '_run10'];
    elseif (phase==2),
        run_code = [root_file, '_run14'];
    elseif (phase==3),
        run_code = [root_file, '_run18'];
    elseif (phase==4),
        run_code = [root_file, '_run22'];
    end
    batch_eye_anal(data_path, run_code);
end
%%%%%%%%%%%%%%%%%%%%%%%%%%%%%%%%%%%%%%%%%%%%%%%%%%%%%%%%%%%%%%%%%%%%%%%%%%
%%%%%%%%%%%%%%%%%%%%%%%%%%%%%%%%%%%%%%%%%%%%%%%%%%%%%%%%%%%%%%%%%%%%%%%%%%
end

%%%%%%%%%%%%%%%%%%%%%%%%%%%%%%%%%%%%%%%%%%%%%%%%%%%%%%%%%%%%%%%%%%%%%%%%%%
%%%%%%%%%%%%%%%%%%%%%%%%%%%%%%%%%%%%%%%%%%%%%%%%%%%%%%%%%%%%%%%%%%%%%%%%%%
% Delete this after subject 20
% for rn=12:num_runs,
%     if (rn < 10),
%         run_code = [root_file, '_run0', int2str(rn)];
%     else
%         run_code = [root_file, '_run', int2str(rn)];
%     end
%     run_file = [data_path, run_code, '.mat'];
%     fprintf(['\nProcessing ', run_code, '...']);
%     load(run_file);
%     batch_bed_file
% end
%%%%%%%%%%%%%%%%%%%%%%%%%%%%%%%%%%%%%%%%%%%%%%%%%%%%%%%%%%%%%%%%%%%%%%%%%%
%%%%%%%%%%%%%%%%%%%%%%%%%%%%%%%%%%%%%%%%%%%%%%%%%%%%%%%%%%%%%%%%%%%%%%%%%%

```

batch_bed_anal_right

```
close all
clear all

FALSE = 0;
TRUE = 1;

RIGHT_VERTICAL = 3;
RIGHT_HORIZONTAL = 5;

num_increase = 2;
num_RMS = 0.25;
min_diff_class = 30;

batch_mode = TRUE;

% get research data folder name
get_PC_bed_path

% get list of patients to be processed
get_patient_list

[num_patients,n] = size(patient_list);

for patnum=1:num_patients,

    file_name = patient_list(patnum,:);
    idx = find(abs(file_name) > 32);           % printable non-blank characters
    file_name = file_name(idx);

    idx = find(file_name == '.');
    if (isempty(idx)),
        root_file = file_name;
    else
        root_file = file_name(1:(idx(1)-1));
    end

    convert_bed_file

    for rn=1:num_runs,
        if (rn < 10),
            run_code = [root_file, '_run0', int2str(rn)];
        else
            run_code = [root_file, '_run', int2str(rn)];
        end
        run_file = [data_path, run_code, '.mat'];

        fprintf('\nProcessing ', run_code, ' ...!');
        load(run_file);

        % create time vector
        clear t
        t = [0:(num_samples-1)] / sample_rate;

        %
        % process right vertical eye position data
        %
        raw_index = RIGHT_VERTICAL;
        cal_index = RIGHT_VERTICAL+num_params;
        which_eye = 'Right Vertical';
        file_ext = '_RV.mat';

        batch_eye_channel

        %
        % process right horizontal eye position data
        %
        raw_index = RIGHT_HORIZONTAL;
```

```

cal_index = RIGHT_HORIZONTAL+num_params;
which_eye = 'Right Horizontal';
file_ext = '_RH.mat';

batch_eye_channel

    end

for phase=5:5:10,
    if (phase==5),
        run_code = [root_file, '_run05'];
    else
        run_code = [root_file, '_run10'];
    end
% This programme analyzes the eye & button data using the button (ANALOG0)
% as the trigger for start of nystagmus. Outputs to a new .txt file for each
% subject, phase (run), and eye.
% This programme was modified from eye_anal to automatically edit Right
% vertical eye data during batch eye processing.
%
% By: David Phillips April 4, 2001

    data_dir=data_path;
    filename=run_code;

fn=[data_dir, filename, '.mat'];
load(fn);
run_file = [data_dir, filename, '_RV.mat'];
load(run_file);

    Button=data(:,6);                                %Retrieve Duration Button
    button_find;

% This part finds the point of local max of eye data between button_start and _stop.
% then it finds the exponential curve & cumulative eye mvmt given that start index.

peakT = 4;          % peakT is number of seconds past button_stop to search

for turn=1:turncount,

    % Find start of eye movement
    end_search=min(button_stop(turn)+(peakT*60),length(Button)); % Ensure no overruns of length
    [peak, index] = max(abs(spv(button_start(turn)+60:end_search)));

    if spv(index) == 0
        worked=0;
    else peak = peak*sign(spv(index));    % Gives Peak the right sign
    end

    start_ind(turn,1)=button_start(turn)+index;
    integsecs=10;                                % Adjust time to fit curve here in secs
    max_pts=integsecs*60;                          % number of points to fit curve
    max_pts=min(start_ind(turn)+max_pts,length(spv)); % Ensure no overruns of length
    num_pts=max_pts-start_ind(turn);
    [A_temp, tau_temp]=expfit(start_ind(turn), spv, num_pts);

    % Append A_temp, tau_temp to A, tau vectors
    A(turn,1)=A_temp;
    tau(turn,1)=tau_temp;

    %----- curve fit goodness-----
    ftest(turn,1)=checkcurve(spv, start_ind(turn), A(turn), tau(turn), num_pts);
    if (ftest(turn)<=3.00)
        fprintf('\nRefit A and tau for Head Turn %4.0f, F-test = %f (<3.00)\n', turn, ftest(turn));
        fprintf('File to edit is: %s', filename);
    end

    %-----cumulative spv-----
    % This integrates the area under the fitted A, tau curve.
    end_eye=10; % for 10sec

```

```

t_matrix=transpose(0:01:10);
curve=A(turn)*exp(-t_matrix/tau(turn));
cum_eye(turn,1)=trapz(t_matrix,curve);
end

% Write to file
write_file = [data_dir, filename, '_RV_results.txt'];
fid = fopen(write_file,'w');
fprintf(fid,'\nBut_Start\tEye_Start\tBut_Dur\t A\t Tau\t Cum_Eye\t F-Test\n');
for turn=1:turncount,
    fprintf(fid,'%8.4ft %6.0ft %8.4ft %8.4ft %8.4ft %8.4ft %8.4ft\n'...
        , button_start_time(turn), start_ind(turn), button_dur(turn), A(turn), tau(turn), cum_eye(turn), flest(turn));
end
fclose(fid);

end

end

```

batch_bed_file.m

```

% create time vector
clear t
t = [0:(num_samples-1)] / sample_rate;

%
% process left vertical eye position data
%
% raw_index = LEFT_VERTICAL;
% cal_index = LEFT_VERTICAL+num_params;
% which_eye = 'Left Vertical';
% file_ext = '_LV.mat';
%
% batch_eye_channel

%
% process right vertical eye position data
%
RIGHT_VERTICAL = 4;
raw_index = RIGHT_VERTICAL;
cal_index = RIGHT_VERTICAL+num_params;
which_eye = 'Right Vertical';
file_ext = '_RV.mat';

batch_eye_channel

%
% process left horizontal eye position data
%
raw_index = LEFT_HORIZONTAL;
cal_index = LEFT_HORIZONTAL+num_params;
which_eye = 'Left Horizontal';
file_ext = '_LH.mat';

batch_eye_channel

%
% process right horizontal eye position data
%
raw_index = RIGHT_HORIZONTAL;
cal_index = RIGHT_HORIZONTAL+num_params;
which_eye = 'Right Horizontal';
file_ext = '_RH.mat';

%batch_eye_channel

```

batch_eye_anal.m

```
function batch_eye_anal(data_dir, filename)
% This programme analyzes the eye & button data using the button (ANALOG0)
% as the trigger for start of nystagmus. Outputs to a new .txt file for each
% subject, phase (run), and eye.
% This programme was modified from eye_anal to automatically edit Left
% vertical eye data during batch eye processing.
%
% By: David Phillips March 28, 2001

ini_bed

fn=[data_dir, filename, '.mat'];
load(fn);
%run_file = [data_dir, filename, '_LV.mat'];
run_file = [data_dir, filename, '_RV.mat'];
load(run_file);

Button=data(:,6); %Retrieve Duration Button

button_find;

% This part finds the point of local max of eye data between button_start and _stop,
% then it finds the exponential curve & cumulative eye mvmt given that start index.

peakT = 4; % peakT is number of seconds past button_stop to search

for turn=1:turncount.

    % Find start of eye movement
    end_search=min(button_stop(turn)+(peakT*60),length(Button)); % Ensure no overruns of length
    [peak, index] = max(abs(spv(button_start(turn)+60:end_search)));

    if spv(index) == 0
        worked=0;
    else peak = peak*sign(spv(index)); % Gives Peak the right sign
    end

    start_ind(turn,1)=button_start(turn)+index;
    integsecs=10; % Adjust time to fit curve here in secs
    max_pts=integsecs*60; % number of points to fit curve
    max_pts=min(start_ind(turn)+max_pts,length(spv)); % Ensure no overruns of length
    num_pts=max_pts-start_ind(turn);
    [A_temp, tau_temp]=expfit(start_ind(turn), spv, num_pts);

    % Append A_temp, tau_temp to A, tau vectors
    A(turn,1)=A_temp;
    tau(turn,1)=tau_temp;

    %----- curve fit goodness-----
    ftest(turn,1)=checkcurve(spv, start_ind(turn), A(turn), tau(turn), num_pts);
    if (ftest(turn)<=3.00)
        fprintf('\nRefit A and tau for Head Turn %4.0f, F-test = %f (<3.00)\n', turn, ftest(turn));
        fprintf('File to edit is: %s', filename);
    end

    %-----cumulative spv-----
    % This integrates the area under the fitted A, tau curve.
    end_eye=10; % for 10sec
    t_matrix=transpose(0:.01:10);
    curve=A(turn)*exp(-t_matrix/tau(turn));
    cum_eye(turn,1)=trapz(t_matrix,curve);
end

% Write to file
%write_file = [data_dir, filename, '_LV_results.txt'];
write_file = [data_dir, filename, '_RV_results.txt'];
fid = fopen(write_file,'w');
```

```

fprintf(fid, '\nBut_Start\tEye_Start\t But_Dur\t A\t Tau\t Cum_Eye\t F-Test\n');
for turn=1:turncount;
    fprintf(fid, '%8.4f\t %6.0f\t %8.4f\t %8.4f\t %8.4f\t %8.4f\t %8.4f\n'...
        . button_start_time(turn), start_ind(turn), button_dur(turn), A(turn), tau(turn), cum_eye(turn), ftest(turn));
end
fclose(fid);

```

bed_classify_phases.m

```

function [fast_start, fast_end] = bed_classify_phases(vel, num_RMS, ...
num_increase, min_diff_class, sample)
%
% bed_classify_phases.m - attempts to detect fast phases in a velocity trace 'vel'
%
% The velocity data is filtered by the AATM algorithm, to calculate an estimate
% of SPV. The difference between the raw eye velocity and the AATM velocity
% is calculated. Any difference which exceeds a specified multiple (num_RMS)
% of the RMS difference, and which also exceeds a specified absolute threshold
% (min_diff_class), is classified as a "fast" point. A fast phase is defined
% as a series of consecutive fast points. A specified number of points
% (num_increase) are added to the beginning and end of the fast phase, to allow
% for transient behaviour, particularly due to digital filtering effects.
% "fast_start" is a vector in which each element is the sample number of the
% start of a fast phase. "fast_end" contains the corresponding sample
% numbers of the ends of the fast phases.
%
% Note: fast phases in the first or last half-second of data will not be properly detected
%
% Suggested values for the input parameters are:
%     vel = eye velocity, calculated by differentiating calibrated eye position
%     num_RMS = 0.25
%     num_increase = 2
%     min_diff_class = 30
%     sample = 60
%
% Written by: MDB 10/1/99
%
last = length(vel);
AATM_transient = num_increase;

% run AATM filter over data
AATM_spv = newAATM(sample+1, vel);           % one second filter window

% find data points for which velocity and AATM are within 'num_RMS'
i = 1 + AATM_transient;
j = last - AATM_transient;
slow = min_threshold( vel(i:j), AATM_spv(i:j), num_RMS, min_diff_class );
slow = [zeros(AATM_transient,1); slow; zeros(AATM_transient,1)];
fast = ~slow;
clear i j AATM_transient

% increase fast phase duration by 'num_increase' sample
% in each direction for transients
if (num_increase > 0),
    fast = filtfilt(ones(num_increase+1,1), 1, fast);
    fast = (fast > 0);
end

% find start and end of each fast phase
fast_diff = filter([1 -1], 1, fast); % two-point difference
fast_start = find(fast_diff > 0);    % 0 to 1 transition
num_start = length(fast_start);
fast_end = find(fast_diff < 0) - 1;  % 1 to 0 transition
num_end = length(fast_end);
if (num_end < num_start),
    fast_end = [fast_end; last];

```

```

    num_end = num_end + 1;
end

clear slow fast num_slow fast_diff num_end num_start

return;

```

bed_eye_channel.m

```

% free up variable space
clear pos vel spv edited_spv filt_spv fast_start fast_end

% detect blinks using raw data, but make interpolations on calibrated data
if (batch_mode)
    pos = deblink(data(:,raw_index), data(:,cal_index), 0, 0);
else
    save_file = [data_path, run_code, file_ext];
    load(save_file);
    fig = figure('Name', 'Review of Despiking Algorithm');
    plot(t, data(:,cal_index), 'y');
    hold on
    plot(t, pos, 'b');
    xlabel('Time (sec)');
    ylabel('Eye Position (deg)');
    title([run_code, '-- ', which_eye]);
    yn = get_yn('Do you want to redo the despiking algorithm?', 'N');
    close(fig);
    if (yn == 'Y'),
        redo_flag = TRUE;
        pos = deblink(data(:,raw_index), data(:,cal_index), -1, -1);
    end
end

% filter eye position data to enhance signal-to-noise ratio
% - one pass of order statistic filter to minimize video quantization,
%   allowing for curved eye movements
% - two passes of fourth-order phase-less Butterworth low-pass filter
%   with 30 Hz corner frequency, to reduce noise
% - two additional passes of order statistic filter, to reduce noise
%   and sharpen corners of nystagmus, allowing for curved eye movements
if (batch_mode | redo_flag)
    pos = filt_position(pos, sample_rate, 2, 3, TRUE);
end

% differentiate eye position to get velocity
if (batch_mode | redo_flag)
    vel = differentiate(pos, sample_rate);
end

% classify fast phases in eye velocity data, and interpolate across
if (batch_mode | redo_flag)
    [fast_start, fast_end] = bed_classify_phases(vel, num_RMS, num_increase, ...
        min_diff_class, sample_rate);
    spv = interpolate(vel, fast_start, fast_end);
end

if (~batch_mode),
    fig = figure('Name', 'SPV from Automated Fast Phase Detection');
    plot(t, vel);
    hold on
    h2 = plot(t, spv, 'b');
    xlabel('Time (sec)');
    ylabel('Eye Velocity (deg/sec)');
    title([run_code, '-- ', which_eye]);
    yn = get_yn('Do you want to change the fast phase detection parameters?', 'N');
    while (yn == 'Y'),
        redo_flag = TRUE;
        new_RMS = input([' # of RMS levels (' , num2str(num_RMS), ') : ']);
    end
end

```



```

        if (isempty(new_RMS),
            new_RMS = num_RMS;
        end
        new_inc = input([' # of transition points (', int2str(num_increase), '): ']);
        if (isempty(new_inc),
            new_inc = num_increase;
        else
            new_inc = round(abs(new_inc));
        end
        new_min = input([' minimum difference threshold (', num2str(min_diff_class), '): ']);
        if (isempty(new_min),
            new_min = min_diff_class;
        else
            new_min = abs(new_min);
        end
        [fast_start, fast_end] = bed_classify_phases(vel, new_RMS, new_inc, ...
                                                    sample_rate);
                                                    new_min;
        spv = interpolate(vel, fast_start, fast_end);
        set(h2, 'YData', spv);
        drawnow
        yn = get_yn('Do you want to change the fast phase detection parameters','N');
    end
    close(fig);
end

% manual editing
if (~batch_mode),
    yn = get_yn('Do you want to manually edit the SPV data','Y');
    if (yn == 'Y'),
        redo_flag = TRUE;
        if (isempty(fast_start),
            d = (spv ~= vel);
            df = diff(d);
            fast_start = find(df > 0);
            fast_end = find(df < 0);
            if (length(fast_start) > length(fast_end)),
                fast_end = [fast_end; length(spv)];
            end
        end
        fig = figure('Name', ['Manual Editing -- ', run_code, ' -- ', which_eye]);
        ed_spv = edit_alg_diff(t, spv, vel, pos, [fast_start fast_end], 'y');
        close(fig);
        yn = get_yn('Do you want to save the newly edited SPV data','Y');
        if (yn == 'Y'),
            edited_spv = ed_spv;
        end
        clear ed_spv
    end
end

% save data in a Matlab-format file
save_file = [run_file(1:(length(run_file)-4)), file_ext];
eval(['save ', save_file, ' pos vel spv edited_spv filt_spv']);

```

button_find.m

```

% Find Button Start & Stop
% By David Phillips, March 30, 2001

button_on=find(Button>=max(Button)-250); % Button Threshold = 100 below maximum

button_sw_temp=find((button_on(2:end)-1)~=button_on(1:end-1)); % Find toggle (on-off)

% Write start & stop of toggle
button_start=[button_on(1);button_on(button_sw_temp+1)];
button_stop=[button_on(button_sw_temp);button_on(end)];

```

```

% Check for correct number of turns

turncount=length(button_start);

if turncount~=14
    fprintf('\nWarning!! Incorrect Number of Turns!!! %4.0f Turns Recorded\n', turncount);
end

button_start_time=button_start/60;
button_dur=(button_stop-button_start)/60;

```

check_curve.m

```

function ftest=checkcurve(spv, startPt, a_check, tau_check, num_pts)
% Checks curve goodness of fit using F-test
% requires spv, startPt, A, tau, number of points
% By David Phillips, March 28, 2001
% SSQT = Total Sum of Squares (fitted-avg)
% SSQE = Error Sum of Squares (point-fitted)
% SSQR = Regress Sum of Squares (SSQT-SSQE)

clear t;
t=rot90([1:num_pts+1]/60,-1); % t=time in sec
modspv=spv(startPt:startPt+num_pts); % modspv is spv for num_pts

curve_vals=a_check*exp(-t/tau_check);

avgspv=mean(modspv);
SSQT=sum((modspv-avgspv).^2);
SSQE=sum((modspv-curve_vals).^2);
SSQR=SSQT-SSQE;

ftest=(SSQR/2)/(SSQE/num_pts-3); % 2 for A, tau, 3 for A, tau, mean

% compare f-test to 3.00 for 2DOF (A, tau), P=0.05, infinite points (==600pts)

```

convert_bed_file.m

```

%data_path = 'C:\MATLAB\data\watson_data\';
%file_name = 'xlrotttest.txt';

fid = fopen([data_path,file_name],'r');

%
% decipher header information
%

% Sometimes, header info is tab-delimited
% In other cases, it is separated by blank spaces
% In either situation, looking for unprintable characters seems to work,
% to find either tab (9) or carriage return (13).
TAB = 9; % tab character seems to be used in header info, instead of blank space
COLON = 58;
BLANK = 32;

iscan_ver = fgets(fid); % ISCAN version number, and file format

% discard two lines
inline = fgets(fid);
inline = fgets(fid);

% subject name
inline = fgets(fid);
l = length(inline);

```

```

cl = find(abs(inline) == COLON);           % look for ":" in string
str = inline( (cl(1)+1) : 1 );
tb = find(abs(str) < BLANK);             % look for "tab" or "cr" in sub-string
subject_name = str( (tb(1)+1) : (tb(2)-1) );

% test date
inline = fgets(fid);
l = length(inline);
cl = find(abs(inline) == COLON);           % look for ":" in string
str = inline( (cl(1)+1) : 1 );
tb = find(abs(str) < BLANK);             % look for "tab" or "cr" in sub-string
test_date = str( (tb(1)+1) : (tb(2)-1) );

% test description
inline = fgets(fid);
tb = find(abs(inline) == COLON);           % look for "colon" in string
l = length(inline);
if (inline(tb(1)+1) <= BLANK),
    test_descr = inline( (tb(1)+2) : (l-1) );
else
    test_descr = inline( (tb(1)+1) : (l-1) );
end

% discard line
inline = fgets(fid);

% number of runs
inline = fgets(fid);
l = length(inline);
cl = find(abs(inline) == COLON);           % look for ":" in string
str = inline( (cl(1)+2) : 1 );
tb = find(abs(str) < BLANK);             % look for "tab" or "cr" in sub-string
num_runs = eval( str(1:(tb(1)-1)) );

% total number of points recorded (i.e. number of samples)
inline = fgets(fid);
l = length(inline);
cl = find(abs(inline) == COLON);           % look for ":" in string
str = inline( (cl(1)+2) : 1 );
tb = find(abs(str) < BLANK);             % look for tab or "cr" in sub-string
total_pts = eval( str(1:(tb(1)-1)) );

% total number of parameters recorded (i.e. number of raw data channels)
inline = fgets(fid);
l = length(inline);
cl = find(abs(inline) == COLON);           % look for ":" in string
str = inline( (cl(1)+2) : 1 );
tb = find(abs(str) < BLANK);             % look for tab/cr in sub-string
num_params = eval( str(1:(tb(1)-1)) );

% discard three lines
inline = fgets(fid);
inline = fgets(fid);
inline = fgets(fid);

% parse out number of points in each run
run_points = zeros(num_runs,1);           % number of samples in each run
run_rate = zeros(num_runs,1);           % sampling rate for each run
run_start = [];                          % start time for each run
for i=1:num_runs,
    inline = fgets(fid);
    l = length(inline);
    tb = find(abs(inline) == TAB);         % look for "tab" in string
    if (inline(l-1) >= BLANK),
        tb = [0, tb, l];
    end
    run_points(i) = eval( inline( (tb(1)+1) : (tb(2)-1) ) );
    run_rate(i) = 60; %eval( inline( (tb(2)+1) : (tb(3)-1) ) );
    run_start = [run_start; inline( (tb(3)+1) : (tb(3)+9) )];
end

```

```

% discard three lines
inline = fgets(fid);
inline = fgets(fid);
inline = fgets(fid);

% parse information for names of channels. and mean and standard deviation
% of each channel over length of runs
param_name = [];
name_len = 10; % allow parameter names up to 10 characters long
all_raw_mean = zeros(num_params,num_runs);
all_raw_std = zeros(num_params,num_runs);
all_cal_mean = zeros(num_params,num_runs);
all_cal_std = zeros(num_params,num_runs);
for i=1:num_params.

    % extract name of parameter
    inline = fgets(fid);
    idx = find(inline == '('); % look for "(" in string
    pn = inline(2: (idx(1)-2));
    l = length(pn);
    if (l < name_len), % pad with blanks
        pn = [pn, blanks(name_len - l)];
    else % truncate length
        pn = pn(1:name_len);
    end
    idx = find(pn < BLANK);
    for k=1:length(idx), % replace tabs with blank characters
        pn(idx(k)) = BLANK;
    end
    param_name = [param_name; pn];

    % extract mean of raw data from same line
    idx = find(inline == ')'); % look for ")" in string
    str = inline( (idx(2)+1) : length(inline) );
    idx = find(abs(str) < BLANK); % look for non-numeric in sub-string
    for j=1:num_runs,
        num = eval(str( (idx(j)+1) : (idx(j+1)-1) ));
        all_raw_mean(i,j) = num;
    end

    % extract standard deviation of raw data
    inline = fgets(fid);
    idx = find(inline == ')'); % look for ")" in string
    str = inline( (idx(2)+1) : length(inline) );
    idx = find(abs(str) < BLANK); % look for non-numeric in sub-string
    for j=1:num_runs,
        num = eval(str( (idx(j)+1) : (idx(j+1)-1) ));
        all_raw_std(i,j) = num;
    end

    % extract mean of calibrated data
    inline = fgets(fid);
    idx = find(inline == ')'); % look for ")" in string
    str = inline( (idx(2)+1) : length(inline) );
    idx = find(abs(str) < BLANK); % look for non-numeric in sub-string
    for j=1:num_runs,
        num = eval(str( (idx(j)+1) : (idx(j+1)-1) ));
        all_cal_mean(i,j) = num;
    end

    % extract standard deviation of calibrated data
    inline = fgets(fid);
    idx = find(inline == ')'); % look for ")" in string
    str = inline( (idx(2)+1) : length(inline) );
    idx = find(abs(str) < BLANK); % look for non-numeric in sub-string
    for j=1:num_runs,
        num = eval(str( (idx(j)+1) : (idx(j+1)-1) ));
        all_cal_std(i,j) = num;
    end
end

```

```

end

% discard three lines
inline = fgets(fid);
inline = fgets(fid);
inline = fgets(fid);
inline = fgets(fid);

num_channels = 2*num_params + 1;      % raw and calibrated, plus sample number

idx = find(file_name == '.');
if (isempty(idx)),
    root_file = file_name;
else
    root_file = file_name(1:(idx(1)-1));
end

for i=1:num_runs,

    % input data for run
    num_samples = run_points(i);

    fprintf('\nConverting ', file_name, ' -- run #', int2str(i), ' (', ...
            int2str(num_samples), ' samples) ...');

    clear data
    data = zeros(num_samples, num_channels);

    for j=1:num_samples,

if (~rem(j,500)),
    fprintf('\n finished %d', j);
end

                inline = fgets(fid);
                idx = find(abs(inline) < BLANK);      % look for non-numeric in string
                if (idx(1) > 2),
                    idx = [1,2,idx];
                elseif (idx(2) > 2),
                    idx = [1,idx];
                end

        for k=1:num_channels,
            num = eval(inline( (idx(k+1)+1) : (idx(k+2)-1) ));
            data(j,k) = num;
        end
    end

    % save data for this run in a separate mat-file
    sample_rate = 60; %run_rate(i);
    start_time = run_start(i,:);
    raw_mean = all_raw_mean(:,i);
    raw_std = all_raw_std(:,i);
    cal_mean = all_cal_mean(:,i);
    cal_std = all_cal_std(:,i);

    if (i < 10),
        out_file = [data_path, root_file, '_run0', int2str(i), '.mat'];
    else
        out_file = [data_path, root_file, '_run', int2str(i), '.mat'];
    end

    param_list = 'data iscan_ver subject_name test_date test_descr num_runs';
    param_list = [param_list, 'total_pts num_params num_samples sample_rate'];
    param_list = [param_list, 'start_time raw_mean raw_std cal_mean cal_std'];
    param_list = [param_list, 'param_name num_channels out_file'];

    eval(['save ', out_file, ', ', param_list]);

    % discard one line

```

```

        inline = fgets(fid);

end

fprintf('\n');

fclose(fid);

```

eye.m

```

close all
clear all

init_bed

batch_mode = FALSE;

% get research data folder name
get_PC_bed_path

% get list of patients to be processed
get_patient_list
[num_patients,n] = size(patient_list);
for patnum=1:num_patients,

    file_name = patient_list(patnum,:);
    idx = find(abs(file_name) > 32);           % printable non-blank characters
    file_name = file_name(idx);

    idx = find(file_name == '.');
    if (isempty(idx)),
        root_file = file_name;
    else
        root_file = file_name(1:(idx(1)-1));
    end

    run=input('\nEnter run number: ', 's');
    rn=str2num(run);
        if (rn < 10),
            run_code = [root_file, ' run0', run];
        else
            run_code = [root_file, '_run', run];
        end
        run_file = [data_path, run_code, '.mat'];
    load(run_file);
    %%%%%%%%%%%
    fprintf('\nWhich eye do you want to use for %s?\n', run_code);
    eyenum=input('LV=1, LH=2, RV=3, RH=4 (LV default): ', 's');
    eyenum=str2num(eyenum);

    if isempty(eyenum)
        eyenum=1;
    end

    if eyenum==2
        eyeext='_LH';
    elseif eyenum==3
        eyeext='_RV';
    elseif eyenum==4
        eyeext='_RH';
    else
        eyeext='_LV';
    end

    run_file = [data_path, run_code, eyeext, '.mat'];
    load(run_file);

```

```

% run_file = [data_path, run_code, '_LV.mat'];
% load(run_file);

Head =data(:,7);

% Anlog1=data(:,15);
%Retrieve Analog 1 from column 15
% Anlog2=data(:,16);
%Retrieve Analog 1 from column 16
% x1=1.1646.*Anlog1; %use x1=6.2189 for subjects 2,4,6,7,9. Use x1=1.1646 for 10,11,12
% x2=1.1646.*Anlog2; %recalibration factor C %-----
% gyroy=filt_gyro_position(x1); %Filter Analog 1 (yaw motions
% gyrop=filt_gyro_position(x2); %Filter Analog 2 (pitch motions

figure(1)
subplot(2,1,1)
x=[1:length(spV)];
plot(x,spV)
subplot(2,1,2)
x=[1:length(Head)];
plot(x,Head)
[x7,y]=ginput(1);
zm=round(x7);
top=max(spV(zm-60:zm+900));
bot=min(spV(zm-60:zm+900));
subplot(2,1,1)
axis([x7-200,x7+500,bot-5,top+5]);

subplot(2,1,2)
h_top=max(Head(zm-60:zm+900));
h_bot=min(Head(zm-60:zm+900));
axis([x7-200,x7+500,h_bot,h_top]);
%-- look for end of head movement----have that be startT
over=10;
% fprintf('Manually change axis until can eye ball end of head peak\n');
%while(over ~= 0)
%-- while not pressing escape key

% endpoint=input('\nEnter end point: ','s');
% x2=str2num(endpoint);

% axis([x2-5,x2+4*60,-200,280]);
% subplot(2,1,1)
% axis([x2-5,x2+4*60,-200,280]);
% subplot(2,1,2)
% quitting=input('\nEnter 0 if done: ','s');
% over=str2num(quitting);
% end

% start=endpoint;%input('Enter start point: ','s');
[start, y] = ginput(1);
startT=round(start); %-- actually in points, not time
peakT = 4;
spV2 = spV;%zeros(size(spV));
nearest = 0;
if y>0
[peak, index] = max(spV(startT:startT+(peakT*60)));
for i = startT:startT+index+600
if spV(i,1)>0
spV2(i,1)=spV(i,1);
nearest = spV(i,1);
else
spV2(i,1) = nearest;
end
end
elseif y<0
[peak, index] = min(spV(startT:startT+(peakT*60)));

```

```

for i = startT:startT+index+600
    if spv(i,1)<0
        spv2(i,1)=spv(i,1);
        nearest = spv(i,1);
    else
        spv2(i,1) = nearest;
    end
end
end
end
%----- Nate's Craziest Idea Yet

[A, tau, endrange]=expfit4(startT, index, spv2);
%[A, tau, endrange]=expfit4(startT, index, spv);
%----- curve fit goodness-----
x=[1:endrange+1]/60;
startpoint=startT+index;
xspv=spv(startpoint:startpoint+endrange);
if y>0
    curve=A*exp(-x/tau);
    cum_eye=trapz(x,curve);
elseif y<0
    curve=-A*exp(-x/tau);
    cum_eye=(trapz(x,curve))*-1;
end

lspv=log(xspv);
lspv=abs(lspv); %---- took abs of lspv to get rid of imaginary parts.
%---- just takes positive values and mag. of imaginary values.
lcurve=log(curve);
%figure
%plot(x,lspv);
%hold on
%plot(x,lcurve);
    lave=sum(lcurve)/(length(lcurve));
residual=lspv-lcurve;
regress=lcurve-lave;
totss=sum((lspv-lave).^2); %sum of squares of deviations of the individual sample
%points from the sample mean (lave)
regss=sum(regress.^2); %sum of squares of the regression components
resss=sum(residual.^2); %sum of squares of the residual components
k=1; %predictor variables in the model-for simple linear regression, k=1
regms=regss/k; %regression mean square
n=endrange;
resms=resss/(n-k-1);
ftest=regms/resms;
fact=5.15;
fprintf('%8.4f\t %8.4f\t %8.4f\t %8.4f\n', A, tau, cum_eye, ftest);
if ftest>fact
    fprintf('satisfies F-test criterion, therefore significant\n')
else fprintf('not significant\n')
end
totss=regss+resss;
Rsquared=regss/totss;
End

```

cum_spv.m

```

close all
clear all

init_bed

batch_mode = FALSE;

% get research data folder name

```



```

get_PC_bed_path

% get list of patients to be processed
get_patient_list
[num_patients,n] = size(patient_list);
for patnum=1:num_patients.

    file_name = patient_list(patnum,:);
    idx = find(abs(file_name) > 32);           % printable non-blank characters
    file_name = file_name(idx);

    idx = find(file_name == '.');
    if (isempty(idx)),
        root_file = file_name;
    else
        root_file = file_name(1:(idx(1)-1));
    end

%runnumber=input('\nEnter number of runs: ', 's');
%runs=str2num(runnumber);
for i=1:1,
    run=input('\nEnter run number: ', 's');
    rn=str2num(run);
    if (rn < 10),
        run_code = [root_file, '_run0', run];
    else
        run_code = [root_file, '_run', run];
    end
    run_file = [data_path, run_code, '.mat'];
load(run_file);
run_file = [data_path, run_code, '_LV.mat'];
load(run_file);
%-----
    Anlog1=data(:,15);
    %Retrieve Analog 1 from column 15
    Anlog2=data(:,16);
    %Retrieve Analog 1 from column 16
x1=5.514451.*Anlog1;           %use x1=6.2189 for subjects 2,4,6,7,9. Use x1=1.1646 for 10,11,12
x2=5.514451.*Anlog2; % recalibration factor C 5.514451 for incremental%-----
    gyroy=filt_gyro_position(x1);           %Filter Analog 1 (yaw motions
    gyrop=filt_gyro_position(x2);           %Filter Analog 2 (pitch motions
%-----
subplot(2,1,1)
x=[1:length(spv)]/60;
plot(x,spv)
subplot(2,1,2)
x=[1:length(gyro)]/60;
plot(x,gyroy)
x=[1:length(gyro)];
%-----
[x,y,key]=ginput(1);
beginramp=round(x);
start=beginramp;
%[x1,y1,key]=ginput(1);
%endpoint=round(x1);
%start=beginramp+3*60;
start=beginramp+7*60;
    endpoint=start+20*60;
stuff=spv(start:endpoint);
%-----
ramp=(endpoint-start)/60
    avg=mean(stuff)
    area=trapz(stuff)/60
area_under_curve=round(area);
end
i=0;
end

```

dave_checkcurve.m

```
% Checks curve goodness of fit using F-test
% requires startPt, endrange, A, tau
% By David Phillips, March 28, 2001

clear t;
t=rot90([1:endrange+1]/60,-1); % t=time in sec
modspv=abs(spv(startPt:startPt+endrange)); % modspv is positive spv for ~ 10sec

neg=sign(y); % neg allows for negative or positive y

lspv=abs(log(modspv)); %---- took abs of modspv to get rid of imaginary parts.
%--- just takes positive values and mag. of imaginary values.

curve=neg*A*exp(-t/tau);
lcurve=abs(log(curve));

% This is faulty - compares residual (straight angled line)
% to regression (horizontal line), then shows that they are sig different

lave=mean(lcurve);
residual=lspv-lcurve;
regress=lspv-lave;
totss=sum((lspv-lave).^2); % sum of squares of deviations of the individual sample
% points from the log curve

mean (lave)
regss=sum(regress.^2);
resss=sum(residual.^2);
k=2; % k-2 for A (1), tau (2)
regms=regss/k; % regression mean square -
% - why isn't above denominator k/length(regress)?
resms=resss/(length(residual)-k);
flest=regms/resms;
fact=3.00; % 3.00 for k=2 (A, tau), P=0.05, infinite points (~=600pts)
if flest>fact
    fprintf('satisfies F-test criterion, therefore significant\n')
else fprintf('not significant\n')
end
totss=regss+resss;
Rsquared=regss/totss;
fprintf('flest = %f, Rsquared = %f\n', flest, Rsquared);

%%%% shows goodness of fit curve %%%
%figure(2)
%hold on
%plot(t,lspv,'o','MarkerSize',4,'MarkerFaceColor','k');
%plot(t,lcurve);
%XaxisLabel = 'time (sec)';
%YaxisLabel = 'spv';
%XLabel(XaxisLabel, 'FontSize', 8, 'FontWeight', 'bold');
%YLabel(YaxisLabel, 'FontSize', 8, 'FontWeight', 'bold');
```

deblink.m

```
function [y, num_blinks, perc_blink] = deblink(x, xcal, low, high, num_increase)

% detects blinks on position trace "x" using threshold "thresh".
% low > 0 ==> use the specified values, call "thresh_blinks"
% low = 0 ==> rely on ISCAN zeros for blinks, call "simple_blinks"
% low < 0 ==> calculate thresholds based on mean and standard deviation
% and iterate with operator control, call "thresh_blinks"
% "xcal" is calibrated position, while "x" is raw data
% detect blinks using "x", but make interpolations on "xcal"
% if "xcal" is empty, assume "x" is calibrated data
% "y" is eye position data with blinks removed by linear interpolation
```

```

%% "num_blinks" is the number of blinks which were detected in the trace
%% "perc_blink" is the percentage of the trace which is defined as a blink
%%
if (low == 0),
    [s,e] = simple_blinks(x, num_increase, 100);
elseif (low > 0),
    [s,e] = thresh_blinks(x, num_increase, low, high, 100);
else
    mn = mean(x);
    sd = std(x);
    low = mn - 3*sd;
    if (low < 0),
        low = 0;
    elseif (low > 500),
        low = 500;
    end
    high = mn + 3*sd;
    if (high < 3500),
        high = 3500;
    elseif (high > 4000),
        high = 4000;
    end

    [s,e] = thresh_blinks(x, num_increase, low, high, 100);
    x2 = interp_blinks( x, s, e);
    fig = figure('Name', 'Specification of Blink Threshold');
    h1 = plot(x, 'y');
    hold on
    h2 = plot(x2, 'b');
    xl = get(gca,'XLim');
    h3 = plot(xl, [low low], 'g');
    h4 = plot(xl, [high high], 'r');

    low2 = input('Specify new value for low threshold (-1 to end): ');
    if (isempty(low2)),
        low2 = 0;
    else
        if (low2 >= 0),
            low = low2;
        end
    end

    high2 = input('Specify new value for high threshold (-1 to end): ');
    if (isempty(high2)),
        high2 = 0;
    else
        if (high2 >= 0),
            high = high2;
        end
    end

    while ((low2 >= 0) | (high2 >= 0)),

        [s,e] = thresh_blinks(x, num_increase, low, high, 100);
        x2 = interp_blinks( x, s, e);
        set(h2, 'YData', x2);
        set(h3, 'YData', [low low]);
        set(h4, 'YData', [high high]);

        low2 = input('Specify new value for low threshold (-1 to end): ');
        if (isempty(low2)),
            low2 = 0;
        else
            if (low2 >= 0),
                low = low2;
            end
        end
    end
end

```

```

        end
    end
    high2 = input('Specify new value for high threshold (-1 to end): ');
    if (isempty(high2)),
        high2 = 0;
    else
        if (high2 >= 0),
            high = high2;
        end
    end
end

end

delete(h4);
delete(h3);
delete(h2);
delete(h1);
close(fig);
clear x2

end

if (isempty(xcal)),
    y = interp_blinks( x, s, c);
else
    y = interp_blinks( xcal, s, c);
end

num_blinks = length(s);
if (num_blinks > 40),
    fprintf('\n  WARNING: dangerously high blink activity (%d blinks)', num_blinks);
end
perc_blink = 100 * (sum(e - s - 1) / length(x));
if (perc_blink > 3),
    fprintf(['\n  WARNING: dangerously high blink activity (%5.2f%%)', perc_blink,37]);
end

end

return;

```

differentiate.m

```

function xprime = differentiate( x, sample )

% differentiate - returns the first time derivative of 'x'
%
% Written by: D. Balkwill 10/20/93
%

A = 1 / sample;
if (sample == 60),
    B = [0.0077, 0.0714, 0.1078, 0.0870, 0, -0.0870, -0.1078, -0.0714, -0.0077];
else
    B = [0.0332, 0.0715, 0.0678, 0.0522, 0, -0.0522, -0.0678, -0.0715, -0.0332];

end
gain = [4 3 2 1] * B(1:4)' * 2;
B = B / gain;
xprime = zero_filter(B, A, x);

clear A B gain

```

edit_alg_diff

```
%  
  
%function edited_spv = edit_alg_diff(t,spv,vel,pos,diffs,colour,gyroYaw)  
  
% This is the main algorithm for the manual editing of  
% slow phase velocity profiles.  
% sample = sampling rate in Hz  
% spv = slow phase eye velocity vector  
% vel = raw eye velocity vector  
% pos = eye position vector  
% colour = flag for colour monitor  
%  
% The user now has the capability of over-riding faulty  
% interpolations made by the detection process. The 'diff_list'  
% script is called to return a list of regions over which the  
% raw velocity and slow phase velocity differ. The format of  
% this list is identical to that of 'flag' in the 'heart' script.  
%  
% If one wishes to re-edit a previously edited SPV profile, then  
% the first line can be deleted so that the 'diffs' list contains  
% the differences between raw and *edited* SPV profiles.  
%  
% If the SPV profile is completely different from the raw  
% velocity (due to low-pass or order-statistic filtering for  
% instance), then the call to 'diff_list' should be removed.  
%  
% written by D. Balkwill -- 11/27/90  
% some portions ruthlessly and shamelessly stripped from  
% scripts by B. McGrath and W. Kulecz  
%  
% Modified: D. Balkwill 10/21/93  
% Changed 'diffs' to an input parameter, since we already know what  
% what it is from having calculated the SPV  
edited_spv = spv; % don't overwrite spv  
%diffs = diff_list(vel,edited_spv);  
num_diffs = length([fast_start fast_end]);  
highs = [];  
num_highs = 0; % number of regions highlighted  
interps = [];  
spv_interps = [];  
num_interps = 0; % number of regions interpolated  
  
l = length(spv);  
sample = round(1/(t(2) - t(1))); % assumes t is periodic  
  
% minimum window height to prevent graph from being dominated by noise  
rms = sqrt(sum(edited_spv.*edited_spv)/l);  
min_height = 3 * rms;  
  
key = 0;  
FINISHED = 27; % escape  
%PAN_LEFT = 28; % left arrow  
%PAN_RIGHT = 29; % right arrow  
%SCROLL_LEFT = 11; % page down  
%SCROLL_RIGHT = 12; % page up  
PAN_LEFT = 107; % 'k'  
PAN_RIGHT = 108; % 'l'  
SCROLL_LEFT = 75; % 'K'  
SCROLL_RIGHT = 76; % 'L'  
ACCEPT = 13; % carriage return  
DELETE_1 = 8; % backspace  
DELETE_2 = 127; % delete  
%ZOOM_IN = 30; % up arrow  
%ZOOM_OUT = 31; % down arrow  
ZOOM_IN = 122; % 'z'  
ZOOM_OUT = 120; % 'x'  
FAST_ZOOM_IN = 46; % decimal
```

```

FAST_ZOOM_OUT = 48; % zero
COMPLETE_PLOT_1 = 97; % 'a' key
COMPLETE_PLOT_2 = 65; % 'A' key
% note: 1, 2, and 3 are reserved for mouse button(s)

num_pick = 0; % number of points picked
os = 1; % offset of start of current trace, in samples
w = 1 - 1; % width of trace, in samples
redraw = 1; % flag for plotting
mf = 1; % magnification factor
mag_thresh = 1 / (sample * 10); % 10 seconds

fprintf('\n !!! Collecting Eye data !!!');
while (key ~= FINISHED)

    if (redraw == 1)
        df = floor(w/2000);
        if (df < 1)
            df = 1;
        end
        er = edited_spv(os:df:os+w);
        tr = t(os:df:os+w);
        vr = vel(os:df:os+w);
        pr = pos(os:df:os+w);

% leave some blank space above and below trace for aesthetics
        mxv = max(er);
        if (mxv < 0)
            mx = mxv * 0.9;
        else
            mx = mxv * 1.1;
        end
        mnv = min(er);
        if (mnv < 0)
            mn = mnv * 1.1;
        else
            mn = mnv * 0.9;
        end
        old = mx - mn;
        if (old < min_height)
            mx = mx + (min_height - old)/2;
            mn = mx - min_height;
        end

% ensure that position data appears on plot
        pr = pr - min(pr) + mnv;

        cla

        hold off
% axis([tr(1) tr(length(tr)) mn mx]);

                %counter=0;
                %Tcount=[0:length(gyro)-1];
                %Create vector 0 to length of Analog1
                %T =(Tcount/60);

%---size gyro to same as eye data---
%if tr(length(tr)) < T(length(T))
% counter=1;
% while tr(length(tr)) > T(counter),
% counter=counter+1;
% end
%elseif tr(length(tr)) > T(length(T))
% counter=1;
% while tr(length(tr)) > T(counter),
% counter=counter+1;
% end

%end
%T=T(1:counter-1);
subplot(2,1,1);
plot(tr,vr,'r-');

```

```

axis([0,floor(tr(length(tr))), min(vr)-2, max(vr)+2]);
                                hold on
                                plot(tr,pr,'g-');

plot(tr,er,'k-');
subplot(2,1,2);
plot(T,gyroy(1:length(T)), 'b-');
axis([0,floor(tr(length(tr))), min(gyroy)-10,max(gyroy)+10]);
                                subplot(2,1,1);

set(gca, 'XLim', [tr(1) tr(length(tr))]);
                                set(gca, 'YLim', [mn mx]);
                                xlabel('black = SPV, red = raw velocity, green = eye position, blue=yaw head
movements');

[x,y,key] = ginput(1);
key
if isempty(key),
    key = ACCEPT;
end

if (key == ZOOM_IN)    % increase magnification factor

    old=mf;
    mf=min(old*2,max(old,floor(1/100)));
    if mf==old    % maximum magnification of 100X
        redraw=0;
    else
        redraw=1;
        w=floor(1/mf);
    end

elseif (key == FAST_ZOOM_IN) % fast two-point zoom

    % first point of region to zoom into
    [t3,y,key] = ginput(1);
    if ((key ~= DELETE_1) & (key ~= DELETE_2))

        % bounds check on first point of region
        if (t3 < tr(1))
            t3 = tr(1);
        elseif (t3 > tr(length(tr)))
            t3 = tr(length(tr));
        end
        x3 = 1 + round(t3 * sample);
        t3 = (x3 - 1)/sample;

        % display first point
        hold on
%-----modified -----
        plot([t3,t3],[mn,mx], 'r');

        hold off
        redraw = 1;

        % second point of region to zoom into
        [t4,y,key] = ginput(1);

        % allow user to abort zoom via delete key
        if ((key ~= DELETE_1) & (key ~= DELETE_2))

            % bounds check on second point of region
            if (t4 < tr(1))
                t4 = tr(1);
            elseif (t4 > tr(length(tr)))
                t4 = tr(length(tr));
            end
            x4 = 1 + round(t4 * sample);
            t4 = (x4 - 1)/sample;

            % display second point
            hold on

```

```

        plot([t4,t4],[mn,mx],r');

    hold off

    % swap order of points if needed
    if(x4 < x3)
        old = x4;
        x4 = x3;
        x3 = old;
    end

    % calculate new magnification parameters
    if(x3 ~= x4)
        os = x3;
        w = x4 - x3;
        mf = 1/w;
    end
end
end

elseif(key==ZOOM_OUT) % decrease magnification

    if(mf == 1) % already completely zoomed out
        redraw = 0;
    else
        redraw=1;
        old =mf;
        mf = max(floor(old/2),1);
        w=floor(1/mf);
        if(w >= 1)
            w = 1 - 1;
        end
        if((os+w)>1)
            os=floor(max(1,1-w));
        end
    end
end

elseif((key == COMPLETE_PLOT_1) | (key == COMPLETE_PLOT_2) | (key == FAST_ZOOM_OUT)) % display entire plot

    os = 1;
    mf = 1;
    w = 1 - 1;
    redraw = 1;

elseif(key==PAN_RIGHT) % increase offset by quarter-screen

    old=os;
    os=floor(max(1,min(1-w,os+0.25*w)));
    if old==os % already panned to end
        redraw=0;
    else
        redraw=1;
    end
end

elseif(key==PAN_LEFT) % decrease offset by quarter-screen

    old=os;
    os=floor(max(1,os-0.25*w));
    if os==old % already panned to beginning
        redraw=0;
    else
        redraw=1;
    end
end

elseif(key==SCROLL_RIGHT) % jump display one screenful right

    old=os;
    os=floor(max(1,min(os+w,1-w)));
    if os==old % already panned to end

```



```

        redraw=0;
    else
        redraw=1;
    end

elseif (key==SCROLL_LEFT) % jump display one screenful left

    old=os;
    os=floor(max(1,os-w));
    if old==os % already panned to beginning
        redraw=0;
    else
        redraw=1;
    end

end

end

if (key==1)
    yinput=[yinput; y]
    xinput=[xinput; x]

end

end
end

```

expCost.m

```

function cost = expCost(params, data)

tau_temp = params(1);
a_temp = params(2);

curveVals = a_temp * exp(-data(:, 1) / tau_temp);
cost = sum((data(:, 2) - curveVals) .^ 2); % sum of least mean squares

```

expfit.m

```

function [a_temp, tau_temp]=dave_expfit(start_ind,spv,num_pts)
%clf
%for startPt = 1:50:1000,
    x = [1:(num_pts+1)]' / 60; % x=time (in secs)
    data = [x, spv(start_ind:start_ind+num_pts)]; % data=[time(in secs), spv]

    startParams = [10, 20];
    options = optimset('Display', 'off');
    bestFitVals = FMINSEARCH('expCost', startParams, options, data);
    tau_temp = bestFitVals(1);
    a_temp = bestFitVals(2);
%end

```

eye_anal.m

```

% This programme analyzes the eye & button data using the button (ANALOG0)
% as the trigger for start of nystagmus. Outputs to a new .txt file for each
% subject and phase (run)
% By: David Phillips March 28, 2001

close all
clear all

init_bed

```

```

batch_mode = FALSE;

% get research data folder name
get_PC_bed_path

% get list of patients to be processed
get_patient_list
[num_patients,n] = size(patient_list);
for patnum=1:num_patients,
    load_file;

    Button_data(:,6); %Retrieve Duration Button
    button_find;

    % This part finds the point of local max of eye data between button_start and _stop.
    % then it finds the exponential curve & cumulative eye mvmt given that start index.

    peakT = 4; % peakT is number of seconds past button_stop to search

    for turn=1:turncount,

        % Find start of eye movement
        end_search=min(button_stop(turn)+(peakT*60),length(Button));
        [peak, index] = max(abs(spv(button_start(turn)+60:end_search))); % Ensure no overruns of length

        if spv(index) == 0
            fprintf('Peak spv = 0. ERROR!!!\n');
        else peak = peak*sign(spv(index)); % Gives Peak the right sign
        end

        start_ind(turn,1)=button_start(turn)+index;
        integsecs=10; % Adjust time to fit curve here in secs
        max_pts=integsecs*60; % number of points to fit curve
        max_pts=min(start_ind(turn)+max_pts,length(spv)); % Ensure no overruns of length
        num_pts=max_pts-start_ind(turn);

        [A_temp, tau_temp]=expfit(start_ind(turn), spv, num_pts);

        % Append A_temp, tau_temp to A, tau vectors
        A(turn,1)=A_temp;
        tau(turn,1)=tau_temp;

        %----- curve fit goodness-----
        ftest(turn,1)=checkcurve(spv, start_ind(turn), A(turn), tau(turn), num_pts);
        if (ftest(turn)<=3.00)
            fprintf('\nRefit A and tau for Head Turn %f, F-test = %f (<3.00)\n', turn, ftest(turn));
        end

        %-----cumulative spv-----
        % This integrates the area under the fitted A, tau curve.
        t_matrix=transpose(0:.01:10); % for 10sec
        curve=A(turn)*exp(-t_matrix/tau(turn));
        cum_eye(turn,1)=trapz(t_matrix,curve);

    end

    % Write to file
    write_file = [data_path, run_code, eyeext, '_results.txt'];
    fid = fopen(write_file,'w');
    fprintf(fid,'\nBut_Start\t Eye_Start\t But_Dur\t A\t Tau\t Cum_Eye\t F-Test\n');
    for turn=1:turncount,
        fprintf(fid,'%8.4f\t %6.0f\t %8.4f\t %8.4f\t %8.4f\t %8.4f\t %8.4f\n'...
            , button_start_time(turn), start_ind(turn), button_dur(turn), A(turn), tau(turn), cum_eye(turn), ftest(turn));
    end
    fclose(fid);

    % Write to Screen
    fprintf('\nBut_Start\tEye_Start\t But_Dur\t A\t Tau\t Cum_Eye\t F-Test\n');
    for turn=1:turncount,
        fprintf('%8.4f\t %6.0f\t %8.4f\t %8.4f\t %8.4f\t %8.4f\t %8.4f\n'...

```

```

        . button_start_time(turn), start_ind(turn), button_dur(turn), A(turn), tau(turn), cum_eye(turn), ftest(turn));
    end

end

```

eye_anal_manual.m

```

% This programme analyzes the eye & button data using a manual click
% as the trigger for start of nystagmus. Outputs to screen.
% By: David Phillips March 28, 2001

```

```

close all
clear all

```

```

init_hed

```

```

batch_mode = FALSE;

```

```

% get research data folder name
get_PC_bed_path

```

```

% get list of patients to be processed
get_patient_list
[num_patients,n] = size(patient_list);
for patnum=1:num_patients,

```

```

    load_file;

```

```

    Button=data(:,6);

```

```

    Head =data(:,7);

```

```

    over=10;

```

```

    c=1;

```

```

    times = [];

```

```

while(c<15)

```

```

    x_length=max(length(spv),length(Button));

```

```

    % Graph full length of run

```

```

    clf;

```

```

    figure(1)

```

```

    hold off;

```

```

    subplot(2,1,1)

```

```

    x=[1:x_length];

```

```

    plot(x,spv)

```

```

    subplot(2,1,2)

```

```

% plot(x,Button)

```

```

% subplot(3,1,3)

```

```

    plot(x,Head)

```

```

    fprintf('\nClick on SPV start to zoom in\n')

```

```

    [zm,y]=ginput(1);

```

```

    zm=round(zm);

```

```

    top=max(spv(zm-60:zm+180));

```

```

    bot=min(spv(zm-60:zm+180));

```

```

    % Graph zoomed region (from -1sec to +15sec)

```

```

%o clf;

```

```

%o figure(1)

```

```

%o hold off;

```

```

%o subplot(2,1,1)

```

```

%o x=[1:x_length];

```

```

%o plot(x,spv, 'r')

```

```

%o axis([zm-60,zm+900,bot,top]); %oNates comment out

```

```

%o %axis([zm-60,zm+900,-60,60]);

```

```

%o

```

```

%o subplot(2,1,2)

```

```

%o % x=[1:x_length];

```

```

%o % plot(x,Button)

```

```

%o % axis([zm-60,zm+900,1000,4000]);

```

```

%o % subplot(3,1,1)

```

```

%o

```

```

% h_top=max(Head(zm-6:zm+900));
% h_bot=min(Head(zm-6:zm+900));
% subplot(3,1,3)
% x=[1:x_length];
% plot(x,Head)
% axis([zm-60,zm+900,h_bot-20,h_top+20]);
% subplot(3,1,3)
%
% %%%%%%%%%%%
%
% fprintf('Select start index by clicking: ');
% [start_click, y]=ginput(1);
% start_click=round(start_click);
% fprintf('%6.0f\n', start_click);
% fprintf('Select end index by clicking');
% [end_click, y]=ginput(1);
% end_click=round(end_click);
% times(c,1)=(end_click - start_click)/60.00;
if (c==1|c==3|c==5|c==7|c==9|c==11|c==13),
    spv_max(c,1)=top;
else
    spv_max(c,1)=bot;
end
c=c+1
%fprintf('%6.0f\n', end_click);
% yn = get_yn('Accept these values?', 'Y');
% if (yn == 'Y'),
%     over = 0;
% end
end

% This part finds the point of local max of eye data between two mouse points.
% then it finds the exponential curve & cumulative eye mvmt given that start index.

% Find start of eye movement
% peak = spv(start_click);

% start_ind=start_click;
% num_pts=end_click-start_ind;
% end_index = end_click; % end of fit
%
% [A temp, tau_temp]=expfit(start_ind, spv, num_pts);
%
% % Append A_temp, tau_temp to A, tau vectors
% A=A_temp;
% tau=tau_temp;
%
% %-----curve fit goodness-----
% flest=checkcurve(spv, start_ind, A, tau, num_pts);
%
% %-----cumulative spv-----
% % This uses spv, not fitted A, tau curve.
% end_eye=10; % for 10sec
% t_matrix=transpose(0:0.1:10);
% curve=A*exp(-t_matrix/tau);
% cum_eye=trapz(t_matrix,curve);
%
% start_time=start_click/60;
% click_dur=end_click/60-start_time;
%
% % ----Open file to be edited-----
% edit_file=[data_path, run_code, eyeext, '_results.txt'];
% edit(edit_file);
%
% % Write to screen
% fprintf('\nClk Start\tClick_Dur\t Eye Start\t || A\t Tau\t Cum_Eye\t F-Test\n');
% fprintf(' %8.4f\t %8.4f\t %6.0f\t %8.4f\t %8.4f\t %8.4f\t %8.4f\n...',
%     , start_time, click_dur, start_ind, A, tau, cum_eye, flest);
%
% % -----Plot fitted line-----

```

```

% time=rot90([1:num_pts+1]/60,-1);
% curveVals = A * exp(-time / tau);
% axismin=min(spv(start_ind:start_ind+num_pts))-5;
% axismax=max(spv(start_ind:start_ind+num_pts))+5;
%
% clf
% hold on
% figure(1)
%
% plot(time, spv(start_ind:start_ind+num_pts),...
% 'o',...
% 'MarkerSize', 4,...
% 'MarkerFaceColor', 'k',...
% 'MarkerEdgeColor', 'k'...
% );
% axis([0,time(end),axismin,axismax]);
%
% plot(time, curveVals,...
% 'LineStyle', '-',...
% 'Color', 'k',...
% 'LineWidth', 0.5);
%
% axis([0,time(end),axismin,axismax]);
%
% XaxisLabel = 'time (sec)';
% YaxisLabel = 'spv';
% xlabel(XaxisLabel, 'FontSize', 8, 'FontWeight', 'bold');
% ylabel(YaxisLabel, 'FontSize', 8, 'FontWeight', 'bold');
%
end

```

filt_position.m

```

function y = filt_position(x, sample_rate, num_lpf, num_OS, quad_flag)

%
% filt_position - filters the eye position with a Butterworth filter,
% using 'filtfilt' to remain phase-less
%
% Written by: D. Balkwill 10/20/93
% Modified by: D. Balkwill 8/17/95
%
% - added "num_lpf" and "num_OS" parameters for
% external control of number of filter stages
%

N1 = sample_rate / 20;
N1 = max(N1, 3);
N1 = min(N1, 10);
N2 = round(1.7 * N1);
N3 = round( (N1 + N2) / 2 );

corner = 28;
[B,A] = butter(2, 2 * corner / sample_rate); % butterworth filter, fc = 28 Hz

% one stage of OS filtering first, to reduce noise
y = OS_lin2(x, N1, N2);
%y = OS_lin2(x, 2*N1, 2*N2); % filters out some of 16 Hz noise

y = filtfilt(B,A,y);
if (num_lpf > 1),
    for i=2:num_lpf,
        y = filtfilt(B,A,y);
    end
end

for i=2:num_OS,
    if (quad_flag),
        y = OS_lin2quad1(y, N1, N2, N3);
    end
end

```

```

        else
            y = OS_lin2(y, N1, N2); % order statistic filter
        end
    end

clear B A N1 N2 N3 i

```

get_hms.m

```

%-- take in head movement clicks of user and calls integrate.m to find area under
%-- specified head movements
%assuming that clicks will increase from hm1 to hm8

fprintf(['\n !! Ready to enter same number of head movements !!!']);

[x,y,key] = ginput(currenteyes) %x in terms of time

h=1;
preseconds=15;
while h <= length(y), %-- goes through each head movement input by user in ascending order

    if yinput(h) > 0 %user wants up head movement
        if xinput(h) < 20 % if it's the very first head movement, initial ave needs be smaller
            hm = [];
            earlysecs = 2;
            earlypoint = earlysecs*60;
            toptreshold = max(gyroy(1:earlypoint));
            avezero = sum(gyroy(1:earlypoint))/(earlypoint);
            i=1;
            else
                preavezero = xinput(h)-preseconds; %getting preseconds of time before the headmovement
                earlysecs = 6 + preavezero; %aveg over 6 secs
                earlypoint = round(earlysecs*60);
                preavezeropoint = round(preavezero*60);
                toptreshold = max(gyroy(preavezeropoint:earlypoint));
                avezero = sum(gyroy(preavezeropoint:earlypoint))/(earlypoint-preavezeropoint);
                i=round(preavezero*60);
            end
            integrateup
            hm = [hm; upinteg];
        elseif yinput(h) < 0 %user wants down head movement
            lowpreavezero = xinput(h)-preseconds; %getting preseconds of time before the headmovement
            lowprepoint = round(lowpreavezero*60);
            lowprepoint2 = round(lowprepoint+6*60); %getting points over which to ave zero
            i=round(lowprepoint2);
            lowthreshold = min(gyroy(lowprepoint:lowprepoint2));
            prelow_avezero = sum(gyroy(lowprepoint:lowprepoint2))/(lowprepoint2-lowprepoint);
            integreatedown
            hm = [hm; downinteg];
        end
        h=h+1;
    end
end

```

get_patient_list.m

```

%
% get_patient_codes - input patient codes for batch processing
%
% D. Balkwill 9/28/93
%

check_flag = 1;
code_length = [];
patient_list = [];
[m,n] = size(patient_list);

```

```

if (exist([data_path,'patient_list.mat']) == 2),
    eval(['load ',data_path,'patient_list.mat']);
    fprintf("\nCurrent patient list:\n");
    for i=1:length(code_length),
        fprintf([patient_list(i,1:code_length(i)), '\n']);
    end
    yn = get_yn('Is this the correct patient list','Y');
    if (yn == 'Y'),
        check_flag = 0;
    else,
        code_length = [];
        patient_list = [];
    end
end

while (check_flag == 1),

    % terminate list by entering no patient code
    patient_code = input('Enter Subject Code (e.g. aim3s5d1): ','s');
    if (isempty(patient_code) == 1),
        check_flag = 0;
        break;
    end

    % add run code to patient list, padding with blanks as needed
    l = length(patient_code);
    if (l < n),
        patient_code = [patient_code, zeros(1,n-l)];
    elseif (l > n),
        patient_list = [patient_list, zeros(m,l-n)];
    end
    patient_list = [patient_list; patient_code];
    [m,n] = size(patient_list);
    code_length = [code_length; l];

end

eval(['save ',data_path,'patient_list.mat patient_list code_length']);

clear check_flag patient_code status l m n i yn

```

get_PC_bed_path

```

%
% This routine searches the MatLab path specification for the main MatLab
% folder (name ends in MATLAB), and looks in that folder for a file named
% research_path, which is to contain a string variable named 'data_path'.
% The contents of 'data_path' is the name of the folder in which the data
% to be analyzed is stored.
%
% Written by: D. Balkwill 10/20/93
% Note: same as 'get_rot_path', but with different file name 'research_path'.

%get MatLab path specification
master_path = [matlabroot, '\'];

% see if rotation path exists, input if it doesn't
status = exist([master_path,'bed_path.mat']);
if (status == 2),
    %eval(['load ',master_path,'bed_path.mat']);
    data_path = ['C:\matlabR12\aim5\ISCAN\'];
else
    %data_path = input('Enter bed data folder specification: ','s');
    data_path = ['C:\matlabR12\aim5\ISCAN\'];
end

```

```

% ensure that : is at end of path
l = length(data_path);
if (data_path(l) ~= '\'),
    data_path = [data_path,'\'];
status = 1; % force save with back-slash path name
end

% save path if it hasn't been before
if (status ~= 2)
    eval(['save ',master_path,'bed_path.mat data_path']);
end

clear a b found status mat_path l skip

```

get_yn.m

```

function yn = get_yn( question, default )

%
% yn - asks a yes/no 'question', allowing an answer of 'Y' or 'N'
%       from the user, and returns the capitalized response letter.
%       If the user response is not 'y', 'n', 'Y', or 'N', the response
%       is set to the 'default' value.
%
% Written by: D. Balkwill 9/28/93
%

if ((default >= 'a') & (default <= 'z')).
    default = default - 'a' + 'A';
end

if (default == 'Y'),
    yn = input( [question,' ([Y]/N) ? ',' ],'s');
    other = 'N';
else
    yn = input( [question,' (Y/[N]) ? ',' ],'s');
    other = 'Y';
end

if (isempty(yn)),
    yn = default;
elseif ((yn >= 'a') & (yn <= 'z')).
    yn = yn - 'a' + 'A';
end

if (yn ~= other),
    yn = default;
end

clear other

```

init_bed.m

```

FALSE = 0;
TRUE = 1;

LEFT_VERTICAL = 2;
%RIGHT_VERTICAL = 3;
LEFT_HORIZONTAL = 4;
%RIGHT_HORIZONTAL = 5;

num_increase = 2;
num_RMS = 0.25;
min_diff_class = 30;

```

integratedown.m

```
%-----  
while gyroy(i) > lowthreshold-2  
    i=i+1; %find place where peak down is below threshold  
end  
  
if gyroy(i-1) > gyroy(i),  
    i=i-1; %backtracks to time when peak down starts  
end  
startlowpoint=i; %point where peak down starts  
startlowtime = round(i/60);  
%----- above finds place where peak starts for head to red  
  
findmin = startlowpoint  
while gyroy(findmin+1) < gyroy(findmin)  
    findmin = findmin+1;  
end  
min_peak = gyroy(findmin)  
findmax = findmin; %goes back up to find end of peak down  
while gyroy(findmax+1) > gyroy(findmax)  
    findmax=findmax+1;  
end  
  
peakdownend = findmax %point where peak down ends  
lowpointlength = findmax-startlowpoint;  
lowheadtime = round(lowpointlength/60); %duration in peak low head movement  
time4eye = (round(0.05*pointlength) + startlowpoint)/60;  
%----- above finds the time duration of the  
%----- head movement upand time to start headmovement integration  
  
i=startlowpoint;  
j=1;  
downinteg = 0;  
timeindex=[];  
  
for k=startlowpoint:findmax,  
    downinteg=downinteg + (gyroy(k)-prelow_avezero)*(1/60); %find magnitude with changing zero  
end  
downinteg  
%subplot(2,1,2)  
%plot([startlowpoint:findmax]/60,gyroy(startlowpoint:findmax))
```

integrateup.m

```
i=1;  
  
while gyroy(i) < tophreshold+2  
    i=i+1; %find place where peak is above threshold  
end  
  
if gyroy(i-1)<gyroy(i),  
    i=i-1; %backtracks to time when peak starts  
end  
startpoint=i;  
starttime = round(i/60);  
%----- above finds place where peak starts for head  
  
findmax = startpoint;  
while gyroy(findmax+1)>gyroy(findmax)  
    findmax=findmax+1;  
end  
max_peak = gyroy(findmax)  
findmin = findmax;  
while gyroy(findmin+1) < gyroy(findmin)
```

```

    findmin=findmin+1;
end
uppeakend = findmin;
pointlength = findmin-startpoint;
headtime = round(pointlength/60);
time4eye = (round(0.05*pointlength)+startpoint)/60;
%----- above finds the time duration of the
%----- head movement upand time to start headmovement integration

i=startpoint;
j=1;
upinteg = 0;
timeindex=[];

for k=startpoint:findmin.
    upinteg=upinteg + (gyroy(k)-avezero)*(1/60);
end
upinteg
%subplot(2,1,1)
figure
plot([startpoint:findmin]/60,gyroy(startpoint:findmin))

```

interp1z.m

```

function y2 = interp1z(x1,y1,x2)
% this function interpolates values with a zero-order hold
% assumes that x1 and x2 are equally spaced.
y2 = interp1(x1,y1,x2,'nearest');
shift_index = floor((size(y2,1))/(2*(size(y1,1))));
y2(shift_index+1:size(y2,1)) = y2(1:size(y2,1)-shift_index);

```

interp_blinks.m

```

function spv = interp_blinks(vel, first, last)

% interp_blinks - Interpolates across eye position blinks by calculating new
% position values to estimate replacement values for blink points.
% New position values are interpolated as first order line segments.
% a zeroth order hold.
%
% Written by: D. Balkwill 11/16/93
%
% Modified from "interpolate.m" by: MDB 10/1/99
%
%

spv = vel;
n = length(first);

% replace old velocities with new ones
delta = last - first + 1;
for i=1:n,
    d = delta(i);
        s = vel(first(i));
        e = vel(last(i));
        spv(first(i):last(i)) = (s * ones(d,1)) + ((e - s) * [0:(d-1)]'/(d-1));
    end
end

```

interpolate.m

```

function spv = interpolate(vel, first, last)

% interpolate - Interpolates across fast phases by calculating new SPV
% values to estimate replacement values for fast phase
% velocity samples. New SPV is the median of the three
% SPV values before the fast phase, and interpolated as
% a zeroth order hold.
%
% Written by: D. Balkwill 11/16/93
%

spv = vel;
n = length(first);
vn = length(vel);

if (n == 0),
    return;
end

% variables for calculation of new interpolation values
a = first;
b = last;
m = n;

% eliminate fast phases which are on time boundaries
start_flag = (first(1) == 1);
end_flag = (last(n) == vn);
if (start_flag), % first phase is at start of time boundary
    a = a(2:m);
    b = b(2:m);
    m = m - 1;
end
if (end_flag), % last phase is at end of time boundary
    a = a(1:m-1);
    b = b(1:m-1);
    m = m - 1;
end

% check that there are any fast phases left to interpolate across
if (m > 0),

    % construct matrix of velocities before fast phase for speed optimization,
    % and calculate new interpolation values as median of previous three points
    overlap = find(a < 4);
    if (~isempty(overlap)),
        a(overlap) = 4 * ones(size(overlap));
    end
    overlap = find(b > (vn-3));
    if (~isempty(overlap)),
        b(overlap) = (vn-3) * ones(size(overlap));
    end
    vel_matrix = [vel(a-1), vel(a-2), vel(a-3)];
    start_values = median(vel_matrix');
    vel_matrix = [vel(b+1), vel(b+2), vel(b+3)];
    end_values = median(vel_matrix');

    % add extrapolation values for fast phases which occurred on time boundaries
    if (start_flag),
        i = last(1) + 1;
        v = median(vel(i:i+2));
        start_values = [v; start_values];
        end_values = [v; end_values];
    end
    if (end_flag),
        i = first(n) - 1;
        v = median(vel(i-2:i));
        start_values = [start_values; v];
        end_values = [end_values; v];
    end
end

```

```

    % replace old velocities with new ones
    delta = last - first + 1;
    for i=1:n
        d = delta(i);
        s = start_values(i);
        e = end_values(i);
        spv(first(i):last(i)) = (s * ones(d,1)) + ((c - s) * [0:1/(d-1):1]');
    end
end

```

end

clear a b m n vn start_flag end_flag overlap vel_matrix start_values end_values i v delta d s e

load_file.m

```

% This loads the appropriate file and eye data for analysis
% Copied from previous eye.m and modified
% By David Phillips, April 1, 2001

file_name = patient_list(patnum,:);
idx = find(abs(file_name) > 32); % printable non-blank characters
file_name = file_name(idx);

idx = find(file_name == '.');
if (isempty(idx)),
    root_file = file_name;
else
    root_file = file_name(1:(idx(1)-1));
end

run=input('\nEnter run number: ', 's');
rn=str2num(run);
    if (rn < 10),
        run_code = [root_file, '_run0', run];
    else
        run_code = [root_file, '_run', run];
    end
run_file = [data_path, run_code, '.mat'];
load(run_file);

fprintf('\nWhich eye do you want to use for %s?\n', run_code);
eyenum=input('LV=1, LH=2, RV=3, RH=4 (LV default): ', 's');
eyenum=str2num(eyenum);

if isempty(eyenum)
    eyenum=1;
end

if eyenum==2
    eyeext='_LH';
elseif eyenum==3
    eyeext='_RV';
elseif eyenum==4
    eyeext='_RH';
else
    eyeext='_LV';
end

run_file = [data_path, run_code, eyeext, '.mat'];
load(run_file);

```

min_threshold.m

function same = min_threshold(x, y, mult, minimum)

```

% threshold - compare two profiles, and reject all points which differ
%
% by more than a specified multiple of the rms, and at
% least by 'minimum' units
% Written by: D. Balkwill 10/20/93
%
d = abs(y - x);
s = sqrt(mean(d .* d));
n = abs(d / s);
same = ((n <= mult) | (d < minimum));
%plot(n)
clear d s n

```

newAATM.m

```

function spv = newAATM(window, vel)

% matAATM - MATLAB implementation of the "newAATM" C-code, since
% the C-code could not be run on the PowerMac as yet.
%
% Written by: MDB 1/18/96
%

% initialize parameter values
ALPHA = 0.44;
BETA = 0.12;
MU = 0.4;

% integer number of samples in sliding window
N = floor(window / 2);
L = round(2 * N + 1);
num_samples = max(size(vel));
stop = num_samples - N;

% initialize skewing parameters
Lalpha = round(L * ALPHA);
Lbeta = round(L * BETA);
M = round(L * MU);

% initialize and sort first window of data
spv = vel;
s = sort(vel(1:L));

% check to see if array is sorted
d = s(2:L) - s(1:(L-1));
j = find(d < 0);
if (~isempty(j))
    fprintf('Array unsorted initially at indices ');
    j
end

% calculate skewness of first window of data
if (s(L - Lbeta) == s(Lbeta))
    Sbeta = 0;
else
    Sbeta = (s(L - Lbeta) + s(Lbeta) - 2 * s(N+1));
    Sbeta = Sbeta / (s(L - Lbeta) - s(Lbeta));
end
K = round(- Sbeta * M);

% new value at centre of window is mean of estimated peak of histogram
spv(N+1) = mean( s( (Lalpha + K + 1):(L - Lalpha + K) ) );
%spv(N+1) = mean( s( (Lalpha + K):(L - Lalpha + K - 1) ) );

% for each value
for n = (N+2):stop,

```



```

                Sbeta = 0;
            else
                Sbeta = (s(L - Lbeta) + s(Lbeta) - 2 * s(N+1));
                Sbeta = Sbeta / (s(L - Lbeta) - s(Lbeta));
            end
            K = round(- Sbeta * M);

            % new value at centre of window is mean of estimated peak of histogram
            spv(n) = mean( s( (Lalpha + K + 1):(L - Lalpha + K) ) );
            %
            spv(n) = mean( s( (Lalpha + K):(L - Lalpha + K - 1) ) );

        end                %else
    end                    %for

clear s N L K num_samples stop i k1 k2 new old
clear ALPHA BETA MU Lalpha Lbeta M

```

OS_lin2.m

```

function y = OS_lin2(x,N1,N2)

% This function performs order statistic filtering (first stage
% of Engelken, 1990) on an input signal x to sharpen corners and
% reduce noise. It uses two windows of length N1 and N2,
% allowing linear root signals. The new value is therefore
% the median of five values.
%
% D. Balkwill 10/28/90

l=length(x);

% calculate window coefficients for forward filters
h1F = PFMH1(N1);
h2F = PFMH1(N2);

% backward filters have same coefficients, but in reverse
h1B = h1F;
for i=1:N1
    h1B(i) = h1F(N1-i+1);
end
h2B = h2F;
for i=1:N2
    h2B(i) = h2F(N2-i+1);
end

% Use Matlab filter command to maximize speed of execution,
% applying forward and backward windows to appropriate range
% of the input signal.
xF1 = filter(h1F,1,x);
xF1 = [x(1:N1)' xF1(N1:1-1)'];
xB1 = filter(h1B,1,x);
xB1 = [xB1(N1+1:l)' x(1-N1+1:l)'];

xF2 = filter(h2F,1,x);
xF2 = [x(1:N2)' xF2(N2:1-1)'];
xB2 = filter(h2B,1,x);
xB2 = [xB2(N2+1:l)' x(1-N2+1:l)'];

y = median([x xF1 xB1 xF2 xB2]');

clear xB1 xF1 xB2 xF2 i h1F h1B h2F h2B

```

OS_lin2quad1.m

```

function y = OS_lin2quad1(x,N1,N2,N3)

% This function performs order statistic filtering (first stage
% of Engelken, 1990) on an input signal x to sharpen corners and
% reduce noise. It uses two linear windows of length N1 and N2,
% and ones second-order window of length N3, so that linear and
% parabolic root signals are preserved. The new value is therefore
% the median of seven values.
%
% D. Balkwill 11/19/93

l = length(x);

% calculate window coefficients for forward filters
h1F = PFMH1(N1);
h2F = PFMH1(N2);
h3F = PFMH2(N3);

% backward filters have same coefficients, but in reverse
h1B = h1F;
for i=1:N1
    h1B(i) = h1F(N1-i+1);
end
h2B = h2F;
for i=1:N2
    h2B(i) = h2F(N2-i+1);
end
h3B = h3F;
for i=1:N3
    h3B(i) = h3F(N3-i+1);
end

% Use Matlab filter command to maximize speed of execution.
% applying forward and backward windows to appropriate range
% of the input signal.
xF1 = filter(h1F,1,x);
xF1 = [x(1:N1)' xF1(N1:-1:1)']';
xB1 = filter(h1B,1,x);
xB1 = [xB1(N1+1:1)' x(1-N1+1:1)']';

xF2 = filter(h2F,1,x);
xF2 = [x(1:N2)' xF2(N2:-1:1)']';
xB2 = filter(h2B,1,x);
xB2 = [xB2(N2+1:1)' x(1-N2+1:1)']';

xF3 = filter(h3F,1,x);
xF3 = [x(1:N3)' xF3(N3:-1:1)']';
xB3 = filter(h3B,1,x);
xB3 = [xB3(N3+1:1)' x(1-N3+1:1)']';

y = median([x xF1 xB1 xF2 xB2 xF3 xB3]');

clear xB1 xF1 xB2 xF2 xB3 xF3 i1 h1F h1B h2F h2B h3F h3B

```

PFMH1.m

```

function h1 = PFMH1(N)

% This calculates the coefficients for a linear order statistic
% window of length N.
%
% D. Balkwill 10/28/90

a = (4*N + 2)/(N*(N-1));
b = 6/(N*(N-1));

```



```
h1 = a * ones(1,N) - b * [1:N];
clear a b ans
```

PFMH2.m

```
function h2 = PFMH2(N)

% This calculates the coefficients for a second-order order statistic
% window of length N.
%
% D. Balkwill 11/19/93

i = [1:N];
h2 = (9 * N * N) + ((9 - 36 * i) * N) + (30 * i .* i) - (18 * i) + 6;
h2 = h2 / (N * (N * N - 3 * N + 2));
%a = (4*N + 2)/(N*(N-1));
%b = 6/(N*(N-1));
%h1 = a * ones(1,N) - b * [1:N];
clear i
```

review_bed.m

```
% batch_bed

close all
clear all

init_bed

batch_mode = FALSE;

% get research data folder name
get_PC_bed_path

% get list of patients to be processed
get_patient_list

[num_patients,n] = size(patient_list);
yinput=[];
xinput=[];
TVspv=[];
Vspv=[];
THspv=[];
Hspv=[];
hm=[];

for patnum=1:num_patients.

    file_name = patient_list(patnum,:);
    idx = find(abs(file_name) > 32);           % printable non-blank characters
    file_name = file_name(idx);

    idx = find(file_name == '.');
    if (isempty(idx)),
        root_file = file_name;
    else
        root_file = file_name(1:(idx(1)-1));
    end

    for rn=5:4:17,

        if (rn < 10),
            run_code = [root_file, '_run0', int2str(rn)];
        else
```

```

        run_code = [root_file, '_run', int2str(m)];
    end
run_file = [data_path, run_code, '.mat'];
    fprintf(['\nProcessing ', run_code, '...']);
load(run_file);

% Anlog1=data(:,15);
    %Retrieve Analog 1 from column 15
% Anlog2=data(:,16);
    %Retrieve Analog 1 from column 16
% x1=6.2189.*Anlog1;
% x2=6.2189.*Anlog2; %recalibration factor C %-----
% gyro=data(:,7);%filt_gyro_position(x1); %Filter Analog 1 (yaw motions
% gyro=filter_gyro_position(x2); %Filter Analog 2 (pitch motions
%
% Tcount=[0:length(gyro)-1];
%Create vector 0 to length of Analog1
% T=(Tcount/60); %Divide Matrix elements by 60

review_bed_file

end
filename = [data_path, run_code, '_Vspv.mat'];
eval(['save ', filename, ' hm Vspv TVspv ']); % hm=chosen gyros
filename = [data_path, run_code, '_Hspv.mat'];
eval(['save ', filename, ' Hspv THspv ']);
end

```

review_bed_file.m

```

% analyzec_bed_data

% create time vector
clear t
t = [0:(num_samples-1)] / sample_rate;
%og=[0:(length(gyro)-1)] / sample_rate;
%
% process left vertical eye position data
%
raw_index = LEFT_VERTICAL;
cal_index = LEFT_VERTICAL+num_params;
which_eye = 'Left Vertical';
file_ext = '_LV.mat';

review_eye_channel
Vspv=yinput;
neyes=length(yinput)
%Vspv = [Vspv;yinput];
%TVspv = [TVspv; xinput];

%-----input-----
%Tcount=[0:length(gyro)-1]; %Create
vector 0 to length of Analog1
%T=(Tcount/60);
%plot(T, gyro)
%--fprintf(['Ready to enter noise offset cutoff, 1-upper, 2-lower']);
%--[x,y,key]=ginput(2);
%--noiseup = y(1);
%--noisedown = y(2);
%--fprintf(['\n !! Ready to enter same number of head movements !!!!!']);
%InputHM = input('\nEnter Number of Head Movements Wanted: ','s');
%num_headmoves = str2num(InputHM);
%-----
if m==5,
    currenteyes = neyes;

```

```

else
    currenteyes = neyes-currenteyes
end

%[x,y,key] = ginput(currenteyes);
get_hms
%--for i=1:currenteyes.
%-- if y(i)<0
%--     y(i) = y(i)-noisedown;
%-- elseif y(i)>0
%--     y(i) = y(i)+noiseup;
%-- else %y(i) = 0
%--     y(i) = y(i)
%-- end
%--end
%while i-2:2:currenteyes, %num_headmoves,
% y(i-1)=y(i-1)+noiseup;
% y(i)=y(i)-noisedown;
%end
%hm=[hm; y];
%
% process right vertical eye position data
%
%raw_index = RIGHT_VERTICAL;
%cal_index = RIGHT_VERTICAL+num_params;
%which_eye = 'right Vertical';
%file_ext = '_RV.mat';

%review_eye_channel

%
% process left horizontal eye position data
%
%raw_index = LEFT_HORIZONTAL;
%cal_index = LEFT_HORIZONTAL+num_params;
%which_eye = 'Left Horizontal';
%file_ext = '_LH.mat';

%review_eye_channel
%Hispv = yinput;
%THispv = xinput;
%
% process right horizontal eye position data
%
%raw_index = RIGHT_HORIZONTAL;
%cal_index = RIGHT_HORIZONTAL+num_params;
%which_eye = 'Right Horizontal';
%file_ext = '_RH.mat';

%review_eye_channel

```

review_eye_channel.m

```

% bed_eye_channel
%

% free up variable space
clear pos vel spv edited_spv fast_start fast_end

% when something is changed in interactive mode, then analysis must be
% redone from that point on
redo_flag = FALSE;

% review, and allow editing, of despiking algorithm
save_file = [data_path, run_code, file_ext];
load(save_file);

```

```

% filter eye position data to enhance signal-to-noise ratio
%   - one pass of order statistic filter to minimize video quantization,
%     allowing for curved eye movements
%   - two passes of fourth-order phase-less Butterworth low-pass filter
%     with 30 Hz corner frequency, to reduce noise
%   - two additional passes of order statistic filter, to reduce noise
%     and sharpen corners of nystagmus, allowing for curved eye movements
if (redo_flag),
    pos = filt_position(pos, sample_rate, 2, 3, TRUE);
end

% differentiate eye position to get velocity
if (redo_flag),
    vel = differentiate(pos, sample_rate);
end

% classify fast phases in eye velocity data, and interpolate across
if (redo_flag),
    [fast_start, fast_end] = bcd_classify_phases(vel, num_RMS, num_increase, ...
        min_diff_class, sample_rate);
    spv = interpolate(vel, fast_start, fast_end);
end

% allow manual editing, if desired
%yn = get_yn('Do you want to manually edit the SPV data','Y');
%if (yn == 'Y'),
    if ((~redo_flag) & (~isempty(edited_spv))),
        [fast_start, fast_end] = diff_list2(vel, spv);
    end
    fig = figure('Name', ['Manual Editing -- ', run_code, ' -- ', which_eye]);
    edit_alg_diff
    clear ed_spv
%end

% save data in a Matlab-format file
save_file = [data_path, run_code, file_ext];
parms_list = ' pos vel spv edited_spv fast_start fast_end num_blinks perc_blink';
eval(['save ', save_file, parms_list]);

```

see_eye.m

```

% See_eye.m
% Plots all phases of button, spv
% By David Phillips
clear all
get_PC_bed_path

% Gather file name from user
filename = input('Enter subject info (e.g. aim3s18d2): ','s');
root_file = [data_path, filename];

x_strt=1;
run_code = [root_file, '_run01.mat'];
load(run_code);

for rn=1:1:num_runs
    run=num2str(rn);
    if (rn < 10),
        run_code = [root_file, '_run0', run];
    else
        run_code = [root_file, '_run', run];
    end
    run_file = [run_code, '.mat'];

```

```

load(run_file);

% for i=1:5:length(data(:,6))
%   Btemp((i+4)/5,1)=data(i,6);
% end
Btemp=data(:,6);

x_len=length(Btemp);
x_end=x_len+x_strt-1;
x=x_strt:1:x_end;

Button(x_strt:x_end,1)=Btemp;
phase(x_strt:x_end,1)=pi;

x_strt=x_end;
end
phase=phase*(max(Button)-2500)/num_runs+2500;

clf;
hold on;
plot(Button); %Button
plot(phase,'r'); % Phase

```

simple_blinks.m

```

function [blink_start, blink_end] = simple_blinks(pos, num_increase, min_diff_class)
%
% simple_blinks.m - attempts to detect the blinks in a position trace 'pos'
%
% The ISCAN blink detection algorithm marks "blink" points as zeros. A blink
% interval is defined as a series of consecutive blink points. A specified
% number of points (num_increase) are added to the beginning and end of the
% blink interval, to allow for transient behaviour. In addition, the blink
% interval is extended to include any consecutive points that differ by more
% than a specified threshold (min_diff_class). "blink_start" is a vector in
% which each element is the sample number of the start of a blink interval.
% "blink_end" contains the corresponding sample numbers of the ends of the
% blink intervals.
%
% Suggested values for the input parameters are:
%   pos = raw eye position, uncalibrated
%   num_increase = 2
%   min_diff_class = 100
%
% Written by: MDB 10/1/99
%
[m,n] = size(pos);
if (m > n), % column vector
    last = m;
    d = [0; abs(diff(pos))];
else % row vector
    last = n;
    d = [0; abs(diff(pos))];
end

% flag "blink" points
fast = (pos == 0);

% increase fast phase duration by 'num_increase' sample
% in each direction for transients
if (num_increase > 0),
    fast = filtfilt(ones(num_increase+1,1), 1, fast);
    fast = (fast > 0);
end

```

```

% find start and end of each fast phase
fast_diff = filter([1 -1], 1, fast); % two-point difference
blink_start = find(fast_diff > 0); % 0 to 1 transition
num_start = length(blink_start);
blink_end = find(fast_diff < 0) - 1; % 1 to 0 transition
num_end = length(blink_end);
if (num_end < num_start),
    blink_end = [blink_end; last];
    num_end = num_end + 1;
end

% extend interval until difference is less than threshold
for i=1:num_end,
    s = blink_start(i);
    while (d(s) > min_diff_class),
        s = s - 1;
    end
    blink_start(i) = s;
    e = blink_end(i);
    while (d(e) > min_diff_class),
        if (e < length(d))
            e = e + 1; %ERROR here is that d(e) index goes higher than length d. This is index exceeds matrix dimension
        else d(e) = min_diff_class; %If difference too high, make it min threshold
        end
    end
    blink_end(i) = e;
end

return;

```

thresh_blinks.m

```

function [blink_start, blink_end] = thresh_blinks(pos, num_increase, ...
                                                high_thresh, min_diff_class, low_thresh)
%
% thresh_blinks.m - attempts to detect the blinks in a position trace 'pos'
%
% The ISCAN blink detection algorithm marks "blink" points as zeros. In some
% cases, a blink may be missed by ISCAN, but the value at that point may be
% above or below a specified non-zero threshold. A blink interval is
% defined as a series of consecutive blink points with values < "low_thresh"
% or > "high_thresh" in addition to the ISCAN zeros. A specified
% number of points (num_increase) are added to the beginning and end of the
% blink interval, to allow for transient behaviour. In addition, the blink
% interval is extended to include any consecutive points that differ by more
% than a specified threshold (min_diff_class). "blink_start" is a vector in
% which each element is the sample number of the start of a blink interval.
% "blink_end" contains the corresponding sample numbers of the ends of the
% blink intervals.
%
% Suggested values for the input parameters are:
%     pos = raw eye position, uncalibrated
%     num_increase = 2
%     min_diff_class = 100
%
% Written by: MDB 10/1/99
%

[m,n] = size(pos);
if (m > n), % column vector
    last = m;
    d = [0; abs(diff(pos))];
else % row vector
    last = n;
    d = [0, abs(diff(pos))];
end

```

```

% flag "blink" points
fast = ((pos <= low_thresh) | (pos >= high_thresh));

% increase fast phase duration by 'num_increase' sample
% in each direction for transients
if (num_increase > 0),
    fast = filtfilt(ones(num_increase+1,1), 1, fast);
    fast = (fast > 0);
end

% find start and end of each fast phase
fast_diff = filter([1 -1], 1, fast); % two-point difference
blink_start = find(fast_diff > 0); % 0 to 1 transition
num_start = length(blink_start);
blink_end = find(fast_diff < 0) - 1; % 1 to 0 transition
num_end = length(blink_end);
if (num_end < num_start),
    blink_end = [blink_end; last];
    num_end = num_end + 1;
end

% extend interval until difference is less than threshold
for i=1:num_end,
    s = blink_start(i);
    while (d(s) > min_diff_class),
        s = s - 1;
    end
    blink_start(i) = s;
    e = blink_end(i);
    while (d(e) > min_diff_class),
        e = e + 1;
    end
    blink_end(i) = e;
end

return;

```

VOR.m

```

% Files must be in same directory as when run this
snumber = input('\n Enter Subject Number: ','s');
% dnumber = input('\n Enter Day: ','s');
run_file = ['S', snumber, 'd1_run08_Vspv.mat'];
load (run_file)
fprintf(['\n Getting file ', run_file, '...']);
VOR1 = Vspv./hm;
run_file = ['S', snumber, 'd2_run08_Vspv.mat'];
load (run_file)
fprintf(['\n Getting file ', run_file, '...']);
VOR2 = Vspv./hm;
run_file = ['S', snumber, 'd3_run08_Vspv.mat'];
load (run_file)
fprintf(['\n Getting file ', run_file, '...']);
VOR3 = Vspv./hm;

VOR=[VOR1;VOR2;VOR3;];
VORdata = [str2num(snumber) VOR];

eval(['save ', [data_path, snumber, 'VOR.mat'], ' VORdata ']);

```

zero_filter.m

```

function y = zero_filter( B, A, x )

```

```

% zero_filter
%
% Performs zero phase shift filtering for FIR filters (ONLY!)
%     by padding signal to be filtered with non-zero values at
%     beginning and end of data sequence.
%     Called with the same parameters and order as Matlab filter command.
%
% Written by: D. Balkwill 10/20/93 (slightly modified from D. Merfeld)
%

% check sizes of vectors
nx=max(size(x));
nB=max(size(B));

% get initial condition for delay
x(nx+1:nx+((nB-1)/2)) = x(nx).*ones(((nB-1)/2),1);
[temp,Zi] = filter( B, A, x(1) .* ones(((nB-1)/2),1) );

% derivative filter with initial condition for phase-shift compensation
x = filter(B,A,x,Zi);
y = x(((nB-1)/2+1):nx+((nB-1)/2));

%clear temp Zi nx nB

```

40/05-28